Ship Structural Integrity Management:
Opportunistic Maintenance Optimization for Naval Supportability

by

João Felipe Costa Casares

A dissertation submitted in partial fulfillment
of the requirements for the degree of
Doctor of Philosophy
(Naval Architecture and Marine Engineering)
in The University of Michigan
2026

Doctoral Committee:

Professor Nickolas Vlahopoulos, Chair
Professor Matthew D. Collette
Professor Romesh Saigal
Professor David J. Singer

“The ship wherein Theseus and the youth of Athens returned had thirty oars, and was preserved by the Athenians down even to the time of Demetrius Phalereus, for they took away the old planks as they decayed, putting in new and stronger timber in their place, insomuch that this ship became a standing example among the philosophers, for the logical question as to things that grow; one side holding that the ship remained the same, and the other contending that it was not the same.”

- Plutarch, around 100 AD (Plutarch 1905)

The Ship of Theseus Paradox

João Felipe Costa Casares

casares@umich.edu

ORCID iD: 0000-0002-2319-8684

© João Felipe Costa Casares 2026

Dedication

To Raffaella, Alice, and Arthur
– my safe harbor and the fair winds that filled my sails.

"There are other places, surely, for other people, but for me there is only one place, Ann Arbor, for there it was I discovered what life's bright possibilities were."
— William Shawn, The New Yorker

Go Blue!

Acknowledgements

I profoundly acknowledge the Brazilian Navy for the opportunity and support during my time at the University of Michigan, which played a crucial role in shaping my academic path. In this regard, I wish to honor the Directorate of Naval Engineering, where I learned to be an engineer. Particularly, my deepest appreciation goes to my colleagues and senior officers, who introduced me to the topic "Structural Integrity Management" and trusted me to carry this flag.

I treasure the Naval Architecture and Marine Engineering Department at the University of Michigan, which has been an incredible source of inspiration and assistance. The professors, staff, and friends within this remarkable community not only provided opportunities and support for my professional growth but also shared valuable insights that significantly enriched this thesis. I will never forget their kindness and generosity, particularly during the unforgettable moment of my son's birth.

I am forever grateful to Professor Nickolas Vlahopoulos, my academic advisor and committee chair, whose unwavering and kind guidance, support, and academic expertise were fundamental in shaping the direction and scholarly rigor of this thesis and inspired me throughout this journey. I also wish to express my sincere appreciation to the other members of the Doctoral Committee — Professors Matthew Collette, Romesh Saigal, and David Singer — for their valuable contributions, insightful feedback, and expertise. I am particularly grateful to Professor Singer, whose dedicated attention and advice on multiple occasions greatly enhanced the quality of this work.

To my honored parents, Paula and Flavio, and beloved brother, Antonio — you have been far more than any son and brother could ever desire. Your unconditional love and lifelong devotion materialized in the values and strength this journey demanded.

To my devoted family, Raffaella, Alice, and Arthur — I owe my greatest gratitude for your infinite love, boundless patience, and constant support. Your belief in my potential has been a guiding light through every challenge, and your presence in my life has made this endeavor possible. I carry this achievement as much for you as it is for me.

To God, who provided me with strength and providence through every storm.

Fair winds and following seas.
Godspeed,

João Felipe Costa Casares

Table of Contents

Dedication ii

Acknowledgements iii

List of Tables viii

List of Figures xii

List of Appendices xviii

List of Abbreviations xx

Abstract xxiii

Chapter 1 Introduction 1

1.1 Problem Overview 6

1.2 Literature Survey 9

1.3 Research Structure 11

1.4 Dissertation Outline 13

Chapter 2 Structural Degradation 15

2.1 Introduction 15

2.2 Literature Survey 16

2.2.1 Corrosion Model Considerations 21

2.2.2 Corrosion Model Requirements and Selection 23

2.3 Corrosion Model 24

2.4 Probabilistic Approach 28

2.5 Simulation, Results, and Validation 31

2.6 Failure Thresholds 34

2.7 Conclusion 38

Chapter 3 Cost and Time 39

3.1 Introduction 39

3.2 Literature Survey 41

3.2.1 Literature Survey: Structural Cost 41

3.2.2 Literature Survey: Expected Cost of Failure 42

3.2.3 Literature Survey: Expected Cost of Opportunity of Non-Planned Unavailability of Naval Vessels 44

3.3 Structural Cost 45

3.3.1 Sequential Workstations 51

3.3.2 CONWIP Workstations 53

3.3.3 Structural Maintenance Time and Cost 65

3.4 Expected Cost of Failure 67

3.5 Expected Cost of Opportunity of Non-Planned Unavailability of Naval Vessels 71

3.5.1 Expected Cost of Opportunity 72

3.5.2 Present Value of the Expected Cost of Opportunity 75

3.5.3 Cost of Opportunity Sensitivity Analysis 76

3.6 Conclusion 79

Chapter 4 Opportunistic Maintenance Optimization 81

4.1 Introduction 81

4.2 Literature Survey 85

4.3 Maintenance Cost and Risk Optimization (MCRO) 89

4.4 Opportunistic Maintenance Cost and Risk Optimization (OMCRO) 90

4.4.1 Time-Grouping Strategy 91

4.4.2 Policy-Grouping Strategy 94

4.4.3 Discussion on the Results of the Grouping Strategies 101

4.4.4 Optimization 103
4.5 The OMCRO framework 107
4.5.1 OMCRO Framework Results 108
4.6 Verification and Validation (V&V) 116
4.6.1 Verification 117
4.6.2 Optimization Validation 118
4.7 Quantitative Maintainability and Availability Analysis 120
4.7.1 Shipyard (SS) Quality (Q) Effects on Maintainability (M) 121
4.7.2 Ship Structure (SoI) Reliability (R) Effects on Maintainability (M) 122
4.7.3 Maintainability (M) Effects on Availability (A) 126
4.7.4 Ship Structure (SoI) Reliability (R) and Shipyard (SS) Quality (Q) Emergent Effects on Maintainability (M) and Availability (A) 132
4.7.5 Qualitative Communication of Quantitative Maintainability and Availability Analysis 135
4.8 Scalability 138
4.9 OMCRO Framework Validation 142
4.10 Conclusion 143
Chapter 5 Thesis Contributions 146
Chapter 6 Future Work 151
Appendices 155
Bibliography 194

List of Tables

Table 1. Life Cycle Processes Outline (ISO/IEC/IEEE 15288 2023; INCOSE 2023). 2

Table 2. RAM Outline (Blanchard 1998; INCOSE 2023). 4

Table 3. Technical Outline. 13

Table 4. Prominent Ship Corrosion Models. 24

Table 5. Environmental Nominal Factors. 26

Table 6. Environmental and Operational parameters. 31

Table 7. Hazard Severity Levels and $PoFT$ 35

Table 8. Activities and Tasks of Ship Repair. 46

Table 9. Entities and Unities of Sequential Workstations. 51

Table 10. Workflow Parameters for Validation. 60

Table 11. TH Average Errors 62

Table 12. Intervention Time. 66

Table 13. Consequence of Failure Components. 67

Table 14. Equivalent Number of Fatalities. 68

Table 15. Sensitivity Analysis on the Cost of Opportunity Parameters. 77

Table 16. Structural Integrity Management KID. 84

Table 17. Structural Cost CS in PV (USD) – Time-Grouping. 93

Table 18. Structural Cost CS in FV (USD) – Time-Grouping. 93

Table 19. Costs in PV and Total Expected Cost CT – Time-Grouping. 94

Table 20. Structural Cost CS in PV (USD) – Policy-Grouping. 100

Table 21. Structural Cost CS in FV (USD) – Policy-Grouping. 100

Table 22. Costs in PV and Total Expected Cost CT – Policy-Grouping. 100

Table 23. Results of the Grouping Strategies. 101

Table 24. OMCRO overall results (Time-Grouping Strategy - 5 elements)..... 109

Table 25. OMCRO overall results (Policy-Grouping Strategy - 5 elements)..... 113

Table 26. Times, Tasks CS, CEF and CEO (FV) Maximum Absolute Differences (Time-Grouping)..... 117

Table 27. CS Absolute Differences (Time-Grouping)..... 117

Table 28. CT Absolute Difference (Time-Grouping). 117

Table 29. Times, Tasks CS, CEF and CEO (FV) Maximum Absolute Differences (Policy-Grouping)..... 117

Table 30. CS Absolute Differences (Policy-Grouping). 118

Table 31. CT Absolute Difference (Policy-Grouping)..... 118

Table 32. Shipyard Quality Effect on CT. 121

Table 33. Ship Structure Thickness and Shipyard Quality Effect on CT. 123

Table 34. Ship E&O and Shipyard Quality Effect on CT..... 123

Table 35. Shipyard Quality Effect on Total Unavailability Time (TUT)..... 127

Table 36. Shipyard Quality Effect on Repair Frequency (RF). 127

Table 37. Ship Structure Thickness and Shipyard Quality Effect on Total Unavailability Time (TUT)..... 128

Table 38. Ship E&O and Shipyard Quality Effect on Total Unavailability Time (TUT). 128

Table 39. Ship Structure Thickness and Shipyard Quality Effect on Repair Frequency (RF).. 129

Table 40. Ship E&O and Shipyard Quality Effect on Repair Frequency (RF)..... 130

Table 41. Environment and Operation parameters (Scalability Simulation)..... 139

Table 42. OMCRO overall results (Time-Grouping Strategy - 200 elements)..... 139

Table 43. OMCRO overall results (Policy-Grouping Strategy - 200 elements)..... 140

Appendix Table A.1. Mean $dn(t)$ parameters from datasets. 155
Appendix Table A.2. Standard Deviation parameters for deck plates. 156
Appendix Table A.3. Space Classes. 157
Appendix Table A.4. Collected data type. 157
Appendix Table A.5. List of Corrosion Models. 162
Appendix Table C.1. Elements' Parameters. 166
Appendix Table D.1. Cost of Failure Parameters (Except for Structural). 167
Appendix Table D.2. Cost of Opportunity Parameters. 168
Appendix Table D.3. Structural Cost Parameters (1-30). 168
Appendix Table D.4. Structural Cost Parameters (31-70). 169
Appendix Table D.5. Structural Cost Parameters (71-110). 170
Appendix Table D.6. Structural Cost Parameters (111-133). 171
Appendix Table E.1. Drydock Costs in PV for Downtime at Year 5. 172
Appendix Table E.2. Quay Costs in PV for Downtime at Year 5. 173
Appendix Table E.3. Drydock Costs in PV for Downtime at Year 10 and 20. 175
Appendix Table E.4. Quay Costs in PV for Downtime at Year 10 and 20. 176
Appendix Table E.5. Drydock Costs in PV for Downtime at Year 15. 177
Appendix Table E.6. Quay Costs in PV for Downtime at Year 15. 178
Appendix Table E.7. Cost of Failure for Single Elements and Associated Unavailability Time. 179
Appendix Table E.8. Probability of Failure Up to First Threshold. 179
Appendix Table E.9. Expected Cost of Failure Up to First Threshold. 179
Appendix Table E.10. Expected Cost of Failure Over Time with Interventions. 180
Appendix Table E.11. Expected Cost of Opportunity Up to First Threshold (without return of capital) 181
Appendix Table E.12. Expected Cost of Opportunity Over Time with Interventions. 181

Appendix Table G.1. Drydock Costs in PV for Downtime at Year 5, 10, 15, and 20. 186

Appendix Table G.2. Quay Costs in PV for Downtime at Year 5, 10, 15, and 20. 187

Appendix Table G.3. Cost of Failure for Policy Elements and Associated Unavailability Time. 189

Appendix Table G.4. Probability of Failure Up to First Threshold. 189

Appendix Table G.5. Expected Cost of Failure Up to First Threshold. 189

Appendix Table G.6. Expected Cost of Failure Over Time with Interventions. 190

Appendix Table G.7. Expected Cost of Opportunity Up to First Threshold (without return of capital). 191

Appendix Table G.8. Expected Cost of Opportunity Over Time with Interventions. 191

List of Figures

Figure 1. Asset Integrity upkeep dynamic. 1

Figure 2. Life cycle processes (INCOSE 2023; ISO/IEC/IEEE 15288 2023). 3

Figure 3. RAMS from a SoS perspective. 4

Figure 4. (a) Tanker side-by-side with the Eiffel Tower. DNV courtesy to EMSA. (EMSA 2005). (b) The author is entering a ship's bottom tank to survey (confined space). 7

Figure 5. Relative number of publications related to the optimization of different maintenance strategies from 2000 to 2020 [www.scopus.com](Pinciroli, Baraldi, and Zio 2023). 10

Figure 6. Keyword co-occurrence network using the VOSviewer. 11

Figure 7. Technical outline structure. 14

Figure 8. Paik model (Paik et al. 2003). Corrosion depth tr as a function of structural age T, coating life TC, transition time Tt and coefficients $C1$ and $C2$. 18

Figure 9. Soares-Garbatov model (Guedes Soares and Garbatov 1999). Thickness wastage $d(t)$ as a function of structural age t, coating life τc, transition time τt, and long-term corrosion wastage thickness $d\infty$. 19

Figure 10. Melchers marine immersion model (Melchers 1997). Thickness wastage as a function of time in Phase 0 and 1 (kinetic controlled); Phase 2 (diffusion controlled); Phase 3 (nutrient controlled); Phase 4 (anaerobic controlled). 20

Figure 11. Qin-Cui model (Qin and Cui 2003). Thickness wastage as a function of time t, the instant Tst at which the pitting corrosion starts, and the time TA when the general corrosion decelerates. 21

Figure 12. (a) Seawater immersion correction factor (Guedes Soares, Garbatov, and Zayed 2011). (b) Marine atmosphere correction factor (Guedes Soares et al. 2009). (c) Oil atmosphere correction factor (Guedes Soares et al. 2008). 26

Figure 13. Generic transverse section of a naval vessel. 31

Figure 14. $PoF(t)$ for Element 1 – Class GE. 33

Figure 15. $PoF(t)$ for Element 2 – Class GG. 33

Figure 16. $PoF(t)$ for Element 3 – Class GG. 33
Figure 17. $PoF(t)$ for Element 4 – Class H. 34
Figure 18. $PoF(t)$ for Element 5 – Class IC. 34
Figure 19. $PoF(t)$ for Element 1 with full renewal (log scale). 36
Figure 20. $PoF(t)$ for Element 2 with full renewal (log scale). 36
Figure 21. $PoF(t)$ for Element 3 with full renewal (log scale). 37
Figure 22. $PoF(t)$ for Element 4 with full renewal (log scale). 37
Figure 23. $PoF(t)$ for Element 5 with full renewal (log scale). 37
Figure 24. Repair Intervention Workflow. 47
Figure 25. Push System. 48
Figure 26. Pull System. 49
Figure 27. CONWIP System. 50
Figure 28. Production and Repair CONWIP workflow. 50
Figure 29. Logistic Operating Curve ($WIP\ x\ TH/rb$) of a line. 59
Figure 30. Logistic Operating Curve ($WIP\ x\ CT/T0$) of a line. 60
Figure 31. Line 1 Model Error. 61
Figure 32. Line 2 Model Error. 61
Figure 33. Line 3 Model Error. 61
Figure 34. Line 4 Model Error. 62
Figure 35. WIP x CT - ce = 1. 63
Figure 36. WIP x CT - ce = 1.5. 64
Figure 37. WIP x CT - ce = 2. 64
Figure 38. Loss of Opportunity from T to PV. 72
Figure 39. Cost of Opportunity Sensitivity Analysis. 78
Figure 40. Maintenance Strategies (Pinciroli, Baraldi, and Zio 2023). 82

Figure 41. Uncertainty and Optimization Problems. 86

Figure 42. GA process (Vu et al. 2014). 88

Figure 43. Design variable, Time Limit, and Operational Window. 91

Figure 44. Combined Costs in FV – Time-Grouping. 94

Figure 45. Decision Tree..... 97

Figure 46. Combined Costs in FV – Policy-Grouping. 100

Figure 47. Results of the Grouping Strategies – Cost USD..... 101

Figure 48. Results of the Grouping Strategies – Cost Contribution Percentage..... 102

Figure 49. Downtime's bounds..... 107

Figure 50. OMCRO overall results (Time-Grouping Strategy - 5 elements). 109

Figure 51. OMCRO CEF and CEO results (Time-Grouping Strategy- 5 elements). 110

Figure 52. OMCRO CS results for downtime at year 5 (Time-Grouping Strategy - 5 elements). 110

Figure 53. OMCRO CS results for downtime at year 10 (Time-Grouping Strategy - 5 elements). 111

Figure 54. OMCRO CS results for downtime at year 15 (Time-Grouping Strategy - 5 elements). 111

Figure 55. OMCRO CS results for downtime at year 20 (Time-Grouping Strategy - 5 elements). 112

Figure 56. OMCRO overall results (Policy-Grouping Strategy - 5 elements). 113

Figure 57. OMCRO CEF and CEO results (Policy-Grouping Strategy- 5 elements)..... 114

Figure 58. OMCRO CS results for downtime at year 5 (Policy-Grouping Strategy - 5 elements). 114

Figure 59. OMCRO CS results for downtime at year 10 (Policy-Grouping Strategy - 5 elements). 115

Figure 60. OMCRO CS results for downtime at year 15 (Policy-Grouping Strategy - 5 elements). 115

Figure 61. OMCRO CS results for downtime at year 20 (Policy-Grouping Strategy - 5 elements). 116

Figure 62. Monte Carlo Simulation for Time-Grouping. 119

Figure 63. Monte Carlo Simulation for Policy-Grouping. 119

Figure 64. Shipyard Quality Effect on CT (Time-Grouping). 122

Figure 65. Ship Structure Thickness and Shipyard Quality Effect on CT. 124

Figure 66. Ship E&O and Shipyard Quality Effect on CT. 124

Figure 67. Ship Structure Thickness and Shipyard Quality Effect on CT (Heatmap). 125

Figure 68. Ship E&O and Shipyard Quality Effect on CT (Heatmap). 125

Figure 69. Shipyard Quality Effect on Total Unavailability Time (TUT). 127

Figure 70. Ship Structure Thickness and Shipyard Quality Effect on Total Unavailability Time (TUT). 129

Figure 71. Ship E&O and Shipyard Quality Effect on Total Unavailability Time (TUT). 129

Figure 72. Ship Structure Thickness and Shipyard Quality Effect on Total Unavailability Time (TUT) (Heatmap). 130

Figure 73. Ship E&O and Shipyard Quality Effect on Total Unavailability Time (TUT) (Heatmap). 131

Figure 74. Five-dimensional (5D) space for Total Expected Cost CT. 133

Figure 75. Five-dimensional (5D) space for Total Unavailability Time (TUT). 133

Figure 76. Five-dimensional (5D) space for Repair Frequency (RF). 134

Figure 77. RAMSQ Chart. 137

Figure 78. RAMSQ Chart (High-Level). 137

Figure 79. OMCRO overall results (Time-Grouping Strategy - 200 elements). 140

Figure 80. OMCRO overall results (Policy-Grouping Strategy - 200 elements). 141

Figure 81. SIM SoS. 154

Appendix Figure A.1. Thickness wastage curve for single-sided model C, simplified model C with original τt, and error. 160

Appendix Figure A.2. Non-Linear Factors $fnli$ for ship space types (A to I). 160

Appendix Figure A.3. Thickness wastage curve for single-sided model C, corrected model C with original τt, and error. 161

Appendix Figure A.4. Probabilistic corrosion model framework. 162

Appendix Figure B.1. Grouping Strategy (Step 1). 163

Appendix Figure B.2. Grouping Strategy (Step 2). 163

Appendix Figure B.3. Grouping Strategy (Step 3): Input Solution. 164

Appendix Figure B.4. Grouping Strategy (Step 3): Iteration 1. 164

Appendix Figure B.5. Grouping Strategy (Step 3): Iteration 2. 164

Appendix Figure B.6. Grouping Strategy (Step 3): Iteration 3. 165

Appendix Figure B.7. Grouping Strategy (Step 3): Iteration 4. 165

Appendix Figure B.8. Grouping Strategy (Step 3): Grouping Solution. 165

Appendix Figure E.1. Drydock Costs in PV for Downtime at Year 5. 173

Appendix Figure E.2. Drydock Times for Downtime at Year 5. 173

Appendix Figure E.3. Quay Costs in PV for Downtime at Year 5. 174

Appendix Figure E.4. Quay Times for Downtime at Year 5. 174

Appendix Figure E.5. Drydock Costs in PV for Downtime at Year 10 and 20. 175

Appendix Figure E.6. Drydock Times for Downtime at Year 10 and 20. 175

Appendix Figure E.7. Quay Costs in PV for Downtime at Year 10 and 20. 176

Appendix Figure E.8. Quay Times for Downtime at Year 10 and 20. 176

Appendix Figure E.9. Drydock Costs in PV for Downtime at Year 15. 177

Appendix Figure E.10. Drydock Times for Downtime at Year 15. 177

Appendix Figure E.11. Quay Costs in PV for Downtime at Year 15. 178

Appendix Figure E.12. Quay Times in PV for Downtime at Year 15. 178

Appendix Figure E.13. Expected Cost of Failure CEF in FV – Time-Grouping. 180

Appendix Figure E.14. Expected Cost of Opportunity CEO in FV – Time-Grouping. 182

Appendix Figure F.1. Grouping Strategy (Step 1). 183

Appendix Figure F.2. Grouping Strategy (Step 2). 183
Appendix Figure F.3. Grouping Strategy (Step 3): Input Solution. 184
Appendix Figure F.4. Grouping Strategy (Step 3): Iteration 1. 184
Appendix Figure F.5. Grouping Strategy (Step 3): Iteration 2. 184
Appendix Figure F.6. Grouping Strategy (Step 3): Iteration 3. 185
Appendix Figure F.7. Grouping Strategy (Step 3): Iteration 4. 185
Appendix Figure F.8. Grouping Strategy (Step 3): Grouping Solution. 185
Appendix Figure G.1. Drydock Costs in PV for Downtime at Year 5, 10, 15, and 20. 187
Appendix Figure G.2. Drydock Times for Downtime at Year 5, 10, 15 and 20. 187
Appendix Figure G.3. Quay Costs in PV for Downtime at Year 5, 10, 15, and 20. 188
Appendix Figure G.4. Quay Times for Downtime at Year 5, 10, 15, and 20. 188
Appendix Figure G.5. Expected Cost of Failure CEF in FV – Policy-Grouping. 190
Appendix Figure G.6. Expected Cost of Opportunity CEO in FV – Policy-Grouping. 192

List of Appendices

Appendix A: Long-Term Single-Sided Model 155
A.1 Step 1: Nominal Short-Term Model for Specific Ship Spaces 155
A.2 Step 2: Nominal Short-Term Single-Sided Model for Multiple Ship Spaces 156
A.3 Step 3: Long-Term Single-Sided Model for Multiple Ship Spaces 158
A.4 Step 4: Long-Term Probabilistic Model for Multiple Ship Spaces 159
Appendix B: Time-Grouping Demonstration 163
B.1 Step 1: Single element time threshold 163
B.2 Step 2: Single element repair (time threshold repetitions) 163
B.3 Step 3: Grouping and Anticipation 164
Appendix C: Elements' Parameters 166
Appendix D: Costs' Parameters 167
D.1 Cost of Failure Parameters (Except Structural) 167
D.2 Cost of Opportunity Parameters 168
D.3 Structural Cost Parameters 168
Appendix E: Time-Grouping Hand Calculation Results 172
E.1 Structural Cost 172
E.2 Expected Cost of Failure 179
E.3 Expected Cost of Opportunity 181
Appendix F: Policy-Grouping Demonstration 183
F.1 Step 1: Single element time threshold 183
F.2 Step 2: Single element repair (time threshold repetitions) 183

F.3 Step 3: Grouping, Policy Application, and Anticipation 184
Appendix G: Policy-Grouping Hand Calculation Results 186
G.1 Structural Cost 186
G.2 Expected Cost of Failure 189
G.3 Expected Cost of Opportunity 191
Appendix H: The OMCRO Framework 193

List of Abbreviations

A	Availability
AI	Artificial Intelligence
AIM	Asset Integrity Management
ALGA	Augmented Lagrangian Genetic Algorithm
CAPEX	Capital Expenditure
CBM+	Condition-Based Maintenance Plus
CBO	Congressional Budget Office
CE	Cost-Effectiveness
CONWIP	Constant Work In Process
CPS	Corrosion Protective Systems
CRO	Cost and Risk Optimization
CS	Classification Societies
CT	Cycle Time
DC	Developed Countries
DES	Discrete Event Simulation
DP	Dynamic Programming
DT	Decision Tree
E&O	Environment and Operation
ESS	Embedded Sensor System
FFS	Fit For Service
FIFO	First In First Out
FOMC	Federal Open Market Committee
FV	Future Value
FY	Fiscal Year
GA	Genetic Algorithm
GAO	Government Accountability Office
GDP	Gross Domestic Product
GT	Group Technology
HR	High Reliability
HRHQ	High Reliability High Quality
HRLQ	High Reliability Low Quality
I2S	Information and Integration Subsystem
IACS	International Association of Classification Societies

ICAF	Implied Cost of Averting a Fatality
JIT	Just In Time
KID	Knowledge, Information, and Data
LCRO	Life Cycle Cost and Risk Optimization
LDC	Less Developed Countries
LQ	Low Quality
LR	Low Reliability
LRHQ	Low Reliability High Quality
LRLQ	Low Reliability Low Quality
M	Maintainability
MA	Mathematical Approaches
MCRO	Maintenance Cost and Risk Optimization
MCS	Monte Carlo Simulation
MDS	Mobile Device System
MDT	Maintenance Downtime
MIP	Mixed Integer Programming
MRP	Material Resource Planning
MSA	Metaheuristic Search Algorithms
MTBM	Mean Time Between Maintenance
MTBR	Mean Time Between Repairs
MVA	Mean Value Analysis
NSS	National Security Strategy
OMCRO	Opportunistic Maintenance Cost and Risk Optimization
OPEX	Operational Expenditure
PDF	Probability Density Function
PM	Policy Matrix
PMC	Policy Matrix for Compartment
PMM	Policy Matrix for Manufacturing
PMT	Policy Matrix for Time
PMTS	Policy Matrix for Tank or Seawater
PMW	Policy Matrix for Welding
PV	Present Value
Q	Quality
QC	Quality Characteristic
R	Reliability
RAMS	Reliability, Availability, Maintainability, and Safety
RAMSQ	Reliability, Availability, Maintainability, Safety, and Quality
RBDO	Reliability-Based Design Optimization
RBI	Risk-Based Inspection
RF	Repair Frequency

RV	Random Variable
S	Safety
SFC	Shop Floor Control
SHM	Structure Health Monitoring
SIM	Structure Integrity Management
SIMS	SIM System
SIP	Stochastic Information Packet
SoI	System of Interest
SoS	System of Systems
SRB	Sulphate-Reducing Bacteria
SS	Support System
TA	Technical Analysis
TDCWM	Time-Dependent Corrosion Wastage Models
TH	Throughput
TM	Technical Management
TUT	Total Unavailability Time
U.S.	United States
USCG	United States Coast Guard
USD	United States Dollar
WIP	Work-In-Process

Abstract

The structure of ships, which are prone to various failure modes, presents challenges due to diverse degradation factors and limited access for inspection, leading to a lack of condition knowledge of structural components. Notably, corrosion is the primary cause of structural failures in sea-going vessels, which has triggered extensive prediction studies. Structural integrity, however, is only one dimension of the problem, as there are also significant management challenges in implementing optimized maintenance strategies in real-world scenarios, where the value of logical and straightforward processes is often overlooked. In this regard, Opportunistic Maintenance Optimization has not been formally explored in the ship industry, despite its potential to take advantage of costly downtimes through a rational process.

Accordingly, this dissertation presents a novel Opportunistic Maintenance Cost and Risk Optimization (OMCRO) framework, designed to optimize opportunistic maintenance decisions on downtimes by minimizing the total expected cost during the life cycle, while respecting safety levels. Hence, this framework leverages opportunistic repair grouping processes during downtime to reduce quantitative operational risks by jointly performing maintenance actions within the same intervention. These grouping strategies comprise two innovative procedures to perform component grouping under the Opportunistic Maintenance: Time-Grouping and Policy-Grouping Strategies.

Consistently, this framework is applied in this dissertation to address the Structural Integrity Management (SIM) of naval vessels, considering an enhanced probabilistic corrosion model for any ship space. Through metaheuristic optimization, it seeks a good trade-off between operational risks and repair costs, providing clear guidance for stakeholders on what, when, and where to survey and repair, as well as understanding the associated costs and risks. This framework is verified through analytical calculations and validated by Monte Carlo Simulation (MCS). Moreover, it is adaptable to multiple systems, as it is based on a logical grouping principle and does not make a distinction on what type of system component is being grouped.

The OMCRO framework is built upon the foundational elements of a leveraged high-level integration concept of Reliability, Availability, Maintainability, and Safety (RAMS) within a

System of Systems (SoS), viewed from a supportability perspective. It clearly redefines Maintainability (M) as an emergent property of both the ship and the shipyard. Consistently, this dissertation develops an analytical model that integrates shipyard processes and Quality (Q) for downtime cost and time prediction, based on a Group Technology (GT) arrangement and Constant Work In Process (CONWIP) discipline. This model is validated using Discrete Event Simulation (DES).

Furthermore, a pioneering economic model is proposed to quantify the Expected Cost of Opportunity of unplanned unavailability of naval vessels, addressing a previously unmodeled expenditure in defense economics. A sensitivity analysis within this model identified the opportunity return horizon as the primary driver, leading to the conclusion that early unexpected downtimes result in higher opportunity losses. Accordingly, this cost is incorporated as an element of operational risk, which also provides a governance-level trigger to reassess remaining service life and evaluate life-extension, repurposing, or decommissioning options under current economic conditions.

As a sensitivity study, the OMCRO framework evaluates the effects of key parameters, such as process capacity and variability, structural thickness, and environmental and operational corrosion factors, indicating how each independently influences downtime frequency and duration. The results, in a cost-effective approach, demonstrate that shipyard Quality (Q) governs downtime average duration, while ship Reliability (R), bounded by Safety (S) levels, drives scheduling frequency independently. However, both integrated factors provide the emergence of Maintainability (M) and Availability (A), quantified by cost and time, respectively. Accordingly, this dissertation proposes adding the Quality (Q) of Support Systems (SS) to the traditional RAMS approach, creating a new leveraged perspective called RAMSQ. This is based on the important role of SS and the need for a SoS perspective to more effectively evaluate and measure Maintainability (M) and Availability (A). Furthermore, this dissertation also provides a qualitative rationale and introduces a RAMSQ Chart, visually mapping how structural Reliability (R) and shipyard Quality (Q) contribute to building Maintainability (M) and Availability (A). The RAMSQ Chart serves as a practical tool for technical and non-technical stakeholders.

The same framework was used to simulate SIM in a scalability demonstration by considering 200 structural elements with different shapes and sizes, localized in a diverse number of compartments, and subjected to a simulated environment and operation. The simulation results

demonstrate the framework's efficacy in aligning with industry standards while offering valuable insights for SIM stakeholders.

Future work should consider shipyard Availability (A) constraints, such as drydocks and quay spaces. Furthermore, expanding the model to support fleet optimization would enable evaluation of trade-offs across multiple assets while accounting for shared support resources. A further avenue is to incorporate structural CAPEX and non-maintenance OPEX into the life cycle trade-off model, and to refine the service-life boundary by incorporating life-extension reinvestment costs, decommissioning expenditures, and post-upgrade failure risks. Finally, the most transformative prospect lies in integrating OMCRO with real-time data through Maintenance 4.0 and Structural Health Monitoring (SHM), enabling adaptive, data-driven solutions using Bayesian Inference, Digital Twins, and AI-enhanced failure prediction models.

Chapter 1 Introduction

“Is a ship that has had all her parts replaced still the same ship?”

- The Ship of Theseus Paradox

The answer to this famous quote depends on the "ship" definition. Most of the descriptions blend two distinct but related concepts in the same definition: material and function. Generalizing: the “ship” is a “material” that performs a “function”. This definition rationale is what sustains the paradox and is not useful to describe ship maintenance.

Breaking this definition into a systems thinking perspective allows one to observe that the material supports the ship's function, but over time, the function itself degrades the material until the support becomes unreliable. Consequently, maintenance will be demanded under a payoff to ensure the material remains reliable enough to support the ship’s function over time. This reliability upkeep dynamic can be generalized for any asset and is metaphorically illustrated in Figure 1.

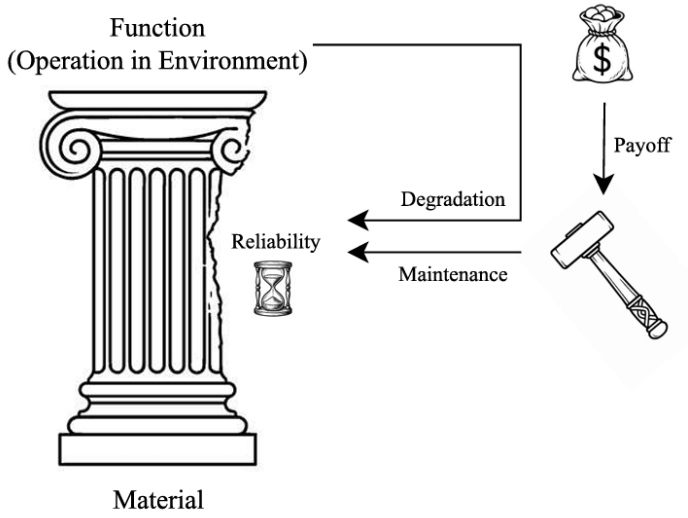


Figure 1. Asset Integrity upkeep dynamic.

Accordingly, the ship will not be the same from a material perspective since parts are replaced at different times. However, it will be the same from the functional perspective if its initial function is still preserved.

Designing and controlling the process presented in Figure 1 and its components over the life cycle of a system is explored by Asset Integrity Management (AIM). It is described as the integration of life cycle processes that aim to ensure the adequate integrity of a physical asset for its mission (Fit For Service - FFS) throughout its life cycle until its disposal. These life cycle processes are well-defined and integrated by (INCOSE 2023; ISO/IEC/IEEE 15288 2023). They are outlined and simplified by Table 1 and illustrated by Figure 2 at a high-level perspective.

Table 1. Life Cycle Processes Outline (ISO/IEC/IEEE 15288 2023; INCOSE 2023).

1	Agreement Processes	Establish agreement between organizations.
2	Organizational Project-Enabling Processes	Provides the resources needed to enable the project to meet the needs and expectations of the organization's stakeholders.
3	Technical Management Processes	Manage the resources and assets allocated by the organization management and apply them to fulfill the agreements between organizations. Uses technical and administrative resources to plan, organize, and control engineering functions.
4	Technical Processes	
4a	Concept Definition	Define high-level problems and opportunities, characterize the solution space, and elicit stakeholders' needs.
4b	System Definition	Define the requirements for the System of Interest (SoI).
4c	System Realization	Transform the requirements into an effective product.
4d	System Deployment and Use	Use the product, provide the required services, sustain the provision of those services, and dispose of the product when it is retired from service.

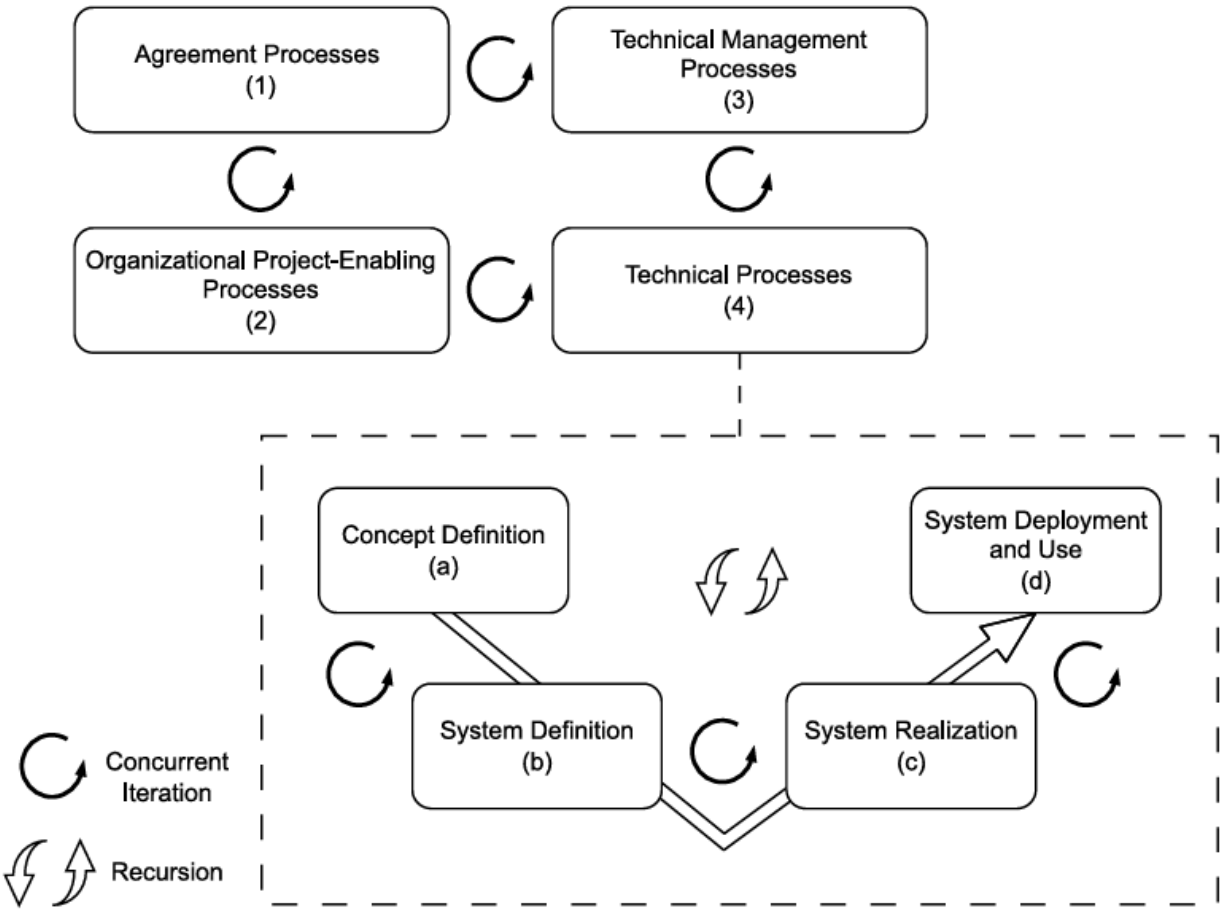


Figure 2. Life cycle processes (INCOSE 2023; ISO/IEC/IEEE 15288 2023).

Every process or subprocess from the life cycle that refers to or impacts the physical integrity of the System of Interest (SoI) is part of the AIM. Specifically, under the system use (process 4d), maintenance is highly strategic while explored as the downstream action to ensure the SoI FFS. In a holistic perspective, the AIM maintenance concept and plan are herein explored under Reliability, Availability, Maintainability, and Safety (RAMS) Engineering. This approach is based on four of the many Quality Characteristics (QC) of a system (INCOSE 2023). Accordingly, their descriptions are outlined in high-level by Table 2, based on (Blanchard 1998; INCOSE 2023) definitions.

Table 2. RAM Outline (Blanchard 1998; INCOSE 2023).

Reliability	The probability that a system satisfactorily performs under a specified time when used in operating conditions.
Availability	The measure of system readiness (the degree, percent, or probability that a system will be FFS).
Maintainability	The ease, accuracy, safety, time, and cost-effectiveness in the performance of maintenance actions.
Safety	The risk measure of harm to people, assets, and the environment.

Accordingly, these QCs are interdependent and have a strong association with logistics engineering, thereby with the supportability QC (INCOSE 2023). As illustrated by Figure 3, their relationship with the System of Systems (SoS), composed of the SoI and Support System (SS), is developed and explored in this dissertation, on a leveraged approach.

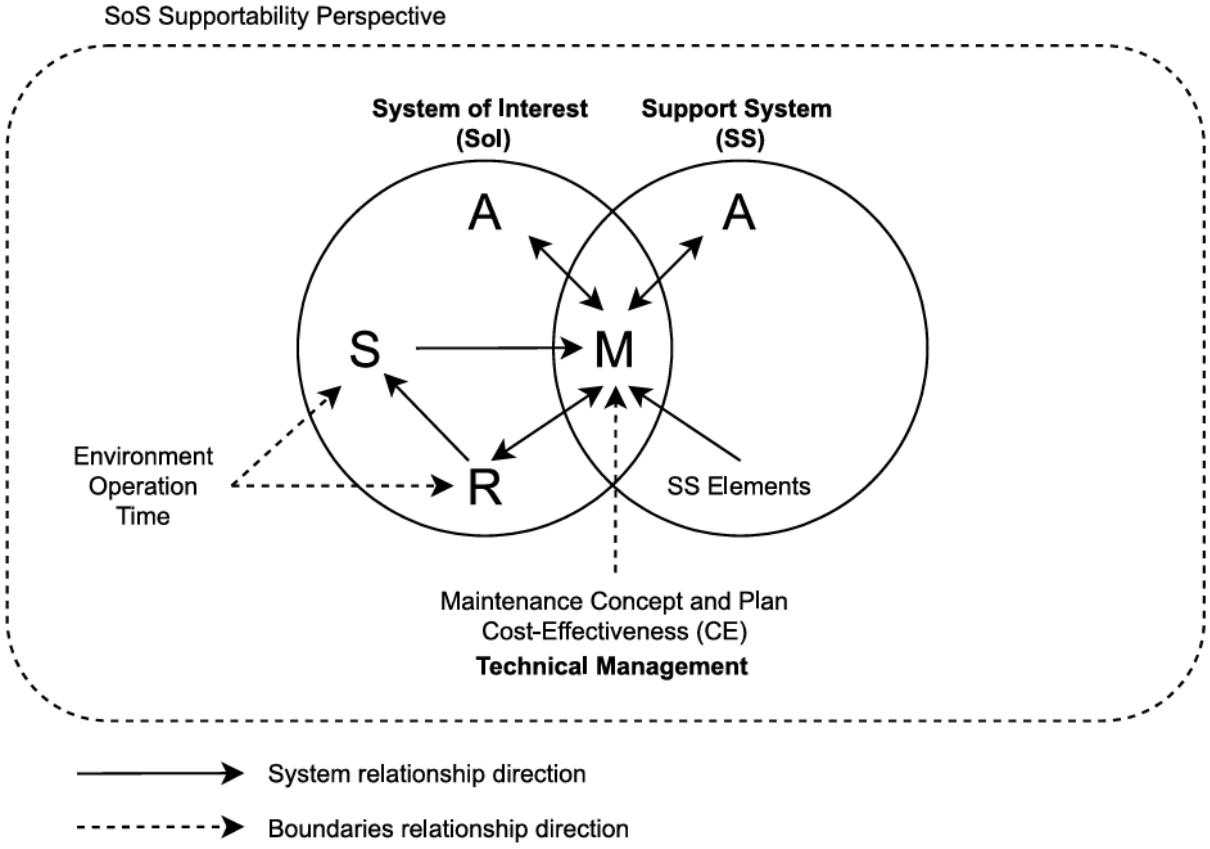


Figure 3. RAMS from a SoS perspective.

Figure 3 can be described by the following dynamics:

I. Environment, operation, time, and system design will have a direct impact on the time-based Reliability (R) and Safety (S) of the SoI.

II. The SoI Safety (S) measure of risk is related to the uncertainty levels of failure, which can be associated with Reliability (R), and the failure severity, which is estimated based on the relation between environment, operation, and the SoI design.

III. Both SoI Reliability (R) and Safety (S) are inputs to Maintainability (M). Accordingly, Reliability (R) will quantify the system deterioration level, while safety will evaluate its impact under acceptable levels. Therefore, deterioration levels related to their acceptable thresholds are necessary information for maintenance decision-making.

IV. Maintenance concept and plan are defined by the Technical Management organization and are inputs to Maintainability (M). Correspondingly, the maintenance concept defines maintenance levels criteria, high-level support policies, and maintainability factors, while the maintenance plan specifies the strategy, process, and elements needed from the SS.

V. Cost-Effectiveness (CE) is also under the Technical Management organization and is a QC of affordability analysis. As defined by (INCOSE 2023), it maximizes value by balancing system performance, cost, and schedule constraints over the life cycle. CE trade-offs are applied in the SoI and SS design, affecting SoI Reliability (R) and SS elements. Since both system designs affect Maintainability (M), CE analysis shall be conducted in the integration domain, and therefore, applied directly to Maintainability (M) to provide optimal decision-making regarding maintenance actions.

VI. Both SoI and SS Availability (A) will enable or constrain maintenance actions on the Maintainability (M) design.

VII. Maintainability (M) is then measured with the information from the SoI time-based risk levels and safety thresholds, with the definition of maintenance concept and plan, by having access to the SS elements while targeting CE, and by assessing SoI and SS availabilities.

VIII. As a Maintainability (M) design result, maintenance action is performed, affecting Availability (A) of both the SoI and the SS, and SoI Reliability (R), upkeeping it under Safety (S) levels.

Considering AIM through the RAMS approach, it becomes possible to analyze, design, and manage logistics and supportability. From this supportability perspective, Maintainability (M) should be seen not only as an inherent characteristic of the System of Interest (SoI), as proposed by Blanchard (1998), but rather as an emergent property resulting from the integration of the SoI, SS, and the Technical Management organization. Similarly, Reliability (R) and Safety (S) are emergent properties influenced by the SoI and its operational scenario, environmental conditions, time, and the Technical Management organization. Finally, Availability (A) is also an emergent property of the SoI and SS, as it depends on maintenance frequency and duration, which are outputs of the emergent Maintainability (M) design.

In the maritime industry, RAMS-based AIM offers a strategic systems-level approach to address the growing challenges of aging fleets in complex operational environments within resource constraints. As such, ship structural integrity, typically regarded as a SoI characteristic, is increasingly perceived as an emergent property from the integration between the ship's physical design (SoI), its operational and environmental conditions over time, maintenance philosophy and planning, and shipyard infrastructure, quality, and personnel (SS); all under cost-effective decision making. This shift in the industry is evident with investments in Digital Twins (DT) and Structural Health Monitoring (SHM) systems, which provide enhanced and timely evaluation of RAMS under system use. In this context, Ship Structural Integrity Management (SIM) can be defined as a subsystem framework of AIM dedicated to the ship structural subsystem.

Consistently, this thesis delves into overlooked opportunities in naval ship SIM, enhancing the understanding of the holistic perspective of ship RAMS and building a quantitative framework for technological development and decision-making. Nevertheless, the framework proposed in this thesis is flexible enough to fit other subsystems and systems, providing opportunities and insights for other industries.

1.1 Problem Overview

Among the subsystems of a ship, the structural subsystem is one of the most complex for predicting failures, due to its inherent complexity, originating from the unique design of each vessel and the different types of degradation caused by diverse operational uses and environmental conditions. This challenge is amplified by the sheer size of the ship structure and the limited access for proper inspection due to confined spaces and sediment accumulation, as illustrated by Figure

4. Therefore, collecting and managing consistent data over the typical lifespan of a vessel (25-40 years) is a considerable task.



(a)



(b)

Figure 4. (a) Tanker side-by-side with the Eiffel Tower. DNV courtesy to EMSA. (EMSA 2005). (b) The author is entering a ship's bottom tank to survey (confined space).

Structural deterioration over time can be observed in the following ways (Wang et al. 2009): coating damage, corrosion, cracking, deformation, and changes in material properties. Among all structural failure modes, general corrosion is considered in this work.

During the 80s and the 90s, many casualties in aging vessels were reported (Paik et al. 2003). Statistical analysis of ship hull structures revealed that 77-79% of structural failures of all ships and 86-92% of those in aged ships were attributed to corrosion (Emi et al. 1991), which motivated the development of a diverse number of studies on practical ship general corrosion wastage models, which are explored in Chapter 2.

Furthermore, the necessity for sustained vessel operations in a resource-constrained context, where CE is crucial, conflicts with the inherent deterioration of ship structures over time, which increases risks to the ship’s safety, cargo, and crew. This dilemma emphasizes the need for an optimized management approach, focusing on activities essential for preserving naval structural integrity, as maintaining adequate structural reliability is pivotal to ensuring the vessel's optimal performance throughout its life cycle. This approach is the core of RAMS-based SIM, presented in the opening section of this Chapter.

Accordingly, in the past decades, the maintenance field has evolved into a strategic asset with substantial industry investment, integrating Industry 4.0 technologies for preventive maintenance through monitoring techniques like condition-based, predictive, and prescriptive methods (Pinciroli, Baraldi, and Zio 2023). Despite advancements in modern maintenance techniques, there exists an untapped opportunity in the ship industry: a repair grouping strategy for the exploitation of expensive system downtime, such as drydocking. This specific type of preventive maintenance strategy, termed Opportunistic Maintenance, can play a crucial role in minimizing costs and the risk of unexpected downtime.

The Opportunistic Maintenance Strategy idea is simple: to perform maintenance in a group of elements or subsystems at the same downtime (Pinciroli, Baraldi, and Zio 2023). Hence, some components are maintained before their individual failure predictions or schedules. However, it is not straightforward to define which components are going to be grouped in this strategy, and when to schedule maintenance considering the opportunistic approach, since there is a mutual effect between grouping decisions and schedules.

Furthermore, the challenges of SIM do not rely solely on technical issues. It is difficult to implement maintenance optimization in real-world scenarios. This problem is due to the complexity that some frameworks present, which are often a “black box” from the perspective of managers and other stakeholders (Pinciroli, Baraldi, and Zio 2023). This aspect can imply a lack of trust in optimal “solvers.” Hence, maintenance optimization frameworks must consider as a value, logical and straightforward processes that can be understood by all decision-makers.

In summary, SIM faces many challenges related to the SoI and its boundaries, including the uniqueness of structural design, variations in operations and environments, and multiple failure modes, as well as challenges related to SS and Technical Management. Indeed, despite recent technological developments, these issues were evidenced by the author as a modern SIM problem at the Ship Repair USA 2023 conference, when shipyard managers disclosed that “nobody knows the true condition of the ship when she arrives at the drydock”. Accordingly, the U.S. Government Accountability Office report (GAO 2020) reveals that “substantial maintenance delays persist at the U.S. Navy's shipyards with 75% of planned maintenance periods completed late for aircraft carriers and submarines in FY 2015-2019, with an average delay of 113 days for carriers and 225 days for submarines”. The report identified two main causes for the delays: Unplanned work and issues with shipyard workforce performance and capacity. As a result, the report concludes that

the Navy "relies on excessive use of overtime". More recently, the GAO reported (GAO 2025) that the "U.S. Navy still faces persistent challenges sustaining combat surface ships, …, lack of sufficient and qualified maintenance personnel, and a continual need to defer maintenance".

To address these problems, the proposed SIM framework in this thesis focuses on supporting the following stakeholders' needs:

I. What, when, and where to survey and repair?
II. What are the costs and risks involved?
III. The process of answering these questions must be logical and straightforward.

1.2 Literature Survey

A maintenance strategy comprises a set of guidelines that dictate how various maintenance tasks are executed on a given asset. As described by (Blanchard 1998), maintenance strategies can be either corrective or preventive, whose subtypes were classified by (Pinciroli, Baraldi, and Zio 2023) in a comprehensive and updated literature survey:

I. Corrective maintenance
II. Preventive maintenance: Scheduled, Opportunistic, Condition-based, Predictive, and Prescriptive.

There is no correct method for determining the optimal maintenance strategy tailored to a particular system (Pinciroli, Baraldi, and Zio 2023). Each maintenance approach possesses distinct attributes; hence, the Technical Management needs to consider multiple factors related to the organization, system type, and its risk levels, spare parts availability, and costs. Additionally, a combination of strategies can be adopted. However, each maintenance strategy requires different amounts of data, technology, and consequently, cost.

The optimization of opportunistic maintenance is not well explored when compared with other strategies, as shown in Figure 5 (Pinciroli, Baraldi, and Zio 2023). In addition, it is not formalized for naval maintenance applications, although it is suitable for exploiting costly downtime in a drydock.

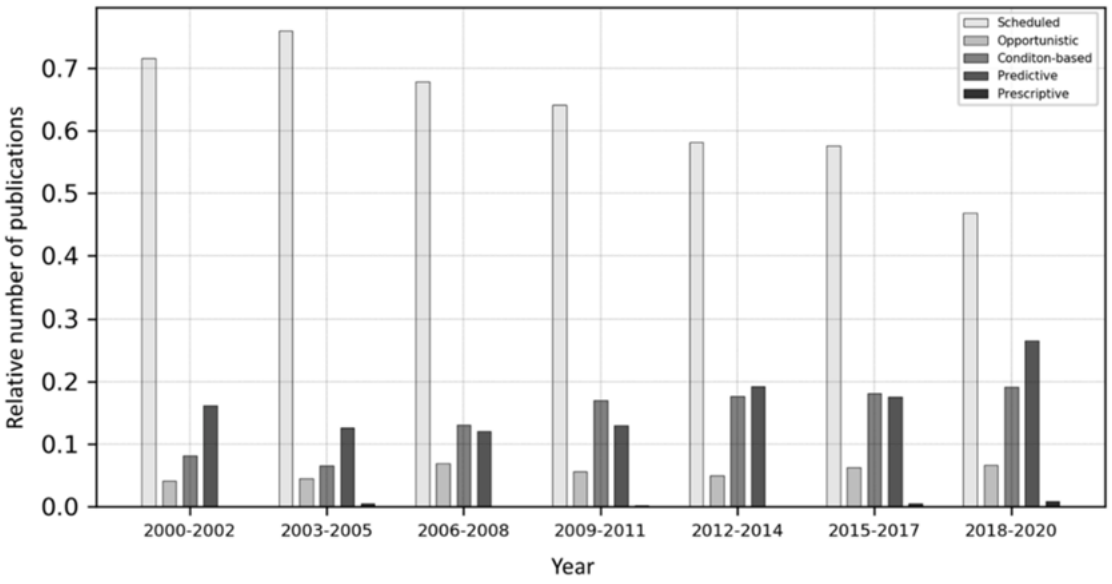


Figure 5. Relative number of publications related to the optimization of different maintenance strategies from 2000 to 2020 [www.scopus.com](Pinciroli, Baraldi, and Zio 2023).

Research in the Scopus® database was conducted (Scopus® 2023) containing in the title, abstract, and keywords, the terms “maintenance” and “risk” and “optimization” or “optimisation”, where close to 3,000 publications were found. When the word “opportunistic” was added, only 38 publications remained. Furthermore, adding the word “ship” or “naval” or “vessel”, only one publication was left; however, it deals with the word opportunistic not in a technical way.

Considering the 38 publications, a bibliometric network was constructed based on keyword co-occurrence using the VOSviewer software, developed by the Centre for Science and Technology Studies of Leiden University (Van Eck and Waltman 2010), and can be visualized in Figure 6. The color of an item is determined by keyword clusters, and the size of the label and the circle is determined by the co-occurrence of the item. The higher the co-occurrence of a keyword, the larger the label and the circle of the item.

As can be seen in Figure 6, there is a relatively low co-occurrence relation between “opportunistic maintenance” and “maintenance optimization” or “optimisations”, and “failure risk”. Also, no application was verified in the ship industry.

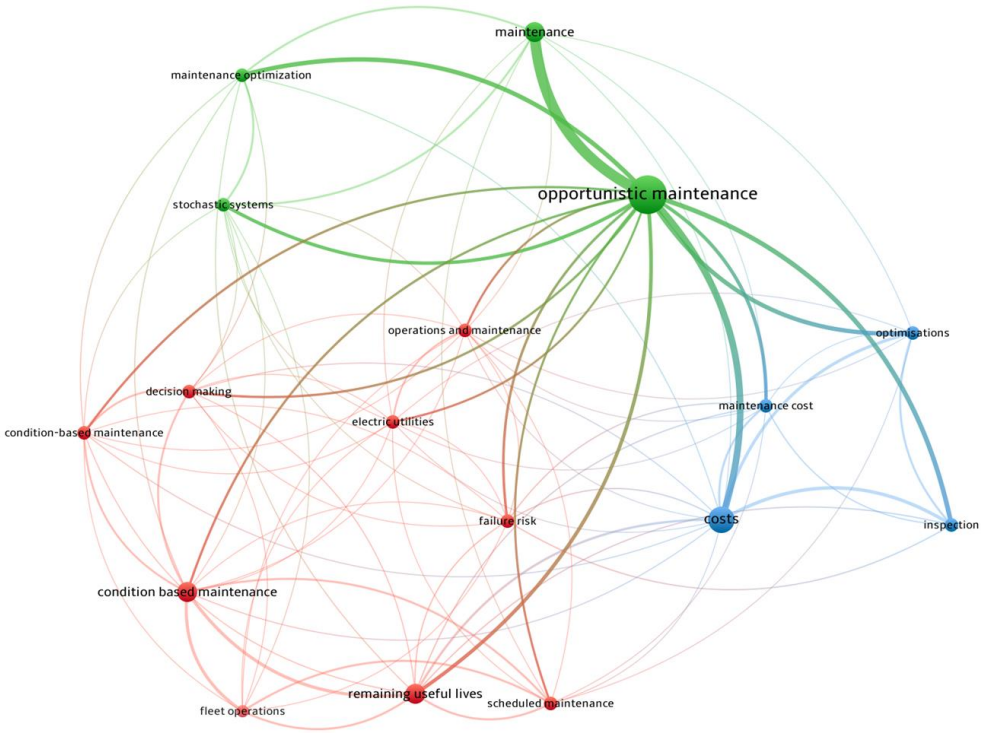


Figure 6. Keyword co-occurrence network using the VOSviewer.

The literature survey indicates that there is scarce research and application on Opportunistic Maintenance optimization, and no precedent work in the ship industry. Therefore, this research will explore this overlooked field to develop a novel Opportunistic Maintenance Strategy framework to address optimized RAMS-based SIM from a supportability perspective.

During the development of this research, a simplified version of it was published by the author (Casares and Vlahopoulos 2024), which pioneered its application in the naval engineering field. In this respect, the referred work was awarded the 2025 Elmer L. Hann Award for best paper in Ship Production at the 2024 SNAME Maritime Convention. Nevertheless, this work is herein enhanced by novel analysis, integration, and impacts of the SS and new economic factors on the system use process, specifically for naval vessels.

1.3 Research Structure

The main goal of this research is to deliver a novel quantitative RAMS-based framework for SIM, named Opportunistic Maintenance Cost and Risk Optimization (OMCRO), considering

the general corrosion failure mode. Hence, this study aims to forecast the likelihood and potential consequences of corrosion-related failures, and the associated risks and costs. These results are evaluated under an Opportunistic Maintenance Strategy while optimizing maintenance scheduling activities to support decision-making. The framework needs to be logical and straightforward to have wide application by the following key stakeholders: academia, engineers, surveyors, shipyards, Classification Societies (CS), and asset managers. Therefore, the deliverable of this framework relies on its key high-level requirements as follows:

I. The parameters input shall be developed in digital spreadsheets.
II. The inputs shall include SoI structural, operational, environmental, cost, and safety-related parameters and SS parameters.
III. The output shall include the probability of structural failure, consequences of failure, risks, costs, intervention duration, and optimal maintenance schedule.
IV. The output shall clearly indicate what, when, and where the structural element is going to be maintained, and what the costs and risks are involved.
V. The probability of failure output shall be validated by simulation.
VI. The intervention time shall be validated by simulation.
VII. The optimal solution output shall be validated by simulation.
VIII. The outputs shall be formatted to be capable of external software importation.
IX. The framework shall perform analysis of different elements as a deliverable demonstration.
X. The verification of the framework shall be carried out in digital spreadsheets.
XI. The output shall be compared with existing structural management practices.
XII. The quantitative output shall be able to communicate qualitative conclusions.

The SIM framework supports Maintainability (M) decision-making regarding structural maintenance scheduling activities, considering economic, reliability, and safety criteria, which depend on failure predictions estimated by time-dependent corrosion wastage models. The incorporated values and their quantifiable measurements are the reduction of repair costs while maintaining reliability; the reduction of unexpected repairs over the ship's life cycle; the improvement of repair budgeting estimation; and the improvement of resource allocation.

1.4 Dissertation Outline

According to the deliverables and requirements of this research, which were described in the Section 1.3, this dissertation is outlined in a structure of chapters and sections, which are related to building knowledge in a logical sequence to develop the OMCRO framework based on the RAMS approach. This Chapter presents the research introduction, while Chapters 5 and 6 present thesis contributions and future work, respectively. The technical sections are outlined with their corresponding chapters in Table 3 and their structured and logical sequence is illustrated by Figure 7. Also, their corresponding non-technical sections include introduction, literature research, and conclusions for all the referred chapters.

Table 3. Technical Outline.

CHAPTER 2	STRUCTURAL DEGRADATION	2.3 Corrosion Model
		2.4 Probabilistic Approach
		2.5 Simulation, Results, and Validation
		2.6 Failure Thresholds
CHAPTER 3	COST AND TIME	3.3 Structural Cost
		3.4 Expected Cost of Failure
		3.5 Expected Cost of Opportunity of Non-Planned Unavailability of Naval Vessels
CHAPTER 4	OPPORTUNISTIC MAINTENANCE COST AND RISK OPTIMIZATION (OMCRO)	4.3 Maintenance Cost and Risk Optimization (MCRO)
		4.4 Opportunistic Maintenance Cost and Risk Optimization (OMCRO)
		4.5 The OMCRO Framework
		4.6 Verification and Validation (V&V)
		4.7 Quantitative Maintainability and Availability Analysis
		4.8 Scalability
		4.9 OMCRO Framework Validation

According to Table 3, the outline can be described as follows:

- **Chapter 2** enhances and validates a time-based probabilistic corrosion model applicable to any ship space, with safety levels defined as probability threshold values. Based on this model, renewal times for individual structural components are estimated.
- **Chapter 3** develops and validates cost and time models for structural interventions, along with risk models that rely on the failure probabilities established in Chapter 2.
- **Chapter 4** develops, verifies, and validates the OMCRO framework, which is built upon the models presented in the previous chapters. The framework serves as a platform for quantitative Maintainability (M) and Availability (A) analysis and is demonstrated under scalability conditions.

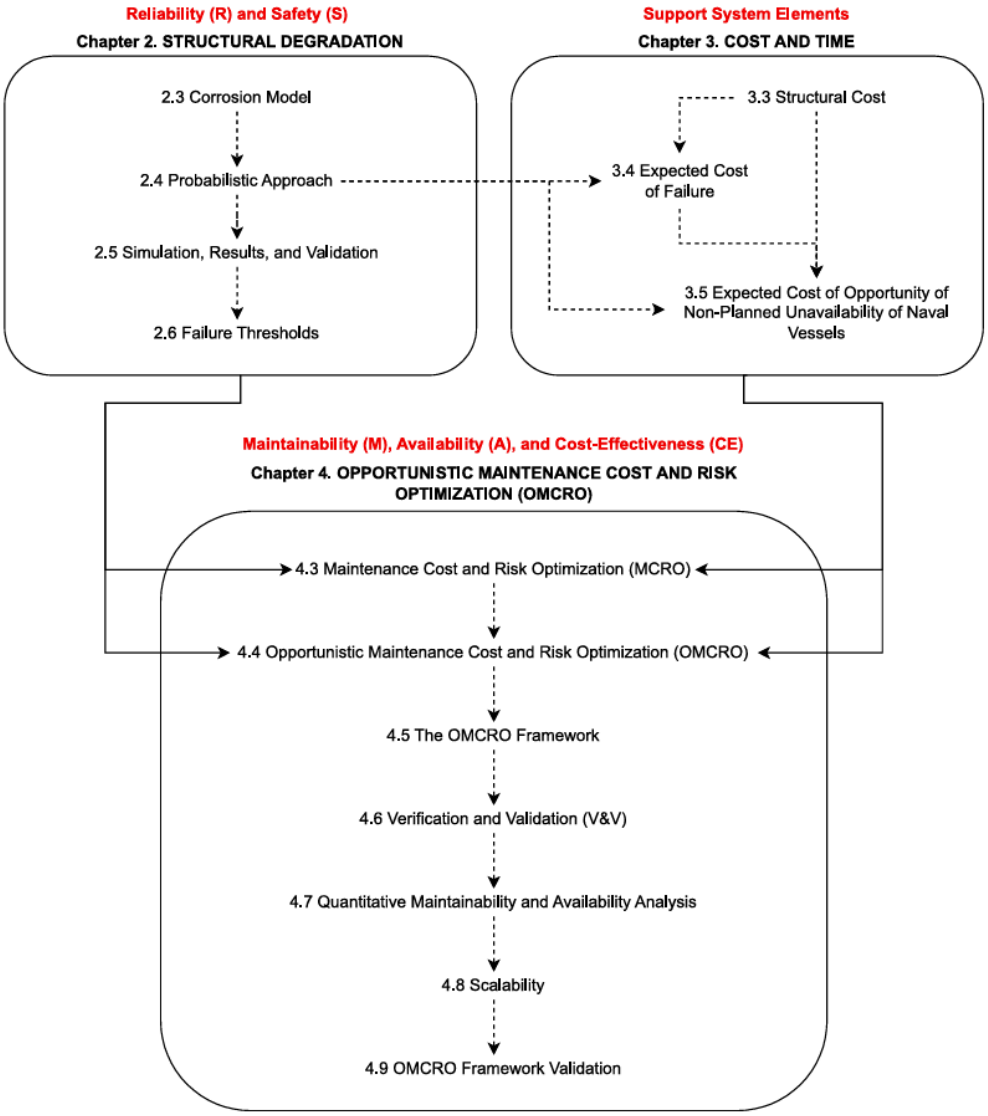


Figure 7. Technical outline structure.

Chapter 2 Structural Degradation

"Rust never sleeps."

- Neil Young (Young 1987)

This Chapter provides a detailed description of the processes carried out to estimate the structural elements' individual repair based on a probabilistic degradation model and safety levels, respectively related to the SoI Reliability (R) and Safety (S) of the RAMS approach.

As mentioned in Section 1.1, although structural degradation can be described in different ways, corrosion is considered in this work for sea-going vessels, since it has been evidenced to be a major issue, as 77-79% of structural failures of all ships and 86-92% of those in aged ships were attributed to corrosion (Emi et al. 1991). Moreover, from a global industrial perspective, the economic impact of corrosion has been estimated at approximately 2.5 trillion USD, representing about 3.4% of the worldwide Gross Domestic Product (GDP) as of 2013 (Koch 2017).

2.1 Introduction

As introduced by Section 1.1, during the 80s and 90s, many casualties, mostly related to corrosion degradation in aging vessels, motivated the development of many studies on practical ship general corrosion wastage models. Although many models can be found in the literature, they are mostly derived from the prominent ones developed during this effort to reduce structural failures (Yamamoto and Ikegami 1996; Paik, Kim, and Lee 1998; Paik et al. 2003; Guedes Soares and Garbatov 1999; Garbatov, Guedes Soares, and Wang 2007; Garbatov and Soares 2008; Melchers 1997; Melchers 2003a; Gardiner and Melchers 2001; Qin and Cui 2003).

All models provide a combination of physical and empirical approaches at different levels. However, the existing corrosion literature lacks sufficient homogeneous data (Melchers 2019), and variability is a considerable factor (Garbatov, Guedes Soares, and Wang 2007), which can be mainly attributed to data collected during diverse environmental and operational conditions of

different ships. Also, thickness measurements are usually related to plates that interface different compartments and are, therefore, subjected to distinct environmental effects. Another challenge is that compartments of the same type and even structural elements inside the same compartment may experience different corrosion rates (Paik, Kim, and Lee 1998).

To address these limitations, past research was conducted considering the non-linear (Guedes Soares and Garbatov 1999) model to account for operation, environment, double-side effects, and uncertainty (Garbatov, Guedes Soares, and Wang 2007; Garbatov and Soares 2008; Guedes Soares et al. 2005; Zayed, Garbatov, and Guedes Soares 2007; Guedes Soares et al. 2008; 2009; Guedes Soares, Garbatov, and Zayed 2011; Zayed, Garbatov, and Guedes Soares 2018). Considering this model, corrosion allowances of ship structures were also investigated based on probabilistic and risk-based assessments (Garbatov 2020), and an enhanced probabilistic framework was developed for corrosion prediction using Bayesian inference (Woloszyk and Garbatov 2024).

This Chapter outlines and explores the previous corrosion models and details the approach based on the non-linear model (Guedes Soares and Garbatov 1999). As an enhancement to previous works, the probabilistic assessment is derived for single-sided models, making it possible to perform estimations on probabilistic corrosion degradation in any desired ship space. Corrosion allowances are not investigated; rather, industry standards of accepted levels of corrosion wastage are used to establish time-based probabilities of failure of ship structures, in which failure is defined as the need for repair. Moreover, the probability of failure threshold is considered dependent on the failure consequence severity and ship type (commercial or naval), which gives an estimation of the time to repair individual components.

2.2 Literature Survey

To forecast corrosion degradation, a comprehensive comparative analysis of prominent models is undertaken to identify the most appropriate approach and model for this purpose.

Two approaches are commonly used in conjunction within the field of corrosion modeling. These approaches can be classified into physical and empirical modeling (Kim, Wong, and Cho 2020):

I. **Physical or phenomenological modeling** involves the development of a model that considers the physical and chemical phenomena and mechanisms underlying corrosion progression. Factors such as the material properties, environmental conditions, and electrochemical processes are considered. The aim is to simulate the corrosion behavior and predict how corrosion progresses over time based on a fundamental understanding of the physical principles involved.

II. **Empirical modeling**, on the other hand, relies on a database of corrosion measurements that have been collected and classified over time. Statistical analyses are then employed to identify patterns and relationships within the data, enabling the model to make predictions regarding future corrosion behavior. Unlike physical modeling, empirical modeling does not require a deep understanding of the underlying physical mechanisms but focuses on observed correlations and trends in the data.

Researchers often combine these two approaches to leverage their respective strengths. By incorporating physical principles into empirical models or by validating and improving physical models using empirical data, more accurate and robust corrosion models can be developed. This combination facilitates a better understanding of the corrosion process and enhances the reliability of predicting corrosion behavior in real-world scenarios.

Concerning (McIntyre 2017) classification, the following types of corrosion can be observed: uniform, localized, galvanic, velocity effects, intergranular, dealloying, cracking phenomena, high-temperature, and microbial effects. In this work, corrosion modeling considers only uniform (general) corrosion, which is characterized by the absence of a significant localized attack and instead progresses uniformly, leading to a gradual and consistent reduction in thickness (McIntyre 2017).

Accordingly, the prominent practical ship models in the literature are outlined as follows (Melchers 2014) and are also referred to as time-dependent corrosion wastage models (TDCWM) (Kim, Wong, and Cho 2020):

I. **Yamamoto-Ikegami model** (Yamamoto and Ikegami 1996): Assumes that general corrosion in steel plates arises from a sequence of three successive mechanisms: deterioration of protective paint coatings, formation of localized pitting points, and subsequent progress of these pitting points. Each process considers probabilistic models to quantitatively predict the corrosion process. The statistical parameters were estimated from a classified dataset and applied to these probabilistic models. The dataset consists of 7,581 thickness measurement points in 27 bulk carriers, classified by location inside ballast and cargo holds.

II. **Paik model** (Paik, Kim, and Lee 1998; Paik et al. 2003) and Figure 8: Assumes that the general corrosion wastage process of steel plates is divided into three phases: life (durability) of the coating, transition to corrosion, and corrosion progress. The first phase is a non-corrosion state, which is assumed to follow a log-normal distribution. The second phase is the time between the coating becoming ineffective and the start of corrosion, which is assumed to be exponentially distributed. The third phase models the corrosion wastage over time that can assume concave, convex, or linear shapes, which depend on the coefficient fitting on empirical data. The database consists of 12,446 thickness measurement points of 109 bulk carriers (Paik et al. 2003), classified into 23 different primary member locations, and 1,937 thickness measurement points in ballast tanks (Paik et al. 2004), classified by location.

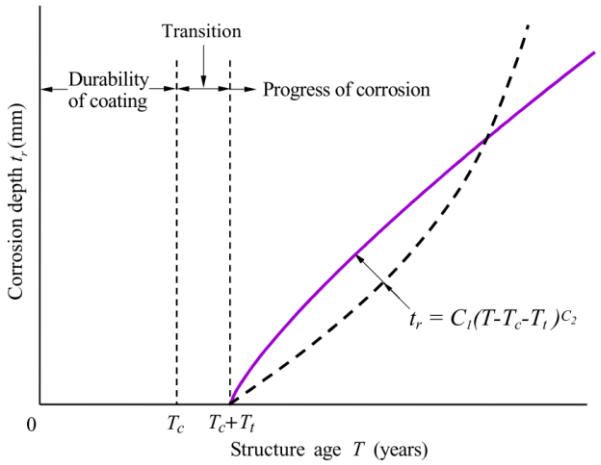


Figure 8. Paik model (Paik et al. 2003). Corrosion depth t_r as a function of structural age T, coating life T_C, transition time T_t and coefficients C_1 and C_2.

III. **Soares-Garbatov model** (Guedes Soares and Garbatov 1999) and Figure 9: Assumes that the general corrosion wastage process of steel plates is divided into three phases: coating, transition, and long-term. In the coating phase, no corrosion is assumed until it reaches the transition phase, when nonlinear corrosion wastage growth takes place, asymptotically reaching a long-term steady-state wastage. This model is described as a solution to a first-order nonhomogeneous linear differential equation. The solution parameters are then calibrated based on an empirical database and account for uncertainty estimation (Garbatov, Guedes Soares, and Wang 2007; Garbatov and Soares 2008). The database includes 1,168 thickness measurement points of deck plates from ballast tanks and 4,665 thickness measurements points of deck plates from cargo tanks. With further research, the model can capture the effect of multiple environmental and operational conditions (Guedes Soares et al. 2005; Zayed, Garbatov, and Guedes Soares 2007; Guedes Soares et al. 2008; 2009; Guedes Soares, Garbatov, and Zayed 2011). In addition, this model can predict corrosion in different ship environments by deriving degradation from both sides of the ship plates (Zayed, Garbatov, and Guedes Soares 2018).

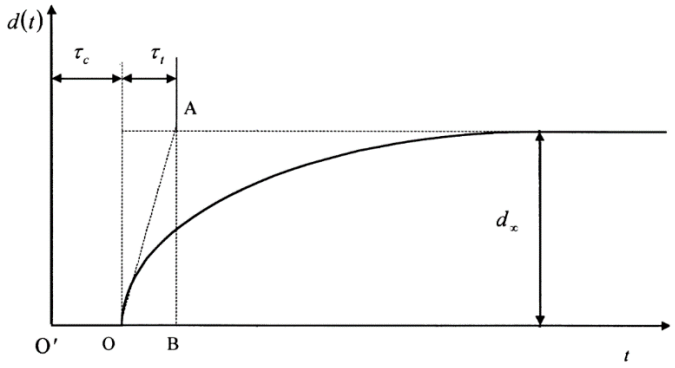


Figure 9. Soares-Garbatov model (Guedes Soares and Garbatov 1999). Thickness wastage $d(t)$ as a function of structural age t, coating life τ_c, transition time τ_t, and long-term corrosion wastage thickness d_∞.

IV. **Melchers marine immersion model** (Melchers 1997; Melchers 2003a; 2003b) and Figure 10: Assumes that the general corrosion wastage process for steel plates subjected to marine immersion is divided into five phases, named 0-4, and does not consider the coating effect. Phase 0 is related to the first exposure and initial chemical reactions; phase 1 is controlled

by oxygen diffusion and the wastage is represented by a linear function (oxygen concentration control); phase 2 is controlled by the limitation of oxygen diffusion due to the build-up of corrosion products (rust layer) on the surface, decreasing the corrosion rate; phase 3 assumes anaerobic conditions and flourishing of sulphate-reducing bacteria (SRB), depending on the nutrients supply; and phase 4 is characterized by a near-steady state corrosion rate that depends on the nutrient supply and loss of rust scales. Each phase is modeled using parameters calibrated from field data and environmental considerations. In addition, the Melchers model accounts for uncertainty and probabilistic estimation (Melchers 2003b).

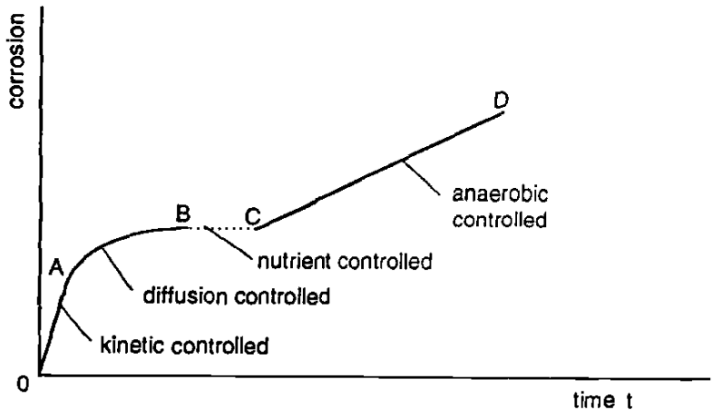


Figure 10. Melchers marine immersion model (Melchers 1997). Thickness wastage as a function of time in Phase 0 and 1 (kinetic controlled); Phase 2 (diffusion controlled); Phase 3 (nutrient controlled); Phase 4 (anaerobic controlled).

Gardiner-Melchers enclosed atmospheric model (Gardiner and Melchers 2001): Assumes that the general corrosion wastage of steel plates is modeled as a linear function of three environmental parameters: time of wetness, salt deposition, and temperature. Atmospheric corrosion phenomena and empirical observations indicate that the corrosion rate varies linearly with temperature and salt deposition. No coating effect or reduction in the corrosion rate due to the corrosion product layer is considered in this model.

V. **Qin-Cui model** (Qin and Cui 2003) and Figure 11: Assumes that corrosion protective systems (CPS) (e.g., coating) gradually degrade as corrosion starts with pitting, before the

CPS loses its complete effectiveness. Three stages are considered: no corrosion, corrosion accelerating, and corrosion decelerating. No corrosion is considered when the CPS is completely effective. Then, in the transition stage, the corrosion rate can be established by equating the volume of pitting corrosion to uniform corrosion (corrosion accelerating). When the CPS loses its complete effectiveness, general corrosion takes place, and the corrosion rate decreases owing to the presence of the corrosion product layer. The Qin-Cui model is flexible since its parameters can be calibrated to represent Paik, Soares-Garbatov, and Melchers' models, and can consider uncertainties. The calibration required a dataset, simulated by Qin-Cui, because the data were not available.

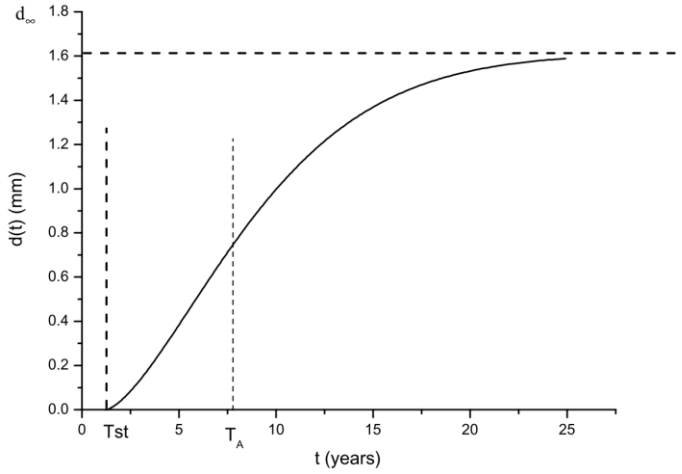


Figure 11. Qin-Cui model (Qin and Cui 2003). Thickness wastage as a function of time t, the instant T_{st} at which the pitting corrosion starts, and the time T_A when the general corrosion decelerates.

2.2.1 Corrosion Model Considerations

All the models provide a combination of physical and empirical approaches at different levels. This combination is particularly important for accounting for the common scatter dataset with which these models work. The following reasons are highlighted for the high variability in the collected data for long-term corrosion wastage analysis:

I. Usually, the only data available are the type of inspected ship, thickness measurement, site of measurement, and time of inspection. Structural renewal between inspections is not usually included in the database, and this would be related to differences in thickness

measurements over the years. In addition, environmental and operational data, which are correlated to differences in corrosion wastage, are not considered in the database.

II. It is challenging to collect and track data from the same site over the years. Usually, for a particular ship compartment type, representative corrosion wastage data of the same compartment type are used (Paik et al. 2004). This causes variability in the data collected, as compartments of the same type can have different environmental and operational characteristics. Additionally, in the same compartment, structural elements are subjected to different environmental influences, and the orientation of structural elements affects corrosion progression (Paik, Kim, and Lee 1998).

III. Thickness measurements are usually related to a single compartment or element structure. However, plates may be the interface between different compartments and are therefore subjected to different environments. This factor causes variability in the data, even when considering the same compartment.

Therefore, the corrosion literature exhibits limited homogeneous data (Melchers 2019), with variability as a defining characteristic (Garbatov, Guedes Soares, and Wang 2007). Hence, efforts to include physical or phenomenological approaches are necessary to consider environmental and operational influences in the models. However, when the environmental effects of natural seawater are reproduced artificially in the laboratory, the results are misleading, considering the complex mix of chemical and biological elements (Melchers 2014). This conclusion reinforces the need for a field dataset consideration over the long term.

Nevertheless, it is difficult to capture long-term corrosion behavior with proper validation, particularly regarding environmental and operational considerations. Accordingly, a field experiment in naval vessels was conducted by (Gudze and Melchers 2008) to validate the mixed influence of the marine immersion model and atmospheric model in seawater ballast tanks, using steel coupons and environmental sensors inside the tanks. The field results were in reasonable agreement with the mean estimated by the models; however, the variability increased significantly over the experiment time. Considering that the experiment lasted for 541 days, one can conclude

that, over a long-term period within different environments and operations, the result may not be broadly applicable.

To address these limitations, Soares (Guedes Soares et al. 2005) considered correction factors to be applied in a nominal model. These factors account for environmental differences from those considered representative of the dataset in which the nominal model was calibrated. Then, these factors are applied for each short-term operation, and the long-term wastage is estimated based on a weighted average of short-term analyses. Conversely, Melchers indicates that the asymptotic decrease in long-term corrosion wastage present in the Soares-Garbatov and Qin-Cui models is not representative of experience with real structures. Indeed, these models do not account for anaerobic conditions and sulfate-reducing bacteria (SRB); however, these effects are localized (McIntyre 2017) and are not considered herein for uniform corrosion prediction.

2.2.2 Corrosion Model Requirements and Selection

As discussed previously, corrosion models have different approaches and limitations. Therefore, it is necessary to establish a series of key requirements that must be fulfilled to achieve the main objectives of this work:

I. Physical and empirical models shall be considered.
II. Uncertainty shall be considered.
III. Long-term estimates shall be considered.
IV. Particular environmental and operational effects shall be considered.
V. The model shall be able to be applied in all compartments of the ship.
VI. The presence of coating shall be considered.
VII. The model shall be built with consideration of both sides' corrosion effects on the structure.

Accordingly, Table 4 indicates the requirements satisfaction concerning the prominent ship corrosion models.

Table 4. Prominent Ship Corrosion Models.

Ship Corrosion Models					
Requirements	**Yamamoto Ikegami**	**Paik**	**Soares Garbatov**	**Melchers**	**Qin Cui**
Physical	X	X	X	X	X
Empirical	X	X	X	X	*[6]
Uncertainty	X	X	X	X	X
Long-term	X	X	X	*[3]	X
Environmental			X	X	
Operational			X	X	
Multi-location	*[1]	*[2]	X	*[4]	
Coating	X	X	X	*[5]	X
Double side			X		

Comments:

1 *Only ballast and cargo spaces in bulk carriers*

2 *Only ballast and structural elements in different locations in bulk carriers*

3 *Only for the marine immersion model*

4 *Only immersion, atmospheric, and their combination (ballast tanks)*

5 *Does not consider coating, but it is possible to implement it*

6 *Does not consider a dataset, but can be calibrated with one*

It can be concluded that the Soares-Garbatov model is the only one that satisfies the key requirements; therefore, it will be selected for this research.

2.3 Corrosion Model

As mentioned in Section 2.2, the Soares-Garbatov non-linear model assumes that the general corrosion wastage process of steel plates is divided into three phases: coating, transition, and long-term. In the coating phase, no corrosion is assumed until it reaches the transition phase, when nonlinear corrosion wastage growth occurs, asymptotically reaching long-term steady-state wastage. Each phase has a respective governing parameter, τ_c (coating life), τ_t (transition time), and d_∞ (long-term corrosion wastage thickness). The model outputs a mean time-based corrosion wastage thickness $d(t)$, described by Figure 9 and Equation 1.

$$d(t) = \begin{cases} d_\infty \left(1 - e^{-\frac{t-\tau_c}{\tau_t}}\right), & t > \tau_c \\ 0, & t \leq \tau_c \end{cases} \quad (1)$$

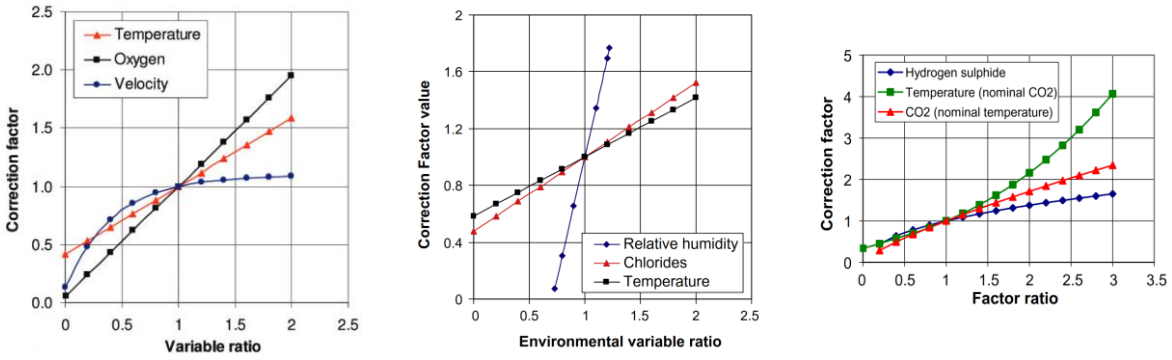
The corrosion rate of change $\frac{d}{dt}[d(t)]$ will eventually approach zero as $d(t)$ approaches d_∞. The rationale behind this assumption is that the presence of the corroded material on the surface of the plate acts as a protective barrier, preventing direct exposure to the corrosive environment and effectively halting the corrosion process. Therefore, any removal of the top corrosion layer from the surface restarts the corrosion rate and growth (Guedes Soares and Garbatov 1999; Jeom K. Paik et al. 2003), which is likely in loaded structures, as dynamic flexing results in the continuous exposure of fresh surfaces to corrosive effects.

The three parameters are then calibrated on empirical datasets (Garbatov, Guedes Soares, and Wang 2007; Garbatov and Soares 2008; Guedes Soares, Garbatov, and Zayed 2011; Zayed, Garbatov, and Guedes Soares 2018). Despite using data for model fitting, high variability is a main feature owing to heterogeneous data, which is a mix of multiple types of ships, different operations, routes, and diverse environments. This issue was highlighted by Melchers (Melchers 2019; Melchers 2014). Indeed, concerning long-term corrosion prediction, the problem becomes much more complex when considering multiple operations and environments over time. Therefore, the calibrated model is considered for specific ship spaces and for short-term operations where environmental conditions are assumed to be constant.

These conditions are related to environmental correction factors for the following environments: seawater immersion, marine atmosphere, and oil atmosphere, respectively, developed by (Guedes Soares, Garbatov, and Zayed 2011), (Guedes Soares et al. 2009), and (Guedes Soares et al. 2008). These correction factors were phenomenologically modeled by analytical formulations as a function of the ratio between the real environmental factors and the nominal ones, related to the dataset fit, as presented in Table 5. These functions were plotted by the same authors and are herein reproduced in Figure 12.

Table 5. Environmental Nominal Factors.

Environmental parameter	Value	Units
Seawater Immersion nominal factors		
Temperature (T_n)	15.5	℃
Dissolved oxygen (O_{2_n})	5.8842	mL/L
Flow velocity (V_n)	10	$knot$
Marine Atmosphere nominal factors		
Chlorides (Cl_n)	180.7	$mg/m^2/day$
Temperature (T_n)	16.2	℃
Relative humidity (Rh_n)	81.9	%
Oil Atmosphere nominal factors		
Temperature (T_n)	28.8	℃
Hydrogen sulfide (H_2S_n)	1197	$ppm\ [vol.]$
Carbon dioxide (CO_{2_n})	6.8	% $[vol.]$



(a) (b) (c)

Figure 12. (a) Seawater immersion correction factor (Guedes Soares, Garbatov, and Zayed 2011). (b) Marine atmosphere correction factor (Guedes Soares et al. 2009). (c) Oil atmosphere correction factor (Guedes Soares et al. 2008).

To deal with the long-term prediction, Appendix A covers a step process to develop a long-term single-sided model for multiple ship spaces, accounting for environmental and operational factors. This process provides modifications on the calibrated (nominal) short-term corrosion wastage mean (Equation 1), termed $d_n(t)$, as to become $d_{L_i}(t)$, the long-term single-sided mean.

This single-sided model is related to just one side of the structural element, making it possible to sum the two sides and model the corrosion degradation of any structural interface with different environments (Zayed, Garbatov, and Guedes Soares 2018).

Modeling in Appendix A has been considered for spaces based on seawater immersion, marine atmosphere, and oil atmosphere environments. However, these environments may coexist in some ship compartments. This is the case for ballast, oil, and compensated tanks:

I. **Ballast tanks** can be fully or partially loaded or empty during operation. The top surface is always in atmospheric conditions, the sides account for contributions of seawater immersion and marine atmospheric environments, and the bottom is always in seawater immersion conditions.

   A. Top of Tank: Marine atmosphere model
   B. Side of Tank: Combined marine atmosphere and seawater immersion models
   C. Bottom of the Tank: Seawater immersion model

II. **Oil tanks** can be fully or partially loaded or empty during operation. All the water present inside the tank is deposited on the tank bottom or evaporated and condensed at the top of the tank. The corrosive environment at the top is generated by water condensation, which absorbs acidic gases from the tank. Tank bottom corrosion occurs because of the presence of layers of water and salt. Therefore, when the tank is loaded, the side shell corrosion can be disregarded because it can be assumed that the water does not deposit on the sides of the tank (Guedes Soares et al. 2008). Therefore, the top and bottom surfaces are always modeled in an oil atmospheric environment, and the side corrosion is only considered in empty or partially loaded conditions.

   A. Top of Tank: Oil atmosphere model
   B. Side of Tank: Combined oil atmosphere model and no corrosion
   C. Bottom of the Tank: Oil atmosphere model

III. **Compensated tanks** are always fully loaded, because oil and seawater share the same environment. During operation, while oil is consumed from the top of the tank, seawater is loaded into the tank. The side shell is then affected by a combination of oil and seawater environments. However, as previously discussed, the corrosion effect of the oil model on the side shell can be neglected.

A. Top of Tank: Oil atmosphere model
B. Side of Tank: Combined seawater immersion and no corrosion
C. Bottom of the Tank: Seawater immersion model

Accordingly, the top and bottom of the tanks need specific corrosion models. Moreover, the approach to deal with multi-environmental contributions in the side of tanks is similar to the assumption of single-sided long-term predictions based on short-term analysis, as presented in Appendix A. Accordingly, a weighted sum of discrete wastage predictions from different models is calculated, where the weight is the relative ratio of the time interval in which each model and environmental conditions remain constant for the specific ship space (Zayed, Garbatov, and Guedes Soares 2007).

2.4 Probabilistic Approach

Although efforts have been made to account for specific environments, operations, and ship spaces, many simplifying assumptions were necessary to establish a useful model. Considering that variability can still be a significant part of the field results, it is still fundamental to consider it.

So far, the model described in Appendix A is mean-modified; hence, this research assumes the premise that the modifications are a consequence of adjustments on the log-normally distributed random variable (RV) $D_n(t)$ of nominal short-term corrosion wastage for specific ship spaces, to become a RV $D_{L_i}(t)$ of long-term single-sided corrosion wastage.

A simple way to specify how $D_n(t)$ can be modified to $D_{L_i}(t)$ is by considering a Total Factor f_T (Appendix Equation A.16). Since f_T is constant for each yearly log-normal distribution, the mean and standard deviation are modified by the same factor (Equation 2-4).

$$D_{L_i}(t) = f_T D_n(t) \tag{2}$$

$$d_{L_i}(t) = f_T dn(t) \tag{3}$$

$$\sigma_{L_i}(t) = f_T \sigma_n(t) \tag{4}$$

Therefore, the modifications already addressed to the mean $d_n(t)$ shall be done to the standard deviation $\sigma_n(t)$. Hence, f_T provides a modification to the single-sided model with environmental and operational effects. The Total Factor f_T is formulated in Appendix A.

With the definition of the log-normal descriptors $d_{L_i}(t)$ and $\sigma_{L_i}(t)$, the RV $D_{L_i}(t)$ is defined. Finally, the double-sided wastage RV $D(t)$ is calculated by the sum of both RV sides $D_{L_i}(t)$ of corrosion wastage thickness (Equation 5).

$$D(t) = D_{L_1}(t) + D_{L_2}(t) \tag{5}$$

It is assumed that different environments on each side of a steel plate can be considered roughly uncorrelated. Therefore, the RVs of corrosion wastage are independent in these cases, since different environments consider distinguished corrosion mechanisms and correction factors. However, in the case where both environments are the same on each side of the steel plate, they are considered dependent with a Correlation Coefficient equal to one. In this case, the total mean and standard deviation are the same as those of the element immersed in a single environment.

The main limitation is that the sum of the two log-normal distributions is not log-normal, and there is no straightforward solution for it (Dufresne 2008). In this case, the Fenton-Wilkinson (F-W) (Fenton 1960) approximation can be done with an equivalent log-normal distribution based on the first (Equation 6) and second (Equation 7) moments. This assumption is not far from reality since the collected data is always double-sided and fits a log-normal distribution. Nevertheless, this approach was compared with a Monte Carlo simulation for validation, showing good agreement (Figure 14 - 18) with minor deviations that do not impact the usefulness of the proposed model, as discussed further.

The mean μ_D and standard deviation σ_D are calculated based on the collected data of corrosion wastage. Therefore, to express the corrosion wastage in a log-normal distribution, it is necessary to express the mean μ_{lnD} and standard deviation σ_{lnD} of the natural logarithm of the RV $D(t)$ (Melchers and Beck 2018) (Equation 8-10)

$$\mu_D = d_{L_1} + d_{L_2} \tag{6}$$

$$\sigma_D = \sqrt{\sigma_{L_1}^2 + \sigma_{L_2}^2} \tag{7}$$

$$V_D = \frac{\sigma_D}{\mu_D} \tag{8}$$

$$\mu_{lnD} = \ln\left[\frac{\mu_D}{(1+V_D^2)^{\frac{1}{2}}}\right] \tag{9}$$

$$\sigma_{lnD} = \sqrt{\ln(1+V_D^2)} \tag{10}$$

To conduct a probabilistic assessment, a specific value d_T is defined, in which the RV $D(t)$ is compared to. It is reasonable to define d_T as the total corrosion allowance of the desired structural element, because this allowance defines the need to repair it. Also, the thickness measurement of structural components is a common way of managing structural repair. Therefore, in this research, failure is defined as the need to repair when the total corrosion allowance is reached, as presented in (Equation 11).

$$p_f(t) = PoF(t) = P(D(t) \geq d_T) \tag{11}$$

A complete framework considering all steps to calculate $PoF(t)$ is illustrated by Appendix Figure A.4 in Appendix A.

2.5 Simulation, Results, and Validation

As a demonstration, the results are provided for five structural elements, localized in a generic transverse section of a naval vessel (Figure 13) with its indicated space classes (Appendix Table A.3) and subjected to a simulated environment and operation (Table 6). The space classes are based on the wastage allowance classification from (IACS 2010).

Table 6. Environmental and Operational parameters.

VESSEL OPERATIONAL PARAMETERS	OPERATION 1	OPERATION 2	OPERATION 3
MEAN SHIP RELATIVE SPEED (knots)	7	12	12
MEAN SEA WATER TEMPERATURE (°C)	20.0	21.4	28.0
MEAN DISSOLVED OXYGEN CONCENTRATION (mL/L)	4	4	5
MEAN ENVIROMENT AIRBORNE CHLORIDES ($mg/m^2/day$)	171.24	171.24	446.58
OPERATION RATIO (%)	80	17	3
RELATIVE HUMIDITY (%)	81.9	81.9	81.9
ENVIRONMENTAL TEMPERATURE (°C)	25.0	25.0	25.0
OIL TANK TEMPERATURE (°C)	27.0	27.0	27.0
H_2S CONCENTRATION IN OIL TANK (ppm)	817	817	817
CO_2 GAS IN OIL TANK (vol %)	10.9	10.9	10.9
FUEL LOADING RATIO (%)	56	70	70
BALLAST RATIO (%)	75	100	100

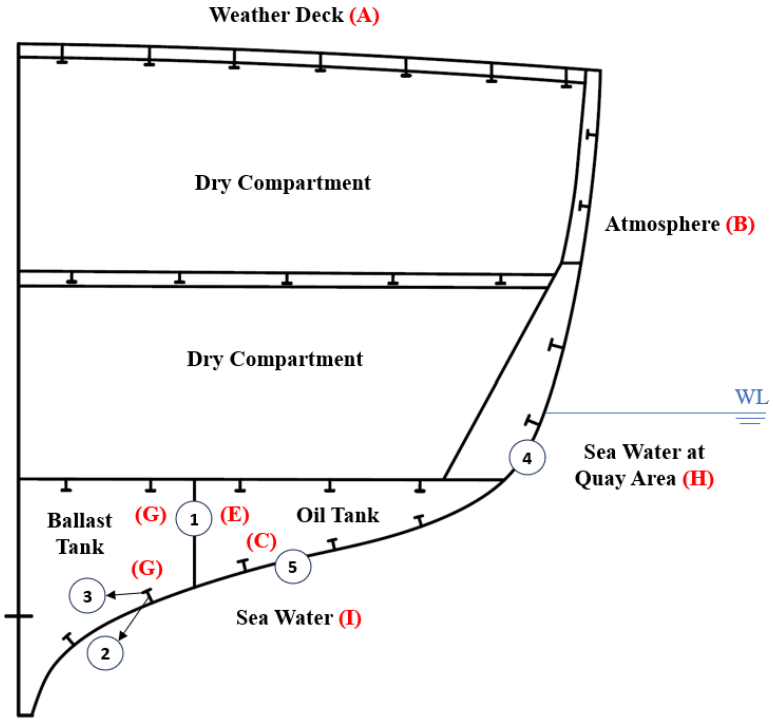


Figure 13. Generic transverse section of a naval vessel.

I. Element 1 is a 6.5 mm thick longitudinal bulkhead that segregates a ballast tank from an oil tank – Class GE.
II. Element 2 is a 5 mm thick longitudinal stiffener web at the bottom of a ballast tank – Class GG.
III. Element 3 is a 10 mm thick longitudinal stiffener flange at the bottom of a ballast tank – Class GG.
IV. Element 4 is a 7.5 mm thick hull plate that segregates the seawater at the quay area from a dry accommodation – Class H.
V. Element 5 is an 8 mm thick hull plate that segregates the seawater from the bottom of the oil tank – Class IC.

The results of the time-based probability of failure for Elements 1-5 are presented in Figure 14 to 18. The wastage to failure d_T is assumed to be 25% of the original thickness. This percentage of wastage is commonly used for structural renewal and is recommended by the United States Coast Guard (USCG) (Ayyub et al. 2002). Classification Societies may indicate different percentages for different structural elements. A validation was also conducted with an interactive Monte Carlo simulation, which was based on SIP (Stochastic Information Packet) using SIPmath™ Tool Modeler in Microsoft® Excel®. For each element side, 1,000 corrosion wastage measurements per year were pseudorandomly generated based on their respective log-normal descriptors. Hence, the sum of both sides' wastage could be calculated, and a frequentist probability of failure could be assessed per year. This simulation aimed to validate the F-W approximation approach.

The model showed consistent results with the simulation. Specifically, Figure 18 presents more deviations than the others, which is explained by the drawbacks of the F-W approximation when dealing with bigger standard deviations, which is the case for seawater models. Nevertheless, as will be covered further in this work, the acceptable levels of probability of failure are sufficiently low to present model consistency.

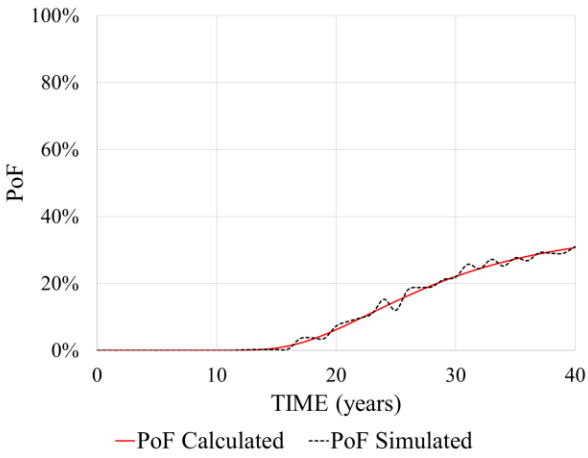


Figure 14. $PoF(t)$ for Element 1 – Class GE.

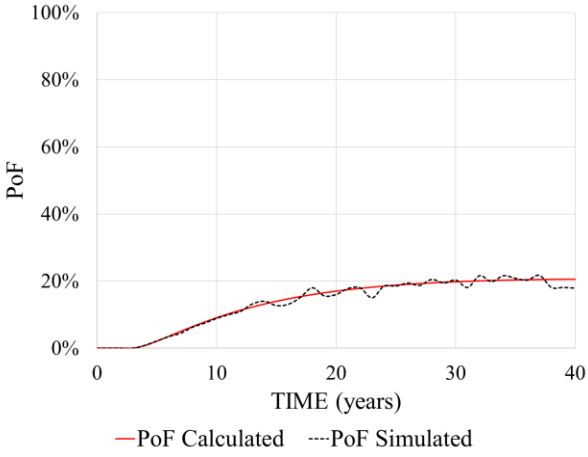


Figure 15. $PoF(t)$ for Element 2 – Class GG.

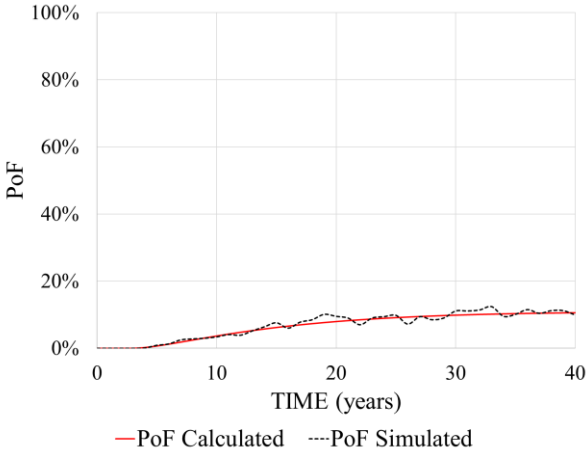


Figure 16. $PoF(t)$ for Element 3 – Class GG.

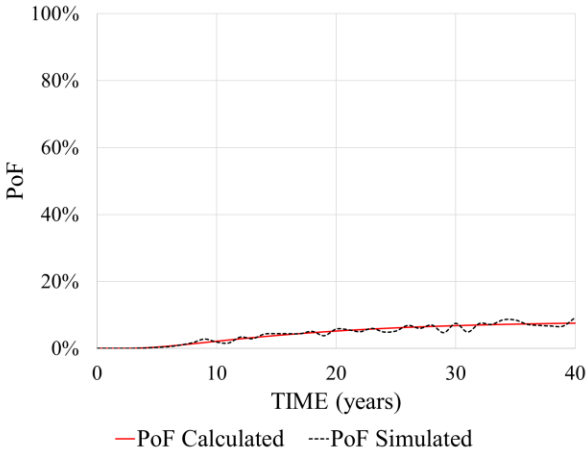


Figure 17. $PoF(t)$ for Element 4 – Class H.

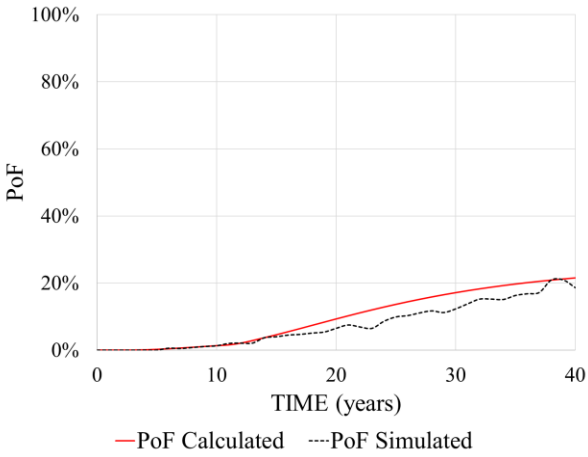


Figure 18. $PoF(t)$ for Element 5 – Class IC.

2.6 Failure Thresholds

Another important point to consider is the target level of the probability of failure, called Probability of Failure Threshold PoF_T. When the probability reaches its threshold, a repair is performed, incurring a structural cost. In this way, repair is never performed beyond the acceptable level of probability of failure (Ayyub et al. 2002).

Notably, (Garbatov 2020) initially references code-prescribed reliability targets but ultimately derives the governing threshold through risk-based cost-benefit optimization against

hull girder collapse consequences, and does not consider structural damage for component renewal.

This work, however, defines and applies reliability targets directly at the component level by assessing failure as the need for repair. Accordingly, it is used (Ayyub et al. 2002) suggestion of considering (Mansour et al. 1997) recommended safety levels for fatigue cracking as a benchmark for corrosion damage. For this research and demonstration, the PoF_T are indicated in (Table 7), as suggested by (Ayyub et al. 2002) and adapted for four severity levels in naval ships.

Table 7. Hazard Severity Levels and PoF_T.

Consequence Level	Damage	Severity	Index PoF_T
Operational	Minor local damage	$S = 1$	1.5 $(6.7 * 10^{-2})$
Impaired Operation	Significant local damage	$S = 2$	2.5 $(6.2 * 10^{-3})$
Abandoned	Severe local damage	$S = 3$	3.5 $(2.3 * 10^{-4})$
Foundered	Hull collapse	$S = 4$	4.0 $(3.2 * 10^{-5})$

It should be noted that the Consequence of Failure (CoF) is independent of the PoF. Therefore, hazard severity is related to the event after failure, and the question one should ask is: what can go wrong after failure, and how severe is it?

This work does not aim to discuss probabilities far from the loss of corrosion allowance, such as the probability of structural element collapse owing to cracking or buckling given the loss of corrosion allowance, or the probability of uncontrolled flooding, given that the watertight hatch does not work, and given the entrance of water in the hull owing to corrosion.

For simplification, the consequence is evaluated considering that after the corrosion wastage reaches the allowance, the element is ineffective in supporting the design loads and to be watertight. This is a conservative assumption because the structural element is designed with a net thickness to sustain loads without allowance for a certain time. However, considering the variability of the already discussed corrosion process and the variability of structural loads during operation, it is practically complex and costly to manage structural renewal based on the

relationship between the strength and stress of each component. This type of approach is justified only by the need for local analysis.

Accordingly, the question that should be asked is: What is the severity level if the corresponding structural element fails to be watertight and to support design loads?

Considering the PoF_T (Table 7), the results of $PoF(t)$ with full renewal repair effect for elements 1-5 are presented in (Figure 19-23). Elements 1, 4, and 5 were classified with the severity level $S = 2$ and elements 2 and 3 with $S = 1$. The rationale is that impaired operation with significant local damage is associated with oil tank and hull loss of watertight, respectively 1, 4, and 5 cases. Elements 2 and 3 are secondary stiffeners inside the ballast tank, not related to watertight loss.

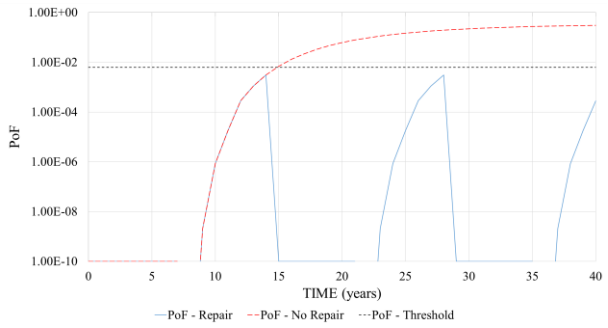


Figure 19. $PoF(t)$ for Element 1 with full renewal (log scale).

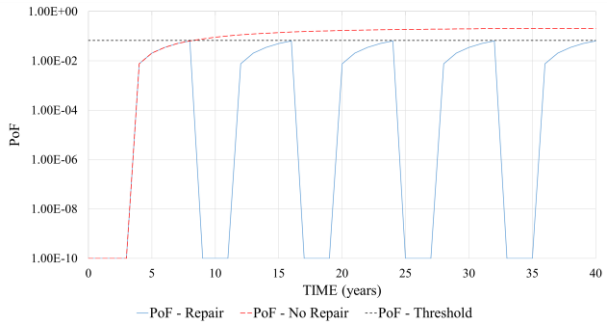


Figure 20. $PoF(t)$ for Element 2 with full renewal (log scale).

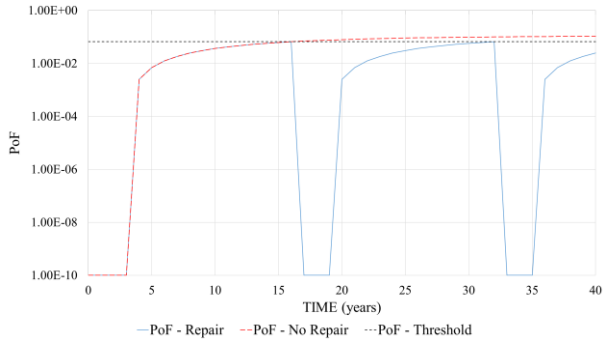


Figure 21. $PoF(t)$ for Element 3 with full renewal (log scale).

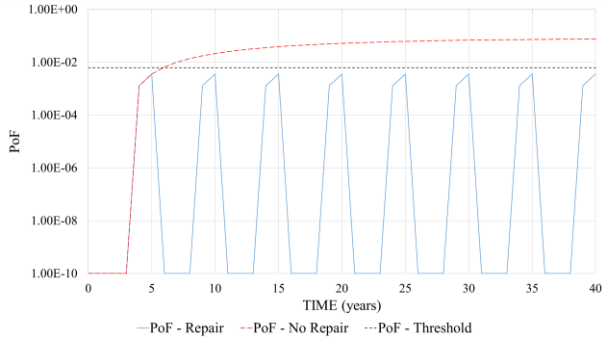


Figure 22. $PoF(t)$ for Element 4 with full renewal (log scale).

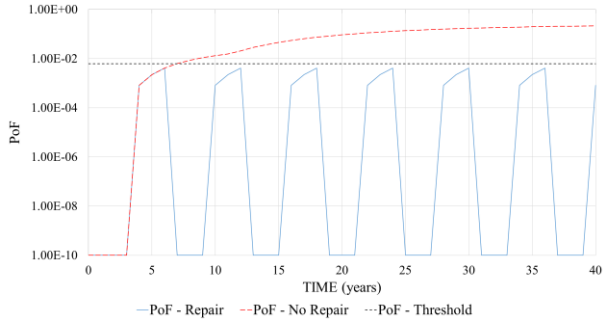


Figure 23. $PoF(t)$ for Element 5 with full renewal (log scale).

Therefore, the repair estimations can be summarized as follows:

I. Element 1: Renew action every 14 years
II. Element 2: Renew action every 8 years
III. Element 3: Renew action every 16 years
IV. Element 4: Renew action every 5 years
V. Element 5: Renew action every 6 years

2.7 Conclusion

In this Chapter, an enhanced time-based probabilistic general corrosion model was developed through comprehensive literature research and detailed model selection and adaptation. Accordingly, the Soares-Garbatov (Guedes Soares and Garbatov 1999) non-linear model was considered, covering many adaptations developed over the years to account for multiple environments, operations, and different ship spaces over the long term. These physics-based adaptations were necessary to deal with heterogeneous data used to calibrate the models and to estimate corrosion behavior related to some ship spaces and interfaces where no data is available.

Nevertheless, variability is still a major aspect of corrosion; therefore, this research adapted this well-known model to account for uncertainties, measured by a time-based probability of failure of structural components in any ship space. The adaptation was successfully validated by MCS. Furthermore, to define the individual renewal time of these components, probability of failure thresholds were suggested according to severity levels for naval vessels.

The results of this Chapter will be necessary inputs for the next chapters, which are related to costs, quantitative risk assessment, and decision-making related to repair downtimes and their duration.

Chapter 3 Cost and Time

"Time is money."

- Benjamin Franklin (Franklin 1762)

This Chapter provides a detailed analytical model of structural elements maintenance completion time and cost, expected costs of failure, and expected costs of opportunity of non-planned unavailability of naval vessels. These models are dependent on the Availability (A) assessment of both SS and SoI, the SS elements, and on the SoI Reliability (R) and Safety (S). Also, they are further integrated with the Cost-Effective (CE) Opportunistic Maintenance Strategy to decide when, where, and what components will be renewed, the costs and operational risks, which will be covered in the Chapter 4. Accordingly, this Chapter covers the integration of both SoI and SS elements regarding Maintainability (M) and Availability (A).

3.1 Introduction

As described by (Blanchard 1998), Maintainability (M) is a design parameter, or a QC, as defined by (INCOSE 2023), which is emergent between the SoI and SS, as expanded by this research in Chapter 1. Therefore, it needs to be measured concerning factors related to SoS design. Accordingly, (Blanchard 1998) proposes a series of metrics or a combination of them to describe Maintainability (M). These metrics are mostly related to time and cost. Specifically, time is related to metrics of the period between interventions (preventive or corrective) and the intervention duration. Correspondingly, cost is related just to the intervention cost itself.

Although many of these metrics are very common in the industry, such as mean time between maintenance (MTBM) or repair (MTBR), along with maintenance or repair costs and time, they are limited in explaining their effects during operation. Consistently, the decision on the number of interventions, their policies, and when they will take place not only affects the maintenance duration and cost, but also quantifiable costs during operation. Therefore, this

Chapter will explore this opportunity by modeling not only intervention completion times and costs but also the overlooked economic impact of maintenance actions during the SoI operation.

As such, three types of SIM costs are herein defined and modeled:

I. **Structural Cost (Section 3.2.1 and 3.3)**: Refers to all the actual expenditure on interventions. Depends on the decisions on the types and numbers of components to be renewed and on the SS elements, such as labor, machines, processes, and variability.

II. **Expected Cost of Failure (Section 3.2.2 and 3.4)**: Related to the economic measure of risk, which is a Safety (S) QC. Hence, although this cost is related to another design parameter, the Structural Cost is necessary to define it, along with other failure costs. Moreover, intervention decisions impact and are impacted by operational risk, hence providing a direct effect on the operational phase. Although this effect is not an actual expenditure, it is a possible one, therefore expressed by the economic impact of the uncertainty.

III. **Expected Cost of Opportunity of Non-Planned Unavailability of Naval Vessels (Section 3.2.3 and 3.5)**: The economic benefits that were forgone when an unplanned intervention was demanded; therefore, related to the tangible operational value of a naval vessel. For merchant ships, this is related to the loss of profit during unplanned idle time (Kuznecovs et al. 2022). However, for naval vessels, which are the focus of this research, it is not straightforward and is commonly overlooked. Therefore, this Chapter will also provide a new economic model to measure this effect for warships.

Considering that these three cost models are monetary-based, their total sum in Present Value (PV) is the necessary Maintainability (M) cost metric, since it accounts for multiple trade-offs which are related to the SoI, SS, and CE decisions.

Regarding the time metric, the total downtime period, as defined as maintenance downtime (MDT) (Blanchard 1998), is still necessary, and is strictly related to cost, as the epigraph to this

Chapter suggests. Moreover, the time between interventions is not based on a mean time of failure, but rather on a probability of failure threshold achievement, which is related to Safety (S) levels, SoI design, environment, and operations. Specifically, these aspects are considered under the Opportunistic Maintenance Strategy, where grouping policies will dictate maintenance under CE. Accordingly, the time between maintenance will herein be named Operational Window (O_W) and will be covered in Chapter 4.

3.2 Literature Survey

The literature survey presented in this section covers the Structural Cost, Expected Cost of Failure, and the Expected Cost of Opportunity of Non-Planned Unavailability of Naval Vessels.

3.2.1 Literature Survey: Structural Cost

Ship structural maintenance is a labor-intensive manufacturing operation that has a decisive impact on ship operational risks and future maintenance scheduling, since repair is a payoff for operational risk reduction as explored by the OMCRO framework developed by (Casares and Vlahopoulos 2024). In this proposed framework, the cost was derived from (Rahman and Caldwell 1995; Rigterink, Collette, and Singer 2013) model, and the downtime duration was based on (Kuznecovs et al. 2022) work. However, the cost model didn't account for many tasks related to pre-survey, survey, repair preparation, post-repair, and activities related to entering and leaving the repair site, such as drydock or a quay. Also, the downtime duration was based on a simple step function related to the total renewal structural steel mass, not accounting for shipyard capacity, sequential tasks, man or machine-hours, and not modeling the analysis for highly demanded maintenance with numerous renewal parts. Furthermore, neither model considered variability in the process, which has a considerable impact on production time and cost (Hopp and Spearman 2011).

Therefore, this work proposes a comprehensive analytical cost and time model of ship structure maintenance based on core shipyard processes, Group Technology (GT) (Flanders 1924; Storch and Lim 1999), and queueing theory related to Constant Work in Process (CONWIP) (Spearman, Woodruff, and Hopp 1990), which is analytically modeled in (Hopp and Spearman 2011). This specific process was studied by (Dong 2013) and (Rodzewicz et al. 2010) as a well-

suited practical policy for ship production operations. The latter specifically modeled ship repair, however, only by using Discrete Event Simulation (DES).

Accordingly, the analytical CONWIP process related to steady-state fabrication and repair workflow is analytically modeled in this work and validated with DES, also identifying the limits of the analytical model. Furthermore, it is implemented in the OMCRO framework in the Chapter 4, from which results allow high-level conclusions that are verified by hand calculation.

This model identifies multiple parameters and variables that contribute to structural maintenance and provides insights into how they impact cost, time, and schedule. Furthermore, under some limitations, this model works as a surrogate for computational analysis under DES, which is based on Monte Carlo approaches. This aspect is advantageous for the OMCRO framework, considering that each feasible solution, under the cost-effective search, calls the cost and time model. Therefore, using a validated analytical model allows it to be incorporated into the optimization framework without significantly increasing the computational effort.

3.2.2 Literature Survey: Expected Cost of Failure

A discussion regarding the definition of risk and the limits of using probability for risk analysis is well explored by (Aven 2010), who questions the common use of expected loss as a risk definition. Indeed, the referred author presents several definitions of risk in the literature, all of which present certain levels of limitations and applications.

In broad and updated terms (ISO 31073 2022) defines risk as the effect of uncertainty on objectives, where the former is related to the deficiency of information related to knowledge and the latter is the result to be achieved (positive, negative, or both). The same standard mentions that risk is usually expressed in terms of risk sources, potential events, their consequences, and their likelihood. Accordingly, risk sources and potential events were explored in Section 2.6, considering the negative result (failure) of structural components. Likelihood is the chance of an event happening, which can be measured qualitatively or quantitatively. Therefore, likelihood is an uncertainty metric. Specifically for quantitative assessment, likelihood is commonly expressed by probability (Aven 2010). Moreover, consequence is the outcome of the event on assessment, which can also be measured qualitatively or quantitatively.

The risk definition in this research is quantitative, expressed by the expected cost of failure as the combination of the estimated probability of failure and its consequences. Therefore, the

likelihood is measured by a frequentist probability of failure, while it is combined with the quantitative monetary cost of failure to measure consequence.

The main limitation of this risk definition is that it misleads rare and extreme events, as it does not accurately represent events with low probability and high consequence. In addition, events with high probability and low consequence have the same results. Another important consideration is that frequentist probability-based risk suggests that it can be highly precise, although significant simplifications and assumptions are necessary in the probability estimation (Aven 2010), as evidenced by Section 2.3. Although many levels of qualitative, quantitative, or semi-quantitative risk approaches exist in the literature, the expected cost of failure approach is common (Ayyub et al. 2002; Melchers and Beck 2018) and very useful, since it expresses risk in a quantifiable monetary approach. Nonetheless, despite precision issues, the model searches for accuracy, especially comparing the effects of maintenance decisions with a systematic metric easily communicated to stakeholders, which is a requirement of this research. Accordingly, the likelihood of failure is considered the estimated probability of failure due to structural degradation based on the corrosion model explored and developed in Chapter 2.

The monetary consequences of failure can cover many domains. Specifically, (Garbatov 2020) explores risk as the expected cost of failure with consequences related to resale (ship loss cost with depreciation), cargo loss, accidental spill of oil, and human costs (loss of life). Similarly, excluding mitigation measures, (Kuznecovs et al. 2022) work cover consequences reflected in the same domains; however, it also considers maintenance cost, since (Garbatov 2020) focus on structural collapse, therefore not assessing upkeep actions. Furthermore, (Kuznecovs et al. 2022) also, associate these cost components with hazard severity levels, which is useful to relate with the probability of failure thresholds, as covered by Section 2.6. Finally, both works are based on monetary consequences reflected in the crew, material, and environment, reinforcing the need to model them. Consistently, considering that (Kuznecovs et al. 2022) models all these domains, including maintenance and hazard severity levels assessment, it is herein selected as a benchmark for naval vessel analysis.

3.2.3 Literature Survey: Expected Cost of Opportunity of Non-Planned Unavailability of Naval Vessels

Opportunity cost is one of the ten principles of economics described by (Mankiw 2015), who defines it as "what we give up to get something." A more formal definition is provided by (Samuelson and Nordhaus 1998), who describe it as "the value of the good or service forgone" in a decision. Therefore, opportunity cost measures the trade-off involved in decision-making within the context of scarce resources in economics.

Accordingly, the cost of opportunity decisions in the private sector can be directly measured by the profit of the foregone alternative. However, the cost of opportunity on defense expenditure is not straightforward to quantify since decisions are not for-profit, while benefits are commonly intangible. This opportunity perspective was notably addressed on April 16th 1953, by the former United States president Dwight D. Eisenhower in a famous quote of his speech "The Chance for Peace" (Eisenhower 1953): "Every gun that is made, every warship launched, every rocket fired signifies, in the final sense, a theft from those who hunger and are not fed, those who are cold and are not clothed. This world in arms is not spending money alone. It is spending the sweat of its laborers, the genius of its scientists, the hopes of its children".

The essence of this trade-off historic statement between military investment versus civilian benefits, namely "guns and butter" (Samuelson and Nordhaus 1998), was earlier believed to be a straightforward negative correlation, according to the classical view that military expenditure can crowd out productive investment. However, this perspective has been deeply explored in the field of defense economics, which assesses the relationship between defense resource allocation and its impact on the economy.

In this context, the prominent work of (Benoit 1978; 1973) revealed that this classical perspective is coherent for developed countries (DC); however, its findings indicated unexpectedly strong positive correlation between the direction of military spending and economic growth in less developed countries (LDC). The evidence of military expense benefits for growth was hypothesized by collateral tangible societal value of defense programs (personnel housing, education, medical care, public works, scientific and technical services, R&D, disaster relief support, etc.) and psychological effects.

Therefore, (Benoit 1978; 1973) conclusions stimulated the debate and development of a great amount of empirical research in the field of defense economics to assess the opportunity cost

of military expense on the economy (Smith 1977; 1980; Grobar and Porter 1987; Sandler and Hartley 1995; Gold 1997; Dunne, Smith, and Willenbockel 2005; Elveren 2022). Specifically, many models were developed, and diverse cross-country correlation analyses provided assessment in this regard, with an overall lack of consensus on these effects (Dunne, Smith, and Willenbockel 2005; Elveren 2022).

Unlike most studies that attempt to model the trade-offs of government investment allocation in the defense sector and civil domains, this work focuses on a specific and often overlooked form of opportunity cost: the inefficient utilization of defense investment at the capital-asset level due to unplanned unavailability. Consistently, the acquisition of a naval vessel shall already account for or expect planned downtimes in the agreement process and other life cycle processes, which are described in Chapter 1. Therefore, planned downtimes are part of the agreed system cost; thus, are the requirements being met. In contrast, unplanned downtimes represent a deviation from requirements and a loss of service availability of government-funded capital assets.

Accordingly, this work proposes and develops a new economic model to quantify the expected cost of opportunity of unplanned unavailability of naval vessels. Moreover, considering uncertainty and diverse consequences related to these expenditures, this expected cost can also be referred to as the Risk of Opportunity. This consideration in the cost assessment is particularly relevant, considering that the last U.S. GAO reports (GAO 2020; 2025) indicate “excessive use of overtime for maintenance activities”.

Building on the “guns and butter” trade-off proposed by (Samuelson and Nordhaus 1998), this dissertation asks whether “good butter” is being traded for a “bad gun”, even when the underlying defense investment itself is justified.

3.3 Structural Cost

Unlike construction, ship repair is not a block-based ship manufacturing and assembly process. It is characterized by an in-situ labor-intensive part replacement or upkeep since parts fail at different times due to their strength, environmental conditions, and ship operations. Even in the same compartment, corrosion degradation can have different rates, and sea load-structure interaction provides different structural responses along the ship. Therefore, variability is a main characteristic of the elements that will be repaired.

Although some parts can be prefabricated and structural deterioration can be predicted for Risk-Based Inspection (RBI) and maintenance planning, a survey is necessary to confirm the repair scope. Despite the variabilities and the survey outputs, the maintenance can be categorized by a standard process (Liker and Lamb 2002). Accordingly, this dissertation identified eight ordered activities, comprising 29 tasks, presented in Table 8 and illustrated by a workflow in Figure 24:

Table 8. Activities and Tasks of Ship Repair.

ACTIVITY		TASK	TASK NAME
1	START INTERVENTION	1	ENTER DRY DOCK / QUAY
2	PRE-SURVEY	2	CLEAN HULL
		3	DRAIN TANK
		4	CLEAN OIL TANK
		5	CLEAN NON OIL TANK
		6	DEGAS TANKS
		7	BUILD SCAFFOLD
3	SURVEY	8	HULL VISUAL SURVEY
		9	NON OIL TANK VISUAL SURVEY
		10	OIL TANK VISUAL SURVEY
		11	ULTRASOUND SURVEY
4	SURVEY REPORT AND REPAIR PREPARATION	12	SURVEY REPORT
		13	REMOVE INTERFERENCES AND OUTLINE REPAIR
5	FABRICATION	14	PROCESS FLAT PLATE
		15	PROCESS FLAT PROFILE
		16	PROCESS FLAT PLATE
		17	PROCESS FLAT PROFILE
		18	PROCESS CURVED PLATE
		19	PROCESS CURVED PROFILE
6	REPAIR	20	CONNECT ELEMENTS
		21	WELD
		22	WELD SURVEY
		23	INTERNAL COAT
		24	EXTERNAL COAT
		25	OUTER HULL COAT
		26	TANK COAT
7	POST-REPAIR	27	REINSTALL INTERFERENCES
		28	REMOVE SCAFFOLDS
8	END INTERVENTION	29	EXIT DRYDOCK / QUAY

Except for all the Fabrication and some Repair activities, all of them are sequential. In other words, each of their previous tasks must be finished before starting the next one in the workflow. Therefore, the workstations that perform these tasks are herein called Sequential Workstations. On the other hand, the tasks inside activities Fabrication and Repair (14 to 22), although ordered, operate in a continuous and steady-state flow of material, generating queues under variability.

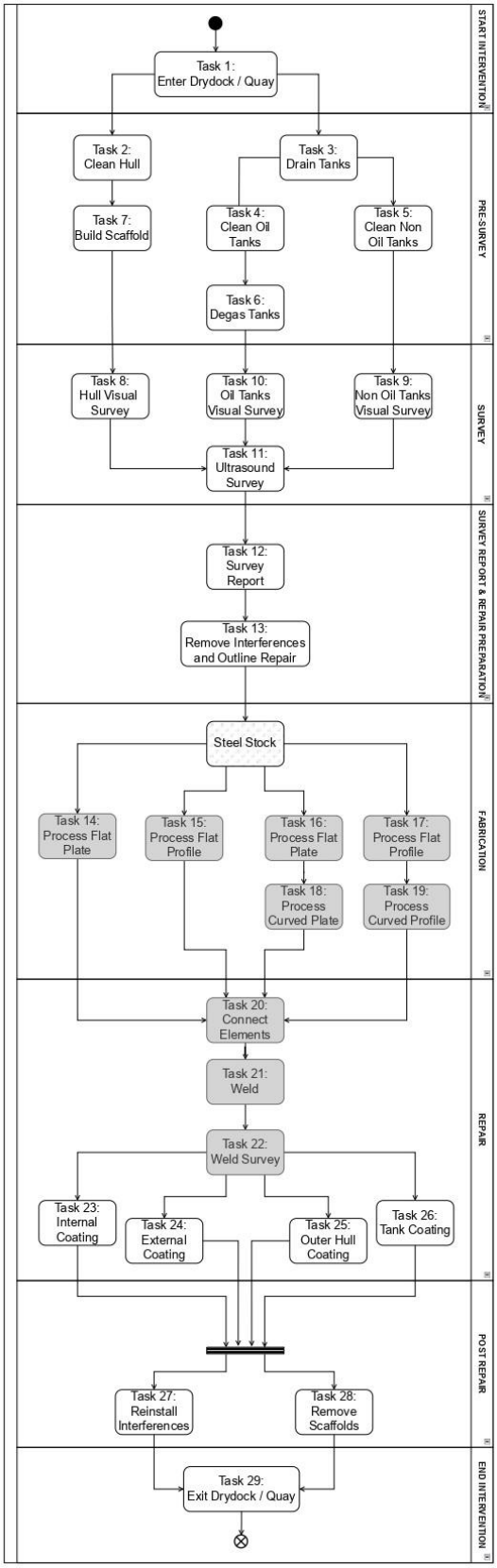


Figure 24. Repair Intervention Workflow.

The continuous flow production system can be arranged and controlled in many ways:

I. **Arrangement**: Even though shipyards may vary in shop floor arrangements and production policies, the core tasks to perform ship repair are very similar and based on the GT manufacturing philosophy, which groups similar components or processes to improve efficiency, reduce production time, and optimize resource utilization. The part families are grouped by similarities in geometry and material during the initial stages, while considering their process flows in subsequent manufacturing stages (Storch and Lim 1999).
In this way, although components have variations, they are herein classified in the same production family: flat plates, curved plates, flat profiles, and curved profiles.
Tasks related to outline repair and intervention removal are concluded during the Repair Preparation activity, which happens before Fabrication and Repair. Therefore, the elements are fabricated, connected to the ship, welded, and weld surveyed in a continuous workflow.

II. **Control**: Production systems can vary from a pure Push to a pure Pull System. Both are described as follows:

A. **Push Systems**: Based on demand forecast with releases triggered by schedule, typically using Material Resource Planning (MRP). Work is pushed through the system regardless of whether the next stage is ready. They are a good fit for production processes that are based on accurate forecasting and can buffer high variation in demand. For this reason, this type of system is loaded with considerable Work in Process (WIP), yielding higher holding costs. The Push System dynamics are illustrated in Figure 25.

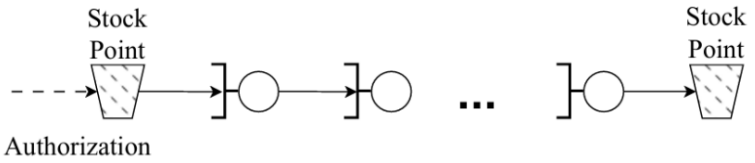


Figure 25. Push System.

B. **Pull Systems**: Based on the Kanban mechanism with releases triggered by authorization. Work is pulled downstream only when the next station allows it. They are related to Lean

Manufacturing and Just In Time (JIT) frameworks, since WIP and its holding costs are highly minimized. Since production happens in response to actual demand, quality is intrinsic to Pull Systems, but the capability of buffering demand variation is limited by low inventory levels. The Pull System dynamics are illustrated in Figure 26.

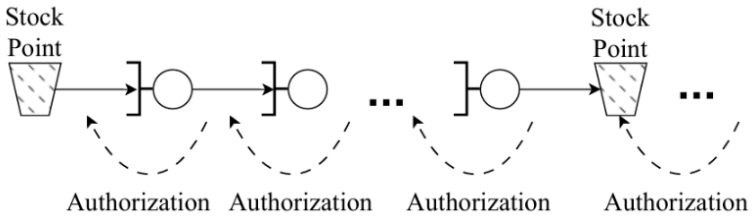


Figure 26. Pull System.

A clear statement is provided by (Hopp and Spearman 2011) to differentiate Push and Pull Systems: “Push Systems control throughput and observe WIP. Pull Systems control WIP and observe throughput”. In this respect, an efficient way to control WIP while maintaining advantageous aspects of the Push System is under the CONWIP System.

C. **CONWIP Systems**: Developed by (Spearman, Woodruff, and Hopp 1990), it presents a compromise system between Push and Pull. This production policy only allows a new job to enter the system when another job departs. Therefore, production is triggered by job completion and, consequently, WIP is capped at a pre-defined level. The mechanism of authorization is similar to Kanban; however, the authorization signal incorporates the whole system under CONWIP discipline. (Hopp and Spearman 2011) identified that this type of system is more efficient and robust than Push Systems. The former is justified by the fact that for the same throughput (TH) level, CONWIP Systems have less WIP and a smaller standard deviation of Cycle Time (CT), and the latter is justified by the fact that it is more robust to errors in WIP. Beyond all these benefits, CONWIP Systems provide a better Shop Floor Control (SFC) mechanism since WIP is directly observable, but not TH. The CONWIP System dynamics are illustrated in Figure 27.

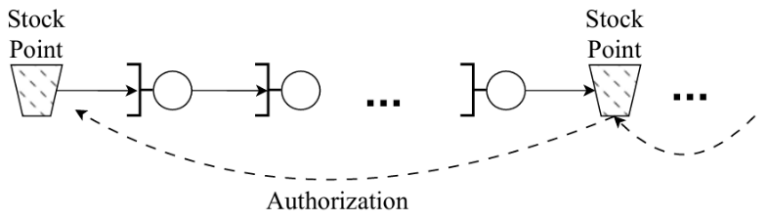


Figure 27. CONWIP System.

As described by (Rodzewicz et al. 2010), the CONWIP approach is well-suited for ship repair operations. It involves scheduling based on key events while maintenance demand is highly variable, characteristic of Push Systems. Also, the renewal of structural elements is based on a repetitive and standardized process of family-type components, commonly associated with Pull Systems.

Considering the previous assumptions, this work models the Repair and Fabrication activities as a CONWIP system arranged by GT, as presented in Figure 28.

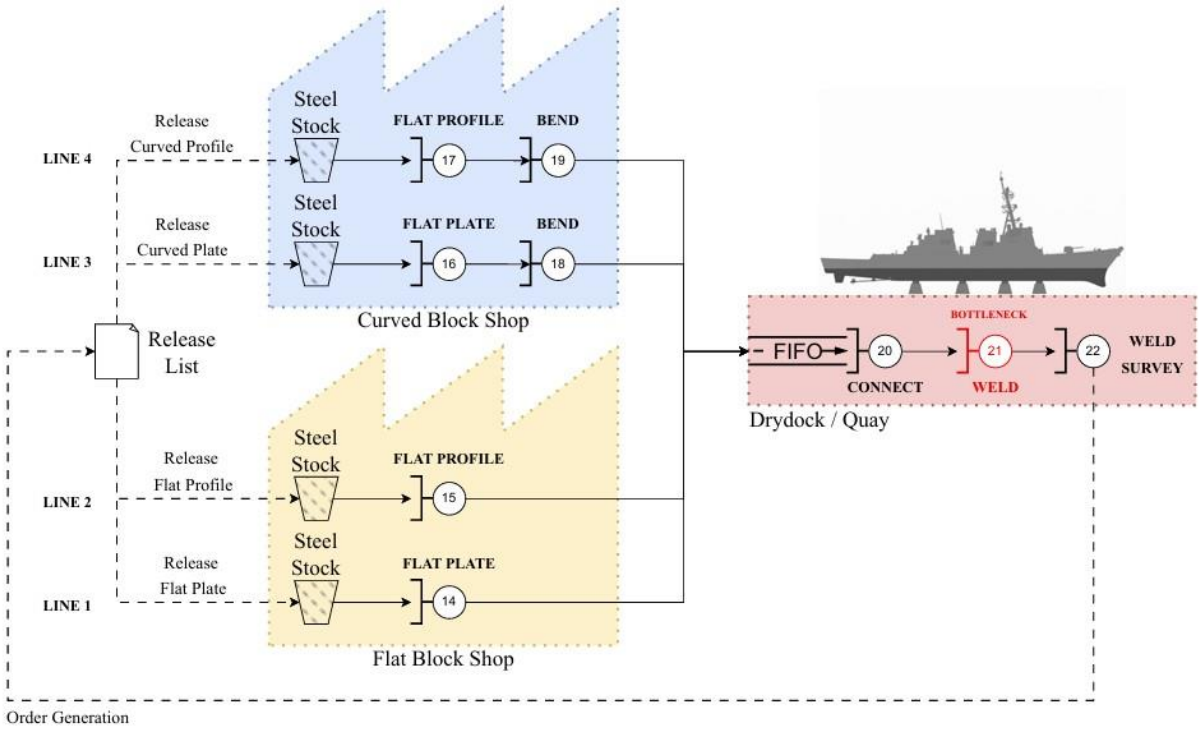


Figure 28. Production and Repair CONWIP workflow.

Accordingly, the workstations that perform the continuous and steady-state flow of material are herein called CONWIP Workstations.

3.3.1 Sequential Workstations

The sequential workstations process a single full batch of entities before allowing the start of the next workstation. Since the vessel itself is the sole production object, each workstation begins immediately upon the previous one's completion. These entities can assume different natures and units, depending on the task. In this work, the tasks performed by the sequential workstations are presented in Figure 24, numbered from 1 to 13 and from 23 to 29. Their respective entities and units $[u_i]$ are presented in Table 9.

Table 9. Entities and Unities of Sequential Workstations.

ACTIVITY		TASK	TASK NAME	ENTITIES AND UNITIES
1	START INTERVENTION	1	ENTER DRY DOCK / QUAY	X
2	PRE-SURVEY	2	CLEAN HULL	HULL AREA (m^2)
		3	DRAIN TANK	ALL TANK VOLUME (m^3)
		4	CLEAN OIL TANK	OIL TANK VOLUME (m^3)
		5	CLEAN NON OIL TANK	NON-OIL TANK VOLUME (m^3)
		6	DEGAS TANKS	OIL TANK VOLUME (m^3)
		7	BUILD SCAFFOLD	NUMBER OF SCAFFOLDS
3	SURVEY	8	HULL VISUAL SURVEY	HULL AREA (m^2)
		9	NON OIL TANK VISUAL SURVEY	NON-OIL TANK VOLUME (m^3)
		10	OIL TANK VISUAL SURVEY	OIL TANK VOLUME (m^3)
		11	ULTRASOUND SURVEY	ELEMENTS SINGLE SIDE AREA (m^2)
4	SURVEY REPORT AND REPAIR PREPARATION	12	SURVEY REPORT	NUMBER OF COMPARTMENTS
		13	REMOVE INTERFERENCES AND OUTLINE REPAIR	NUMBER OF INTERFERENCE ELEMENTS
5 - 6	FABRICATION AND REPAIR	CONWIP WORKSTATIONS		
6	REPAIR	23	INTERNAL COAT	ELEMENTS INTERNAL AREA (m^2)
		24	EXTERNAL COAT	ELEMENTS EXTERNAL AREA (m^2)
		25	OUTER HULL COAT	ELEMENTS OUTER HULL AREA (m^2)
		26	TANK COAT	ELEMENTS TANK AREA (m^2)
7	POST-REPAIR	27	REINSTALL INTERFERENCES	NUMBER OF INTERFERENCE ELEMENTS
		28	REMOVE SCAFFOLDS	NUMBER OF SCAFFOLDS
8	END INTERVENTION	29	EXIT DRYDOCK / QUAY	X

The completion time of the workstation i is the Random Variable (RV) T_i, which can assume a generic distribution. Hence, the RV cost function C_i can be defined by a fixed (material-related) parameter a_i $[USD]$ and a time-based (labor-related) cost parameter b_i $[USD/h]$, as presented by Equation 12:

$$C_i(T_i) = a_i + b_i T_i \tag{12}$$

As proved by Equation 13 to 15, the mean cost $\mu_{C_i} = E[C_i]$ can be expressed as a function of the mean time of completion $\mu_{T_i} = E[T_i]$. The proof is based on the expected cost of a function (Devore 2009), considering that $c_i(t)$ is the cost function of the variable of integration t and that $f_i(t)$ is the Probability Density Function (PDF) of T_i.

$$\mu_{C_i} = E[C_i] = \int_0^\infty c_i(t) f_i(t) dt \tag{13}$$

$$a_i \left(\int_0^\infty f_i(t) dt \right) + b_i \left(\int_0^\infty t f_i(t) dt \right) = a_i + b_i E[T_i] \tag{14}$$

$$\mu_{C_i} = a_i + b_i \mu_{T_i} \tag{15}$$

Equation 15 indicates that the mean cost of each workstation is a function of the mean time of completion, whichever generic time distribution and standard deviation it may have.

For its application, Equation 15 can be modified to consider man-hours or machine-hours $[mh]$ cost parameter β_i $[USD/mh]$ with m_i resources in the workstation i. Also, the fixed cost can be assumed as a function of the number of resources, with a cost parameter α_i $[USD/m]$. All these assumptions are presented in Equation 16 and 17.

$$a_i = \alpha_i m_i \quad ; \quad b_i = \beta_i m_i \tag{16}$$

$$\mu_{C_i} = \alpha_i m_i + \beta_i m_i \mu_{T_i} \quad (17)$$

The mean time of completion μ_{T_i} at workstation i is based on the number of resources m_i, the mean process time t_{e_i} of a single resource per entity unit $[h/u_i]$, and the number of entities n_i $[u_i]$ to be processed, as described by Equation 18.

$$\mu_{T_i} = \frac{t_{e_i} n_i}{m_i} \quad (18)$$

Applying Equation 18 to Equation 17, the expected cost for the workstation i can be defined. It is presented by Equation 19, which is a function of its fixed cost parameter α_i $[USD/m]$, man or machine-hour cost parameter β_i $[USD/mh]$, the process time parameter t_{e_i} of a single resource per entity unit $[h/u_i]$, and the number of entities n_i $[u_i]$, which is a variable output from the OMCRO framework.

$$\mu_{C_i} = \alpha_i m_i + \beta_i t_{e_i} n_i \quad (19)$$

3.3.2 CONWIP Workstations

The CONWIP system only allows a new job to enter the beginning of the workflow routing when one is released at the end. In this way, the Work-in-Process (WIP) is considered constant, while the release of jobs triggers the production authorization of new ones. The CONWIP mechanism is illustrated on Figure 27.

(Hopp and Spearman 2011) provides an analytical model for the CONWIP system based on a Mean-Value Analysis (MVA) with an iterative procedure to evaluate cycle time (CT), throughput (TH), and work-in-process (WIP) of the line and workstations. The main assumption is to model the CONWIP System as a closed queueing network, where jobs are instantly sent back to the beginning of the routing after they are released. For this purpose, all jobs are assumed to be identical. Accordingly, for a simple CONWIP line as illustrated by Figure 27, the iterative process follows the steps and formulations provided by (Hopp and Spearman 2011), and presented by Equation 20 to 24:

Step 1. $$WIP_i(0) = 0\,; TH(0) = 0 \tag{20}$$

Step 2. $$CT_i(w) = \frac{t_{e\,i}^2}{2}[ce_i^2 - 1]TH(w-1) + [WIP_i(w-1) + 1]t_{e_i} \tag{21}$$

Step 3. $$CT(w) = \sum_{i=1}^{n} CT_i(w) \tag{22}$$

Step 4. $$TH(w) = \frac{w}{CT(w)} \tag{23}$$

Step 5. $$WIP_i(w) = TH(w)CT_i(w) \tag{24}$$

Back to Step 2.

Given:

I.	w:	Defined WIP level of the CONWIP line
II.	$CT_i(w)$:	Cycle time in the workstation i for the line WIP level w
III.	$WIP_i(w)$:	Work-in-process at the workstation i for the line WIP level w
IV.	$TH(w)$:	Line throughput for WIP level w
V.	t_{e_i}	Mean process time of workstation i
VI.	c_{e_i}	Coefficient of Variation (CoV) of the process time of workstation i

However, the proposed workflow is not built with a single routing or single product as represented by Figure 27, although this dissertation still considers that all jobs require equal process time in their respective workstations. As illustrated in Figure 28, the Fabrication and Repair workflow has four routings related to different GT, which end up sharing resources in the connecting, welding, and weld-surveying workstations, where welding is the bottleneck task. Furthermore, all workstations may have multiple parallel resources. These complex

implementations are then modeled with simplifying assumptions, although they are approximate solutions. Therefore, this work also validates these analytical approximate solutions with DES.

Accordingly, to address the multiple routing arrangements, four CONWIP loops are modeled, one for each routing, where the shared resources are located. Each one of these loops links the release of jobs from the workflow to authorize the ingress of the respective job type in its respective line, as shown in Figure 28. Also, it is assumed that the inventory of raw material, localized in front of the workflow, will always fulfill the downstream demand since inventory management is not part of this work. Instead, the WIP level w_k of each line k is the only parameter under control.

To handle multiple parallel workstations, (Hopp and Spearman 2011) suggests approximating it with a single fast machine. In other words, to model the workstation with an equivalent mean process time by dividing the original process time by the number m_i of parallel machines, as presented by Equation 25.

$$t_{e_i}^* = \frac{t_{e_i}}{m_i} \tag{25}$$

However, this approximation underestimates the CONWIP performance (Hopp and Spearman 2011), hence the analytical model is more conservative.

To deal with shared resources, it is herein considered that they work based on a first-in, first-out (FIFO) process order. Nonetheless, (Hopp and Spearman 2011) states that the challenge with shared resources is that the release of jobs from a line is impacted by the others, therefore suggesting preallocating capacity as a simplifying model adaptation. This process can be done considering that each GT-based job type k (flat plate, curved plate, flat profile, and curved profile) use a p_k percentage of the time on each shared resource.

Since all workstations spend the same time on all different types of jobs, over the long run, they will be devoting equivalent proportional time related to the respective workload type they process. Of course, this approximation is consistent with heavy traffic load and with low fluctuation on the line volumes (Hopp and Spearman 2011). At low utilization, resources aren't saturated, and the lines have smaller interference with each other; therefore, the pre-allocated

capacity is too pessimistic, making the system seem slower than it really is. Accordingly, this model will be limited to heavy-load and steady traffic.

Consistently, in a busy system, it is reasonable to assume that p_k is equivalent to the ratio of the loaded WIP level w_k at line k to all WIP of the workflow, as presented by Equation 26.

$$p_k = \frac{w_k}{\sum_{i=1}^{4} w_k} = \frac{w_k}{w} \tag{26}$$

To preallocate capacity on the shared resource within the line k, the respective shared resource workstation process time shall be divided by p_k. The combined approximations of process times regarding the use of multiple machines and shared resources are presented by Equation 27.

$$t_{e_i}^{**} = \frac{t_{e_i}}{m_i p_k} \tag{27}$$

Considering the modeling simplifying assumptions to account for multiple machines and shared resources, the four routings can be analyzed as separate CONWIP lines, where each line k has its respective w_k level. Also, according to the definition of the CONWIP system, w_k is the sum of the WIP level $WIP_i(w_k)$ from all c individual workstations i of the line k, as presented by Equation 28.

$$w_k = \sum_{i=1}^{c} WIP_i(w_k) \tag{28}$$

With Equation 20 to 28, it is then possible to calculate the throughput $TH(w_k)$, work-in-process $WIP_i(w_k)$, and cycle time $CT_i(w_k)$ for all workstations i and of every line k.

It is assumed that the workflow is always in a steady-state condition, so when the first job enters the line, it is already packed with WIP being processed for another previous production release list (i.e., another ship at a different drydock or quay). Therefore, to estimate the completion time of the job j to leave the system, (Baker and Trietsch 2009) defines it as equal to CT_j plus the release date r_j, when the job arrives at the system, as modeled by Equation 29.

$$C_j = CT_j + r_j \tag{29}$$

Equation 29 can be used to calculate the completion time of the last job j, which is called the makespan (C_{max}) in the scheduling literature. In this work, the CT of a station is independent of the job type. Therefore, the release date r_{last} of the last of any N jobs is logically the time needed for the first $N-1$ jobs to ingress the system, flowing through it, as modeled by Equation 30.

$$r_{last} = \frac{N-1}{TH} \tag{30}$$

With the same rationale, the completion time for the full amount of n_k jobs at the workstation i at the k line is equal to the individual $CT_i(w_k)$ of the last job plus the time it waits for the first $n_k - 1$ entities to enter the station, as shown by Equation 31.

$$C_{max_{ik}} = CT_i(w_k) + \frac{n_k - 1}{TH(w_k)} \tag{31}$$

For shared resources, the total duration time of the workstation i can be modeled by Equation 32.

$$C_{max_i} = \max\left(C_{max_{ik}}\right) \; ; \; k = 1, 2, 3, 4 \tag{32}$$

Equation 22 provides the total cycle time $CT(w_k)$ of each line k as the sum of the cycle times of its individual workstations. Therefore, following the same principle from Equation 30 and 31, each line completion time (line makespan) C_{max_k} is equal to the $CT(w_k)$ of the last job in the line, plus the time it waits for the first $n_k - 1$ jobs to enter the line, as modeled by Equation 33.

$$C_{max_k} = CT(w_k) + \frac{n_k - 1}{TH(w_k)} \tag{33}$$

The whole Fabrication and Repair workflow completion time of all n jobs (makespan) C_{max} is equal to the maximum line makespan (Eq. 20).

$$C_{max} = \max\left(C_{max_k}\right) \; ; \; k = 1,2,3,4 \tag{34}$$

Equation 34 provides the time between the end of Task 13 and the beginning of Task 23, as indicated by Figure 24. This time will also contribute to the drydock or quay duration and cost.

3.3.2.1 CONWIP Workflow Costs and Behavior

Concerning the CONWIP workstations' costs, the model provided by Equation 35 is analogous to Equation 17, corresponding to a fixed and time-based term. Furthermore, it also considers a holding cost term with a holding cost parameter γ_i $[USD/WIP]$ and the workstation WIP level $w_i = \ WIP_i(w_k)$.

$$\mu_{C_i} = \alpha_i m_i + \beta_i m_i C_{max_i} + \ \gamma_i w_i \tag{35}$$

In Equation 35, the first term (1) does not depend on WIP but on capacity. The last term (3) is a linear holding cost function of the workstation WIP level w_i. The second term (2) is a function of CT and TH, which are linked with the WIP level by Little's Law (Hopp and Spearman 2011). The line dynamics can be described as follows:

I. **Best-Case Performance**: No variability case ($c_{e_i} = 0$) for the whole line. When the line is loaded below a critical WIP level w_{0_k}, the $CT(w_k)$ is constant and equal to the raw process time T_{0_k} of the line, which is the minimum $CT(w_k)$. This happens while $TH(w_k)$ increases linearly with WIP, equal to w_k/T_{0_k}, according to Little's Law, until it reaches the bottleneck rate r_{b_k}, which is the maximum $TH(w_k)$ (100% utilization). When at the bottleneck rate, the $CT(w_k)$ increases linearly and is equal to w_k/r_{b_k}.

II. **Worst-Case Performance**: Related to batch move behavior. In other words, the line is made up of sequential workstations. Therefore, all processes are completed in the previous

workstation before starting in the next one. Accordingly, the $CT(w_k)$ increases linearly with WIP level, equal to $w_k T_{0_k}$, while the $TH(w_k)$ is fixed at the minimum level $1/T_{0_k}$.

The line with variability will perform between the upper bound performance (best-case) and the lower bound performance (worst-case). Accordingly, with a heavier WIP load, $CT(w_k)$ behaves in a non-linear pattern, asymptotically increasing with WIP level and following the best-case curve (Figure 30). This happens while $TH(w_k)$ increases in a nonlinear asymptotic pattern, following r_{b_k} (Figure 29). Increasing variability will always degrade the line performance

Figure 29 and Figure 30 respectively illustrate the $TH(w_k)$ and $CT(w_k)$ performance in function of WIP level w_k. This relationship is provided by so-called Logistic Operating Curves (LOC) (Lödding 2013), considered herein with $TH(w_k)$ normalized by the line bottleneck rate r_{b_k}, and $CT(w_k)$ normalized by the line raw process time T_{0_k}. The curves are built with the CONWIP model for the Best-Case, Worst-Case, and performances with increasing variability ($c_e = 1$ and 1.5) for the same capacity.

As observed, line performance degrades with variability. Additionally, increasing capacity by means of increasing r_b and decreasing T_0 will improve performance. These results confirm that the CONWIP analytical model is verified and aligns with the Factory Physics principles proposed by (Hopp and Spearman 2011).

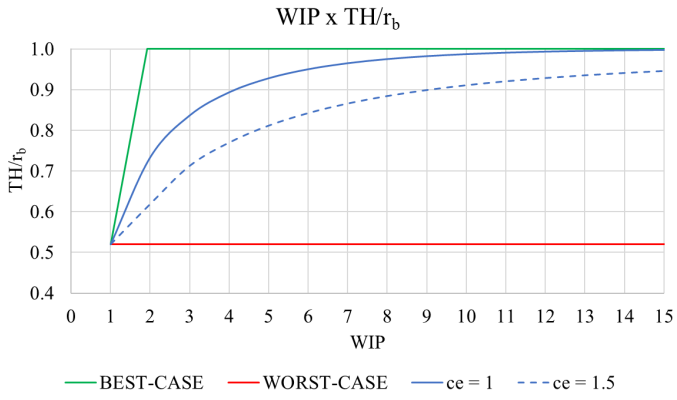


Figure 29. Logistic Operating Curve ($WIP\ x\ TH/r_b$) of a line.

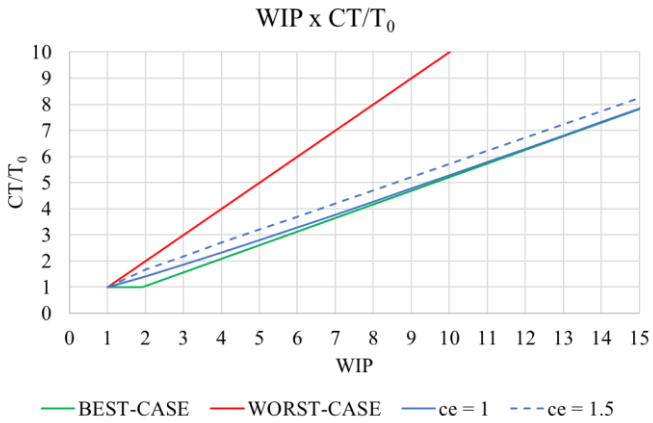


Figure 30. Logistic Operating Curve ($WIP\ x\ CT/T_0$) of a line.

3.3.2.2 CONWIP Model Validation

To validate the proposed analytical model, a DES was conducted using 1.000 steady-state simulations with different line WIP levels w_k (5, 10, 20, and 40), capacities m_i (1, 2, and 3), and process variabilities c_{e_i} (1, 1.5, and 2). For this validation, it was assumed that all lines WIP levels w_k are equal, therefore $p_k = 0{,}25$. Also, the DES was carried out using Jaamsim® software with Lognormal process time distributions to represent a generic and feasible time distribution in the workstations.

The workflow parameters are presented in Table 10, and the DES results for all lines' throughput $TH(w_k)$ are compared against the analytical solution in all cases of capacity and variability.

Table 10. Workflow Parameters for Validation.

TASK	t_e	c_e	m
14	0.33	1 : 1.5 : 2	1 to 3
15	0.50	1 : 1.5 : 2	1 to 3
16	0.33	1 : 1.5 : 2	1 to 3
17	0.50	1 : 1.5 : 2	1 to 3
18	0.67	1 : 1.5 : 2	1 to 3
19	0.67	1 : 1.5 : 2	1 to 3
20	1.75	1 : 1.5 : 2	1 to 3
21	2.40	1 : 1.5 : 2	1 to 3
22	0.17	1 : 1.5 : 2	1 to 3

The relative errors between the simulation and the analytical model, as a function of WIP levels, are presented to all lines in Figure 31 to 34. Accordingly, the average TH errors for all lines within the same WIP level and variability are presented in Table 11.

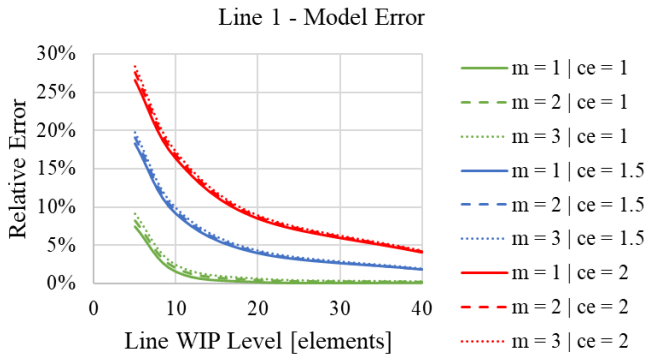


Figure 31. Line 1 Model Error.

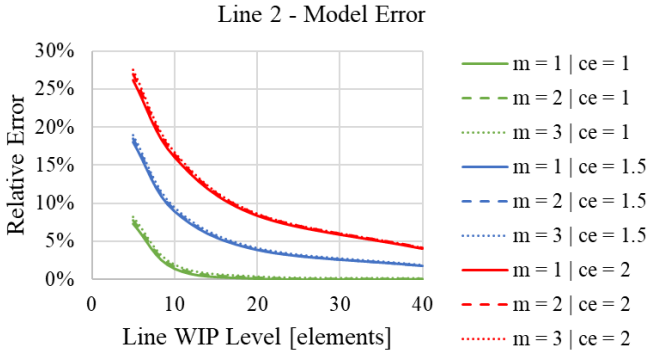


Figure 32. Line 2 Model Error.

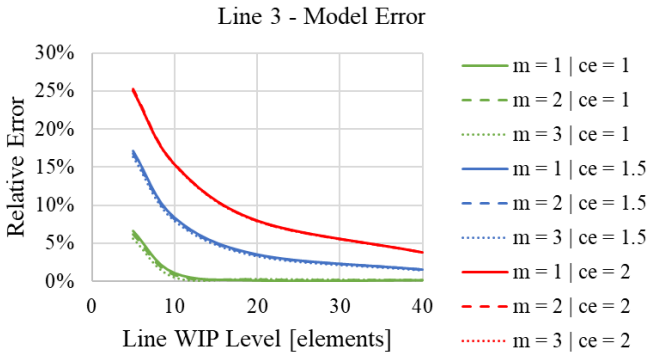


Figure 33. Line 3 Model Error.

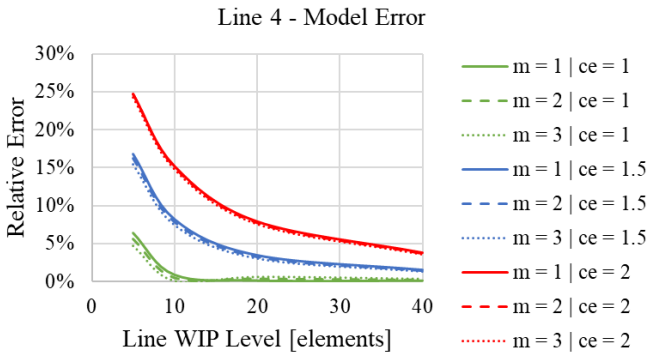


Figure 34. Line 4 Model Error.

Table 11. TH Average Errors.

TH AVERAGE ERROR			
WIP	LINE 1		
	ce = 1	ce = 1.5	ce = 2.0
5	8.3%	19.1%	27.5%
10	2.0%	9.5%	16.8%
20	0.4%	4.1%	8.7%
40	0.2%	1.9%	4.2%
WIP	LINE 2		
	ce = 1	ce = 1.5	ce = 2.0
5	7.7%	18.5%	26.9%
10	1.7%	9.2%	16.4%
20	0.3%	4.0%	8.5%
40	0.1%	1.8%	4.1%
WIP	LINE 3		
	ce = 1	ce = 1.5	ce = 2.0
5	6.1%	16.8%	25.1%
10	0.8%	8.2%	15.4%
20	0.2%	3.4%	7.9%
40	0.1%	1.5%	3.8%
WIP	LINE 4		
	ce = 1	ce = 1.5	ce = 2.0
5	5.6%	16.2%	24.6%
10	0.5%	7.8%	15.0%
20	0.4%	3.3%	7.7%
40	0.2%	1.4%	3.7%

As expected, the errors drastically decrease with heavier traffic and increase with variability. Another effect is that errors can marginally fluctuate with the increase in parallel

machines for the same load. This effect can be explained by the introduced error in the model simplification for a single machine analysis. This error increases with more parallel machines; however, since more capacity decreases utilization for the same WIP level, the lines become more independent, approaching no inflation in process times, which breaks the model assumption on capacity preallocation. Therefore, although errors will decrease with traffic load (larger WIP) and less variability (smaller c_e), the model is less reliable with more parallel machines for the same WIP, since it decreases utilization. However, it can be verified in Figure 31 to 34 that the error variation regarding capacity change is irrelevant when compared with the variability and WIP level effects.

For all lines, the average throughput relative error at the maximum load ($WIP = 40$) is 0.2% ($c_e = 1$), 1.7% ($c_e = 1.5$), and 3.9% ($c_e = 2$). These results are coherent to the CONWIP analytical model expectations since (Baker and Trietsch 2009) mentions reasonable approximations for c_e between 0.5 and 2. Also, the validation confirms the assumption taken on Equation 26.

To validate and illustrate the production system dynamics, Figure 35 to 37 presents the DES results in comparison to the analytical model behavior of the first line cycle time CT_1 for all capacities and variabilities.

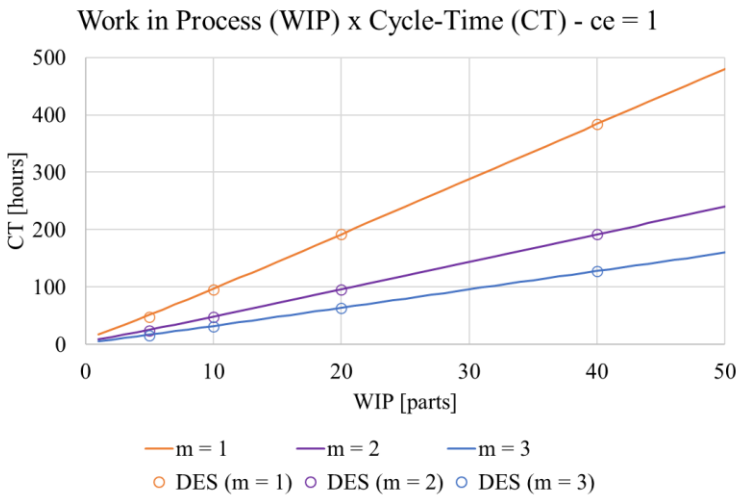


Figure 35. WIP x CT - c_e = 1.

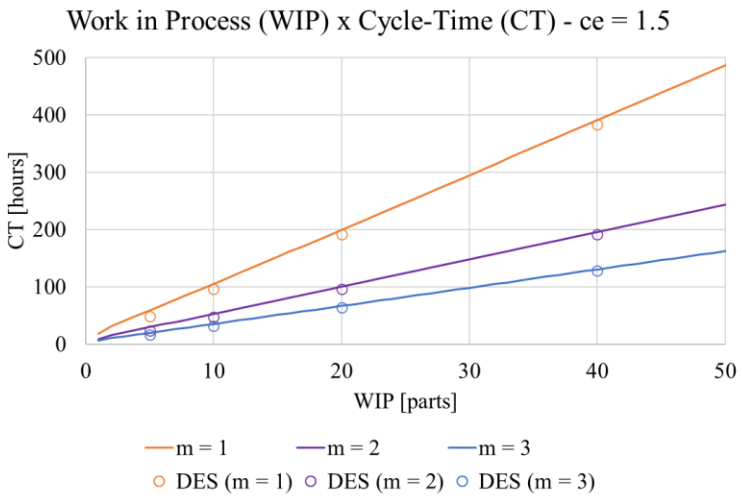


Figure 36. WIP x CT - c_e = 1.5.

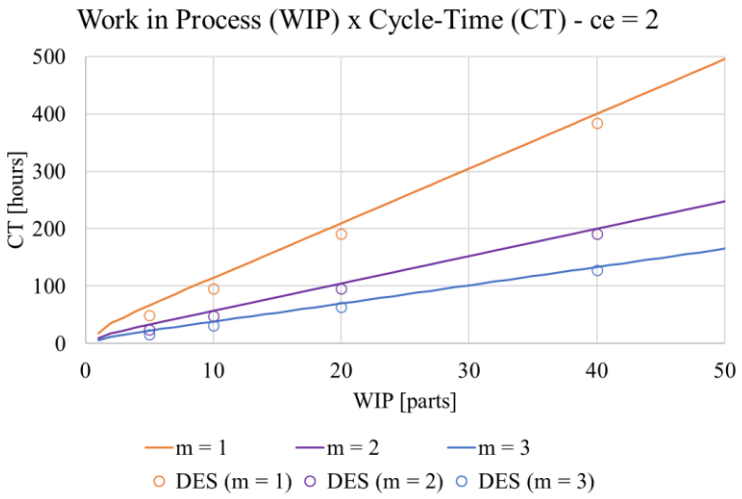


Figure 37. WIP x CT - c_e = 2.

As expected, the CT increases with variability and decreases with capacity. Also, the model prediction degrades with increased variability and is less accurate for low traffic conditions, as mentioned before. Although the range of the model's usefulness has been identified, it is worth mentioning that the expected errors are conservative in any case. In other words, the real-world scenario (modeled by simulation) performs better than the analytical model.

3.3.3 Structural Maintenance Time and Cost

Considering the completion time and cost models for the sequential and CONWIP workstations, and the workflow diagram presented in Figure 24, the Intervention Time T_I can be quantified by Table 12, while the Intervention Cost C_I is the sum of all workstations' costs.

The workstations with tasks 1 to 13 and from 23 to 29 are defined as sequential workstations with their inherent time and cost models in Section 3.3.1. The workstations with tasks 14 to 22 are CONWIP workstations in continuous, steady, and loaded traffic, with their dedicated and validated analytical time and cost models in the Section 3.3.2.

If the intervention is performed in drydock, all tasks are considered. However, if the intervention is done at the quay area and drydock is not needed, tasks 2 and 8 are discarded.

On all fixed and time-based costs, a respective percentage of markup is applied to define the established shipyard prices, which are, in turn, the shipowner's costs that define C_I.

Another considerable expenditure is the Downtime Cost C_{DT}, which is based on the total completion time of the intervention at the drydock T_{I_D} and at the quay area T_{I_Q} and its respective drydock P_D or quay P_Q prices per day, as presented in Equation 36.

$$C_{DT} = P_D T_{I_D} + P_Q T_{I_Q} \tag{36}$$

With both C_I and C_{DT}, the Structural Cost is then defined by Equation 37.

$$C_S = C_I + C_{DT} \tag{37}$$

Table 12. Intervention Time.

TASK	START TIME	END TIME
1	0	E1 = μ_{T_1}
2	E1	E2 = E1 + μ_{T_2}
3	E1	E3 = E1 + μ_{T_3}
4	E3	E4 = E3 + μ_{T_4}
5	E3	E5 = E3 + μ_{T_5}
6	E4	E6 = E4 + μ_{T_6}
7	E2	E7 = E2 + μ_{T_7}
8	E7	E8 = E7 + μ_{T_8}
9	E5	E9 = E5 + μ_{T_9}
10	E6	E10 = E6 + $\mu_{T_{10}}$
11	max(E8, E8, E10)	E11 = max(E8, E9, E10) + $\mu_{T_{11}}$
12	E11	E12 = E11 + $\mu_{T_{12}}$
13	E12	E13 = E12 + $\mu_{T_{13}}$
14	E13	E14 = E13 + $C_{max_{14}}$
15	E13	E15 = E13 + $C_{max_{15}}$
16	E13	E16 = E13 + $C_{max_{16}}$
17	E13	E17 = E13 + $C_{max_{17}}$
18	E13 + CT_{16}	E18 = E13 + CT_{16} + $C_{max_{18}}$
19	E13 + CT_{17}	E19 = E13 + CT_{17} + $C_{max_{19}}$
20	E21 - CT_{21} - $C_{max_{20}}$	E20 = E21 - CT_{21}
21	E22 - CT_{22} - $C_{max_{21}}$	E21 = E22 - CT_{22}
22	E13 + C_{max} - $C_{max_{22}}$	E22 = E13 + C_{max}
23	E22	E23 = E22 + $\mu_{T_{23}}$
24	E22	E24 = E22 + $\mu_{T_{24}}$
25	E22	E25 = E22 + $\mu_{T_{25}}$
26	E22	E26 = E22 + $\mu_{T_{26}}$
27	max(E23, E24, E25, E26)	E27 = max(E23, E24, E25, E26) + $\mu_{T_{27}}$
28	max(E23, E24, E25, E26)	E28 = max(E23, E24, E25, E26) + $\mu_{T_{28}}$
29	max(E27, E28)	E29 = max(E27, E28) + $\mu_{T_{29}}$
		$\boldsymbol{T_I = E29\ in\ days}$

3.4 Expected Cost of Failure

The risk definition used in this project is the expected cost of failure (C_{EF}), which considers two dimensions of risk: probability of failure ($PoF = p_f$) and consequence of failure (CoF) expressed as the cost of failure (C_f), as shown by Equation 38.

$$C_{EF} = p_f \, C_f \tag{38}$$

The probability of failure is developed in Section 2.4, while the consequences of failure, reflected in the crew, material, and environmental cost components, are estimated based on (Kuznecovs et al. 2022) considerations, excluding mitigation measures. The same reference also indicates that these cost components are dependent on the hazard severity levels. In this case, this research presents an adaptation for naval vessels, matching Table 7 hazard severity levels. These adaptations are presented in Table 13.

Table 13. Consequence of Failure Components.

Severity	Social	Structural	Ship Loss	Payload Loss	Oil Loss*
$S = 1$	X	X			
$S = 2$	X	X			
$S = 3$	X	X			X
$S = 4$	X		X	X	X

* For replenishment tankers

Therefore, the cost of failure (C_f) is presented by Equation 39.

$$C_f(S) = C_{social} + C_{structural} + C_{ship} + C_{payload} + C_{oil} \tag{39}$$

Except for the Structural Cost, developed in Section 3.3, formulations for each specific cost are referred to (Kuznecovs et al. 2022), and are presented as follows:

I. Social Cost:

The social cost (C_{social}) refers to the costs of injuries and loss of human life as a consequence of failure. However, valuing human life is uncomfortable, as it cannot be reduced to simple monetary terms. An alternative and common approach is to express it as costs per fatality averted, known as the Implied Cost of Averting a Fatality (ICAF) (DNV 2002), also used in (Garbatov 2020) work. It is always considered as a cost component, which formulation is presented by Equation 40 to 42 and by Table 14 (Kuznecovs et al. 2022).

$$C_{social} = F.ICAF \tag{40}$$

$$ICAF = \frac{GDP.L_E}{4}.\frac{1-w}{w} \tag{41}$$

$$w = \frac{k_L}{24(365)} \tag{42}$$

Table 14. Equivalent Number of Fatalities.

Equivalent Number of Fatalities	
Severity	***F***
$S = 1$	0.01
$S = 2$	0.1
$S = 3$	1
$S = 4$	10

Considering:

A. F: Equivalent number of fatalities as presented in Table 14
B. $ICAF$: Optimum acceptable implied cost of averting a fatality
    1. GDP: Gross Domestic Product per capita

2. L_E: Life expectancy
3. w: Proportion of life spent in economic activity
    a. k_L: Labor Utilization (hours worked per capita)

Notably, since ICAF depends on national GDP, life expectancy, and working hours, the model is sensitive to national context, limiting its use for cost comparisons across different countries.

II. Structural Cost:

The structural cost ($C_{structural}$) was modeled in Section 3.3

III. Ship Loss:

The ship loss cost (C_{ship}) is just considered in the event of maximum severity. In this case, the total economic value of the ship is considered. which is time-dependent and decreases linearly with the yearly-based depreciation rate. Equation 43 presents the ship loss cost.

$$C_{ship} = P_{ship_{new}} - P_{d_s} T_{age} \tag{43}$$

Considering:

A. $P_{ship_{new}}$: Newbuilding price of the ship
B. P_{d_s}: Depreciation rate of the ship
C. T_{age}: Vessel's age

IV. Payload Loss:

The payload loss cost ($C_{payload}$) is just considered in the event of maximum severity. For a naval vessel, this may correspond to the loss of mission-critical onboard or embarked assets, such as aircraft, boats, mission modules, or other operational equipment. In this case, the total

economic value of the payload is considered, which is time-dependent and decreases linearly with the yearly-based depreciation rate. Equation 44 presents the payload loss cost.

$$C_{payload} = P_{payload_{new}} - P_{d_p} T_{age} \quad (44)$$

Considering:

A. $P_{payload_{new}}$: New payload price
B. P_{d_p}: Depreciation rate of the payload
C. T_{age}: Payload's age

V. Oil Loss:

The oil loss cost (C_{oil}) is related only to replenishment tankers (naval auxiliary ships), in which oil is a payload. This cost is related to the oil leakage after the loss of watertightness of the hull in the cargo tank. Also, two severities are considered: foundered ($S = 4$) and abandoned ($S = 3$). For the foundered condition, the total amount of ship cargo oil is considered, as shown by Equation 45.

$$C_{oil} = 7.33 P_{oil} V_{T_{oil}} \quad (45)$$

For the abandoned condition, the amount of oil in a specific cargo tank is considered, as shown in Equation 46.

$$C_{oil} = 7.33 P_{oil} V_{oil} \quad (46)$$

Considering:

A. P_{oil}: Market oil price per volume
B. $V_{T_{oil}}$: Volume of all cargo tanks
C. V_{oil}: Volume of specific cargo oil tank

3.5 Expected Cost of Opportunity of Non-Planned Unavailability of Naval Vessels

Naval vessels are complex systems procured based on a considerable number of requirements, including expected or planned downtimes. Unexpected downtimes, however, result in social, maintenance, and material loss costs that fall outside the budget. As described by (Kuznecovs et al. 2022), in commercial vessels, also incur costs due to loss of economic revenue, taken as opportunity costs. However, naval vessels do not have economic revenue or cash flows, as their existence is related to the intangible National Security Strategy (NSS). Although naval vessels do not provide revenue, they are government assets and shall be perceived as public investments delivering intangible benefits.

To maintain these intangible benefits, unplanned maintenance actions are sometimes required to ensure proper reliability for a ship to continue performing its functions. The costs associated with maintenance decisions are, thus, unplanned allocations of public capital that displace alternative uses of these resources, which could otherwise generate tangible returns elsewhere. Therefore, the minimum acceptable intangible benefit associated with maintenance can be related to the tangible benefits foregone due to downtime, since, in the absence of such a benefit, maintenance would not be economically justifiable.

Hence, when the ship is idle due to unplanned downtime and no operational intangible benefit is delivered, the remaining effect is the loss of potential capital return, which can be quantified as opportunity cost. Accordingly, this work identifies two distinct sources of opportunity cost associated with unplanned naval vessel unavailability:

I. **Unbudgeted costs**: The unexpected social, maintenance, and material loss consequences are covered by resources that were allocated elsewhere, causing opportunity losses in return of capital.

II. **Budgeted costs**: The difference between the already budgeted operational and support (O&S) expenditure during operation and the O&S expenditure during idle time is an opportunity loss. More specifically, it represents resources allocated exclusively to non-idle functions that were not performed. Thus, had the downtime been planned, this portion of the budget could have been reduced or reallocated elsewhere, yielding tangible benefits.

3.5.1 Expected Cost of Opportunity

The Expected Cost of Opportunity or Risk of Opportunity C_{EO_j} for a single element j is formulated as:

$$C_{EO_j} = p_{f_j}(t).C_{o_j}(t) \tag{47}$$

Where $C_{o_j}(t)$ is the Cost of Opportunity and $p_{f_j}(t)$ is the yearly-based probability of failure for a single element j, which demands downtime on failure.

In this work, $C_{o_j}(t)$ is defined as the forgone return on capital corresponding to the sum of budgeted and unbudgeted costs associated with component j during its downtime period t_{u_j}. This tangible loss represents the financial benefit that could otherwise be obtained through alternative public capital allocation.

The real annual rate of return for public investment is denoted by r, and the loss of opportunity is related to the future return of capital from time t to a forgone investment horizon T, as illustrated in Figure 38. In this context, the Present Value (PV) represents the current state, while the Future Value (FV), at time t, corresponds to the occurrence of unexpected downtime. As a benchmark, the investment horizon T may be assumed equal to the ship's service life, as defined by its requirements.

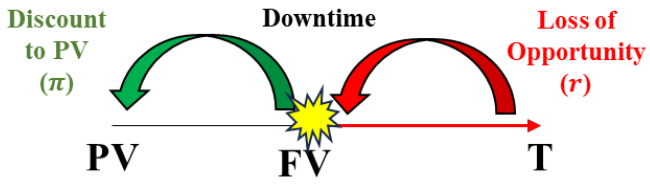


Figure 38. Loss of Opportunity from T to PV.

With this benchmark, the opportunity cost horizon T represents the limit of the foregone alternative value within the remaining planned service life of the vessel. While broader opportunity

costs associated with alternative uses of resources may exist beyond this horizon, such effects are outside the scope of the present model. Accordingly, the proposed formulation assumes that alternative value streams emerge with the commissioning of the vessel and are extinguished at the end of its planned service life. Under this definition, opportunity cost is directly associated with the operational tangible value of keeping the vessel as an available option; consequently, this value is assumed to be zero at the end of the service life.

Therefore, the Cost of Opportunity $C_{o_j}(t)$ can be modeled as follows:

$$C_{o_j}(t) = \left[C_{f_j}(t) + \Delta C_{os_j}(t)\right].[(1+r)^{T-t} - 1] \tag{48}$$

In Equation 48, $C_{f_j}(t)$ is the unbudgeted consequence cost of failure of the element j at year t based on severity levels as presented in Section 3.4.

The Exclusively Non-Idle O&S Cost $\Delta C_{os_j}(t)$ is related to the difference between the budgeted O&S total expenditures during the year t, proportional to the downtime duration, and the O&S expenditures of the idle ship during the same time.

Therefore, $\Delta C_{os_j}(t)$ is a fraction α of the annual budgeted O&S total expenditures $C_{os}(t)$, at year t, exclusively related to the non-idle state of the ship, and proportional to the downtime duration t_{u_j} in days, given by the time to repair the element j and its associated elements by specific grouping policies as presented in Chapter 4. The downtime duration is, then, a function of the shipyard quality (capacity and variability), as well as the number and types of elements to be repaired. This relation is presented by Equation 49:

$$\Delta C_{os_j}(t) = \alpha . C_{os}(t) . \frac{t_{u_j}}{365} \tag{49}$$

The operational and support costs $C_{os}(t)$ include routine ship operation and maintenance, personnel compensation and benefits, operational activities, training, support contractors, fuel, and consumables. Hence, $C_{o_j}(t)$ can be formulated by Equation 50:

$$C_{o_j}(t) = \left[C_{f_j}(t) + \alpha . C_{os}(t) . \frac{t_{u_j}}{365}\right] . [(1 + r)^{T-t} - 1] \quad (50)$$

Accordingly, the Expected Cost of Opportunity or Risk of Opportunity $C_{EO_j}(t)$ as a Future Value (FV) at time t can be rewritten by Equation 51 and 52.

$$C_{EO_j}(t) = p_{f_j}(t) . \left[C_{f_j}(t) + \alpha . C_{os}(t) . \frac{t_{u_j}}{365}\right] . [(1 + r)^{T-t} - 1] \quad (51)$$

or

$$C_{EO_j}(t) = \left[C_{EF_j}(t) + p_{f_j}(t) . \alpha . C_{os}(t) . \frac{t_{u_j}}{365}\right] . [(1 + r)^{T-t} - 1] \quad (52)$$

Where $C_{EF_j}(t)$ is the quantitative risk defined as the Expected Cost of Failure for an element j at time t, developed in Section 3.4.

It is relevant to note that Equation 51 and 52 capture the following effects:

I. The higher the Probability of Failure, which grows with degradation over time, the higher the Expected Cost of Opportunity.
II. The higher the Consequence of Failure, which depends on severity, the higher the Expected Cost of Opportunity.
III. The higher the exclusively non-idle O&S costs, the higher the Expected Cost of Opportunity. Particularly, O&S Costs are very closely related to the size of units. Therefore, the bigger the ship, the higher the Expected Cost of Opportunity.
IV. The number, type of elements, and shipyard quality will affect downtime duration, affecting the Expected Cost of Failure, thus the Expected Cost of Opportunity.
V. The higher the government risk option for opportunity resource allocation, the higher the interest rate, and the higher the Expected Cost of Opportunity. It is reasonable to assume that open-market industries face higher investment risk than governments and therefore

require higher rates of return. Hence, a conservative and appropriate benchmark for public investment is a risk-free rate, herein taken as the nominal Federal Funds (Fed) Rate.

VI. The higher the inflation, the higher the nominal interest rate (Fed rate), the higher the Expected Cost of Opportunity.

VII. The higher the investment horizon, the higher the Expected Cost of Opportunity.

3.5.2 Present Value of the Expected Cost of Opportunity

Since the Federal Open Market Committee (FOMC) target rate varies over time, a long-term nominal rate i is considered. To obtain the real rate of return, the Federal Reserve's target inflation rate π is herein considered by the Fisher Equation, Equation 53 (Fisher 1907).

$$r = \frac{1+i}{1+\pi} - 1 \tag{53}$$

For relatively low inflation rates, this expression is commonly approximated by Equation 54:

$$r \cong i - \pi \tag{54}$$

Therefore, the Total Expected Cost of Opportunity C_{EO} for n components is expressed in PV by Equation 55, where π is the discount rate.

$$C_{EO} = \sum_{j=1}^{n} \left[\frac{C_{EF_j}(t)}{(1+\pi)^t} + \frac{p_{f_j}(t).\alpha.C_{os}(t).\frac{t_{u_j}}{365}}{(1+\pi)^t} \right].[(1+r)^{T-t} - 1] \tag{55}$$

Furthermore, if the future costs in time t, $C_{EF_j}(t)$ and $C_{os}(t)$, are assumed to evolve solely according to the target inflation rate π, the C_{EO} in PV can be simplified by Equation 56, which will be considered in this work.

$$C_{EO} = \sum_{j=1}^{n} \left[C_{EF_j} + p_{f_j}(t).\alpha.C_{os}.\frac{t_{u_j}}{365} \right].[(1+r)^{T-t} - 1] \quad (56)$$

3.5.3 Cost of Opportunity Sensitivity Analysis

The economic model presented by Equation 56 is sensible to the following effects:

I. Time-based degradation driven by environmental and operational conditions.
II. Failure consequence costs in social, material, and environmental dimensions.
III. Ship size and Operational and Support (O&S) cost parameters.
IV. Duration of unavailability, which depends on the number and type of components under maintenance as well as shipyard quality.
V. Interest rates, inflation indices, and investment horizon.

To understand the effects and behavior of the proposed model regarding its parameters, a sensitivity analysis was conducted by evaluating the risk of opportunity output of a single element against the variation of each parameter, where all the others remain constant. For a comparative assessment, the sensitivity analysis is conducted under the relative variation of nominal parameters while evaluating the relative output of the risk of opportunity. This assessment is conducted in the PV by considering estimated data at the fifth year of life. Accordingly, the results are presented in the Table 15 and Figure 39.

Table 15. Sensitivity Analysis on the Cost of Opportunity Parameters.

	t	5	NOMINAL COST	$ 2,453.36
	Probability of Failure (P_f)		Cost of Failure (C_f)	
NOMINAL VALUES	0.01		$ 150,000.00	
RELATIVE VALUES	VALUE	RELATIVE OUTPUT	VALUE	RELATIVE OUTPUT
0.25	0.0025	0.250	$ 37,500.00	0.794
0.5	0.005	0.500	$ 75,000.00	0.863
0.75	0.0075	0.750	$ 112,500.00	0.931
1	0.01	1.000	$ 150,000.00	1.000
1.25	0.0125	1.250	$ 187,500.00	1.069
1.5	0.015	1.500	$ 225,000.00	1.137
2	0.02	2.000	$ 300,000.00	1.274
2.5	0.025	2.500	$ 375,000.00	1.411
3	0.03	3.000	$ 450,000.00	1.548
	Non-Idle Fraction of C_{OS} (α)		Cost of Operation and Support (C_{OS})	
NOMINAL VALUES	0.1		$ 145,000,000.00	
RELATIVE VALUES	VALUE	RELATIVE OUTPUT	VALUE	RELATIVE OUTPUT
0.25	0.025	0.456	$ 36,250,000.00	0.456
0.5	0.05	0.637	$ 72,500,000.00	0.637
0.75	0.075	0.819	$ 108,750,000.00	0.819
1	0.1	1.000	$ 145,000,000.00	1.000
1.25	0.125	1.181	$ 181,250,000.00	1.181
1.5	0.15	1.363	$ 217,500,000.00	1.363
2	0.2	1.726	$ 290,000,000.00	1.726
2.5	0.25	2.089	$ 362,500,000.00	2.089
3	0.3	2.452	$ 435,000,000.00	2.452
	Unavailability Time (t_u)		Real Rate of Return (r)	
NOMINAL VALUES	10		0.025	
RELATIVE VALUES	VALUE	RELATIVE OUTPUT	VALUE	RELATIVE OUTPUT
0.25	2.5	0.456	0.00625	0.219
0.5	5	0.637	0.0125	0.457
0.75	7.5	0.819	0.01875	0.717
1	10	1.000	0.025	1.000
1.25	12.5	1.181	0.03125	1.308
1.5	15	1.363	0.0375	1.644
2	20	1.726	0.05	2.407
2.5	25	2.089	0.0625	3.308
3	30	2.452	0.075	4.370
	Investment Horizon [Ship Lifespan] (T)			
NOMINAL VALUES	20			
RELATIVE VALUES	VALUE	RELATIVE OUTPUT		
0.25	5	0.000		
0.5	10	0.293		
0.75	15	0.625		
1	20	1.000		
1.25	25	1.425		
1.5	30	1.905		
2	40	3.063		
2.5	50	4.546		
3	60	6.444		

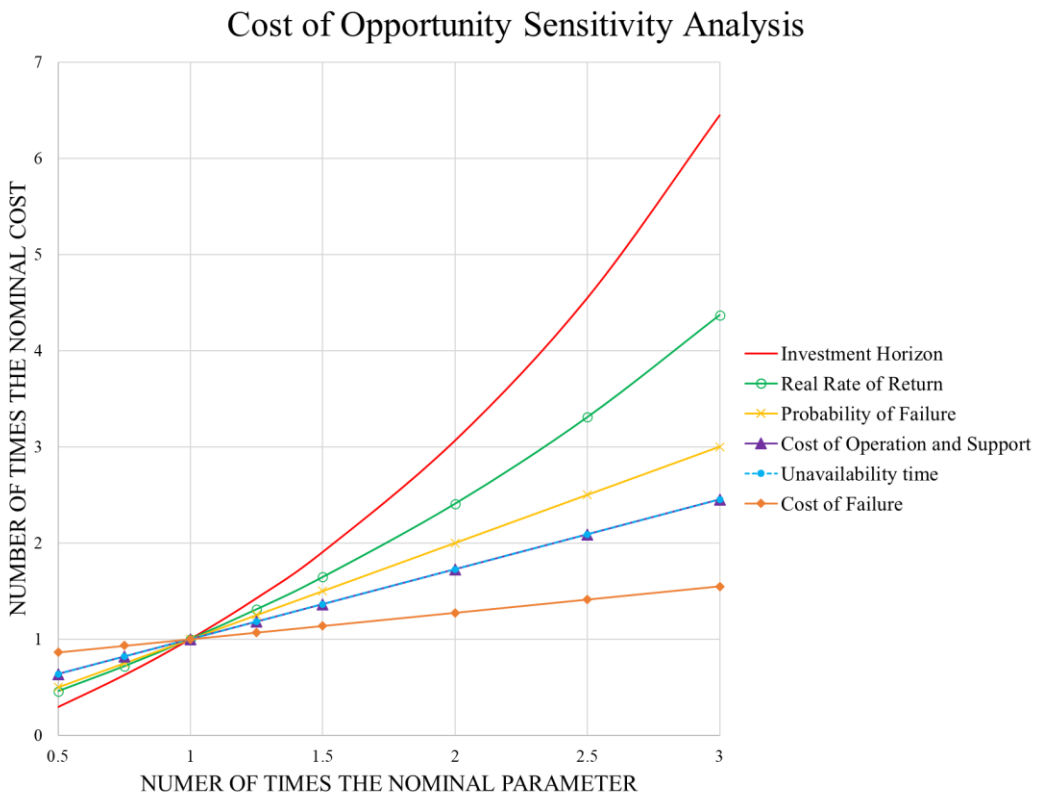


Figure 39. Cost of Opportunity Sensitivity Analysis.

As can be concluded from Figure 39, the Probability of Failure (p_f), Downtime Duration (t_u), Operational & Support Cost (C_{os}), and Cost of Failure (C_f) exhibit a linear influence on the Risk of Opportunity, in decreasing order of relative importance.

In contrast, the investment horizon T and the real rate of return r display a strongly nonlinear and increasing impact on the Risk of Opportunity, with T being the dominant factor. As expected, higher real rates of return r significantly amplify opportunity costs. However, a key insight from this analysis is that, for an evaluation year t, the effect of the fixed investment horizon T outweighs all other parameters.

Accordingly, the sensitivity analysis indicates that early unexpected downtimes in a naval vessel's life result in the highest opportunity costs, whereas late unplanned downtimes incur much lower costs. This model behavior is consistent with economic model assumptions regarding a finite investment horizon, since the loss of vessel function near the end of service life implies limited foregone value, given that most of the vessel's required operational value has already been delivered.

3.6 Conclusion

This Chapter delved into modeling the downtime duration, related costs, and expected costs regarding maintenance decisions by considering the emergent Maintainability (M) aspects between the SoI and the SS. Accordingly, three types of SIM costs were identified, explored, and modeled: Structural Cost (Section 3.2.1 and 3.3), Expected Cost of Failure (Section 3.2.2 and 3.4), and Expected Cost of Opportunity of Non-Planned Unavailability of Naval Vessels (Section 3.2.3 and 3.5). The conclusions on the research conducted on these cost types are described as follows:

I. **Structural Cost:** A comprehensive intervention workflow was analytically modeled with sequential and CONWIP discipline workstations. Accordingly, the arrangement and parts flow were based on GT, and the tasks were modeled to represent typical and logical intervention processes for ship repair. In this workflow, the CONWIP model was adapted to consider multiple and shared resources. Furthermore, DES validated this simplification on Jaamsim® software, which indicated that the analytical model errors are conservative and decrease while increasing the line load and decreasing variability, as expected. This new analytical repair model not only quantifies the Structural Cost, but is also necessary to develop the Expected Cost of Failure. It is also built to be incorporated under the OMCRO framework, explored in Chapter 4, which works as a platform to explore optimal decision-making regarding ship maintenance for corroded steel vessels. Accordingly, the analytical modeling can be incorporated into the optimization framework without great computational effort.

II. **Expected Cost of Failure:** The concept of risk was explored and defined as the monetary quantification of uncertain structural failure consequences on the crew, material and environment. This failure was limited to the “need for repair”, according to renewal decision thresholds, and does not account for mitigation measures or local assessments on stress and strength. Consistently, the uncertainty was measured as the probability of failure developed in Chapter 2, while the consequences were modeled by monetary units according to the cost of averting fatalities, structural costs (developed in this Section), costs for replacing the ship and payload, and costs

associated with oil spills. The assessment on these already explored domains was adapted for naval vessels and associated with the same hazard severity levels that defined probability of failure thresholds in Section 2.6. The Expected Cost of Failure models the risk of failure and is used as a component of the risk of opportunity (item III). Both are operational risks and part of the optimization trade-off on the cost-effective assessment modeled by Chapter 4.

III. **Expected Cost of Opportunity of Non-Planned Unavailability of Naval Vessels:** This work introduces a novel practical engineering-economic model to quantify the opportunity cost of unplanned naval vessel unavailability, with its rationale contextualized by defense economics and focused on a distinct asset-level question. Planned downtimes are treated as an agreement to capital asset acquisition and therefore excluded from opportunity cost, while unplanned downtimes are modeled as a foregone return and economic inefficiency from public investment. The proposed model integrates the expected cost of unplanned downtime by considering (1) the unbudgeted cost of failure and (2) the budgeted but not allocated operation and support costs during unavailability, to estimate the foregone return of capital. It incorporates parameters related to degradation, operation, safety, material, maintenance, and macroeconomics, and was particularly applied to corrosion-driven failure mode. Sensitivity analysis indicates that the investment horizon of the foregone alternative is the dominant driver of opportunity cost, resulting in significantly higher penalties for early-life unplanned downtime.

The implementation of this model in the OMCRO framework is expected to increase the cost between downtimes, affecting the trade-off between risk and planned maintenance.

Chapter 4 Opportunistic Maintenance Optimization

"The time to repair the roof is when the sun is shining."
- John F. Kennedy (Kennedy 1962)

This Chapter introduces the novel Opportunistic Maintenance Cost and Risk Optimization (OMCRO) framework, which provides support for cost-effective decision making based on the RAMS architecture proposed in Chapter 1. The new approach modifies an already established Cost and Risk Optimization (CRO) problem formulation (Melchers and Beck 2018; Ayyub et al. 2002) by considering an optimized scheduling and grouping of multiple components to be opportunistically repaired, thus exploiting the expensive downtime. This problem is solved using grouping strategies and a Genetic Algorithm (GA) to minimize the total cost over the operational use of the system during its life cycle. The OMCRO framework is verified, validated, and used in an unprecedented quantitative analysis conducted to enhance the understanding of the Maintainability (M) behavior as an emergent factor of ship structure (SoI) Reliability (R) and shipyard (SS) Quality (Q), leveraging a RAMSQ concept. In this regard, the quantitative results are translated into qualitative communication by developing a RAMSQ Chart. Therefore, the proposed framework is built upon a logical and straightforward process that can be understood by all stakeholders, creating trust in decision-making, which is valuable for implementation. This unique framework is flexible and can be applied to any system and subsystem with multiple failure modes.

4.1 Introduction

As introduced in Section 1.2, the maintenance strategy is a component of the maintenance plan, and it can be either corrective or preventive (Pinciroli, Baraldi, and Zio 2023; Blanchard 1998), with different types for the latter. Moreover, there is no correct strategy; rather, the Technical Management needs to consider many factors to adopt and tailor a strategy or a

combination of them for a particular system. This decision must consider that each maintenance strategy requires different amounts of data, technology, and, consequently, cost. Accordingly, the increasing amounts of data required for the different maintenance strategies are presented in Figure 40 (Pinciroli, Baraldi, and Zio 2023), which highlights that the RAMS approach is incorporated into all preventive strategies.

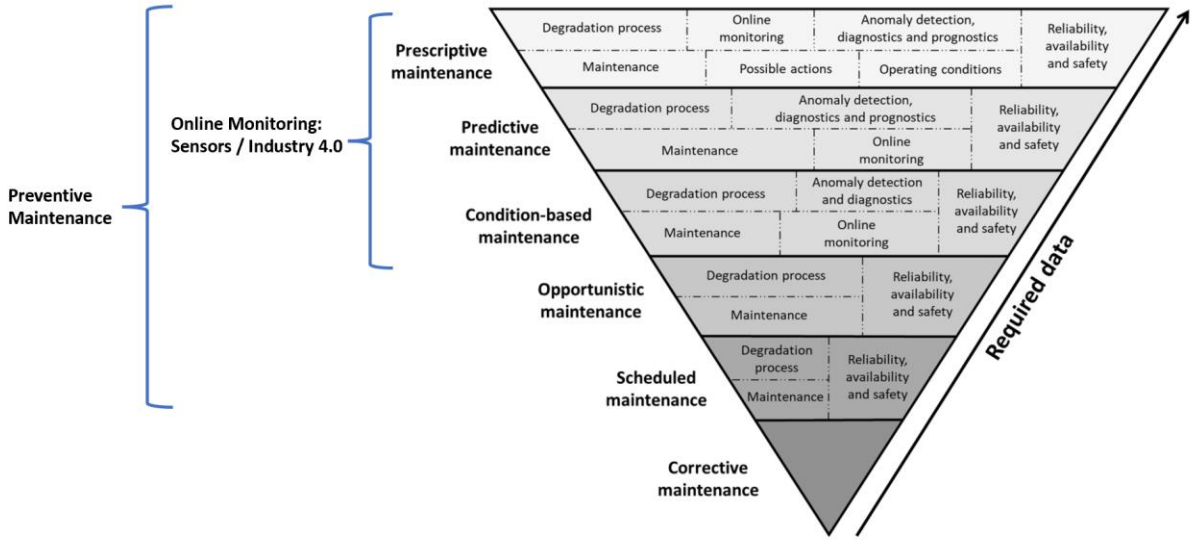


Figure 40. Maintenance Strategies (Pinciroli, Baraldi, and Zio 2023).

As mentioned in Section 1.2, the optimization of opportunistic maintenance is not well explored when compared with other strategies, as shown in Figure 5 (Pinciroli, Baraldi, and Zio 2023). In addition, it is not formalized for naval maintenance applications, although it is suitable for exploiting costly downtimes.

Even though this is an overlooked field, the opportunistic maintenance strategy concept is straightforward, as the benefits of grouping elements or subsystems under the same maintenance action to exploit downtime are well understood by stakeholders. However, the decision process on what and when to group, supporting a cost-effective solution, is complex, since there is a mutual effect between grouping decisions and schedules.

As discussed by (Pinciroli, Baraldi, and Zio 2023), the definitions of the variables, objective function, and constraints in the optimization process for a cost-effective solution depend

on the knowledge, information, and data (KID) of the SoI, SS, environment, and operation. The same work identifies and classifies KID topics and types as follows:

I. KID topic:

A. Maintenance
B. Reliability, availability, and safety
C. Degradation process
D. Health state detection
E. Diagnostics
F. Prognostics
G. Operating conditions
H. Objective function

II. KID type:

A. Expert knowledge
B. Models
C. Data
    1. Numerical
    2. Textual
    3. Images

KID types and industry domains were correlated by (Pinciroli, Baraldi, and Zio 2023). Accordingly, it is possible to conclude that almost all industries, specifically those related to the naval industry, utilize all types of KID.

Considering the decisions made up to this point, it is possible to describe the KID topics and types that apply to the SIM framework proposed by this research. Consistently, Table 16 correlates and outlines each KID topic to all KID types. All of them are related to a specific chapter covered in this dissertation. Moreover, they are all technically developed with new contributions, except specific tasks related to health state detection, diagnostics, and prognostics, which require data collection with online monitoring, surveys, and models of belief state updates. Although these Industry 4.0 tasks are very important for implementation and decision support updates, they are not considered in this current research, although they were explored and proposed as a future framework in Chapter 6.

Table 16. Structural Integrity Management KID.

SIM KID	TYPE		
TOPIC	**Expert Knowledge**	**Models**	**Data**
Maintenance	Known maintenance strategy, intervention actions, workflow, and related parameters (This Chapter and Chapter 3)	Model intervention time and costs (This Chapter and Chapter 3)	Numerical: Parameters for time and cost models (Chapter 3)
Reliability and Safety	Known definition of failure and probability of failure thresholds (Chapter 2)	Models of probability of failure and quantitative risk (Chapter 2 and Chapter 3)	Numerical: Parameters of degradation and risk models (Chapter 2 and Chapter 3)
Degradation Process	Known degradation parameters (Chapter 2)	Model system degradation considering uncertainty (Chapter 2)	Numerical: Parameters of the degradation model (Chapter 2)
Health State Detection*	Degradation estimation based on OMCRO framework (This Chapter), survey, and online monitoring systems*	Inspection Plan guided by the previous OMCRO framework solution (This Chapter) and online monitoring systems*	Numerical, Textual, and Images: The data collection validates or updates the belief state of degradation*
Diagnostics*	Current health state of detection*	Model updates OMCRO belief diagnostics*	Numerical: The current health state of detection validates or updates the belief diagnostics*
Prognostics*	Current diagnostics* and prognostics assessment based on the OMCRO model (This Chapter)	Model updates* OMCRO prognostics (This Chapter)	Numerical: Current diagnostics* and risk parameters to update belief prognostics (This Chapter, Chapter 2, and Chapter 3)
Operation Condition	Known operational and environmental parameters needed to simulate degradation models (Chapter 2)	Model of estimated operational and environmental conditions (Chapter 2) and online monitoring systems*	Numerical: Collected data* and operational and environmental parameters (Chapter 2)
Objective Function	This work (Chapter 2, Chapter 3, and This Chapter)	OMCRO framework (Chapter 2, Chapter 3, and This Chapter)	Numerical: Collected data* and cost and risk parameters (Chapter 2, Chapter 3, and This Chapter)
* Data collection with online monitoring systems, surveys, and belief state updates are not considered in this current research but were explored and proposed as a future framework (Chapter 6)			

According to the KID definition and developments up to this point, the OMCRO model is herein explored, developed, verified, validated, and used under simulation scenarios. The

quantitative results are also explained in a qualitative rationale for clear communication with stakeholders.

4.2 Literature Survey

Maintenance optimization literature was explored in a comprehensive and updated survey by (Pinciroli, Baraldi, and Zio 2023). The authors related optimization criteria to industrial fields of application. The criteria considered are:

I. Economic
II. Safety
III. Management
IV. Performance
V. Temporal
VI. Practicality

The most common criteria across the industries are economic and safety, which look for CE while complying with the RAMS approach. In this case, Safety (S) is related to Reliability (R), although they do not imply the same thing. According to discussions in Chapter 1, Maintainability (M) and Availability (A) are emergent qualities that are output from the integration of SoI, SS, environment, and operation. Therefore, CE, R, and S were selected for an integrated assessment and are described as follows:

I. Economic (CE): Minimize maintenance cost
II. Reliability (R) and Safety (S): Minimize quantitative risk bounded by safety levels
III. Output: Optimal Maintainability (M) and Availability (A) over the operational life

Furthermore, as mentioned in Section 2.4, the degradation model accounts for uncertainty, which is measured by probability. Melchers and Beck (Melchers and Beck 2018) described how uncertainty can be approached by different complexity levels of optimization problems, as illustrated in Figure 41.

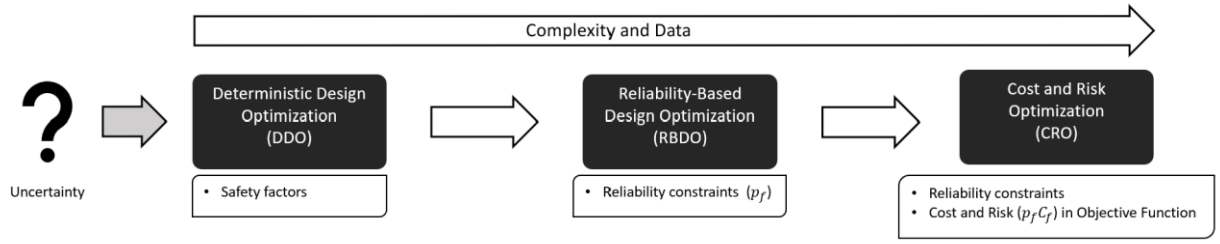


Figure 41. Uncertainty and Optimization Problems.

Therefore, although economic and reliability are two different criteria, (Melchers and Beck 2018; Ayyub et al. 2002) converge in the use of a single objective function, which includes both, by using the total expected cost. Hence, the idea is to consider a trade-off between economy (life cycle cost) and risk (expected cost). This trade-off problem is called Life Cycle Cost and Risk Optimization (LCRO) (Melchers and Beck 2018) and is expressed as the most complex problem in Figure 41.

Since the modeling scope of this research problem is only on the system use, and not the whole life cycle, the objective function can be reduced to a Maintenance Cost and Risk Optimization (MCRO) approach, as presented in Equation 57.

$$\begin{gathered} \text{minimize } C_T \\ C_T = C_M + C_{EF} + C_{EO} \\ \text{subject to } p_f(t) \leq p_{f_T} \end{gathered} \tag{57}$$

Considering:

I. C_T: Total Expected Cost
II. C_M: Maintenance Cost
III. C_{EF}: Expected Cost of Failure
IV. C_{EO}: Expected Cost of Opportunity

Considering that the maintenance activity in this work is related to the structural system, C_M is considered the Structural Cost C_S as defined by Section 3.3.

In a review conducted by (Pinciroli, Baraldi, and Zio 2023), optimization approaches were related to the desired outcomes. The optimization approaches incorporated in the maintenance strategies are presented:

I. Mathematical Approaches (MA)
II. Mixed Integer Programming (MIP)
III. Dynamic Programming (DP)
IV. Metaheuristic Search Algorithms (MSA)

Among these, MSA and DP are the only ones described that work with the desired outcome of optimal grouping of components for maintenance, a requirement of the opportunistic strategy that has not been well explored in the literature using optimization approaches, as previously mentioned.

The issue with using the DP approach is the complexity of working with multiple components to achieve a main and shared goal. In addition, the definition of transition probabilities is not only time-dependent but also dependent on the grouping decision, which increases the complexity of this approach.

Therefore, this study considers the MSA approach using a Genetic Algorithm (GA). The GA was chosen because of its known popularity and its fit in the yearly-discrete-based domain of maintenance scheduling. In addition, (Pinciroli, Baraldi, and Zio 2023) indicated that GA was used before in opportunistic maintenance research conducted by Vu *et al.* (Vu et al. 2014), which stated that it is a relevant optimization approach for the maintenance framework and can significantly reduce computational time.

Specifically, GA utilizes the existing population or solutions as the foundation for producing children that will constitute the next evolutionary phase in each progressive phase. This involves selecting parents, a subset of individuals from the current population, who contribute their genetic traits (vector components) to shape the traits of their children. Preference is given to individuals with higher fitness scores when picking parents. Fitness scores represent a quantifiable measure of how well a candidate solution solves the problem.

The GA, therefore, explores and exploits solutions by working with three distinct categories of children for subsequent generations:

I. **Elite Children:** Individuals from the current generation are distinguished based on their superior fitness scores. These individuals are automatically granted passage to the next generation.

II. **Crossover Children:** Emerge from the combination of vectors from a designated pair of parents.

III. **Mutation Children:** Generated by the introduction of random modifications or mutations to the genetic composition of a single parent.

Figure 42 illustrates the GA process (Vu et al. 2014):

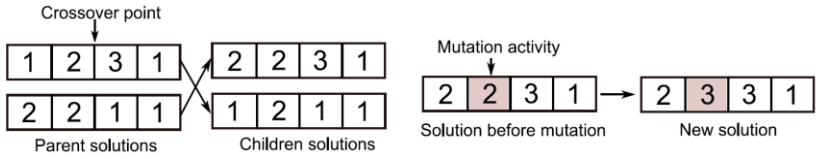


Figure 42. GA process (Vu et al. 2014).

Therefore, the optimization assessment is structured as follows:

I. Maintenance strategy: Opportunistic Maintenance
II. Optimization criteria: Economic (CE), Reliability (R), and Safety (S)
III. Optimization problem: Maintenance Cost and Risk Optimization (MCRO)
IV. Optimization constraint: Probability of failure threshold
V. Optimization approach: Genetic Algorithm (GA)

So far, the optimization problem has only been explored for single elements. However, for opportunistic maintenance, the grouping decision process during the downtime must be considered. In this regard, previous work has been conducted to account for the repair management of multiple components (Vu et al. 2014; Dylan 2015; Saydam and Frangopol 2015). Although all of them use GA as an optimization approach, (Vu et al. 2014) only considers economic criteria, (Dylan 2015) does not consider risk, and (Saydam and Frangopol 2015) do not consider an opportunistic approach. Therefore, the MCRO is adapted to the novel OMCRO framework to cover all the proposed decisions.

4.3 Maintenance Cost and Risk Optimization (MCRO)

There is convergence between (Melchers and Beck 2018; Ayyub et al. 2002) in using the reliability constraint in the MCRO problem. This constraint is expressed by the probability of failure threshold. Also, the significant difference between the Reliability-Based Design Optimization (RBDO) and the MCRO is that, in the latter, reliability is not only a constraint but part of the objective function (Melchers and Beck 2018).

Therefore, it is necessary to establish acceptance targets for engineering decisions. Accordingly, (Ayyub et al. 2002) presents three methods to select these targets:

I. **Expert Opinion:** Expert judgment and elicitation.
II. **Code Calibration:** Rules and guidelines (e.g., Classification Societies).
III. **Economic Model:** Target is a design variable for the optimization process.

In this study, the reliability constraint is defined by a probability of failure threshold, treated as an expert-defined input. Therefore, Expert Opinion is adopted as the target selection method, as already explored in Section 2.6 to define probability of failure thresholds for structural damage, as suggested by (Mansour et al. 1997). Therefore, the optimization problem for a single component is related to Equation 57 and can be expressed by Equation 58.

$$\begin{gathered}\text{Find } \boldsymbol{t}_{\boldsymbol{m}}^{*} \text{ which minimizes } \sum_{t=1}^{t=T_l} C_T(t, \boldsymbol{t_m}) \\ \text{subject to } p_f(t) \leq p_{f_T} \\ \text{Where:} \\ C_T(t, \boldsymbol{t_m}) = \delta_{tt_{m_j}} C_S + p_f(t, \boldsymbol{t_m})(C_f + C_o)\end{gathered} \tag{58}$$

Considering:

I. All costs in Present Value (PV) using the inflation rate as a discount
II. t: Time in years
III. T_L: Last year in which the analysis is being conducted (time limit)
IV. $\boldsymbol{t_m}$**:** Array of n decided years for maintenance downtime, where t_{m_j} is the j^{th} downtime year
V. $C_T(t, \boldsymbol{t_m})$: Total Expected Cost at time t
VI. $\delta_{tt_{m_j}}$: Kronecker Delta for maintenance downtime

$$\delta_{tt_{m_j}} = \begin{cases} 0\,, & t \neq t_{m_j}\ ,\ \ j: 1 \dots n \\ 1\,, & t = t_{m_j}\ ,\ \ j: 1 \dots n \end{cases}$$

VII. C_S: Structural Cost.
VIII. $p_f(t, \boldsymbol{t_m})$: Time-Based Probability of Failure with renewal ($p_f = 0$) when $t = t_{m_j}$
IX. C_f: Cost of Failure (Equation 39)
X. $C_{EF} = p_f C_f$: Expected Cost of Failure (Risk) (Equation 38)
XI. C_o: Cost of Opportunity (Equation 50)
XII. $C_{EO} = p_f C_o$: Expected Cost of Opportunity (Risk of Opportunity) (Equation 47)
XIII. p_{f_T}: Probability of failure threshold

4.4 Opportunistic Maintenance Cost and Risk Optimization (OMCRO)

Equation 58 indicates the MCRO problem for a single component. Considering that downtime is expensive, many components can be renewed together using an opportunistic approach.

The probability of failure of a single component depends on the last time this component was decided to be renewed. Accordingly, the repair time mutually depends on the group of elements to be repaired. Therefore, the decision on how many and which components will be renewed together, and when and how many downtimes will occur to repair these elements over the operational phase of the life cycle, requires a grouping strategy.

4.4.1 Time-Grouping Strategy

Similar to MCRO for a single component, the grouping strategy also considers maintenance downtimes ($\boldsymbol{t_m}$) as a design variable. It is important to mention that the number of downtimes, thus, the number of design variables in $\boldsymbol{t_m}$ is not previously defined, although this number is bounded by an analysis horizon and operational window.

The analysis horizon, or Time Limit (T_L), is defined as the maximum year a maintenance strategy can be developed. Therefore, it is the latest domain bound for $\boldsymbol{t_m}$ since no renewal is considered at and after T_L.

The Operational Window ($\boldsymbol{O_w}$) is defined as the time intervals between consecutive maintenance downtimes, in other words, the differences between consecutive design variables in $\boldsymbol{t_m}$, as presented by Equation 59. No repair is conducted during an operational window.

$$O_{w_i} = t_{m_{i+1}} - t_{m_i} \tag{59}$$

Figure 43 illustrates the relationship between the design variable $\boldsymbol{t_m}$, the time limit T_L , and the operational window $\boldsymbol{O_w}$. The number of downtimes, hence the number of elements in $\boldsymbol{t_m}$ is n. It is important to highlight that the design variable $\boldsymbol{t_m}$ and the operational window $\boldsymbol{O_w}$ are integer arrays, and that the structural renewal is completed in no longer than one year.

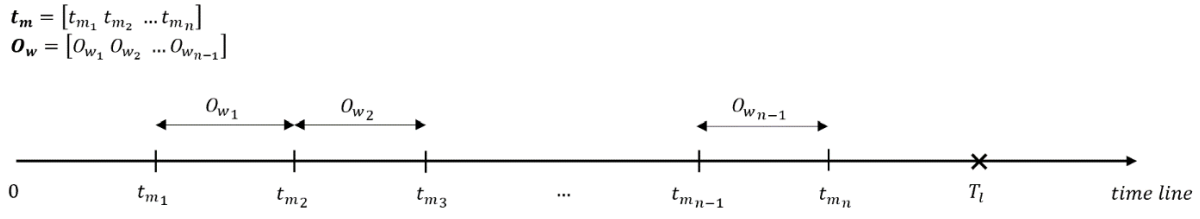


Figure 43. Design variable, Time Limit, and Operational Window.

The $\boldsymbol{t_m}$ solution, thus $\boldsymbol{O_w}$, will deterministically define the grouping of elements. This statement is significant for the optimization process and is justified by the Time Grouping Strategy, which is a straightforward three-step process, described as follows:

I. Step 1: Single element time threshold

The p_f and p_{f_T} are combined to define a renewal time threshold for each element.

II. Step 2: Single element repair (time threshold repetitions)

At the time thresholds, the elements are expected to be individually renewed to "as new" condition, and as the degradation process restarts, the threshold times are repeated over time.

III. Step 3: Grouping and Anticipation

When an element threshold renewal time occurs inside an operational window, the renewal will be grouped in the immediate previous maintenance downtime. This guarantees that no repair is conducted inside an operational window and that repairs are never performed after safety limits are reached. Another consideration is that the previous grouping process affects the future time thresholds of single elements since the grouping may anticipate repair, but never delay. To consider this anticipation effect in future time thresholds, the number of years the element is anticipated due to grouping is propagated to future repeated time thresholds of the same element.

4.4.1.1 Time-Grouping Results

The step-by-step process description is demonstrated by hand calculation, presented in Appendix B. This example considers a solution where $\boldsymbol{t_m}$ = [5 10 15 20] for $T_L = 25$ years to group the five elements presented in Figure 13 with failure times already predicted in Figure 19 to 23.

Therefore, considering the input solution $\boldsymbol{t_m}$ = [5 10 15 20] for $T_L = 25$, the groups $\boldsymbol{G_m}$ are defined:

I. Year 5: [2, 4, 5]
II. Year 10: [1, 2, 4, 5]
III. Year 15: [2, 3, 4, 5]
IV. Year 20: [1, 2, 4, 5]
V. $\boldsymbol{G_m}$ = {[2, 4, 5], [1, 2, 4, 5], [2, 3, 4, 5], [1, 2, 4, 5]}

Considering the groups, it is then possible to hand-calculate, using Microsoft® Excel® spreadsheets, the Structural Cost C_S, the Expected Cost of Failure C_{EF}, and the Expected Cost of Opportunity C_{EO} with the models described in Chapter 2 and Chapter 3. Accordingly, environmental and operational parameters are presented by Table 6, and the elements' and costs' parameters are respectively presented in Appendix C and D.

Therefore, Appendix E presents the results for the intervention's cost and time for all tasks in each downtime, also C_S, C_{EF}, and C_{EO} over time. The overall result for C_S is presented in USD PV by Table 17, and as FV by Table 18. Also, the overall results for C_{EF} and C_{EO} are respectively presented in Appendix Figure E.13 and E.14 as FV.

Consistently, Figure 44 provides the combination of all costs over time in FV, while the sum of the costs in PV, which is the Total Expected Cost C_T, is presented by Table 19. Discussions on the results are presented in Section 4.4.3.

Table 17. Structural Cost C_S in PV (USD) – Time-Grouping.

YEARS	ELEMENTS	DRYDOCK	QUAY	TOTAL
5	**[2, 4, 5]**	$ 476,590.79	$108,716.50	$ 585,307.29
10	**[1, 2, 4, 5]**	$ 569,050.68	$108,716.50	$ 677,767.18
15	**[2, 3, 4, 5]**	$ 521,102.53	$108,716.50	$ 629,819.02
20	**[1, 2, 4, 5]**	$ 569,050.68	$108,716.50	$ 677,767.18
			TOTAL	$ 2,570,660.68

Table 18. Structural Cost C_S in FV (USD) – Time-Grouping.

YEARS	ELEMENTS	DRYDOCK	QUAY	TOTAL
5	**[2, 4, 5]**	$ 526,194.74	$120,031.80	$ 646,226.54
10	**[1, 2, 4, 5]**	$ 693,669.61	$132,524.80	$ 826,194.41
15	**[2, 3, 4, 5]**	$ 701,335.39	$146,318.09	$ 847,653.48
20	**[1, 2, 4, 5]**	$ 845,579.38	$161,547.00	$ 1,007,126.38

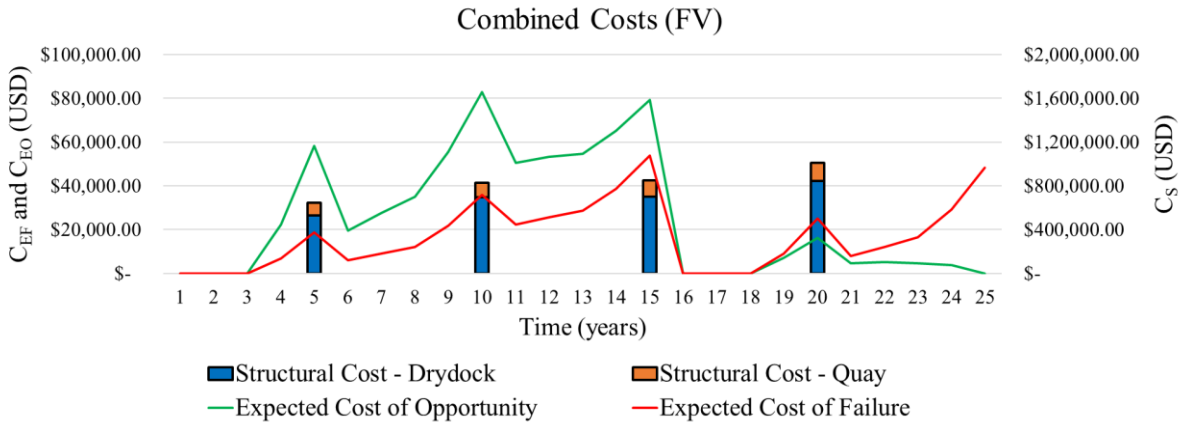


Figure 44. Combined Costs in FV – Time-Grouping.

Table 19. Costs in PV and Total Expected Cost C_T – Time-Grouping.

STRUCTURAL COST	$ 2,570,660.68
EXPECTED COST OF FAILURE	$ 317,290.31
EXPECTED COST OF OPPORTUNITY	$ 519,655.72
TOTAL EXPECTED COST	**$ 3,407,606.71**

4.4.2 Policy-Grouping Strategy

So far, the Grouping Strategy has just considered grouping decisions based on time thresholds. However, stakeholders may decide to consider other aspects for grouping decisions, such as location, repair practical aspects, manufacturing needs, relations between elements, and any other decision. Therefore, this Section explores the already developed Time-Grouping Strategy with more advanced considerations. These new considerations are termed Policies, and their implementation is based on four steps:

I. Step 1: Definition of Policies

Define which policy elements shall be verified by relationship and which policy elements shall be verified against specifications.

II. Step 2: Definition of Matrices

Each specified policy requires an N2 matrix to describe the interrelationship between elements or a standard matrix for proper element specifications. This work considers the N2 Matrix as a binary (elements, elements) matrix that stores the relationship between elements of a system. Therefore, given that m_{ij} is a matrix element, Equation 60 describes the N2 matrix.

$$m_{ij} = \begin{cases} 1, & if\ the\ rule\ is\ verified\ true \\ 0, & if\ the\ rule\ is\ verified\ false \end{cases} \tag{60}$$

The matrix is N2 if m_{ij} verifies rules between elements. The matrix is standard (elements, k) if it verifies rules between elements and k specifications.

III. Step 3: Decision Tree (DT)

The decision to group elements or not is defined based on a Decision Tree (DT) of interconnected policies, represented by matrices. Each DT node verifies the satisfaction of policies by every element.

IV. Step 4: Policy Matrix

When following the rules in the DT logical sequence, it is possible to define a final matrix that combines all relations between elements concerning all policies. Therefore, defining an overall policy.

The Policy-Grouping Strategy starts with the definition of groups based on the Time-Grouping Strategy. The results are then modified to reflect the satisfaction of the adopted policies.

4.4.2.1 Policy-Grouping Results

The step-by-step process description is demonstrated by hand calculation. This is done by still considering the five elements presented in Figure 13, with failure times already predicted in Figure 19 to 23. The Time-Grouping Strategy is the initial grouping driver in which the Policy-Grouping Strategy will be incorporated. Therefore, the policy steps are applied inside Step 3 of the Time-Grouping Strategy, and are exemplified as follows:

I. Step 1: Definition of Policies

A. Both in the same or adjacent compartments
B. Both are welded together
C. Both time threshold differences are smaller than 2x the minimum operation window (Operational Window Limit = 3 years)
D. Both are repaired together due to manufacturing needs
E. Both are inside tank or outer hull below the seawater

II. Step 2: Definition of Matrices

N2 Matrices:

A. PMC: Policy Matrix for Compartment (Policy A)
B. PMW: Policy Matrix for Welding (Policy B)
C. PMT: Policy Matrix for Time (Policy C)
D. PMM: Policy Matrix for Manufacturing (Policy D)

Standard Matrix (elements, 2):

E. PMTS: Policy Matrix for Tank or Seawater (Policy E)

III. Step 3: Decision Tree (DT)

The DT (Figure 45) is then built as a connection of multiple binary matrices (Equation 61 to 65). The PMW and PMM are the only matrices that need to be input by the user, as the others can be built based on the already input parameters. The N2 matrices' diagonals reflect the self-relation of the element, which can be discarded. Therefore, the diagonal of the N2 binary matrices is flagged with the number 2.

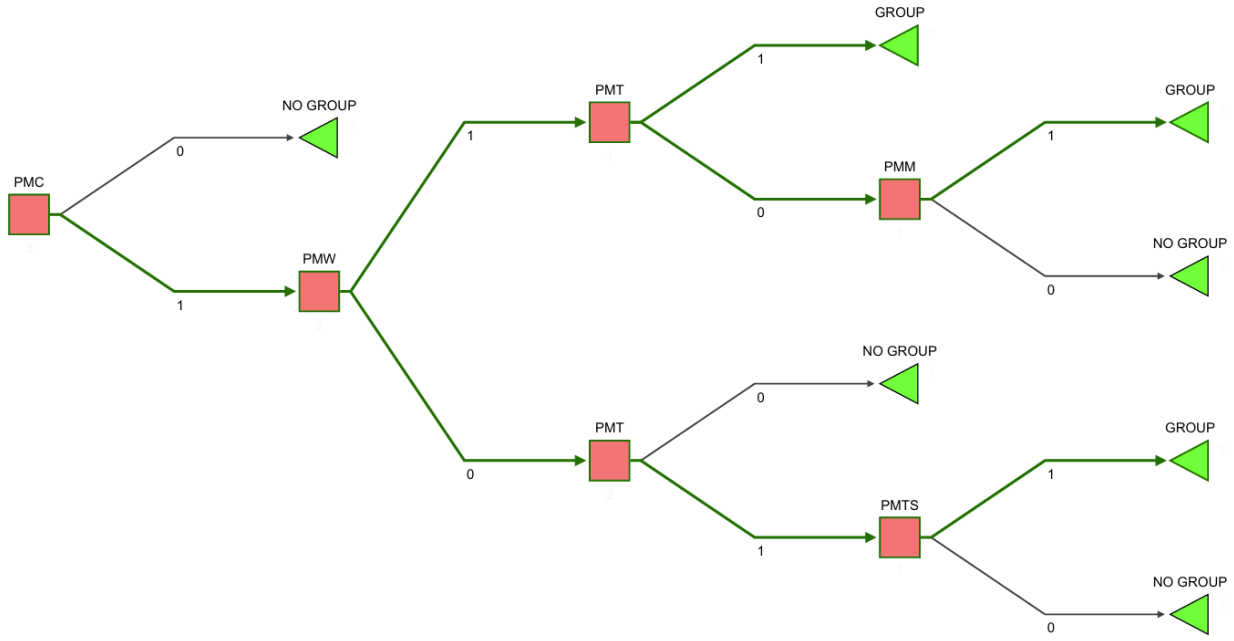


Figure 45. Decision Tree.

$$PMC = \begin{bmatrix} 2 & 1 & 1 & 0 & 1 \\ 1 & 2 & 1 & 0 & 0 \\ 1 & 1 & 2 & 0 & 0 \\ 0 & 0 & 0 & 2 & 0 \\ 1 & 0 & 0 & 0 & 2 \end{bmatrix} \quad (61)$$

$$PMW = \begin{bmatrix} 2 & 0 & 0 & 0 & 0 \\ 0 & 2 & 1 & 0 & 0 \\ 0 & 1 & 2 & 0 & 0 \\ 0 & 0 & 0 & 2 & 0 \\ 0 & 0 & 0 & 0 & 2 \end{bmatrix} \quad (62)$$

$$PMT = \begin{bmatrix} 2 & 1 & 1 & 0 & 0 \\ 1 & 2 & 0 & 1 & 1 \\ 1 & 0 & 2 & 0 & 0 \\ 0 & 1 & 0 & 2 & 1 \\ 0 & 1 & 0 & 1 & 2 \end{bmatrix} \quad (63)$$

$$PMM = \begin{bmatrix} 2 & 0 & 0 & 0 & 0 \\ 0 & 2 & 1 & 0 & 0 \\ 0 & 0 & 2 & 0 & 0 \\ 0 & 0 & 0 & 2 & 0 \\ 0 & 0 & 0 & 0 & 2 \end{bmatrix} \quad (64)$$

$$PMTS = \begin{bmatrix} 1 & 0 \\ 1 & 0 \\ 1 & 0 \\ 0 & 1 \\ 1 & 1 \end{bmatrix} \quad (65)$$

IV. Step 4: Policy Matrix

The Policy Matrix (PM) (Equation 66) is defined based on the previous matrices connected in the DT.

$$PM = \begin{bmatrix} 2 & 1 & 1 & 0 & 0 \\ 1 & 2 & 1 & 0 & 0 \\ 1 & 0 & 2 & 0 & 0 \\ 0 & 0 & 0 & 2 & 0 \\ 0 & 0 & 0 & 0 & 2 \end{bmatrix} \quad (66)$$

The Policy Matrix reflects that:

I. When Element 1 is repaired, 2 and 3 are repaired
II. When Element 2 is repaired, 1 and 3 are repaired
III. When Element 3 is repaired, 1 is repaired

Therefore, the Policy Matrix solution is then incorporated into the Time-Grouping Strategy. Whenever an element is grouped by time, it must be checked if a policy requires other

elements to be grouped. After checking that these new elements are not already grouped, they will be grouped by policy and propagate anticipation for future time thresholds, similar to Step 3 of the Time-Grouping Strategy. Again, the new grouped elements will be checked to verify if they require other elements to be grouped by policy. This process is repeated iteratively until there are no more elements to be grouped by policy. Accordingly, this process is demonstrated by hand calculation in Appendix F. Furthermore, this example considers a solution where $\boldsymbol{t_m}$ = [5 10 15 20] for $T_L = 25$ years to group the five elements presented in Figure 13 with failure times already predicted in Figure 19 to 23.

Therefore, considering the input solution $\boldsymbol{t_m}$ = [5 10 15 20] for $T_l = 25$, the groups $\boldsymbol{G_m}$ are defined:

I. Year 5: [1, 2, 3, 4, 5]
II. Year 10: [1, 2, 3, 4, 5]
III. Year 15: [1, 2, 3, 4, 5]
IV. Year 20: [1, 2, 3, 4, 5]
V. $\boldsymbol{G_m}$ = {[1, 2, 3, 4, 5], [1, 2, 3, 4, 5], [1, 2, 3, 4, 5], [1, 2, 3, 4, 5]}

Considering the groups, it is then possible to hand-calculate, using Microsoft® Excel® spreadsheets, the Structural Cost C_S, the Expected Cost of Failure C_{EF}, and the Expected Cost of Opportunity C_{EO} with the models described in Chapter 2 and Chapter 3. Accordingly, environmental and operational parameters are presented by Table 6, and the elements' and costs' parameters are respectively presented in Appendix C and D.

Therefore, Appendix G presents the results for the intervention's cost and time for all tasks in each downtime, also C_S, C_{EF}, and C_{EO} over time. The overall result for C_S is presented in USD PV by Table 20, and as FV by Table 21. Also, the overall results for C_{EF} and C_{EO} are respectively presented in Appendix Figure G.5 and G6 as FV.

Consistently, Figure 46 provides the combination of all costs over time in FV, while the sum of the costs in PV, which is the Total Expected Cost C_T, is presented by Table 22. Discussions on the results are presented in Section 4.4.3.

Table 20. Structural Cost C_S in PV (USD) – Policy-Grouping.

YEARS	ELEMENTS	DRYDOCK	QUAY	TOTAL
5	**[1,2,3,4,5]**	$ 614,130.63	$ 108,716.50	$ 722,847.12
10	**[1,2,3,4,5]**	$ 614,130.63	$ 108,716.50	$ 722,847.12
15	**[1,2,3,4,5]**	$ 614,130.63	$ 108,716.50	$ 722,847.12
20	**[1,2,3,4,5]**	$ 614,130.63	$ 108,716.50	$ 722,847.12
			TOTAL	$ 2,891,388.50

Table 21. Structural Cost C_S in FV (USD) – Policy-Grouping.

YEARS	ELEMENTS	DRYDOCK	QUAY	TOTAL
5	**[1,2,3,4,5]**	$ 678,049.84	$ 120,031.80	$ 798,081.63
10	**[1,2,3,4,5]**	$ 748,621.81	$ 132,524.80	$ 881,146.61
15	**[1,2,3,4,5]**	$ 826,538.97	$ 146,318.09	$ 972,857.06
20	**[1,2,3,4,5]**	$ 912,565.81	$ 161,547.00	$ 1,074,112.80

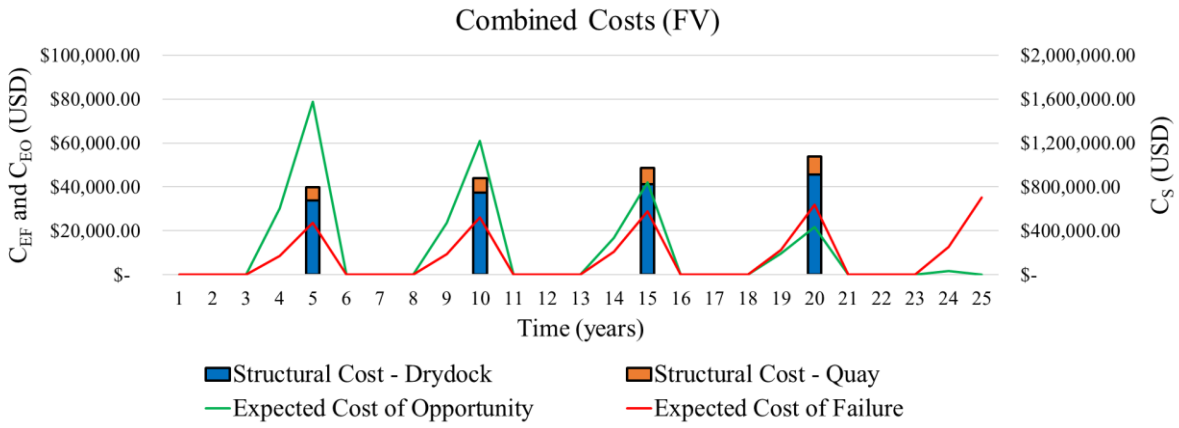


Figure 46. Combined Costs in FV – Policy-Grouping.

Table 22. Costs in PV and Total Expected Cost C_T – Policy-Grouping.

STRUCTURAL COST	$ 2,891,388.50
EXPECTED COST OF FAILURE	$ 146,199.43
EXPECTED COST OF OPPORTUNITY	$ 235,558.96
TOTAL EXPECTED COST	**$ 3,273,146.89**

4.4.3 Discussion on the Results of the Grouping Strategies

Observing Figure 44 and 46, it is evident that C_S is a payoff for risk reduction. The quantification of this effect validates the SoI upkeep dynamics discussed in Chapter 1 and metaphorically illustrated by Figure 1.

Accordingly, the risks increase with time between maintenance actions and are renewed following repair interventions. Moreover, the risk of opportunity decreases as the investment horizon is approached, representing zero value at the end of the vessel's service life. This behavior is consistent with the model assumptions, as previously discussed, which imply higher opportunity costs for early unexpected downtimes and assume zero operational tangible value at the end of the service life.

The overall results of the grouping strategies from Sections 4.4.1.1 and 4.4.2.1 are consolidated in Table 23. The same information is illustrated by Figure 47 and 48.

Table 23. Results of the Grouping Strategies.

	TIME-GROUPING [MILLIONS USD]	COST CONTRIBUTION PERCENTAGE	POLICY-GROUPING [MILLIONS OF USD]	COST CONTRIBUTION PERCENTAGE
STRUCTURAL COST	$ 2.57	75.44%	$ 2.89	88.34%
EXPECTED COST OF FAILURE	$ 0.32	9.31%	$ 0.15	4.47%
EXPECTED COST OF OPPORTUNITY	$ 0.52	15.25%	$ 0.24	7.20%
TOTAL EXPECTED COST	**$ 3.41**	100%	**$ 3.27**	100%

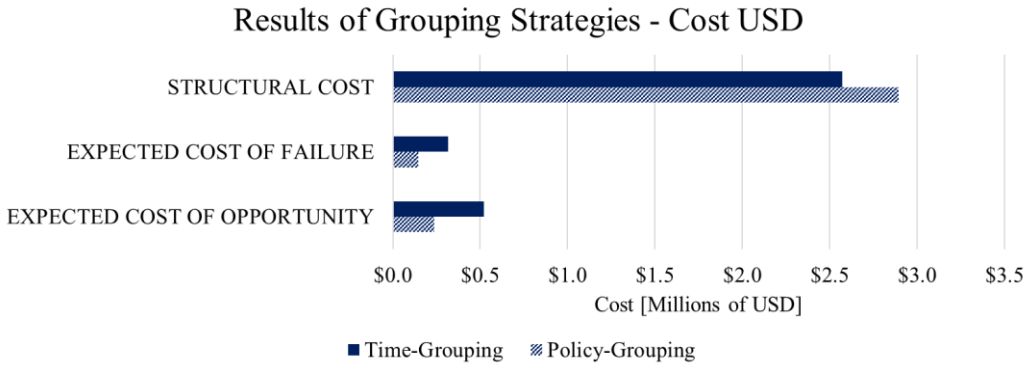


Figure 47. Results of the Grouping Strategies – Cost USD.

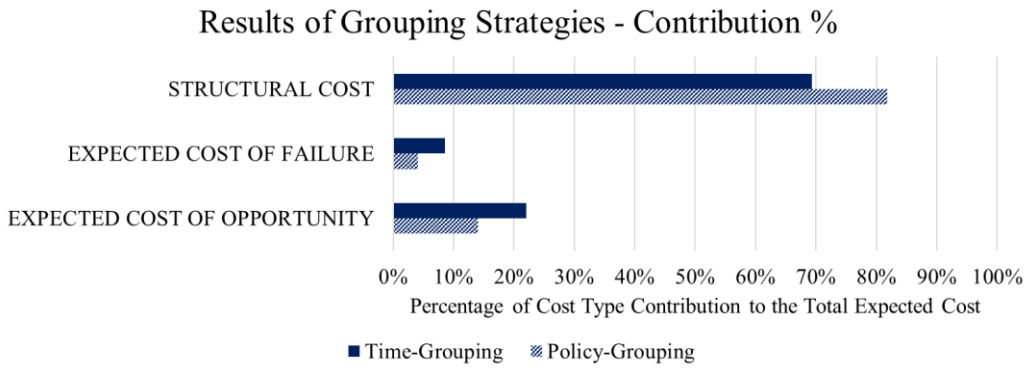


Figure 48. Results of the Grouping Strategies – Cost Contribution Percentage.

Using both grouping strategies, it is also evident that C_S represents the highest contribution to C_T, although the ratio will possibly change with different and more elements under analysis. In any case, it can be verified that C_{EO}, usually overlooked, has a relevant contribution, being greater than C_{EF} in this analysis. Also, C_{EO} has a similar behavior as C_{EF}, explained by the latter being part of its equation as the unbudgeted contribution, as discussed in Chapter 3.

Another quantitative evidence is that, for the same maintenance decision on downtimes, the Policy-Grouping Strategy resulted in a higher C_S when compared to the Time-Grouping Strategy, as expected, considering more elements to repair per downtime. However, this increase in C_S contribution yielded a significant reduction in C_{EF} and C_{EO}. Consistently, the relative contribution to C_T had an increase of 13% in C_S followed by a reduction of 5% in C_{EF} and 8% in C_{EO}. In absolute values, the Policy-Grouping Strategy obtained a better solution, with a cost reduction of 4% on C_T related to the Time-Grouping Strategy. The same effect was observed by (Casares and Vlahopoulos 2024) while using a simplified cost model and by not accounting for C_{EO}. Although this effect is not guaranteed for other analyses, it provides evidence that the trade-off is relevant. Consistently, anticipating and grouping more elements can possibly output a better result overall when considering risks of failure and opportunity.

According to the model behavior, there is an instant where the service life enters a regime where the risk of opportunity is lower than the risk of failure, which occurs at 18 years of life in this demonstration. In this regime, Maintainability (M) primarily sustains technical compliance for Reliability (R) and Safety (S) rather than recoverable Availability (A) tangible value. Although the opportunity horizon is bounded by the planned end-of-life, which is 25 years in this demonstration, the crossover between C_{EO} and C_{EF} provides an economic trigger for reconsidering

the service life boundary. When this crossover occurs, stakeholders may evaluate life-extension programs, repurposing strategies, or decommissioning alternatives, incorporating the associated capital reinvestment or disposal costs, which can be assessed in future work.

4.4.4 Optimization

Considering the grouping strategies presented in Sections 4.4.1 and 4.4.2, which will generate groups $\boldsymbol{G_m}$ based on a solution $\boldsymbol{t_m}$, the novel OMCRO is a modification of the MCRO approach, presented by Equation 58. This modification accounts for executing the Time-Grouping or Policy-Grouping Strategy for each feasible solution in the GA metaheuristic search. Therefore, the OMCRO problem can be expressed by Equation 67.

$$For\ \ n = n_{MIN} \dots n_{MAX} \tag{67}$$

$$Find\ \boldsymbol{t_m^*}\ which\ minimizes \sum_{t=1}^{t=T_l} C_T(t, \boldsymbol{t_m}, \boldsymbol{G_m})$$

$$Where:$$

$$C_T(t, \boldsymbol{t_m}, \boldsymbol{G_m}) = \delta_{tt_{m_j}} C_S\left(\boldsymbol{G_{m_j}}\right) + \sum_{k=1}^{n_e} p_{f_{k,j}}(t, \boldsymbol{t_m}, \boldsymbol{G_m})(C_{f_k} + C_{o_k})$$

$$subject\ to$$

$$\max(\boldsymbol{O_w}) - O_{w_{UB}} \leq 0$$

$$O_{w_{LB}} - \min(\boldsymbol{O_w}) \leq 0$$

$$O_{w_L} - t_{m_1} \leq 0$$

$$t_{m_1} - t_{es} \leq 0$$

$$t_{es} + 1 - t_{m_{2\dots n}} \leq 0$$

$$t_{m_{2\dots n}} - t_{ee} \leq 0$$

Considering:

I. All costs in Present Value (PV) using the inflation rate as a discount
II. n: Number of maintenance downtimes

III. n_{MIN}: Minimum number of maintenance downtimes

IV. n_{MAX}: Maximum number of maintenance downtimes

V. t: Time in years

VI. T_L: Time Limit or Analysis Horizon

VII. $\boldsymbol{t_m}$: Array of n decided years for maintenance downtime, where t_{m_j} is the j^{th} downtime year

VIII. $\boldsymbol{G_{m_j}}$: Array of n arrays of elements grouped for maintenance in the j^{th} downtime year

IX. $C_T(t, \boldsymbol{t_m}, \boldsymbol{G_m})$: Total Expected Cost at time t

X. $\delta_{tt_{m_j}}$: Kronecker Delta for maintenance downtime

$$\delta_{tt_{m_j}} = \begin{cases} 0\,, & t \neq t_{m_j}\ ,\ j: 1 \dots n \\ 1\,, & t = t_{m_j}\ ,\ j: 1 \dots n \end{cases}$$

XI. $C_S\left(\boldsymbol{G_{m_j}}\right)$: Structural Cost of the elements grouped in the j^{th} downtime year

XII. n_e: Number of elements in the analysis

XIII. $p_{f_{k,j}}(t, \boldsymbol{t_m}, \boldsymbol{G_m})$: Time-based probability of failure. Element k grouped in $\boldsymbol{G_{m_j}}$ is renewed ($p_{f_{k,j}} = 0$) when $t = t_{m_j}$

XIV. C_{f_k}: Cost of Failure of the element k with consequence severity S_k (Equation 39)

XV. $C_{EF_k} = p_{f_{k,j}} C_{f_k}$: Expected Cost of Failure (Risk) (Equation 38)

XVI. C_{o_k}: Cost of Opportunity of element k (Equation 50)

XVII. $C_{EO_k} = p_{f_{k,j}} C_{o_k}$: Expected Cost of Opportunity (Risk of Opportunity) (Equation 47)

XVIII. p_{f_T}: Probability of Failure Threshold

XIX. $\boldsymbol{O_w}$: Operational Window

XX. $O_{w_{UB}}$: Operational Window upper bound

XXI. $O_{w_{LB}}$: Operational Window lower bound

XXII. O_{w_L}: Operational Window limit

XXIII. t_{es}: First element time threshold (repeated over time without anticipation)

XXIV. t_{ee}: Last element time threshold (repeated over time without anticipation)

A detailed description of the rationale and constraints of Equation 67 is presented:

$$O_{w_{UB}} = t_{es} \tag{68}$$

$$O_{w_{LB}} = \max\left(\max(\boldsymbol{F_e} - \boldsymbol{t_m}), O_{w_L}\right) \tag{69}$$

$$n_{MIN} = \left\lfloor \frac{(t_{ee} - t_{es}) - t_{es}}{t_{es}} + 1 \right\rfloor = \left\lfloor \frac{t_{ee}}{t_{es}} - 1 \right\rfloor \tag{70}$$

$$n_{MAX} = \left\lfloor \frac{\left(t_{ee} - O_{w_L}\right)}{O_{w_L}} + 1 \right\rfloor = \left\lfloor \frac{t_{ee}}{O_{W_L}} \right\rfloor \tag{71}$$

I. $\boldsymbol{t_m}$ is sorted in increasing order.

II. The probability of failure threshold (p_{f_T}) is not explicitly included in the Objective Function and Constraints, which is a modification from the single-component MCRO. However, it is still a part of it since p_{f_T} is necessary to calculate the time thresholds that are required to form the groups $\boldsymbol{G_m}$.

III. O_{w_L} is a parameter defined by the stakeholder since it is the minimum desired operational window. In other words, it is the minimum time one wishes the system to operate without downtime.

IV. Equation 68: The maximum operational window max ($\boldsymbol{O_w}$) must be smaller than or equal to $O_{W_{UB}}$, which is equal to the first element time threshold (t_{es}), otherwise, the first element would fail in the time between the analysis start and the end of the first operational period.

V. Equation 69: The minimum operational window min ($\boldsymbol{O_w}$) must be bigger than or equal to $O_{W_{LB}}$, which is equal to the max $\left(\max(\boldsymbol{F_e} - \boldsymbol{t_m}), O_{w_L}\right)$. This means that it must be bigger than the minimum desired operational window (O_{w_L}) or the maximum difference between

the maintenance threshold time of the first element to be grouped F_{e_j} and its downtime t_{m_j}, whatever is greater. This guarantees that there will not be empty groups.

VI. The first downtime t_{m_1} must be greater than or equal to the operational window limit O_{W_L}, to avoid a first downtime during the first operation.

VII. The first downtime t_{m_1} must be smaller than or equal to the first element time threshold t_{es}, otherwise, the first element would not be grouped.

VIII. All the other downtimes ($t_{m_{2\ldots n}}$) must be greater than or equal to the next year after the first element and smaller than or equal to the last one (t_{ee}).

IX. The number of design variables n, or the number of downtimes is not defined previously. However, there are physical bounds that constrain its minimum value n_{MIN} and its maximum value n_{MAX}.

A. Equation 70: The lower bound n_{MIN} can be calculated considering the minimum number of operational windows that could fit inside the analysis horizon. The n_{MIN} can be calculated by dividing the minimum possible time between thresholds $[(t_{ee} - t_{es}) - t_{es}]$ by the maximum operational window $O_{w_{UB}} = t_{es}$. Specifically, $(t_{ee} - t_{es})$ is the earliest possible last downtime. Also, since n is an integer and one unit greater than the number of operational windows, one must be summed, and a floor function is applied.

B. Equation 71: For the upper bound n_{MAX}, the opposite approach is done while dividing the maximum possible time between thresholds $(t_{ee} - O_{w_L})$ by the minimum operational window $O_{w_{LB}} = O_{w_L}$. Specifically, t_{ee} is the least possible last downtime. Also, one must be summed up, and a floor function is applied.

C. Figure 49 illustrates both cases.

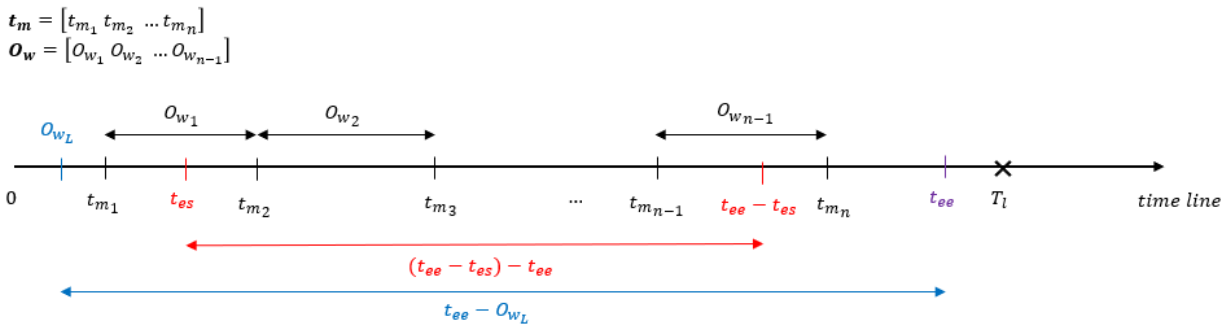


Figure 49. Downtime's bounds.

X. A GA optimization is applied to each possible number of downtimes, and the one with the minimum solution overall is $\boldsymbol{t_m^*}$.

XI. The GA optimization type is a modified integer approach of the Augmented Lagrangian Genetic Algorithm (ALGA), which works with non-linear constraints.

4.5 The OMCRO framework

Considering the integration of the corrosion model framework to calculate the probability of failure of each structural element subjected to environmental and operational long-term effects (Chapter 2), the models for cost and time (Chapter 3), and the OMCRO model (This Chapter), it is possible to build a framework, as shown in Appendix H.

Parameter inputs are built in Microsoft® Excel® spreadsheets and include ship structure, shipyard, operational, environmental, economic, and safety-related parameters. Ideally, spreadsheets are a straightforward way to gather and manage stakeholders' information, which is one of this thesis's requirements.

The output includes the probability of failure of each element, the Structural Cost, Expected Cost of Failure, Expected Cost of Opportunity, Total Expected Cost, and optimal renewal schedule related to these costs. Therefore, the output indicates what, when, and where elements will be renewed, and what costs and risks are involved.

The OMCRO framework consists of 31 integrated MathWorks® MATLAB® algorithms, where the GA optimization is carried out using Global Optimization Toolbox supported by Parallel Computing.

4.5.1 OMCRO Framework Results

A simulation was carried out considering the five elements (Figure 13) discussed so far and the input parameters presented in Appendices C and D, with $T_L = 25$ and $O_{W_L} = 3$. The optimization solution output is $\boldsymbol{t}_{\boldsymbol{m}}^{*}$ = [5 10 15 20] for both Time and Grouping-Strategy cases.

The OMCRO framework results for the Time-Grouping Strategy are presented in Section 4.5.1.1, and the results for Policy-Grouping Strategy are presented in Section 4.5.1.2. These results are automatically extracted and plotted by the framework using MathWorks® MATLAB®.

4.5.1.1 OMCRO Time-Grouping Results

This Section presents the results for the OMCRO simulation using five elements with the Time-Grouping Strategy. Accordingly, Table 24 and Figure 50 provide the overall results of grouping, costs, and times, while Figure 51 plots the risks (C_{EF} and C_{EO}) in FV over time. Moreover, Figure 52 to 55 plot the completion time and C_S in FV for all intervention tasks of each downtime.

Table 24. OMCRO overall results (Time-Grouping Strategy - 5 elements).

```
Optimized Solution:
--------------------------------------------------------------------
Total Cost Results (USD) in PV:
            CostEvaluation                 CostResult
    ___________________________________    __________

    "Structural Cost (PV)"                 2570660.75439073
    "Expected Cost of Failure (PV)"        317290.345769575
    "Expected Cost of Opportunity (PV)"     519655.73273058
    "Total Expected Cost (PV)"             3407606.83289088

--------------------------------------------------------------------
Total Unavailability Result (days): 162
--------------------------------------------------------------------
General Result:
    RepairNumber    Years    NumberOfElements    StructuralCost_FV    DrydockDays    QuayDays    UnavailabilityDays
    ____________    _____    ________________    _________________    ___________    ________    __________________

          1             5            3              646226.50374626          21           17              38
          2            10            4              826194.457486806         25           17              42
          3            15            4              847653.535344651         23           17              40
          4            20            4              1007126.43350701         25           17              42

--------------------------------------------------------------------
```

```
Elements per repair:
    Year: 5
    _______

        2
        4
        5

    Year: 10
    ________

        1
        2
        4
        5

    Year: 15
    ________

        2
        3
        4
        5

    Year: 20
    ________

        1
        2
        4
        5
```

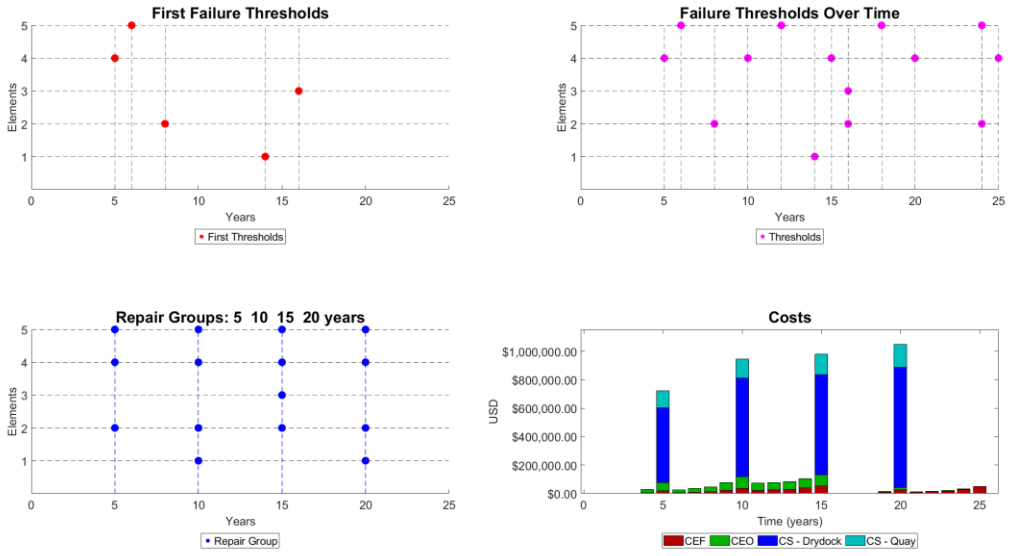


Figure 50. OMCRO overall results (Time-Grouping Strategy - 5 elements).

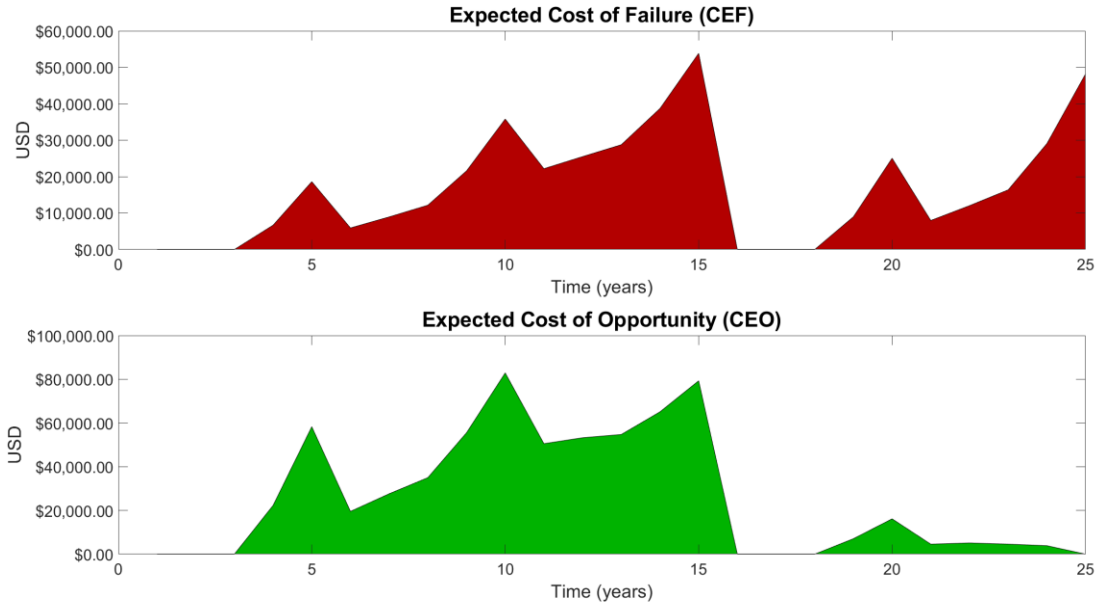


Figure 51. OMCRO C_{EF} and C_{EO} results (Time-Grouping Strategy- 5 elements).

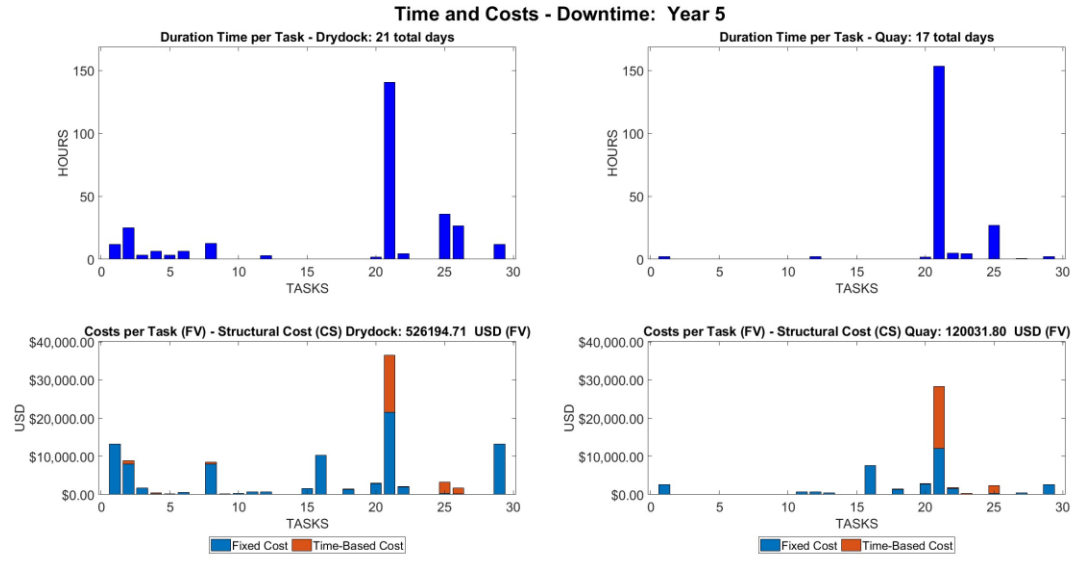


Figure 52. OMCRO C_S results for downtime at year 5 (Time-Grouping Strategy - 5 elements).

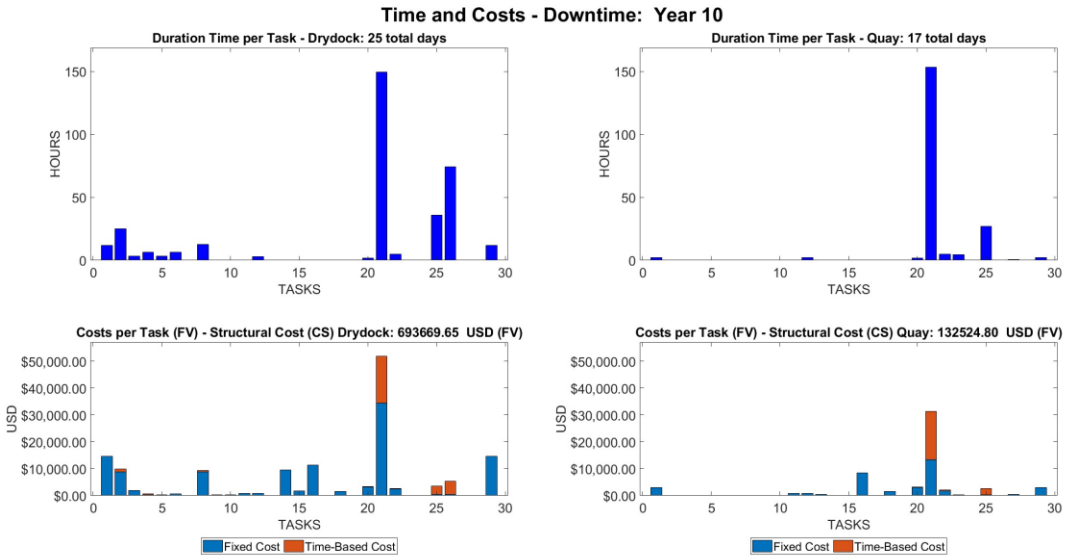


Figure 53. OMCRO C_S results for downtime at year 10 (Time-Grouping Strategy - 5 elements).

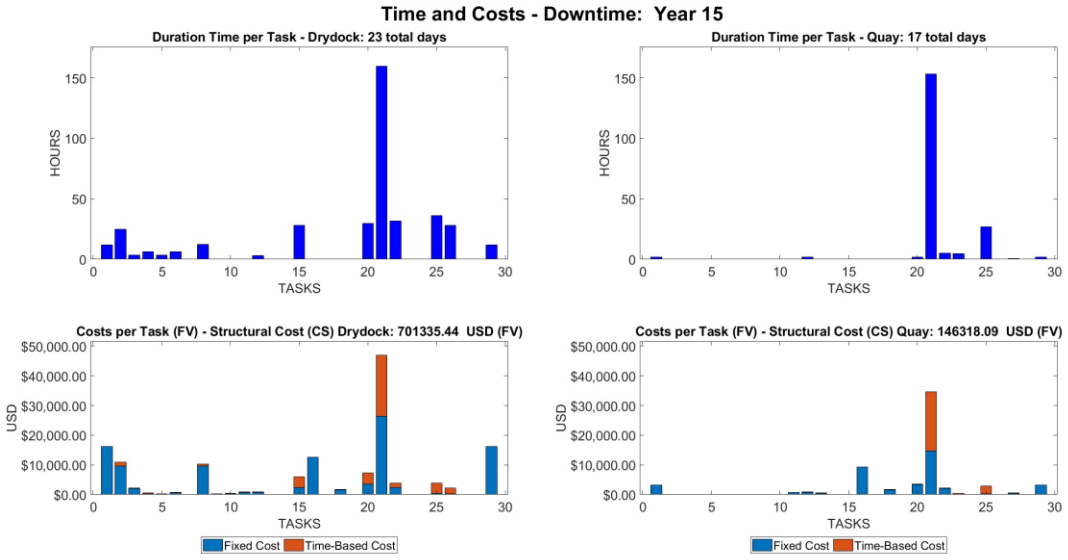


Figure 54. OMCRO C_S results for downtime at year 15 (Time-Grouping Strategy - 5 elements).

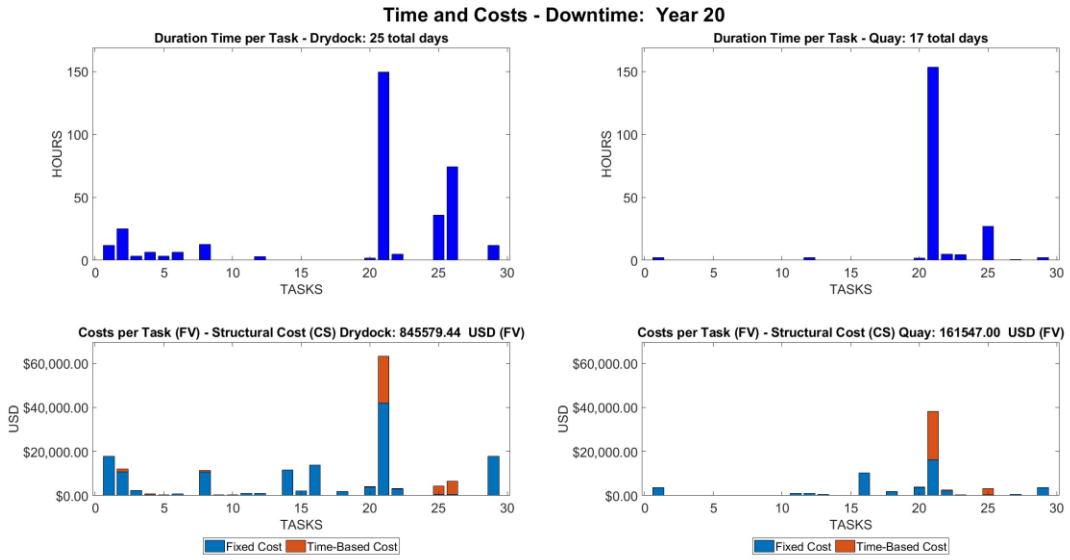
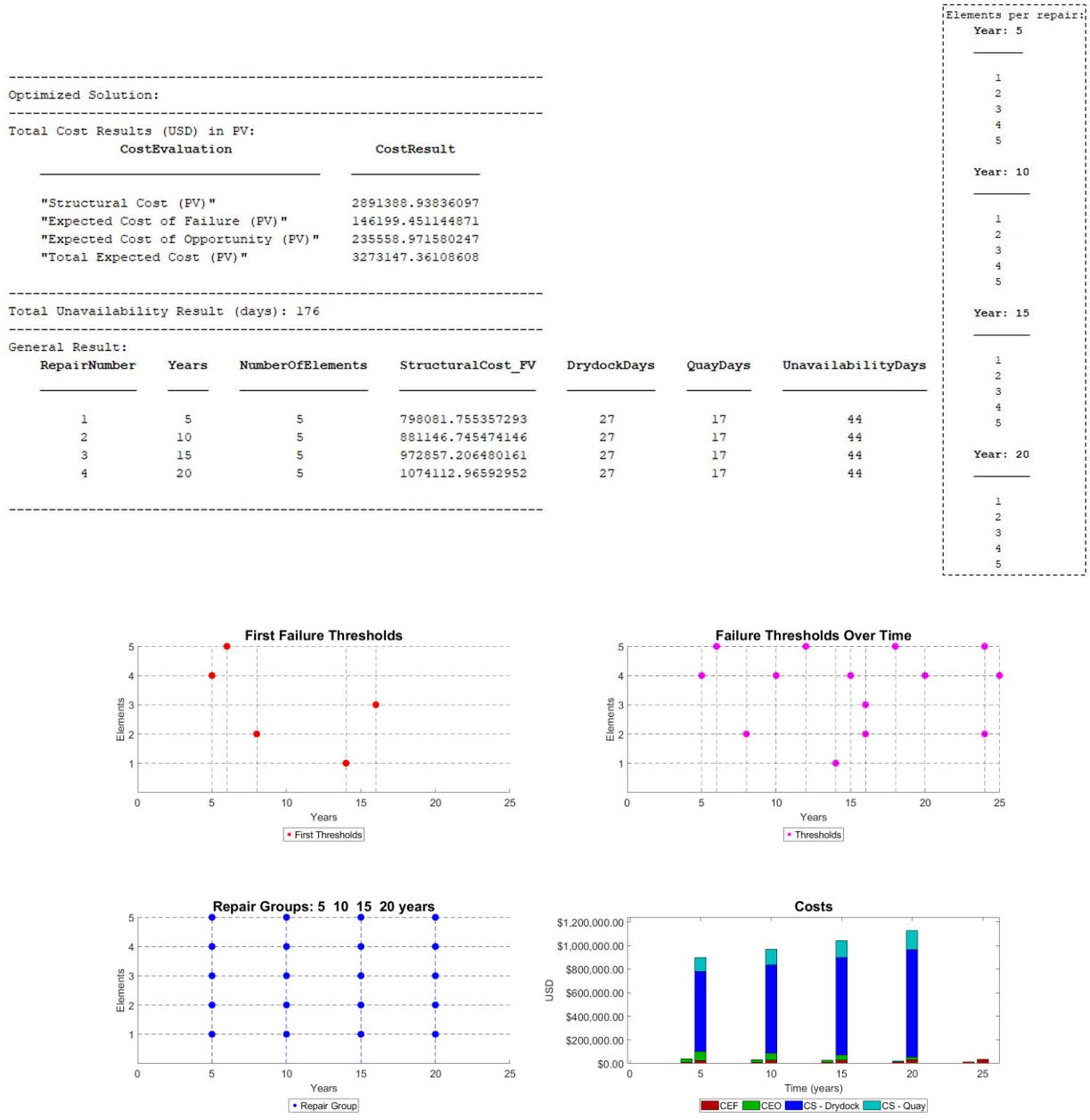


Figure 55. OMCRO C_S results for downtime at year 20 (Time-Grouping Strategy - 5 elements).

4.5.1.2 OMCRO Policy-Grouping Results

This Section presents the results for the OMCRO simulation using five elements with Policy-Grouping Strategy. Accordingly, Table 25 and Figure 56 provide the overall results of grouping, costs, and times, while Figure 57 plots the risks (C_{EF} and C_{EO}) in FV over time. Moreover, Figure 58 to 61 plots the completion time and C_S in FV for all intervention tasks of each downtime.

Table 25. OMCRO overall results (Policy-Grouping Strategy - 5 elements).



Optimized Solution:

Total Cost Results (USD) in PV:

CostEvaluation	CostResult
"Structural Cost (PV)"	2891388.93836097
"Expected Cost of Failure (PV)"	146199.451144871
"Expected Cost of Opportunity (PV)"	235558.971580247
"Total Expected Cost (PV)"	3273147.36108608

Total Unavailability Result (days): 176

General Result:

RepairNumber	Years	NumberOfElements	StructuralCost_FV	DrydockDays	QuayDays	UnavailabilityDays
1	5	5	798081.755357293	27	17	44
2	10	5	881146.745474146	27	17	44
3	15	5	972857.206480161	27	17	44
4	20	5	1074112.96592952	27	17	44

Elements per repair:

Year: 5

1
2
3
4
5

Year: 10

1
2
3
4
5

Year: 15

1
2
3
4
5

Year: 20

1
2
3
4
5

Figure 56. OMCRO overall results (Policy-Grouping Strategy - 5 elements).

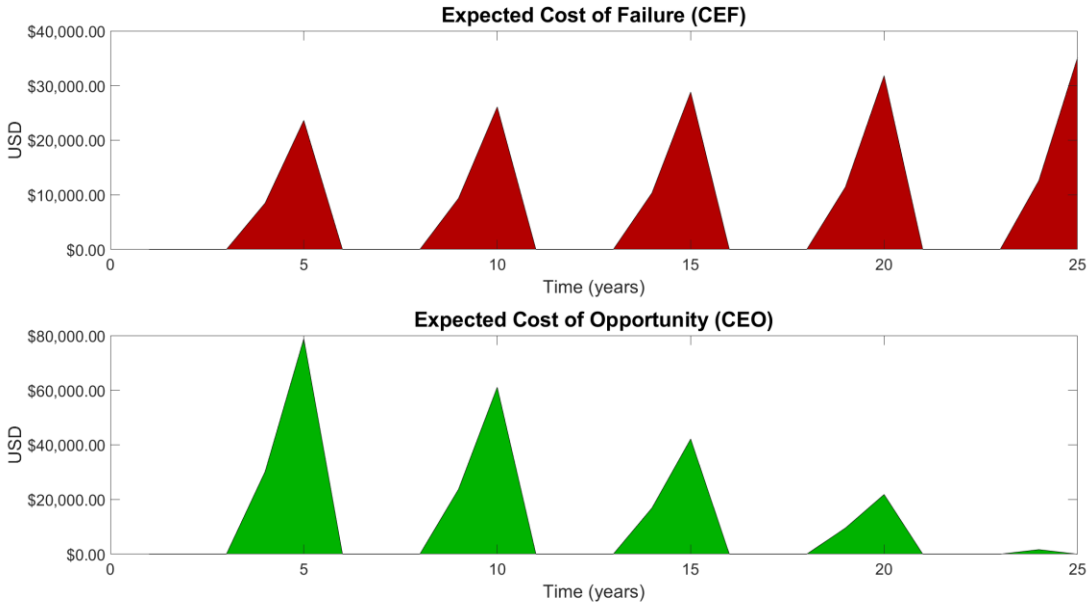


Figure 57. OMCRO C_{EF} and C_{EO} results (Policy-Grouping Strategy- 5 elements).

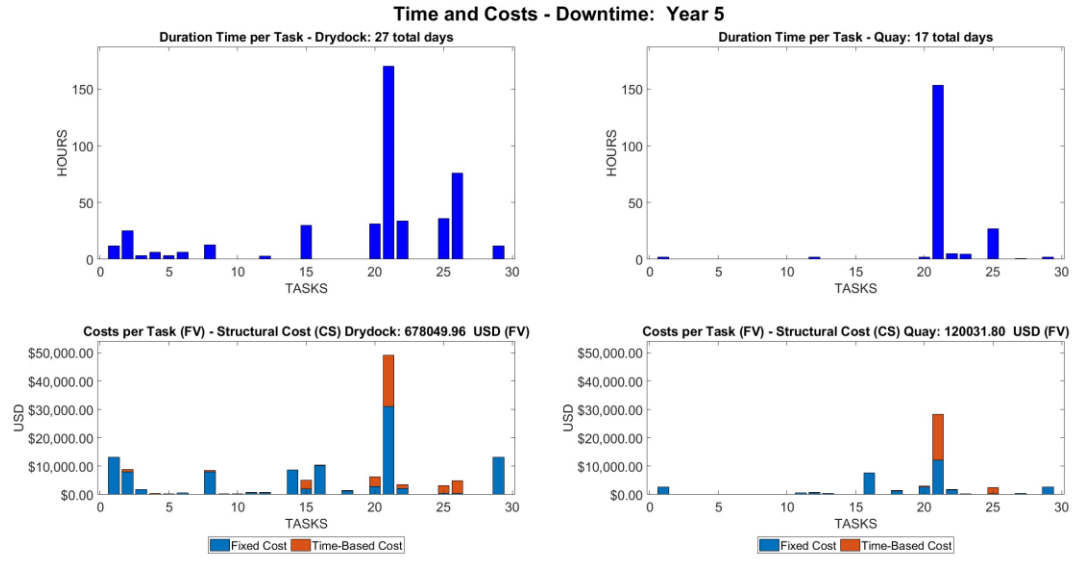


Figure 58. OMCRO C_S results for downtime at year 5 (Policy-Grouping Strategy - 5 elements).

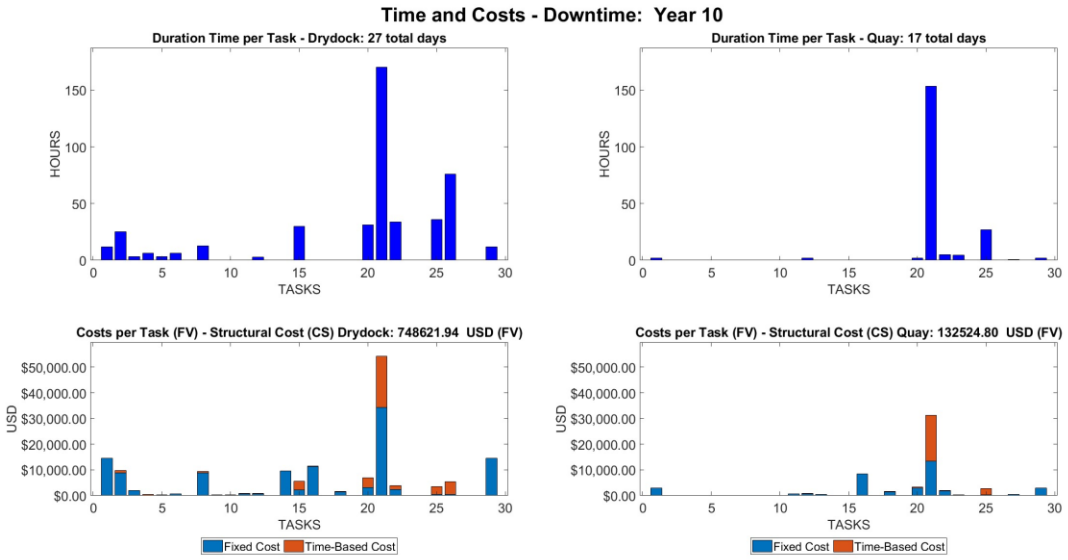


Figure 59. OMCRO C_S results for downtime at year 10 (Policy-Grouping Strategy - 5 elements).

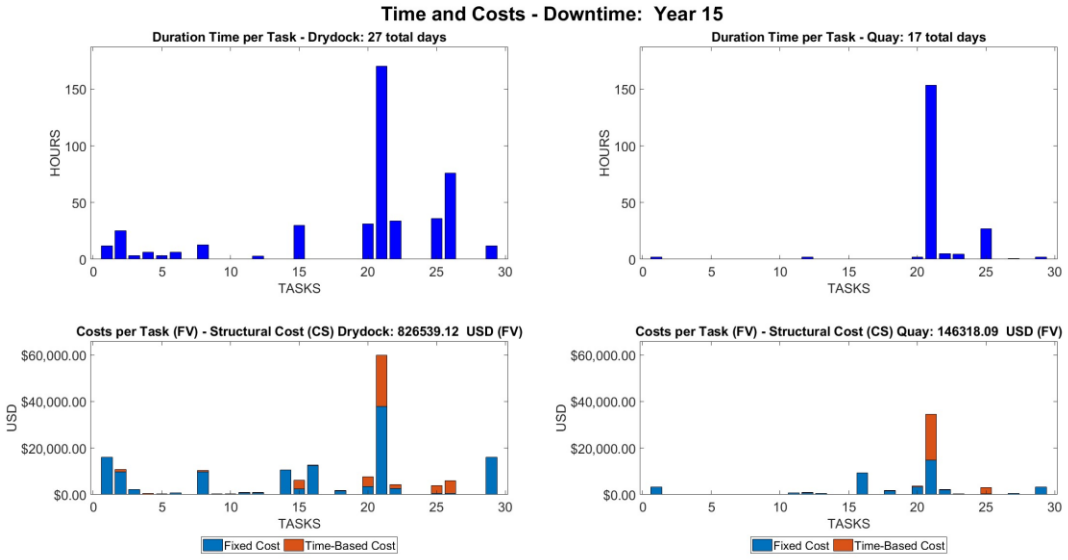


Figure 60. OMCRO C_S results for downtime at year 15 (Policy-Grouping Strategy - 5 elements).

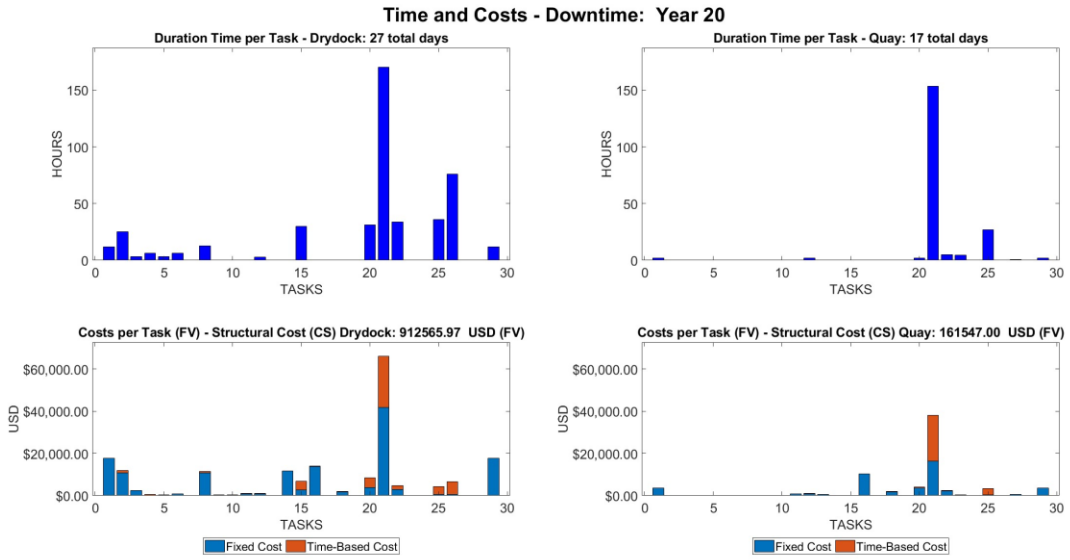


Figure 61. OMCRO C_S results for downtime at year 20 (Policy-Grouping Strategy - 5 elements).

4.6 Verification and Validation (V&V)

Verification and Validation, also known as V&V, are fundamental tasks to test the integrity of the system against its requirements. Accordingly, the Verification process confirms whether the system components were made "right", while the Validation process confirms whether the "right" system was made (INCOSE 2023)

In this regard, Verification is carried out in a piece-wise inspection using Microsoft® Excel® spreadsheets for hand calculation on all outputs, as presented in Section 4.6.1. Moreover, the Optimization Validation is carried out by MCS on MathWorks® MATLAB® to check the optimal solution, as presented in Section 4.6.2. Also, overall Validation results are presented in the Section 4.9 regarding the OMCRO framework by considering the 12 high-level requirements listed in Section 1.3.

Accordingly, the results provided in Section 4.5.1.1 and 4.5.1.2 are tested under a V&V process.

4.6.1 Verification

The hand calculations for $\boldsymbol{t_m^*}$ = [5 10 15 20] were carried out by the Sections 4.4.1.1 and 4.4.2.1 using Microsoft® Excel® spreadsheets, with the piece-wise results evidenced by Appendix E and G, respectively. Accordingly, the tasks' completion times, tasks' C_S, overall C_{EF} and C_{EO} (FV) maximum absolute differences between hand calculation and the OMCRO framework are presented by Table 26 and 29. The overall differences for C_S are presented by Table 27 and 30, and the differences for C_T are presented in Table 28 and 31.

Table 26. Times, Tasks C_S, C_{EF} and C_{EO} (FV) Maximum Absolute Differences (Time-Grouping).

COMPLETION TIME	5.00E-08
TASK STRUCTURAL COST (PV)	7.20E-02
C_{EF} (FV)	5.11E-03
C_{EO} (FV)	1.69E-03

Table 27. C_S Absolute Differences (Time-Grouping).

PRESENT VALUE						
YEARS	ELEMENTS	DRYDOCK	QUAY	TOTAL	MATLAB	DIFFERENCE
5	**[2, 4, 5]**	$ 476,590.79	$ 108,716.50	$ 585,307.29	$ 585,307.25	$ 0.03
10	**[1, 2, 4, 5]**	$ 569,050.68	$ 108,716.50	$ 677,767.18	$ 677,767.22	$ 0.04
15	**[2, 3, 4, 5]**	$ 521,102.53	$ 108,716.50	$ 629,819.02	$ 629,819.06	$ 0.04
20	**[1, 2, 4, 5]**	$ 569,050.68	$ 108,716.50	$ 677,767.18	$ 677,767.22	$ 0.04
			TOTAL	$ 2,570,660.68	$ 2,570,660.75	$ 0.08
FUTURE VALUE						
YEARS	ELEMENTS	DRYDOCK	QUAY	TOTAL	MATLAB	DIFFERENCE
5	**[2, 4, 5]**	$ 526,194.74	$ 120,031.80	$ 646,226.54	$ 646,226.50	$ 0.04
10	**[1, 2, 4, 5]**	$ 693,669.61	$ 132,524.80	$ 826,194.41	$ 826,194.46	$ 0.05
15	**[2, 3, 4, 5]**	$ 701,335.39	$ 146,318.09	$ 847,653.48	$ 847,653.54	$ 0.05
20	**[1, 2, 4, 5]**	$ 845,579.38	$ 161,547.00	$ 1,007,126.38	$ 1,007,126.43	$ 0.06

Table 28. C_T Absolute Difference (Time-Grouping).

STRUCTURAL COST	$ 2,570,660.68
EXPECTED COST OF FAILURE	$ 317,290.31
EXPECTED COST OF OPPORTUNITY	$ 519,655.72
TOTAL EXPECTED COST	**$ 3,407,606.71**
MATLAB	**$ 3,407,606.83**
DIFFERENCE	$ 0.12

Table 29. Times, Tasks C_S, C_{EF} and C_{EO} (FV) Maximum Absolute Differences (Policy-Grouping).

COMPLETION TIME	5.00E-08
TASK STRUCTURAL COST (PV)	7.20E-02
C_{EF} (FV)	5.34E-03
C_{EO} (FV)	2.31E-03

Table 30. C_S Absolute Differences (Policy-Grouping).

PRESENT VALUE						
YEARS	ELEMENTS	DRYDOCK	QUAY	TOTAL	MATLAB	DIFFERENCE
5	**[1,2,3,4,5]**	$ 614,130.63	$ 108,716.50	$ 722,847.12	$ 722,847.23	$ 0.11
10	**[1,2,3,4,5]**	$ 614,130.63	$ 108,716.50	$ 722,847.12	$ 722,847.23	$ 0.11
15	**[1,2,3,4,5]**	$ 614,130.63	$ 108,716.50	$ 722,847.12	$ 722,847.23	$ 0.11
20	**[1,2,3,4,5]**	$ 614,130.63	$ 108,716.50	$ 722,847.12	$ 722,847.23	$ 0.11
			TOTAL	$ 2,891,388.50	$ 2,891,388.94	$ 0.44
FUTURE VALUE						
YEARS	ELEMENTS	DRYDOCK	QUAY	TOTAL	MATLAB	DIFFERENCE
5	**[1,2,3,4,5]**	$ 678,049.84	$ 120,031.80	$ 798,081.63	$ 798,081.76	$ 0.12
10	**[1,2,3,4,5]**	$ 748,621.81	$ 132,524.80	$ 881,146.61	$ 881,146.75	$ 0.13
15	**[1,2,3,4,5]**	$ 826,538.97	$ 146,318.09	$ 972,857.06	$ 972,857.21	$ 0.15
20	**[1,2,3,4,5]**	$ 912,565.81	$ 161,547.00	$ 1,074,112.80	$ 1,074,112.97	$ 0.16

Table 31. C_T Absolute Difference (Policy-Grouping).

STRUCTURAL COST	$ 2,891,388.50
EXPECTED COST OF FAILURE	$ 146,199.43
EXPECTED COST OF OPPORTUNITY	$ 235,558.96
TOTAL EXPECTED COST	**$ 3,273,146.89**
MATLAB	**$ 3,273,147.36**
DIFFERENCE	$ 0.47

The differences between hand calculation and the OMCRO framework are 5.10^{-8} h for completion time and less than 0.50 USD for costs, which is a negligible margin attributed to rounding. Therefore, the OMCRO framework is considered verified.

4.6.2 Optimization Validation

Also, to verify whether the result $\boldsymbol{t_m^*}$ is the best solution, an MCS was conducted using MathWorks® MATLAB® software based on the generation of uniformly distributed pseudorandom integers as $\boldsymbol{t_m}$ candidates. The solution considered 1,000,000 simulations for each number n of design variables, from n_{MIN} to n_{MAX}. The Monte Carlo code applies bound constraints when generating candidate solutions and filters them with constraints that cannot be applied when generating the candidates. Therefore, it is expected that many solutions will be discarded because of their infeasibility.

Figure 62 and 63 present feasible solution plots of $\boldsymbol{t_m}$ candidates (scatter marks) for Time-Grouping and Policy-Grouping, respectively, and compares them with the optimal solution $\boldsymbol{t_m^*}$ (red line). Each scatter mark color represents a feasible solution of a specific number of design variables (downtimes). The y-axis represents C_T costs related to the feasible solutions, while the x-axis represents realizations of the simulation.

It can be concluded that the optimal solution is the global minimum of the simulation results. Therefore, the results are consistent, and the optimal solution is validated. Moreover, it should be noted that the OMCRO called the Objective Function 25,885 and 25,615 times, respectively, for Time and Policy-Grouping, while the MCS required 4.10^6 calls. This fact also validates the usefulness of the optimization framework.

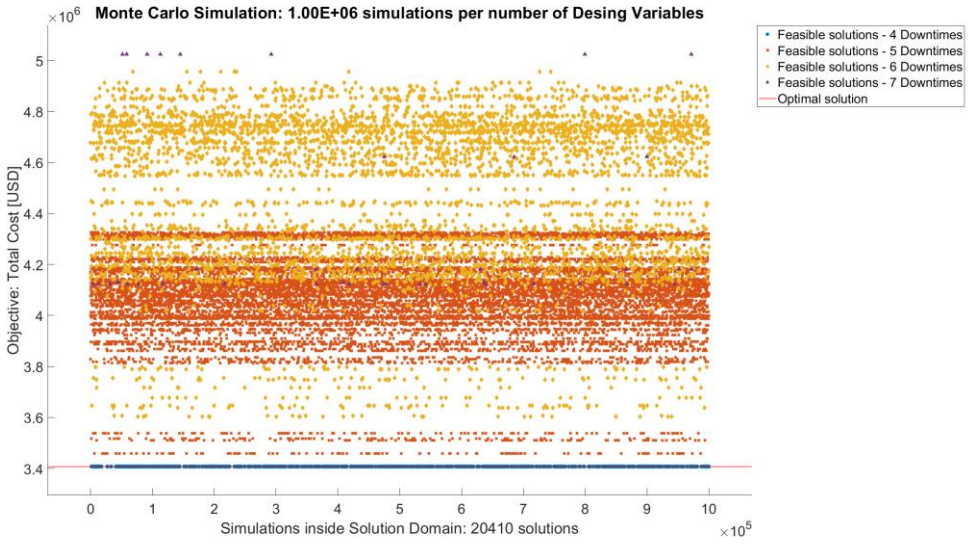


Figure 62. Monte Carlo Simulation for Time-Grouping.

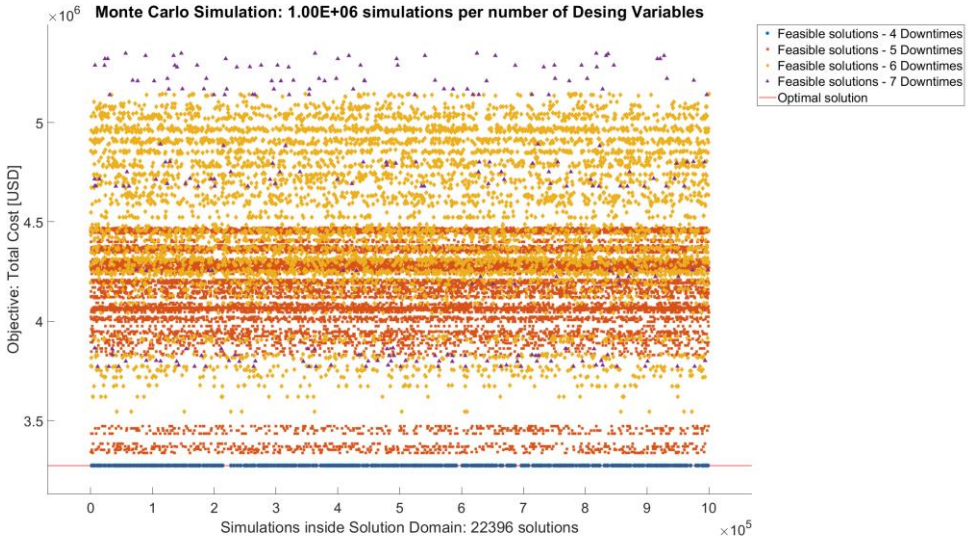


Figure 63. Monte Carlo Simulation for Policy-Grouping.

4.7 Quantitative Maintainability and Availability Analysis

The OMCRO framework, verified and validated, is used in this Section as a platform to analyze and quantify the Maintainability (M) and Availability (A) emergent properties of both SoI (ship structure) and SS (shipyard). Maintainability (M) is quantified by the Total Expected Cost C_T, while Availability (A) is quantified by Total Unavailability Time (TUT) and Repair Frequency (RF).

The simulations are applied in different scenarios for the five elements discussed in this work (Figure 13), by independently varying factors for a sensitivity analysis. In these simulations, it was set a fixed T_L = 25 and O_{W_L} = 3, all under Time-Grouping Strategy, since it is less constrained to study sensitivity effects.

Accordingly, as introduced in Chapter 1 and illustrated by Figure 3, Maintainability (M) and Availability (A) are analyzed in this work with the following specific relationships by their respective detailed Sections:

I. **Maintainability (M) is affected by shipyard (SS) capacity and variability**
   Section 4.7.1.
II. **Maintainability (M) is affected by the ship structure's (SoI) Reliability (R)**
   Section 4.7.2.
III. **Maintainability (M) affects the ship structure's (SoI) Reliability (R) with repair actions**
   Section 4.4.4. Renewed elements are set with $p_f = 0$ under OMCRO grouping decisions.
IV. **Maintainability (M) is affected by the ship structure's (SoI) Safety (S) levels**
   Sections 2.6, 4.4.1, and 4.4.2. Safety levels provide time thresholds for renewal, which are inputs to grouping strategies under the OMCRO framework.
V. **Maintainability (M) affects both the ship structure's (SoI) and the shipyard's (SS) Availability (A)**
   Section 4.7.3.
VI. **Maintainability (M) is affected by ship (SoI) and shipyard Availability (A)**
   Chapter 6. Not considered in this thesis, however, availability constraints can be incorporated in future work.

VII. Maintainability (M) is affected by decisions on Maintenance Concept and Plan based on CE

Maintenance Concept classifies maintenance actions on the shipyard's drydock and quay area (Chapter 3); Maintenance Plan defines Opportunistic Maintenance Strategy with Time-Grouping and Policy-Grouping Strategies (Section 4.4); Decisions based on CE are performed under the OMCRO framework's Objective Function (Section 4.4.4).

4.7.1 Shipyard (SS) Quality (Q) Effects on Maintainability (M)

This Section provides the developments, results, and conclusions regarding a sensitivity analysis to understand the shipyard (SS) behavior on Maintainability (M) under CE, supported by the OMCRO framework. This analysis is conducted by independently varying capacity and variability, which define Quality (Q) in this work.

In a sensitivity analysis, multiplicative factors are applied to parameters of Section D.3 of Appendix D. Accordingly, the capacity factors are applied in five levels (0.25, 0.5, 1, 2, 4) to all capacity parameters: 3, 7, 11, 15, 19, 23, 27, 31, 35, 39, 46, 51, 52, 58, 59, 65, 71, 77, 83, 89, 99, 103, 107, 111, 115, 118. Also, the variability (coefficient of variation) is applied in three levels (0.5, 1, 1.5), by modifying all standard deviation parameters concerning their respective means. The standard deviation parameters are numbered as 54, 61, 67, 73, 79, 85, 91. All other parameters remain constant. As a reference, the parameter's values provided by Section D.3 of Appendix D are normalized with a capacity factor of 1 and a variability equal to 1.5.

Consistently, the Total Expected Cost C_T results are presented by Table 32 and by Figure 64.

Table 32. Shipyard Quality Effect on C_T.

COST (Millions USD)		Normalized Capacity				
		0.25	0.5	1	2	4
Variability	1.5	10.22	5.63	3.41	2.34	1.92
	1	9.57	5.33	3.23	2.24	1.89
	0.5	9.03	5.05	3.09	2.17	1.82

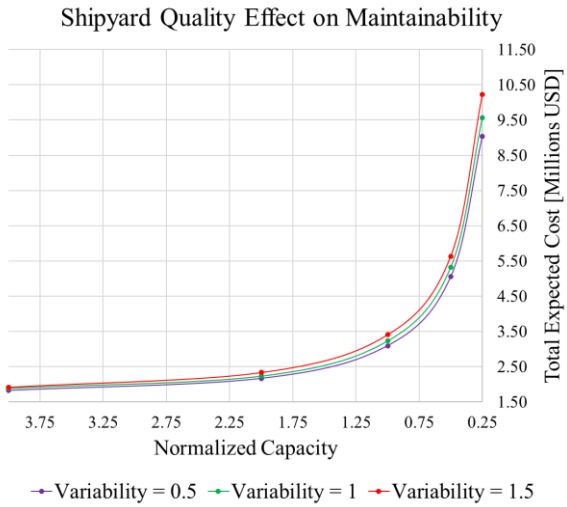


Figure 64. Shipyard Quality Effect on C_T (Time-Grouping).

It is evident that reducing capacity yields a highly non-linear increase in cost, and increasing variability will always degrade performance, especially for lower capacities. However, variability has a marginal impact when compared to capacity, which is the main impact on quality. Its non-linear effect is justified by the cycle time's sharp increase with utilization approaching 100%, since the decrease in capacity is evaluated while considering the load constant. These effects are also observed by (Hopp and Spearman 2011).

4.7.2 Ship Structure (SoI) Reliability (R) Effects on Maintainability (M)

This Section provides the developments, results, and conclusions regarding a sensitivity analysis to understand the ship structure (SoI) Reliability (R) behavior on Maintainability (M) under CE, supported by the OMCRO framework. This analysis is conducted by independently varying structure thickness and Environment and Operation (E&O) corrosion parameters. These parameters quantify Reliability (R) with the probabilistic corrosion model developed in Chapter 2. Both parameters are modified in the following ways:

I. The original thickness is multiplied by factors (0.5, 1, 1.5, 2). As a reference, the thickness values provided by Appendix C are normalized with a factor equal to 1.
II. Among all E&O corrosion parameters described by Table 5, seawater and atmospheric temperature were selected for this sensitivity analysis, since they

respectively impact corrosion degradation in seawater immersion, and in marine and oil atmosphere. Accordingly, the temperature parameters are also multiplied by factors (0.5, 1, 1.5, 2). As a reference, the nominal parameters are the ones described by Table 5, which are mentioned in the developments of (Guedes Soares, Garbatov, and Zayed 2011; Guedes Soares et al. 2009; 2008). Furthermore, one single operation type was considered, and ballast and oil tanks were assumed 50% loaded.

The sensitivity of both Reliability (R) parameters is tested under an independent variation of shipyard (SS) capacity, which is the main quality driver. Accordingly, the normalized capacity, described in Section 4.7.1, is multiplied by factors (0.5, 1, 1.5, 2). Consistently, the Total Expected Cost C_T results are presented by the Table 33 and Figure 65 for the thickness effect, and by Table 34 and Figure 66 for E&O impact.

Table 33. Ship Structure Thickness and Shipyard Quality Effect on C_T.

COST (Millions USD)		Normalized Thickness			
		0.5	1	1.5	2
Normalized Capacity	2	2.96	2.34	1.36	1.09
	1.5	3.35	2.67	1.56	1.24
	1	4.29	3.41	1.95	1.54
	0.5	7.10	5.63	3.17	2.53

Table 34. Ship E&O and Shipyard Quality Effect on C_T.

COST (Millions USD)		Normalized E&O Parameter			
		0.5	1	1.5	2
Normalized Capacity	2	2.01	2.27	2.93	2.98
	1.5	2.28	2.58	3.32	3.38
	1	2.92	3.29	4.23	4.30
	0.5	4.81	5.42	6.99	7.09

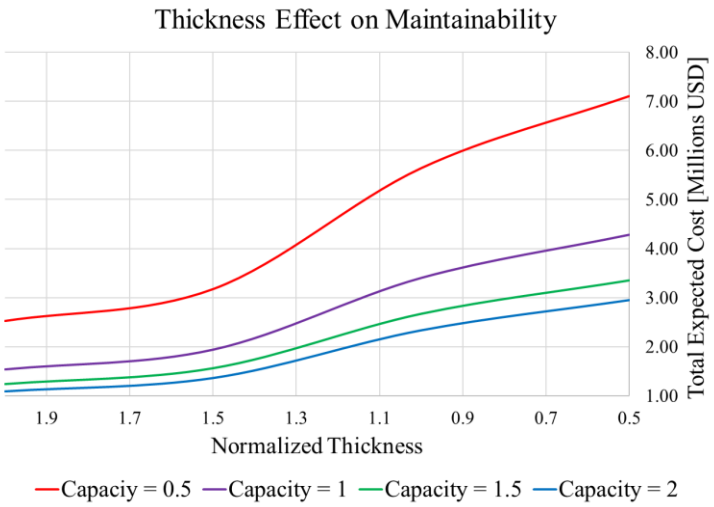


Figure 65. Ship Structure Thickness and Shipyard Quality Effect on C_T.

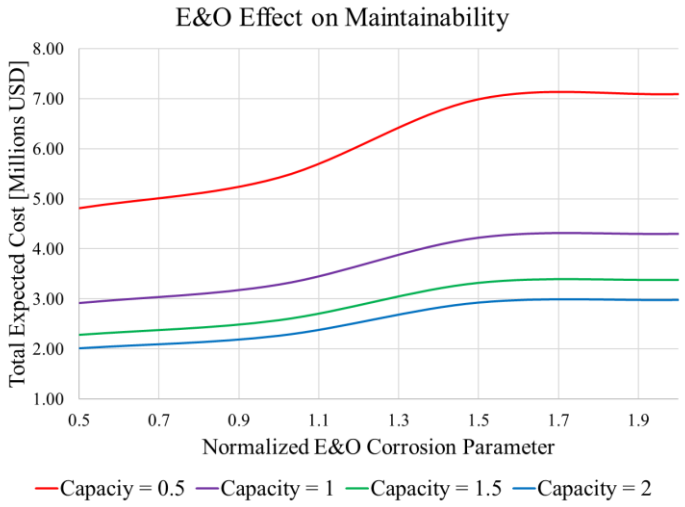


Figure 66. Ship E&O and Shipyard Quality Effect on C_T.

The same Total Expected Cost C_T results are also plotted in a heatmap, where the normalized capacity varies on the y-axis while the normalized thickness (Figure 67) or E&O normalized parameters (Figure 68) varies in the x-axis.

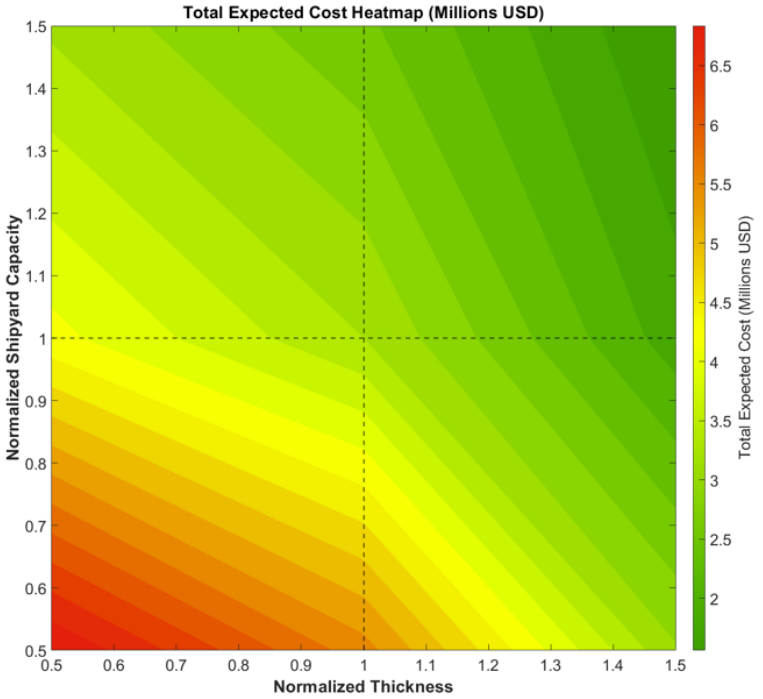


Figure 67. Ship Structure Thickness and Shipyard Quality Effect on C_T (Heatmap).

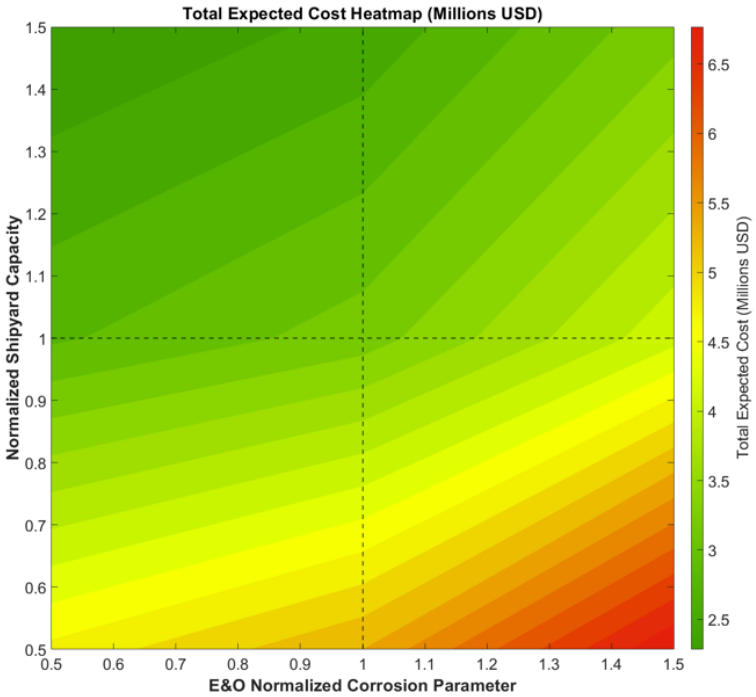


Figure 68. Ship E&O and Shipyard Quality Effect on C_T (Heatmap).

The results provide quantitative evidence that reducing structure thickness or increasing E&O corrosion parameters decreases reliability, thus increasing cost. This effect is non-linear, as observed by Figure 65 and 66, with a reduction in the rate of change of cost while decreasing reliability for E&O analysis, where it reaches a steady state condition. Accordingly, this effect is explained by the fact that the probability of failure increases up to its threshold, therefore defining the time to renew. Hence, the maintenance time lower bound is the next year after coating loses efficiency; therefore, it is the earliest possible renewal in the model, which is eventually achieved by sufficiently low reliability. Therefore, decreasing Reliability (R) over this level will not change the solution for a given fixed capacity. Moreover, the ship structure reliability reduction effects are enhanced by capacity reduction, which provides a non-linear steep increase in cost, already explored in Section 4.7.1.

4.7.3 Maintainability (M) Effects on Availability (A)

The OMCRO framework outputs on Maintainability (M) are strictly related to Availability (A) effects, as discussed in Chapter 1 and Section 4.7 descriptive text. These effects are investigated for the same cases presented in Sections 4.7.1 and 4.7.2, respectively, with quality and reliability sensitivities. For both cases, Availability (A) is quantified by Total Unavailability Time (TUT) of the ship and Repair Frequency (RF).

A single downtime, in extreme cases, may surpass 365 days (one year) in idle time. Although this case was not achieved during simulation, they are not valid under the OMCRO framework, which is discretized in yearly based evaluations. This capacity enhancement in the model is included as future work in Chapter 6. However, for Maintainability (M) analysis, they are valid indications of extreme unavailability.

4.7.3.1 Shipyard (SS) Quality (Q) Effects on Availability (A)

The sensitivity analysis conducted using the OMCRO framework is described in Section 4.7.1. Accordingly, shipyard (SS) Quality (Q) is defined by capacity and variability, where capacity is the main aspect. Therefore, the impacts of capacity on Availability (A) regarding TUT of the ship are described by Table 35 and Figure 69, while quantifications on RF are described by Table 36.

Table 35. Shipyard Quality Effect on Total Unavailability Time (TUT).

TOTAL UNAVAILABILITY TIME (days)		Normalized Capacity				
		0.25	0.5	1	2	4
Variability	1.5	599	305	162	89	51
	1	554	287	149	81	50
	0.5	521	267	141	80	46

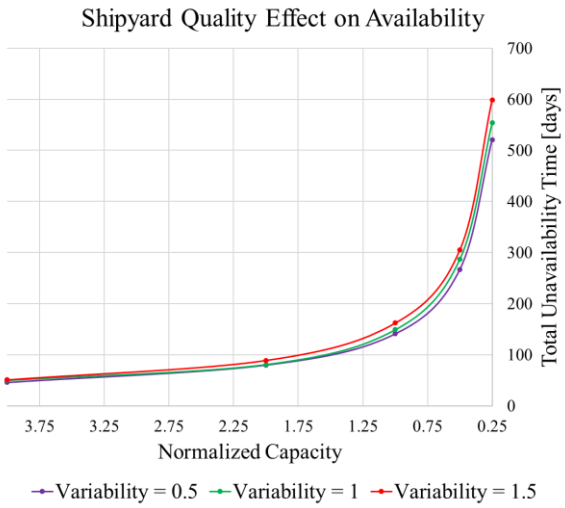


Figure 69. Shipyard Quality Effect on Total Unavailability Time (TUT).

Table 36. Shipyard Quality Effect on Repair Frequency (RF).

SOLUTION (downtime years)		Normalized Capacity				
		0.25	0.5	1	2	4
Variability	1.5	[5 10 15 20] (RF = 4)	[5 10 15 20] (RF = 4)	[5 10 15 20] (RF = 4)	[5 10 15 20] (RF = 4)	[5 10 15 20] (RF = 4)
	1	[5 10 15 20] (RF = 4)	[5 10 15 20] (RF = 4)	[5 10 15 20] (RF = 4)	[5 10 15 20] (RF = 4)	[5 10 15 20] (RF = 4)
	0.5	[5 10 15 20] (RF = 4)	[5 10 15 20] (RF = 4)	[5 10 15 20] (RF = 4)	[5 10 15 20] (RF = 4)	[5 10 15 20] (RF = 4)

It can be noted that the TUT has a steep non-linear increase when reducing capacity, and a marginal underperformance with larger variability, especially for lower capacity. These are the same effects justified in Section 4.7.1, which are consistent with Factory Physics' laws (Hopp and Spearman 2011).

Regarding the RF measure, it is evident that the optimal solution output by the OMCRO framework is equal for all cases, although costs vary for each case, as presented in Table 32. This

is justified by the fact that Quality (Q) does not change grouping results, since the ship renewal thresholds are the same. Furthermore, the repair processes, although with different performances, are also the same. Therefore, the variation on shipyard Quality (Q), despite having a significant impact on costs, does not change the optimal downtime decision, since it has an equal impact on all solutions.

4.7.3.2 Ship Structure (SoI) Reliability (R) Effects on Availability (A)

The sensitivity analysis conducted using the OMCRO framework is described in Section 4.7.2. Accordingly, the ship structure (SoI) Reliability (R) is defined by structure thickness and E&O corrosion parameters. The sensitivity of both Reliability (R) parameters is tested under an independent variation of the shipyard (SS) capacity.

Therefore, the impacts of these factors on Availability (A) regarding Total Unavailability Time (TUT) are presented by the Table 37 and Figure 70 for thickness, and by Table 38 and Figure 71 for E&O. Quantifications on Repair Frequency (RF) are described by Table 39 and Table 40 for thickness and E&O effect, respectively.

Table 37. Ship Structure Thickness and Shipyard Quality Effect on Total Unavailability Time (TUT).

TOTAL UNAVAILABILITY TIME (days)		Normalized Thickness			
		0.5	1	1.5	2
Normalized Capacity	2	133	89	53	42
	1.5	165	111	66	52
	1	242	162	97	76
	0.5	456	305	183	144

Table 38. Ship E&O and Shipyard Quality Effect on Total Unavailability Time (TUT).

TOTAL UNAVAILABILITY TIME (days)		Normalized E&O Parameter			
		0.5	1	1.5	2
Normalized Capacity	2	73	88	133	133
	1.5	90	109	165	165
	1	133	160	242	242
	0.5	251	301	456	456

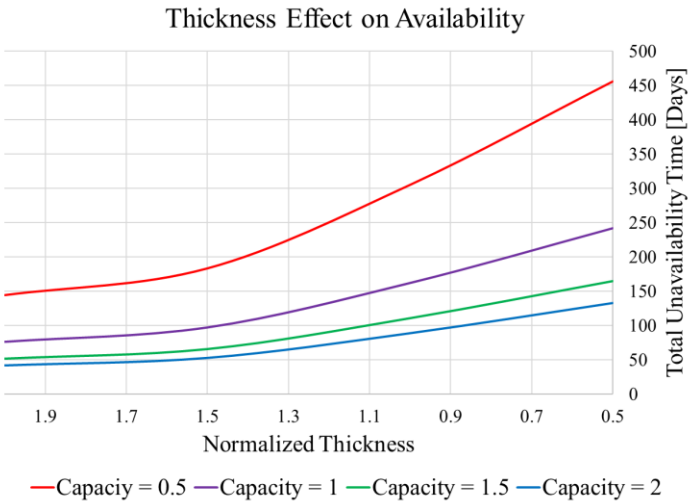


Figure 70. Ship Structure Thickness and Shipyard Quality Effect on Total Unavailability Time (TUT).

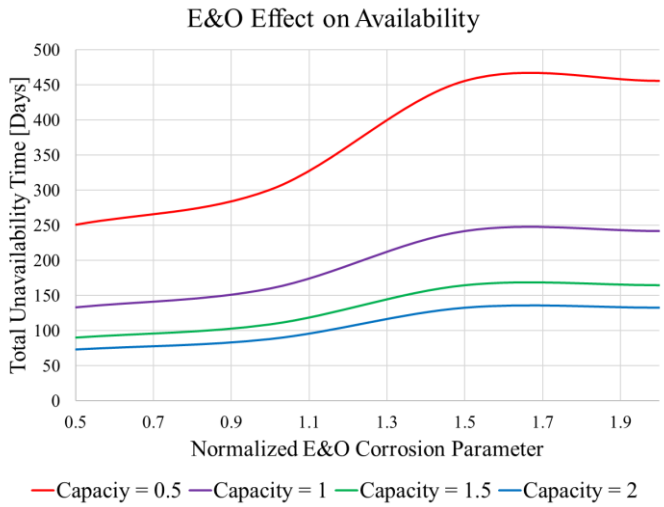


Figure 71. Ship E&O and Shipyard Quality Effect on Total Unavailability Time (TUT).

Table 39. Ship Structure Thickness and Shipyard Quality Effect on Repair Frequency (RF).

SOLUTION (downtime years)		Normalized Thickness			
		0.5	1	1.5	2
Normalized Capacity	2	[3 6 9 13 17 21] (RF = 6)	[5 10 15 20] (RF = 4)	[6 9 12 18] (RF = 4)	[8 17] (RF = 2)
	1.5	[3 6 9 13 17 21] (RF = 6)	[5 10 15 20] (RF = 4)	[6 9 12 18] (RF = 4)	[8 17] (RF = 2)
	1	[3 6 9 13 17 21] (RF = 6)	[5 10 15 20] (RF = 4)	[6 9 12 18] (RF = 4)	[8 17] (RF = 2)
	0.5	[3 6 9 13 17 21] (RF = 6)	[5 10 15 20] (RF = 4)	[6 9 12 18] (RF = 4)	[8 17] (RF = 2)

Table 40. Ship E&O and Shipyard Quality Effect on Repair Frequency (RF).

SOLUTION (downtime years)		Normalized E&O Parameter			
		0.5	1	1.5	2
Normalized Capacity	2	[6 12 16 19] (RF = 4)	[5 10 15 20] (RF = 4)	[3 7 11 14 18 21] (RF = 6)	[3 6 9 13 17 21] (RF = 6)
	1.5	[6 12 16 19] (RF = 4)	[5 10 15 20] (RF = 4)	[3 7 11 14 18 21] (RF = 6)	[3 6 9 13 17 21] (RF = 6)
	1	[6 12 16 19] (RF = 4)	[5 10 15 20] (RF = 4)	[3 7 11 14 18 21] (RF = 6)	[3 6 9 13 17 21] (RF = 6)
	0.5	[6 12 16 19] (RF = 4)	[5 10 15 20] (RF = 4)	[3 7 11 14 18 21] (RF = 6)	[3 6 9 13 17 21] (RF = 6)

The same TUT results are also plotted in a heatmap, where the normalized capacity varies in the y-axis while the normalized thickness (Figure 72) or E&O normalized parameters (Figure 73) varies in the x-axis.

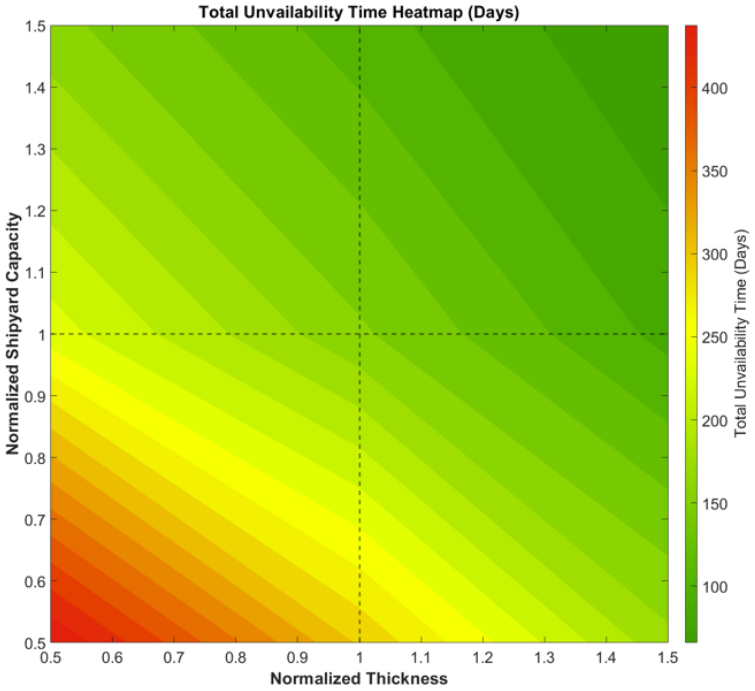


Figure 72. Ship Structure Thickness and Shipyard Quality Effect on Total Unavailability Time (TUT) (Heatmap).

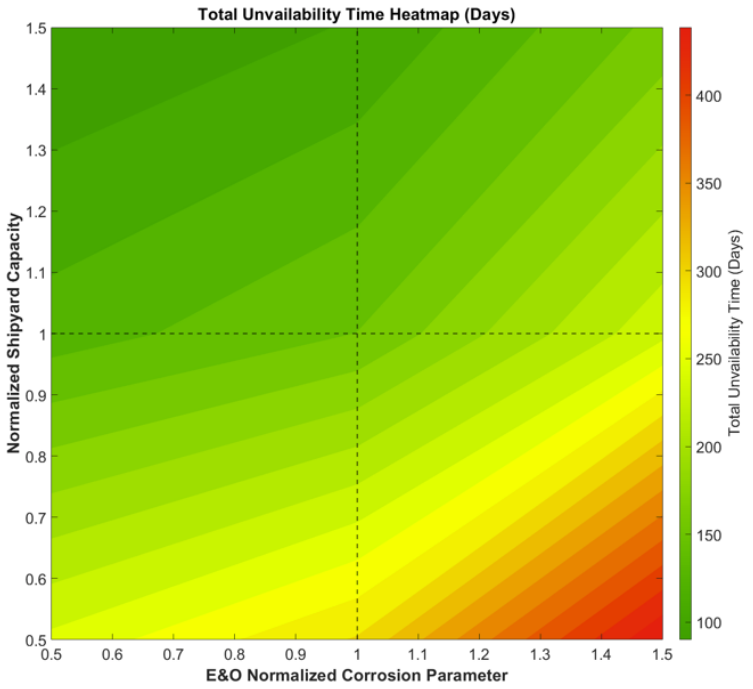


Figure 73. Ship E&O and Shipyard Quality Effect on Total Unavailability Time (TUT) (Heatmap).

The results provide quantitative evidence that reducing structure thickness or increasing E&O corrosion parameters decreases Reliability (R), thus increasing the TUT. This effect is non-linear, as observed by Figure 70 and 71, with a reduction in the rate of change of unavailability for E&O analysis, where it reaches a steady state condition. This behavior was observed and justified in Section 4.7.2

Moreover, the ship structure's Reliability (R) reduction effects are enhanced by capacity reduction, which provides a non-linear steep increase in TUT, already explored in Section 4.7.3.1.

It is also evident that the optimal solution output by the OMCRO framework increases RF when reducing Reliability (R). Accordingly, when varying factors by (0.5, 1, 1.5, 2), the RF output is (6, 4, 4, 2) for the thickness factor and (4, 4, 6, 6) for the E&O factor, respectively. This effect is explained by the increase in the probability of failure; therefore, reducing individual time thresholds and consequently demanding more frequent interventions.

4.7.4 Ship Structure (SoI) Reliability (R) and Shipyard (SS) Quality (Q) Emergent Effects on Maintainability (M) and Availability (A)

Considering the sensitivity analysis and rationales provided by Sections 4.7.1, 4.7.2, and 4.7.3, this Section combines the previous effects of ship structure (SoI) Reliability (R), and shipyard (SS) Quality (Q) on Maintainability (M) and Availability (A). In this regard, Reliability (R) sensitivity is investigated by independently varying the ship structure's thickness and E&O corrosion parameter by factors (0.5, 1, 1.5). Similarly, Quality (Q) sensitivity is observed by independently varying capacity and variability by factors (0.5, 1, 1.5).

Considering the multi-dimensional analysis of the problem and looking for a straightforward sensitivity visualization, this work proposes a nested multivariate function visualization. Accordingly, to represent it in a 2D plot, the outer y and inverted x axis respectively represent shipyard capacity and E&O corrosion parameters, while for each point in this domain, an inner x and inverted y axis respectively represent the ship structure's thickness and shipyard variability.

Therefore, the sensitivity analysis is conducted in four independent dimensions to obtain a fifth dependent outcome in both Maintainability (M) and Availability (A). Accordingly, Figure 74, Figure 75, and Figure 76 represent a discrete five-dimensional (5D) space for Total Expected Cost C_T, Total Unavailability Time (TUT), and Repair Frequency (RF).

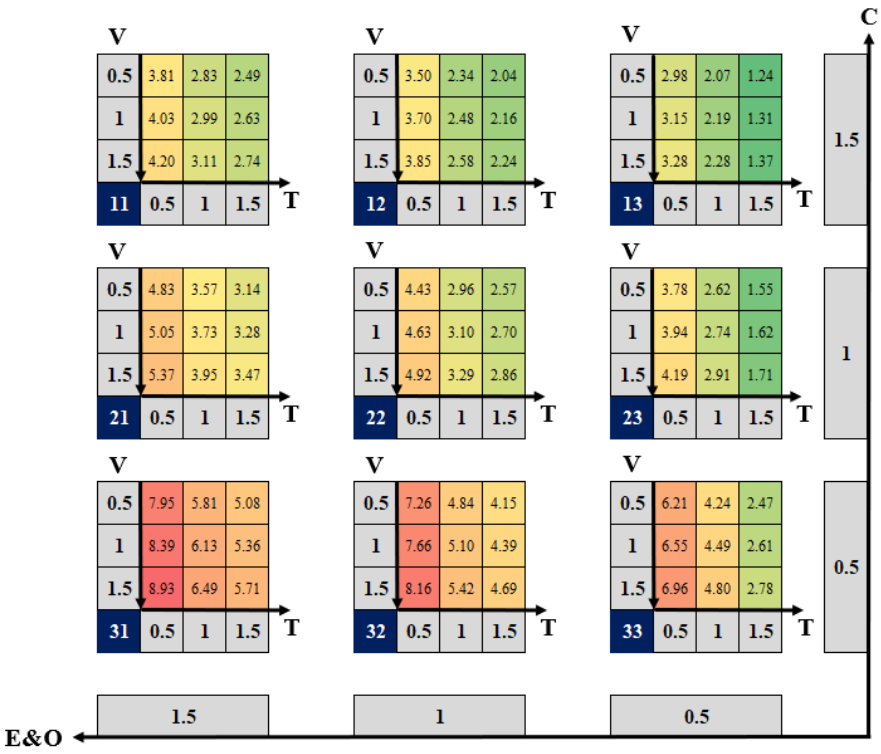


Figure 74. Five-dimensional (5D) space for Total Expected Cost C_T.

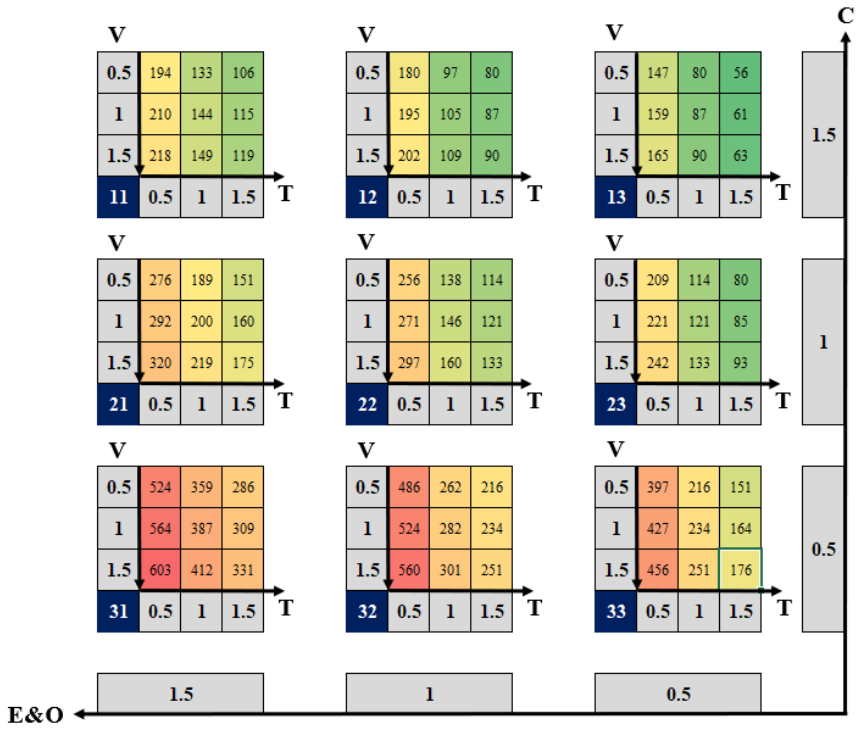


Figure 75. Five-dimensional (5D) space for Total Unavailability Time (TUT).

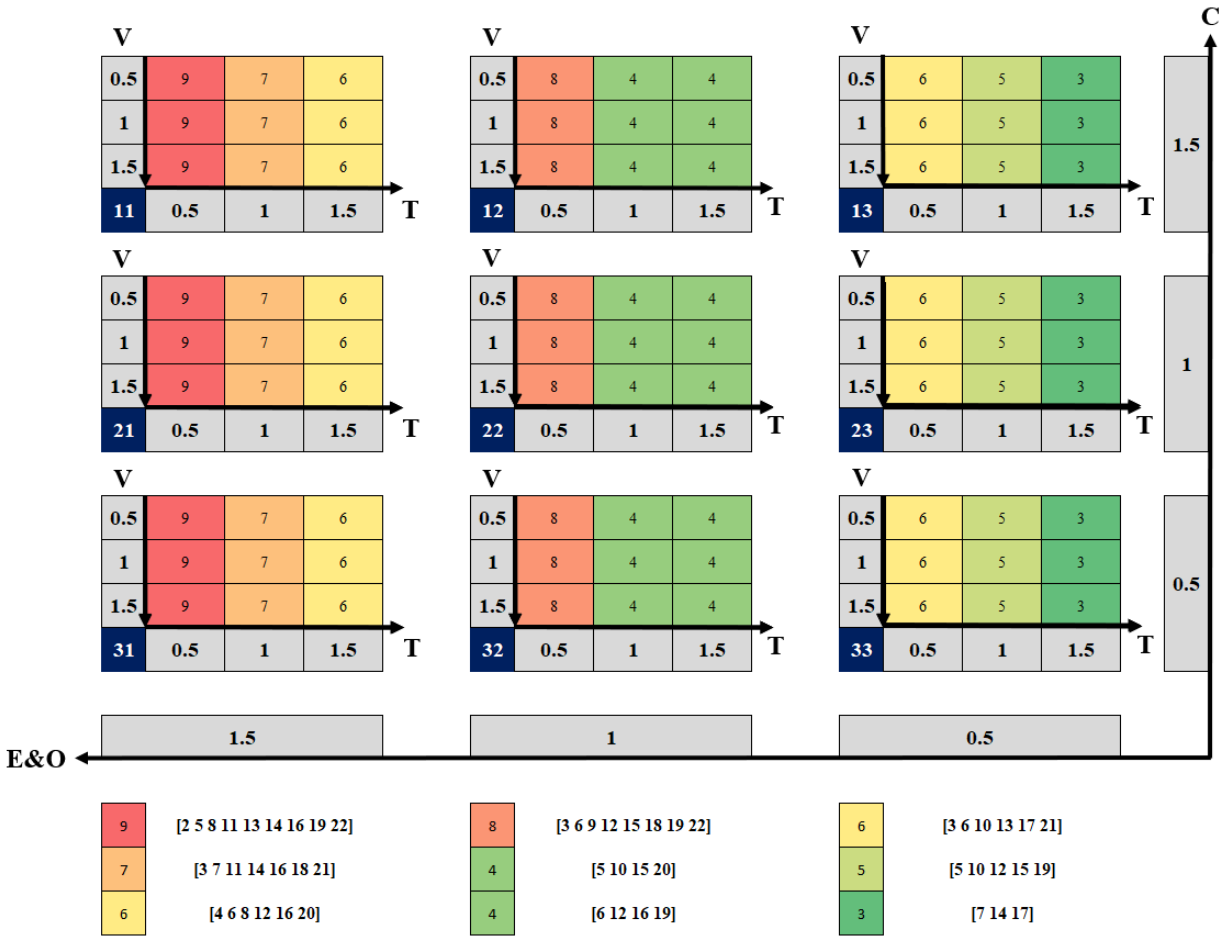


Figure 76. Five-dimensional (5D) space for Repair Frequency (RF).

The combined effects are consonant with the previous investigations presented in Sections 4.7.1, 4.7.2, and 4.7.3:

I. Increase in costs (C_T) and idle times (TUT), in other words, decrease in Maintainability (M) and Availability (A), are driven by a decrease in ship structure (SoI) Reliability (R), shipyard (SS) Quality (Q), or both.

II. Increase in Repair Frequency (RF) is solely driven by a decrease in ship structure (SoI) Reliability (R). The shipyard (SS) Quality (Q) doesn't impact RF.

III. Reliability (R) is positively correlated to the ship structure's thickness and negatively correlated to E&O corrosion parameters. Also, Quality (Q) is positively correlated to the shipyard's capacity and negatively correlated to the shipyard's variability.

Another important finding provided by the quantitative analysis is that the downtime solutions are the same when varying Quality (Q) for the same configuration and workflow process. Therefore, although C_T and TUT vary with Quality (Q), the downtime solution remains the same. This result provides evidence that, in the optimal domain, the shipyard (SS) Quality (Q) drives TUT, while the ship structure (SoI) Reliability (R) drives RF and optimal schedule, independently. The integration of both effects drives cost and unavailability time. This is a notable and straightforward conclusion that can leverage the understanding of Maintainability (M) and Availability (A) to support decision-making.

4.7.5 Qualitative Communication of Quantitative Maintainability and Availability Analysis

Despite the complex optimized trade-offs with quantification of times, costs, and decisions, it is useful to qualify some aspects of the SIM dynamics. This qualification can provide a way to easily communicate with non-technical stakeholders and drive some high-level thoughts that can explain good and bad decisions in the industry.

As demonstrated in this work, SIM must be perceived as a System of Systems (SoS) discipline, here considered ship structure (SoI) and shipyard (SS):

I. Ship Structural System (SoI):

The ship's structural system is designed with corrosion margins and is bounded by environmental conditions. Therefore, ship-environment interactions will define the degradation rate and will dictate the components' renewal time thresholds. Accordingly, low-reliability (LR) structures are associated, in extreme bounds, with low thickness in highly corrosive environments (e.g., light-weight steel patrol vessels operating in warm seas and atmosphere). These systems require frequent and available support. Conversely, high reliability (HR) structures are associated, in extreme bounds, with high thickness in low corrosive environments (e.g., polar icebreakers operating in high latitudes). These

systems are steadfast for longer periods without maintenance. As a drawback, HR structures, as opposed to LR, require higher CAPEX and potentially yield higher fuel consumption in OPEX with increasing thickness. This trade-off was not analyzed in this work; rather, it was considered as future work in Chapter 6.

II. Shipyard System (SS):

The shipyard is the system responsible for providing direct supportability. As verified in this work, the optimal intervention is not straightforward due to grouping strategies and trade-offs between structural and expected costs. Moreover, it was verified that Quality (Q) has a major effect on the downtimes' cost and time, while the optimal schedule, which has the same solution for different SS capacities and variabilities, is robust for a specific grouping strategy and shipyard process, given a fixed SoI Reliability (R). The decrease in Quality (Q) is described by a steep non-linear increase in cost and idle time for lower capacities and a marginal underperformance for higher variabilities, especially in low-capacity scenarios. Accordingly, high quality (HQ) is indicated by high capacity and low variability; on the other hand, low quality (LQ) is herein defined by low capacity and high variability. As a disadvantage, HQ systems are more expensive to implement, require constant quality control, investment in training, and need to be constantly loaded. This trade-off was not analyzed in this work and was considered future work in Chapter 6.

Therefore, considering the relevant impact of SS and by considering the fundamental SoS perspective for an emergent quantification and qualification in Maintainability (M) and Availability (A), this dissertation proposes the consideration of SS Quality (Q) in the RAMS approach, renamed RAMSQ. Therefore, a qualitative perspective of this emergent behavior is provided by RAMSQ Charts, presented by Figure 77 and Figure 78, where the latter is illustrated in a higher-level description. The RAMSQ Charts qualitatively demonstrate conclusions, based on quantitative results, that the shipyard (SS) and ship structures (SoI) have independent contributions to SIM and produce emergent Maintainability (M) and Availability (A). Accordingly, SS quality drives repair duration, while SoI reliability drives repair schedule and frequency. Both effects define Maintainability (M) and Availability (A), quantified in cost and time, respectively.

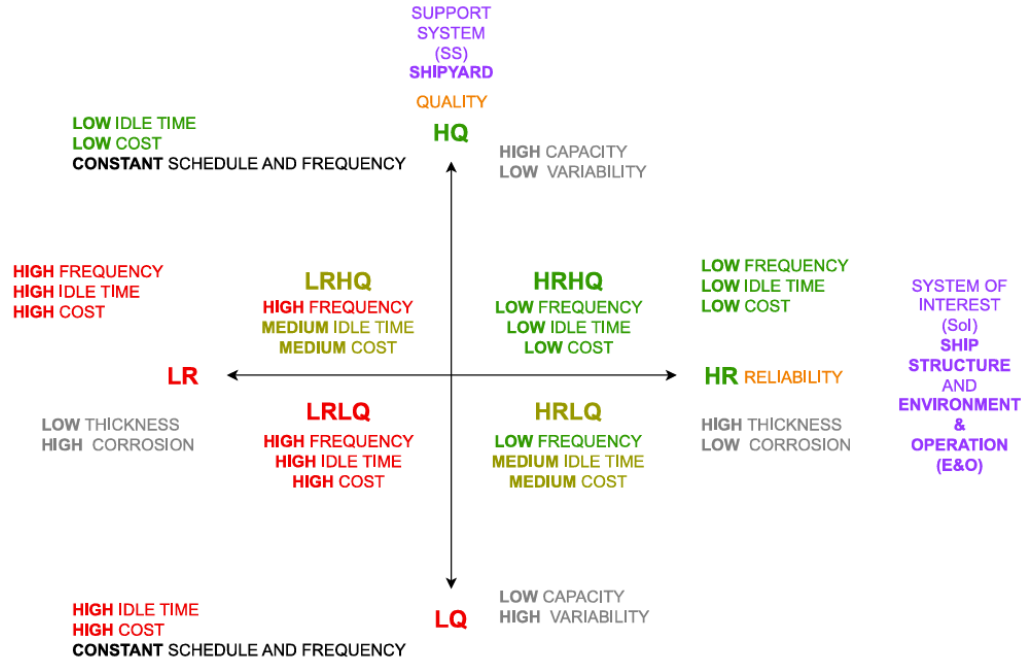


Figure 77. RAMSQ Chart.

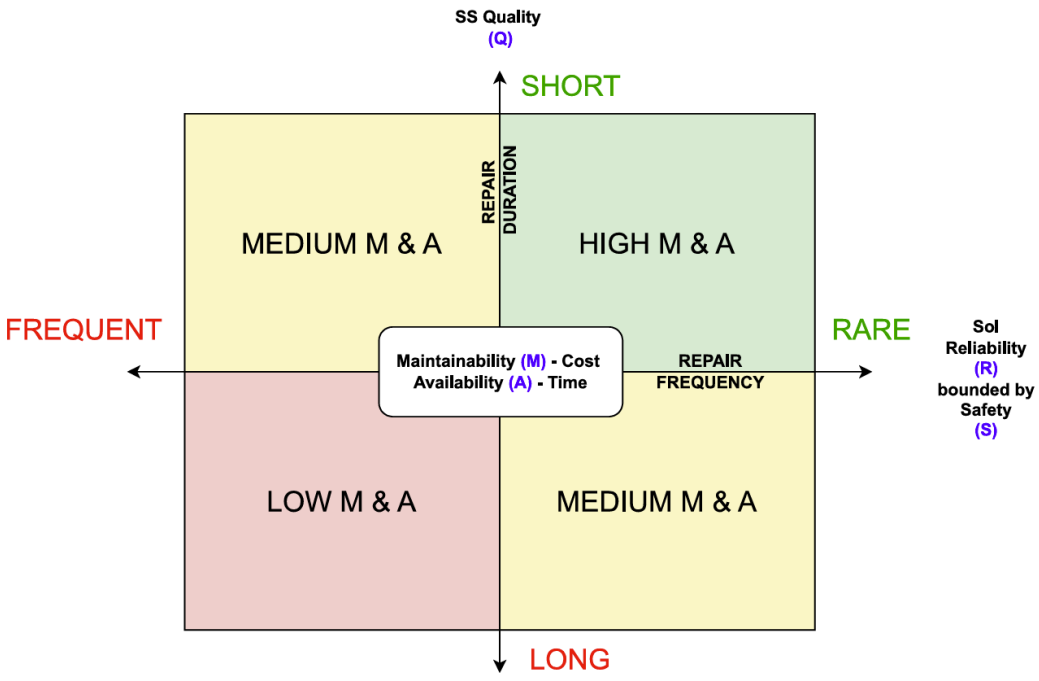


Figure 78. RAMSQ Chart (High-Level).

The RAMSQ Chart is based on the quantitative evidence provided by the OMCRO simulation analysis, as presented in Section 4.7.4. Furthermore, the HQ implementation cost, and

CAPEX and OPEX increase, with larger thickness values for HR, were not considered in this work. This consideration would change the quantitative results, increasing costs in the first (HRHQ), second (LRHQ), and fourth (HRLQ) quadrants, reducing their performance difference from the third quadrant (LRLQ). This analysis is considered for future work in Chapter 6.

Accordingly, the SoS HRHQ has the best performance, while LRLQ presents the worst case. Intermediate SoS (HRLQ and LRHQ) presents potentially close performance on cost and idle time. However, the former provides high repair frequency of short downtimes, while the latter presents low repair frequency of long downtimes.

Although the LRLQ condition is the most critical, it is also common. This situation typically arises when the emergent property of the SoS context is overlooked in favor of exclusive cost reduction strategies, or at the shipyard level (reduced quality), or at the ship level (thinner structures). The risk is greater when ships of the same class are repeatedly serviced by the same shipyard. In such cases, some ships remain idle for extended periods, while others either wait for maintenance or continue operating to maintain fleet availability. However, these ships often operate without adequate reliability, increasing risks to the crew, vessel, and cargo. Over time, these ships experience further degradation, potentially leading to unplanned downtime with more severe damage. This, in turn, extends idle periods and delays maintenance for other ships, creating a cascading and chronic effect that can significantly reduce long-term fleet performance. For design purposes, understanding this relationship, which persists for the vessel's life span (25-40 years), is critical. This fleet effect was not quantified in this thesis, but is suggested in future work in Chapter 6.

It is worth mentioning that other aspects of the structural system (SoI), not related to Reliability (R), impact the downtime costs and time. These elements are related to inherent characteristics of the ship, such as ship size, structural elements' shape, size, and location, and the need to remove interferences. All these aspects are considered in the model, but were not evaluated in the quantitative sensitivity, since they remained constant for the RAMSQ analysis.

4.8 Scalability

For scalability evaluation, the OMCRO framework is used in a more comprehensive simulation to apply SIM for 200 structural elements of a generic lightweight naval vessel. The elements have different shapes and sizes and are localized in a diverse number of compartments

subjected to a simulated environment and operation, as presented in Table 41. The elements have thicknesses varying from 4 to 7 mm (Casares and Vlahopoulos 2024). Moreover, the costs' parameters are the ones presented in Appendix D.

Table 41. Environment and Operation parameters (Scalability Simulation).

VESSEL OPERATIONAL PARAMETERS	OPERATION 1	OPERATION 2	OPERATION 3
MEAN SHIP RELATIVE SPEED (knots)	8	10	15
MEAN SEA WATER TEMPERATURE (°C)	20.0	22.0	28.0
MEAN DISSOLVED OXYGEN CONCENTRATION (mL/L)	4	4	4
MEAN ENVIROMENT AIRBORNE CHLORIDES ($mg/m^2/day$)	170.00	180.00	400.00
OPERATION RATIO (%)	75	20	5
RELATIVE HUMIDITY (%)	81.9	81.9	81.9
ENVIRONMENTAL TEMPERATURE (°C)	25.0	24.0	27.0
OIL TANK TEMPERATURE (°C)	24.0	24.0	26.0
H_2S CONCENTRATION IN OIL TANK (ppm)	817	817	817
CO_2 GAS IN OIL TANK (vol %)	10.9	10.9	10.9
FUEL LOADING RATIO (%)	60	70	50
BALLAST RATIO (%)	75	100	100

The overall results are presented for Time-Grouping in Table 42 and Figure 79, and for Policy-Grouping in Table 43 and Figure 80.

Table 42. OMCRO overall results (Time-Grouping Strategy - 200 elements).

```
------------------------------------------------------------------
Optimized Solution:
------------------------------------------------------------------
Total Cost Results (USD) in PV:
              CostEvaluation                CostResult
    ____________________________________    __________

    "Structural Cost (PV)"                  4.0415e+06
    "Expected Cost of Failure (PV)"         9.3855e+05
    "Expected Cost of Opportunity (PV)"     1.1108e+06
    "Total Expected Cost (PV)"              6.0908e+06

------------------------------------------------------------------
Total Unavailability Result (days): 210
------------------------------------------------------------------
General Result:
    RepairNumber    Years    NumberOfElements    StructuralCost_FV    DrydockDays    QuayDays    UnavailabilityDays
    ____________    _____    ________________    _________________    ___________    ________    __________________

         1            4            14              5.7643e+05            22            0              22
         2            7             4              2.9016e+05            10            0              10
         3           10            14              6.4915e+05            22            0              22
         4           13            96              1.5067e+06            35           33              68
         5           17            33              1.1895e+06            30           19              49
         6           21            19              1.0755e+06            26           13              39

------------------------------------------------------------------
```

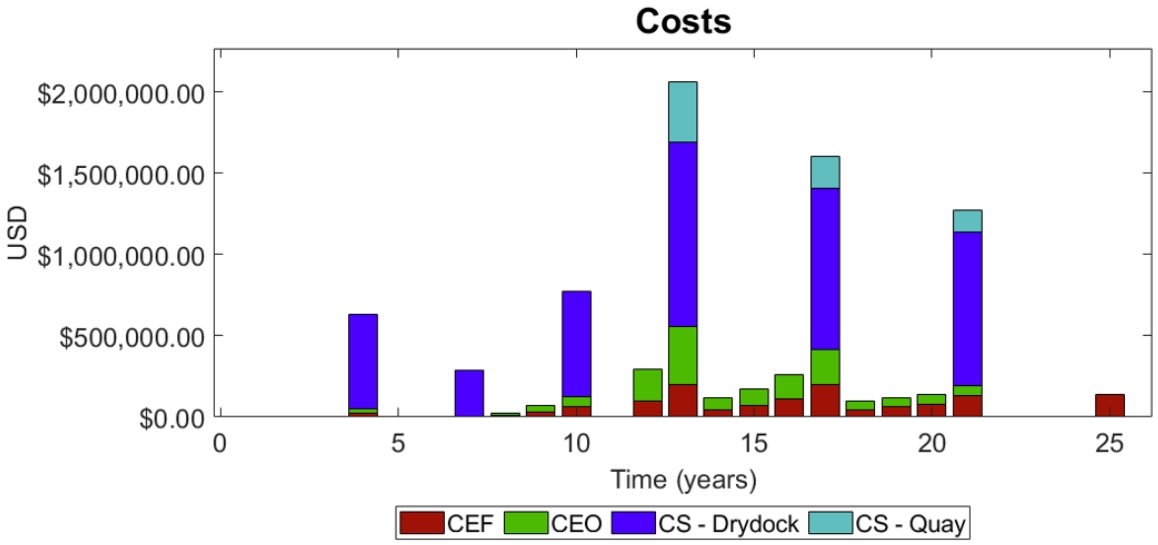


Figure 79. OMCRO overall results (Time-Grouping Strategy - 200 elements).

Table 43. OMCRO overall results (Policy-Grouping Strategy - 200 elements).

```
------------------------------------------------------------------
Optimized Solution:
------------------------------------------------------------------
Total Cost Results (USD) in PV:
              CostEvaluation                 CostResult
    ____________________________________    __________

    "Structural Cost (PV)"                  4.561le+06
    "Expected Cost of Failure (PV)"         9.0061e+05
    "Expected Cost of Opportunity (PV)"     1.1278e+06
    "Total Expected Cost (PV)"              6.5896e+06

------------------------------------------------------------------
Total Unavailability Result (days): 215
------------------------------------------------------------------
General Result:
    RepairNumber    Years    NumberOfElements    StructuralCost_FV    DrydockDays    QuayDays    UnavailabilityDays
    ____________    _____    ________________    _________________    ___________    ________    __________________

          1           3             14              5.6512e+05            22            0              22
          2           6             14              5.9971e+05            22            0              22
          3           9             14              6.3642e+05            22            0              22
          4          13            146              2.1191e+06            51           42              93
          5          17             14              7.4567e+05            22            0              22
          6          21             26              1.2017e+06            34            0              34

------------------------------------------------------------------
```

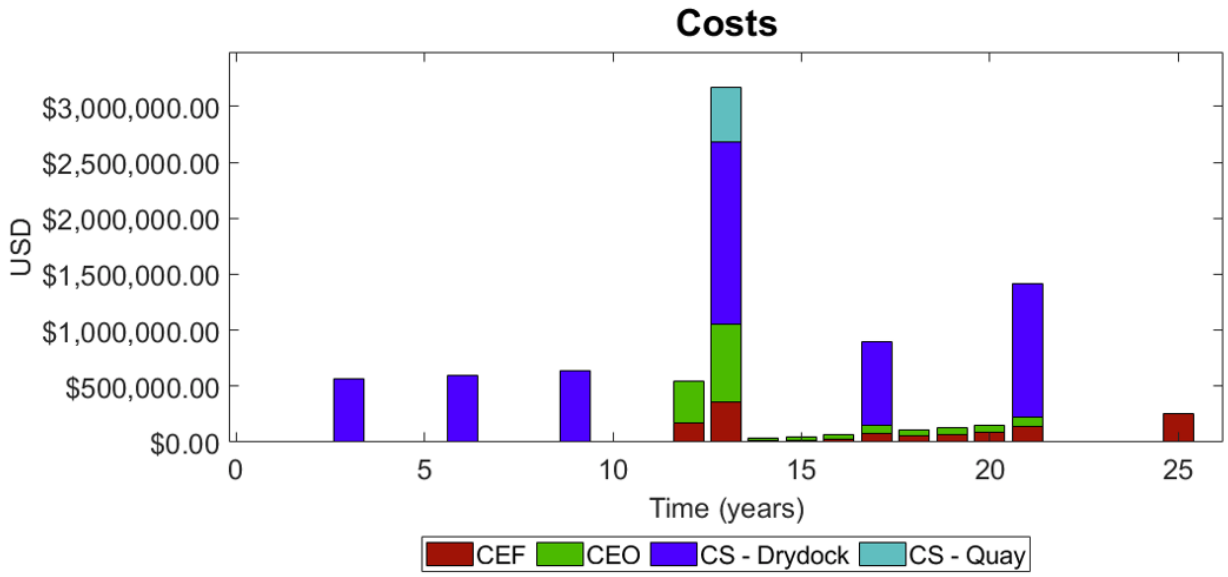


Figure 80. OMCRO overall results (Policy-Grouping Strategy - 200 elements).

Time-Grouping presented the optimal solution $\boldsymbol{t}_{\boldsymbol{m}}^{*} = [4\ 7\ 10\ 13\ 17\ 21]$ while Policy-Grouping presented a close solution $\boldsymbol{t}_{\boldsymbol{m}}^{*} = [3\ 6\ 9\ 13\ 17\ 21]$. However, the Time-Grouping outperformed Policy-Grouping Strategy in terms of cost, as opposed to the 5-elements' simulation conducted earlier in this Chapter. In this regard, the Policy-Grouping Strategy increased C_S and decreased C_{EF}, since more elements are grouped per downtime. However, opposed to the 5-elements' simulation, C_{EO} increased. This can be explained by the fact that grouping more elements increased the idle time parameter of the budgeted cost term of C_{EO}, outweighing the reduction in C_{EF}, which is the unbudgeted cost term of C_{EO}.

Considering the five and 200 elements simulations, the schedule interval between downtimes is 3 – 5 years, which is very close to the IACS rules for intermediate and special survey intervals (IACS 2022). Furthermore, it is evident that the most significant risks and maintenance costs occur close to 15 years, which aligns with the IACS enhanced inspection scope beyond this age (IACS 2022). This indicates that the combination of corrosion allowance, failure probability thresholds by severity level, and cost-effectiveness optimization yields results aligned with reality and industry best practices.

4.9 OMCRO Framework Validation

The 12 high-level requirements of the OMCRO framework, presented in Section 1.3, are checked with the developments of this thesis, as follows:

I. The parameters input shall be developed in digital spreadsheets.
   - (Table 6, Appendix C, D, and H)

II. The inputs shall include SoI structural, operational, environmental, cost, and safety-related parameters and SS parameters.
   - (Table 6, Appendix C, D, and H)

III. The output shall include the probability of structural failure, consequences of failure, risks, costs, intervention duration, and optimal maintenance schedule.
   - (Section 4.5.1 and Appendix H)

IV. The output shall clearly indicate what, when, and where the structural element is going to be maintained, and what the costs and risks are involved.
   - (Section 4.5.1 and Appendix H)

V. The probability of failure output shall be validated by simulation.
   - (Section 2.5)

VI. The intervention time shall be validated by simulation.
   - (Section 3.3.2.2)

VII. The optimal solution output shall be validated by simulation.
   - (Section 4.6.2)

VIII. The outputs shall be formatted to be capable of external software importation.
   - (MathWorks® MATLAB® exports spreadsheets)

IX. The framework shall perform analysis of different elements as a deliverable demonstration.
   - (Section 4.5.1 and 4.8)

X. The verification of the framework shall be carried out in digital spreadsheets.
   - (Section 4.6.1)

XI. The output shall be compared with existing structural management practices.
   - (Section 4.8)

XII. The quantitative output shall be able to communicate qualitative conclusions.
   - (Section 4.4.3, 4.7.5, and 4.8)

4.10 Conclusion

This Chapter provided a comprehensive research on maintenance, indicating that the Opportunistic Maintenance Strategy is an unexplored field, especially in the ship industry. In this respect, Chapter 1 provided a high-level description of the maintenance problem and presented the building blocks based on RAMS. This basis supports the development of a framework for CE Maintainability (M) for naval supportability regarding the integration of ship structure (SoI) and shipyard (SS). Accordingly, This Chapter details the knowledge, information, and data (KID) to develop an Opportunistic Maintenance framework, which is supported by the previous developments in this thesis.

Consistently, previous literature was explored, and a novel Opportunistic Maintenance Cost and Risk Optimization (OMCRO) framework was developed. The framework is built in a comprehensive architecture of 31 integrated codes on MathWorks® MATLAB®, with approximately 200 different types of parameters. The model accounts for economic, reliability, and safety considerations, leveraging an opportunistic repair grouping process as a payoff for quantitative risk reduction, with the objective of minimizing the Total Expected Cost (C_T) with optimal scheduling. This process is a new development with simple steps to group multiple repair-interlinked components, detailed in separate sections for Time-Grouping and Policy-Grouping Strategies. Accordingly, it was demonstrated that Policy-Grouping, which increases the number of components to be repaired, can potentially provide a better overall solution by outweighing the Structural Cost (C_S) with higher reduction in risks – Expected Cost of Failure (C_{EF}) and Expected Cost of Opportunity (C_{EO}). Although this result does not necessarily hold for other analyses, such as the 200-element simulation, it provides evidence of the trade-off relevance. Also, the relative behavior of C_{EF} and C_{EO} provides not only a maintenance-level economic indicator but also a governance-level signal. Their crossover acts as an economic trigger for reassessing remaining service-life assumptions, enabling structured evaluation of life extension, repurposing, or decommissioning alternatives under updated economic conditions.

Through GA optimization, the model seeks a good trade-off between operational risks (C_{EF} and C_{EO}) and repair costs (C_S), providing clear guidance for stakeholders on what, when, and where to survey and repair, as well as understanding the associated costs and risks. It was used to simulate Structural Integrity Management (SIM), considering five structural elements of a generic naval

vessel transverse section subjected to a simulated environment and operation. The results were successfully verified by hand calculation and validated by Monte Carlo simulations.

By using the verified and validated OMCRO framework, a novel quantitative analysis was conducted, leveraging the understanding of the Maintainability (M) and Availability (A) behavior as an emergent factor of ship structure (SoI) and shipyard (SS). Accordingly, quantitative impacts of SoI Reliability (R), bounded by Safety (S) levels, and SS Quality (Q) were investigated on Maintainability (M) and Availability (A) by a cost-effective (CE) perspective. Therefore, complying with the RAMS foundation. The following relations were quantified for optimum costs and schedules:

I. Shipyard (SS) Quality (Q) is quantified by process capacity and variability (coefficient of variation).
II. Ship structure (SoI) Reliability (R) is quantified by structure thickness and environmental and operational (E&O) corrosion parameters.
III. Maintainability (M) is quantified by Total Expected Cost (C_T).
IV. Availability (A) is quantified by Total Unavailability Time (TUT) and Repair Frequency (RF).
V. Decrease in capacity reduces Quality (Q) by yielding a steep non-linear increase in Total Expected Cost (C_T) and Total Unavailability Time (TUT).
VI. Increase in variability reduces Quality (Q) by marginally increasing Total Expected Cost (C_T) and Total Unavailability Time (TUT), with enhanced effect for low-capacity scenarios.
VII. Variations in shipyard (SS) Quality (Q), given the same process, do not yield changes on optimal schedule and Repair Frequency (RF), which remain constant.
VIII. Decrease in ship structure (SoI) thickness reduces Reliability (R), providing a non-linear increase in Total Expected Cost (C_T) and Total Unavailability Time (TUT).
IX. Increase in E&O corrosion parameters reduces Reliability (R), providing a non-linear increase in Total Expected Cost (C_T) and Total Unavailability Time (TUT), with reduced rates for high E&O corrosion parameters.
X. Decrease in Reliability (R) yields a change in optimal schedule and an increase in Repair Frequency.

XI. The shipyard (SS) quality drives downtime duration, while the ship structure (SoI) reliability drives downtime schedule and frequency, independently. The integration of both effects drives Maintainability (M) and Availability (A), related to cost and time, respectively. This is a notable and straightforward conclusion that can leverage the understanding of Maintainability (M) and Availability (A), and support decision-making.

The quantitative findings on RAMS' relationships were plotted in different graphs for easy comprehension. The results propose adding the Quality (Q) of Support Systems (SS) to the traditional RAMS (Reliability, Availability, Maintainability, and Safety) approach, creating a new leveraged perspective called RAMSQ. This is based on the important role of a SoS perspective to better understand and measure Maintainability (M) and Availability (A).

Nonetheless, a qualitative rationale and a new RASMQ Chart were developed for clear communication with non-technical stakeholders on the fundamental impacts of decision-making regarding aspects of Maintainability (M) and Availability (A) on ship design and operation.

Furthermore, to demonstrate the OMCRO framework's scalability capacity, a simulation was successfully conducted considering 200 structural elements with different shapes and sizes, localized in a diverse number of compartments, and subjected to a simulated environment and operation. Its results demonstrate the framework's efficacy in aligning with industry standards while offering valuable insights for academia, engineers, surveyors, shipyards, Classification Societies, and asset managers involved in ship structural integrity management. Furthermore, the proposed framework is built upon a logical and straightforward process that can be understood by all stakeholders, creating trust in decision-making, which is valuable for implementation.

Finally, the framework structure is modular and flexible to accommodate improvements. When an enhanced or a particular corrosion or cost model becomes available, it is easy to incorporate. Also, it is capable of application with multiple systems, not only ship structure, since it is based on a logical grouping principle and does not make a distinction on what type of system component is being grouped.

Chapter 5 Thesis Contributions

"Imagination is more important than knowledge. For knowledge is limited, whereas imagination embraces the entire world."

- Albert Einstein (Einstein 1929)

This Chapter presents the key contributions of the research conducted in this dissertation, which are aligned with the problem formulation and objectives. Accordingly, this work addresses critical gaps in existing literature and industry, proposes novel methodologies, and offers theoretical and practical insights relevant to the fields related to SIM: Naval Architecture (structural integrity), Systems Engineering (life cycle and RAMS), and Industrial and Operations Engineering (analytical modeling, production, and optimization). Each contribution is discussed concerning the challenges it resolves and the originality it demonstrates:

I. Leveraged high-level concept for RAMS integration with emergent Maintainability (M) and Availability (A) for AIM

Chapter 1 introduces RAMS as the building blocks to sustain the Asset Integrity Management framework. More specifically, Figure 3 provides a novel, clear mapping of RAMS integration under a SoS perspective between SoI and SS. In this regard, Maintainability (M) is conceived as an emergent Quality Characteristic (QC) of the systems integration and not just related to the SoI, as previously indicated in the existing classic literature. Furthermore, Maintainability (M) emergence affects and is affected by Availability (A) of both SoI and SS. Accordingly, this perspective is proven fundamental through this dissertation's results and conclusions.

II. Leveraged time-based probabilistic general corrosion model for any ship space

Chapter 2 explores foundational and recent works on general corrosion modeling of ship steel structures. Therefore, deriving a probabilistic assessment of single-sided models makes it possible to perform estimations on time-based probabilistic corrosion degradation in any desired ship space. The development is founded on authoritative references, while the innovations were validated by Monte Carlo Simulation (MCS).

III. Provided novel integration of shipyard processes and quality for a comprehensive analytical structural cost and production time model

Chapter 3 provides a comprehensive analytical cost and time model of ship structure maintenance based on core shipyard processes, Group Technology (GT), and queueing theory related to Constant Work in Process (CONWIP). A validation is presented for the continuous fabrication and repair workflow by Discrete Event Simulation (DES), also identifying the limits of the analytical model. This model acknowledges multiple parameters and variables that contribute to structural maintenance and provides insights into how they impact cost, time, and schedule. Furthermore, under some limitations, this model works as a surrogate for computational analysis under DES, which is based on Monte Carlo approaches. This aspect is advantageous under the OMCRO framework, considering that each feasible solution under the Genetic Algorithm (GA) metaheuristic search calls the cost and time model. Therefore, using a validated analytical model allows it to be incorporated into the optimization framework without significantly increasing the computational effort.

IV. Developed a novel economic model to describe the Expected Cost of Opportunity of non-planned unavailability of naval vessels, providing a governance-level signal for reassessing remaining service life

Chapter 3 discusses the concept of opportunity cost in the field of defense economics and identifies it as an overlooked potential expenditure regarding unplanned idle times. Accordingly, the proposed risk of opportunity formulation

combines unbudgeted failure costs and budgeted but non-allocated operation and support costs, while accounting for the foregone return on public capital using a risk-free option. The opportunity cost is directly associated with the operational tangible value of keeping the vessel as an available option. Accordingly, sensitivity analysis indicates that the investment horizon of the foregone alternative is the dominant contributor to the risk of opportunity, leading to higher costs for early unexpected downtimes and naturally diminishing effects as the vessel approaches the end of its service life. Therefore, this cost is incorporated as an element of operational risk. Accordingly, the relationship between the Risk of Opportunity and the Risk of Failure triggers a governance-level signal for reassessing remaining service-life assumptions, enabling structured evaluation of life extension, repurposing, or decommissioning alternatives under updated economic conditions.

V. Pioneered the application of the Opportunistic Maintenance Strategy in the naval engineering field

Chapter 1 and Chapter 4 introduces the concept of Opportunistic Maintenance Strategy and identifies it as an overlooked advantage to leverage SIM, particularly considering issues presented in the problem overview. In this regard, a cost-effective approach within this strategy was identified and distilled into knowledge, information, and data (KID) architecture as building blocks for a comprehensive framework. This pioneering approach was communicated to the academic field by the author's work (Casares and Vlahopoulos 2024).

VI. Developed original Opportunistic Grouping Strategies

Chapter 4 details a step-by-step process of two innovative procedures to perform components grouping under the Opportunistic Maintenance Strategy: Time and Policy-Grouping Strategies. Accordingly, the processes are simple and straightforward, providing a clear understanding of results and easy incorporation in algorithms, being computationally efficient. The procedure for the two strategies is illustrated by hand calculation.

VII. Developed a novel decision-making framework: OMCRO

Chapter 4 presents a novel Opportunistic Maintenance Cost and Risk Optimization (OMCRO) framework, featuring 31 integrated codes and approximately 200 parameters (Appendix H), which is designed to optimize maintenance decisions. The framework integrates economic, reliability, and safety considerations, leveraging an opportunistic repair grouping process as a payoff for quantitative risk reduction. Specifically, it is applied in this dissertation to address SIM of naval ships, considering probabilistic corrosion models. Through metaheuristic optimization, it seeks a good trade-off between operational risks and repair costs, providing clear guidance for stakeholders on what, when, and where to survey and repair, as well as understanding the associated costs and risks. Furthermore, the model is extensively verified by hand calculation inspection, and its optimal solution is validated by Monte Carlo Simulation (MCS). Accordingly, the optimization is proven to be extremely faster when compared to random trials.

Simulation results demonstrate the framework's efficacy in aligning with industry standards while offering valuable insights for academia, engineers, surveyors, shipyards, Classification Societies, and asset managers involved in SIM. Also, it is flexible and capable of application with multiple systems since it is based on a logical grouping principle and does not make a distinction on what type of system component is being grouped.

VIII. Leveraging RAMS to RAMSQ: Obtained new quantitative results on the effects of SoI Reliability (R) and SS Quality (Q) on Maintainability (M) and Availability (A).

Chapter 4 uses the validated OMCRO framework for an innovative quantitative analysis performed to understand how Maintainability (M) and Availability (A) emerge from the interaction between ship structure (SoI) and shipyard (SS) characteristics, aligning with the RAMS approach presented in Chapter 1. Key variables were quantified: shipyard Quality (Q) by process capacity and variability; ship structure Reliability (R) by structure thickness and corrosion parameters; Maintainability (M) by Total Expected Cost; and Availability (A) by Total Unavailability Time (TUT) and Repair Frequency (RF). The results quantify that

reductions in capacity or increases in variability sharply raise costs and idle times, while reduced thickness or increased corrosive environment also lead to a rise in costs and idle times. The analysis further showed that while shipyard Quality (Q) directly affects the average duration of downtimes, it does not influence scheduling and repair frequency; this is instead governed by the structural Reliability (R) of the ship. These two factors are independent, but together define the emergent Maintainability (M) and Availability (A) in the SoS perspective. This distinction simplifies the understanding of Maintainability (M) and Availability (A) and supports informed decision-making by clearly identifying how shipyard and structural factors impact operational efficiency.

The results propose adding the Quality (Q) of Support Systems (SS) to the traditional RAMS (Reliability, Availability, Maintainability, and Safety) approach, creating a new leveraged perspective called RAMSQ. This is based on the important role of SS and the need for a SoS perspective to better understand and measure Maintainability (M) and Availability (A).

IX. Provided new qualitative rationale and developed a new RAMSQ Chart based on the quantitative findings

Chapter 4 not only provides new and dedicated graphs for quantitative results but also translates them into a qualitative rationale to support broader understanding. Accordingly, a new RAMSQ Chart is developed, providing clear communication on how decisions related to shipyard Quality (Q) and structural Reliability (R) influence Maintainability (M) and Availability (A). This chart serves as a useful tool for non-technical stakeholders, helping them understand the fundamental impacts of their decisions on ship design and operation, and reinforcing the framework's value in guiding effective and informed maintenance strategies.

Chapter 6 Future Work

"A problem well-stated is a problem half-solved."

- Charles Kettering (often attributed - exact origin of this quote is not documented)

This Chapter explores potential areas of interest for future research and industrial applications based on the knowledge built in this dissertation. The suggestions are outlined and detailed as follows:

I. Shipyard (SS) Availability (A) as a constraint to ship (SoI) support

In this dissertation, the shipyard was modeled without bounds on availability to support the ship. Therefore, there is an opportunity to consider the effects of limited resources, such as drydocks and quay spaces, to constrain the OMCRO decisions. Also, by considering that the shipyard shares resources with other ships, effects on costs, idle times, and safety would be enhanced, especially for the LRLQ SoS type.

II. Fleet optimization

In this dissertation, only one ship was considered in the model. However, the effects of optimizing a fleet can bring more value to ship owners, since decisions must be made on trade-offs within diverse assets. Also, by considering fleet and limited support resources in the shipyard, waiting times would be considered part of idle times, and operation beyond safety thresholds could be evaluated.

III. Life Cycle Cost (LCC) consideration

This dissertation did not consider CAPEX and non-maintenance OPEX related to ship structures, such as construction cost and fuel consumption, respectively. This consideration would decrease the benefit of larger thickness in the trade-off since it would imply higher construction costs and higher fuel consumption over the life

cycle. In this respect, the future work could also consider the benefits of curved plates for hydrodynamic hull shape to reduce fuel consumption, but also consider the cost increase in curved shapes, which is already accounted for in the current model. This trade-off was explored by (Dylan 2015).

IV. Reassessing remaining service-life assumptions

The crossover between Risk of Opportunity and Risk of Failure represents an economic inflection point within the bounded service-life horizon. When the Risk of Opportunity becomes lower than the Risk of Failure, the economic burden associated with preserving reliability outweighs the value of maintaining the operational availability option under the current assumptions. This condition does not prescribe an immediate action; rather, it functions as a trigger for reassessing the remaining service-life boundary.

If life extension or repurposing is considered, the renewed availability horizon must be evaluated together with the required capital reinvestment and the residual risk of unexpected failure following the upgrade. Notably, a failure occurring shortly after a life-extension investment results in amplified economic loss due to the recent capital allocation. Conversely, if decommissioning becomes a viable alternative, disposal costs and potential replacement expenditures must be incorporated into the evaluation. Therefore, the risk crossover initiates a structured second-order economic assessment of remaining life decisions.

V. Industry implementation with maintenance 4.0

A. The current framework presents a whole prediction for the ship's lifespan. However, not all predicted conditions will be realized during each ship intervention, and not all indicated repairs will be conducted. Therefore, the OMCRO framework needs to be updated to the current condition every time information is gathered. Accordingly, a new simulation is necessary after each downtime. Moreover, the probabilities of failure must be updated by current observation, which can be done through Bayesian Inference, explored by (Sadeghian 2022; Woloszyk and Garbatov 2024).

B. Other types of maintenance actions can be modeled, such as coating without replacing, and by considering levels of maintenance quality (good, fair, and poor) related to restored condition. The former consideration was approached by (Ayyub et al. 2002).

C. The OMCRO framework has the potential to be implemented within online Structural Health Monitoring (SHM) and be absorbed by frameworks similar to the U.S. Navy CBM+ (DoDI 4151.22 2020). Accordingly, three main systems can be incorporated: Embedded Sensor System (ESS), Mobile Device System (MDS), and SIM System (SIMS). The ESS includes environmental and operational sensors installed in a mesh at different ship compartments and tanks, the MDS provides qualitative and quantitative data gathering by surveyors, and the SIMS integrates, stores, and presents, in a Digital Twin, all collected data and the generated technical data by the OMCRO output. To provide the latter, the SIMS accounts with a Technical Analysis (TA) module to predict failure as well as with a Technical Management (TM) algorithm to optimize opportunistic maintenance and support decision-making. All data is ingested and transits through an Information and Integration Subsystem (I2S), which contains the server, database, system backend, and frontend in dashboards and Digital Twin. The collected data and the proposed framework can also contribute to the application of future AI-based preventive maintenance. The proposed high-level framework is illustrated in Figure 81, where the developments of this dissertation fit TA and TM.

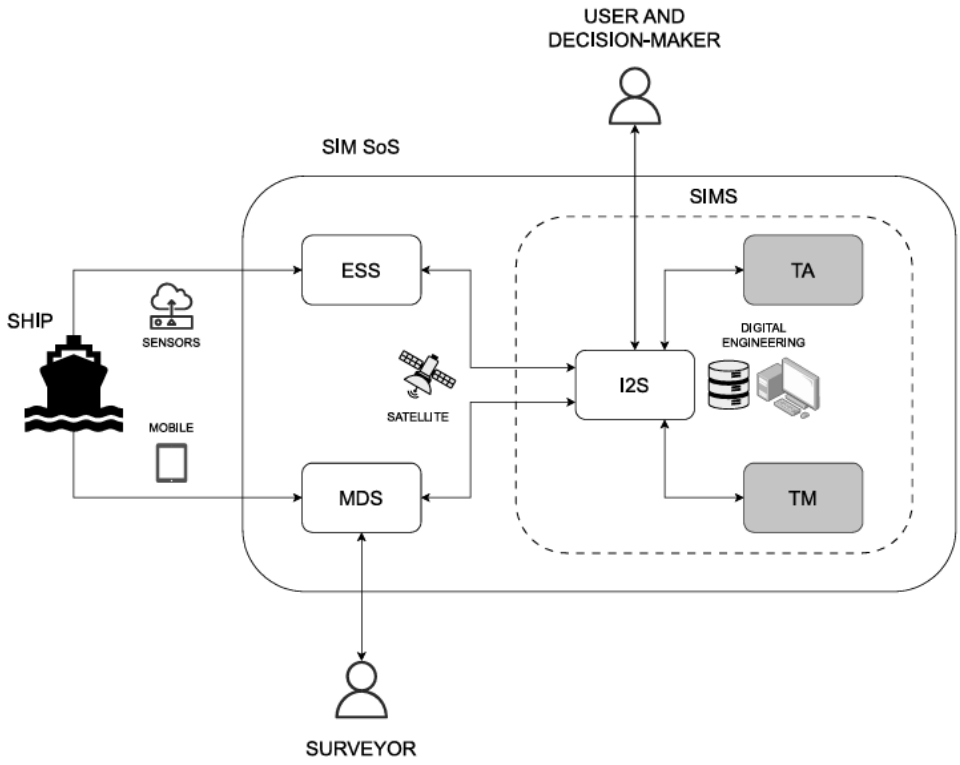


Figure 81. SIM SoS.

Appendices

Appendix A: Long-Term Single-Sided Model

A.1 Step 1: Nominal Short-Term Model for Specific Ship Spaces

Based on the datasets (Garbatov, Guedes Soares, and Wang 2007; Garbatov and Soares 2008; Guedes Soares, Garbatov, and Zayed 2011; Zayed, Garbatov, and Guedes Soares 2018), the time-based corrosion wastage thickness fits a log-normal distribution. The nominal parameters for the time-based mean $d_n(t)$ (Appendix Table A.1) are obtained for specific ship spaces: bottom plates, deck plates for ballast tanks, and oil cargo tanks. The time-based standard deviation $\sigma_n(t)$ for deck and bottom plates are presented in (Appendix Table A.2, Appendix Equation A.1-A.2), respectively.

Appendix Table A.1. Mean $d_n(t)$ parameters from datasets.

Data type	d_∞ (mm)	τ_c (year)	τ_t (year)
Deck Plates-Ballast Tanks	1.85	10.54	17.54
Deck Plates-Cargo Tanks	1.91	11.49	11.23
Bottom Plates	1.42	3.17	14.14

$$\sigma_n(t) = a\ln(t) - b \tag{A.1}$$

$$\sigma_n(t) = 7.16\log(t - \tau_c + 11.60) - 7.41 \tag{A.2}$$

Appendix Table A.2. Standard Deviation parameters for deck plates.

Data type: Deck Plates	a	b
Ballast Tanks	0.384	0.710
Cargo Tanks	0.834	1.838

A.2 Step 2: Nominal Short-Term Single-Sided Model for Multiple Ship Spaces

The double-sided model is divided into two single-sided models. The long-term corrosion wastage depth d_{∞_i} of the side i is calculated considering a margin factor f_i^m, which is defined as the ratio between the corrosion allowance d_{was_i} of the interested side i and the sum of the corrosion allowances from both sides $\sum_{j=1}^{2} d_{was_j}$ (Appendix Equation A.3-A.4) (Zayed, Garbatov, and Guedes Soares 2018).

$$f_i^m = \frac{d_{was_i}}{\sum_{j=1}^{2} d_{was_j}} \tag{A.3}$$

$$d_{\infty_i} = f_i^m \, d_{\infty} \tag{A.4}$$

The single-sided long-term wastage, defined as a reference $d_{\infty_{r_i}}$, is scaled to estimate the long-term corrosion wastage d_{∞_i} of areas without data. The scale factor f_i^s is defined as the ratio between the corrosion wastage allowance of the space of interest d_{was_i} and the reference $d_{was_{r_i}}$ (Appendix Equation A.5-A.6) (A. Zayed, Garbatov, and Soares 2018).

$$f_i^s = \frac{d_{was_i}}{d_{was_{r_i}}} \tag{A.5}$$

$$d_{\infty_i} = f_i^s \, d_{\infty_{r_i}} \tag{A.6}$$

A list of nine ship space classes (A to I) (Appendix Table A.3) and the associated corrosion allowances were presented in (Zayed, Garbatov, and Guedes Soares 2018) and refers to the wastage allowance classification from (IACS 2010). The same list was used to classify the collected data for calibration (Appendix Table A.4).

Appendix Table A.3. Space Classes.

Compartment Type and Structural Member/Place	Class
Ballast water tank (within 3m below tank top)*	F
Ballast water tank (elsewhere)	G
Cargo oil tank (bottom / inner bottom plating)	C
Cargo oil tank (within 3m below tank top)*	D
Cargo oil tank (elsewhere)	E
Exposed to the atmosphere (weather deck plating)	A
Exposed to the atmosphere (other members)	B
Exposed to seawater (shell plating at quay area)	H
Exposed to seawater (elsewhere)	I

* Only applicable to cargo and ballast tanks with weather deck as the tank top

Appendix Table A.4. Collected data type.

Data type	Element Class
Deck Plates-Ballast Tanks	AF
Deck Plates-Cargo Tanks	AD
Bottom Plates	GI

The reference space coating life τ_c is considered the same for the double-sided model. Concerning the transition time, based on a regression analysis, the authors estimated τ_{t_i} with respect to d_{∞_i} (Appendix Equation A.7) (A. Zayed, Garbatov, and Soares 2018).

$$\tau_{t_i} = 7.59 \ln\left(d_{\infty_i}\right) + 15.29 \tag{A.7}$$

A.3 Step 3: Long-Term Single-Sided Model for Multiple Ship Spaces

To consider specific environmental and operational effects, multiplicative correction factors are applied to the previous model, increasing or decreasing the wastage prediction based on environmental conditions in the short-term. Subsequently, the short-term analysis is combined for a long-term prediction by considering routes with different environments and the time spent in these areas. These two considerations are defined as follows (Guedes Soares et al. 2008; 2009; Guedes Soares, Garbatov, and Zayed 2011):

1. **Environment**: Parameters in which the models were calibrated previously are extracted from a large heterogeneous dataset. Therefore, the environmental parameters for which the generic model (nominal model) was based were estimated as the mean of the available environmental data for different areas. These environmental parameters are considered reference values x_{j_r} to those of interest x_j. The correction factor $f_k(x_j)$ is based on the respective ratios between the environmental parameter x_j and its reference value x_{j_r}, corresponding to the effect of j^{th} environmental parameter x_j in the k^{th} operational short-term interval. The m environmental parameters, their ratios, and correction factors are presented for seawater immersion (Guedes Soares et al. 2008), marine atmosphere (Guedes Soares et al. 2009), and oil environment (Guedes Soares, Garbatov, and Zayed 2011).

2. **Operation**: The long-term corrosion is a large number of short-term intervals where the environmental conditions can be considered constant. Therefore, the long-term single-sided corrosion wastage $d_{L_i}(t)$ is a weighted sum of the considered short-term corrosion wastages, where the weight p_k is the relative duration of the k^{th} operational short-term interval of N number of short-term intervals.

Therefore, it is possible to determine the Environmental and Operational Factor $f_{e\&o_i}$, which will allow defining a long-term corrosion wastage model for the side i in multiple ship spaces subjected to different environmental and operational factors (Appendix Equation A.8-A.9):

$$d_{L_i}(t) = \sum_{k=1}^{N} p_k \prod_{j=1}^{m} f_{k_i}(x_j)\, d_{n_i}(t) = f_{e\&o_i} d_{n_i}(t) \tag{A.8}$$

$$f_{e\&o_i} = \sum_{k=1}^{N} p_k \prod_{j=1}^{m} f_{k_i}(x_j) \tag{A.9}$$

A.4 Step 4: Long-Term Probabilistic Model for Multiple Ship Spaces

First, the Side Factor f_{S_i} is defined (Equation A.10) to attribute a simplified short-term mean model for side i (Appendix Equation A.12).

$$f_{S_i} = f_i^m f_i^s \tag{A.10}$$

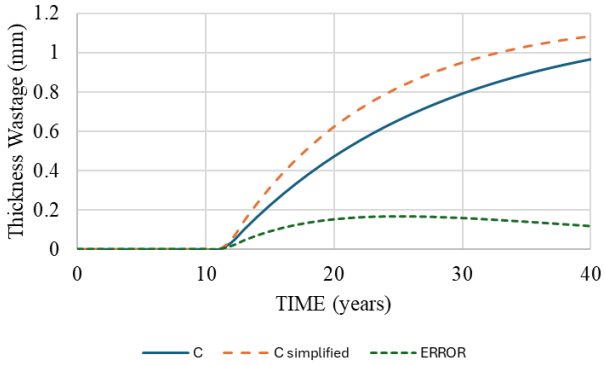
$$d_{\infty\, i} = f_{S_i} d_\infty \tag{A.11}$$

$$d_{n_i}(t) = d_{\infty_i}\left(1 - e^{-\frac{t-\tau_c}{\tau_t}}\right) \cong f_{S_i} d_n(t) = d_{n_{i_*}}(t) \tag{A.12}$$

It should be noted that (Appendix Equation A.12) is an approximate assumption since τ_t is dependent on d_{∞_i} (Appendix Equation A.7), which is calculated by f_{S_i} (Appendix Equation A.11). Therefore, the modification is not linear. Indeed, it was verified that assuming no modification on τ_t from its original double-sided model presents a quantifiable error. The biggest difference was verified as 0.167 mm (25% error) in a 40-year period for type C space (bottom of cargo oil tank), which is not acceptable (Appendix Figure A.1). As a note, both double-sided calibrated models AD and AF consider space A, which is used as a reference for space B. To select

an original τ_t in this case, it was chosen $\tau_t = 17.54$ for space A and 11.23 for space B, with the rationale of minimum error.

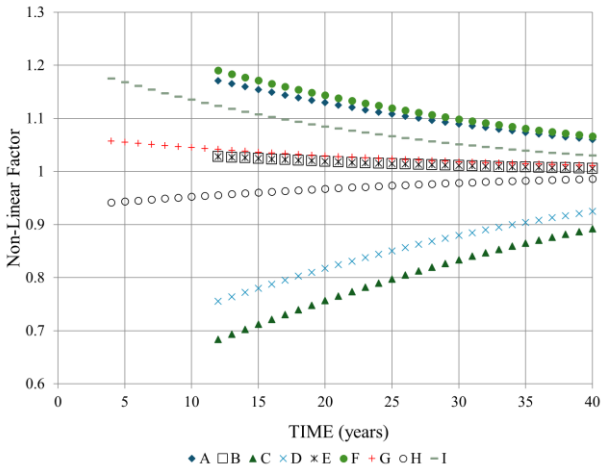
Appendix Figure A.1. Thickness wastage curve for single-sided model C, simplified model C with original τ_t, and error.



Given the quantifiable error, it is possible to define a Non-Linear Factor f_{nl_i} (Appendix Equation A.13) to correct the deviations. The f_{nl_i} values for all nine ship space types (A to I) are presented in (Appendix Figure A.2) and are considered constant within a yearly period.

$$f_{nl_i} = \frac{d_{n_i}(t)}{d_{n_{i_*}}(t)} \tag{A.13}$$

Appendix Figure A.2. Non-Linear Factors f_{nl_i} for ship space types (A to I).

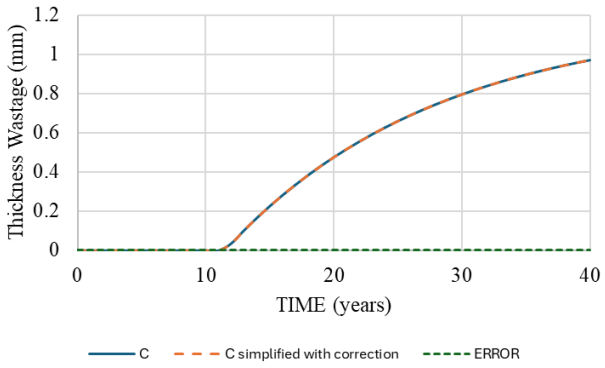


Therefore, the Corrected Side Factor f_{CS_i} (Appendix Equation A.14) can be applied to $d_n(t)$ as to obtain $d_{n_i}(t)$ (Appendix Equation A.15). The error for type C space (Appendix Figure A.1) is then corrected (Appendix Figure A.3).

$$f_{CS_i} = f_{S_i} f_{nl_i} \tag{A.14}$$

$$d_{n_i}(t) = f_{CS_i} d_n(t) \tag{A.15}$$

Appendix Figure A.3. Thickness wastage curve for single-sided model C, corrected model C with original τ_t, and error.

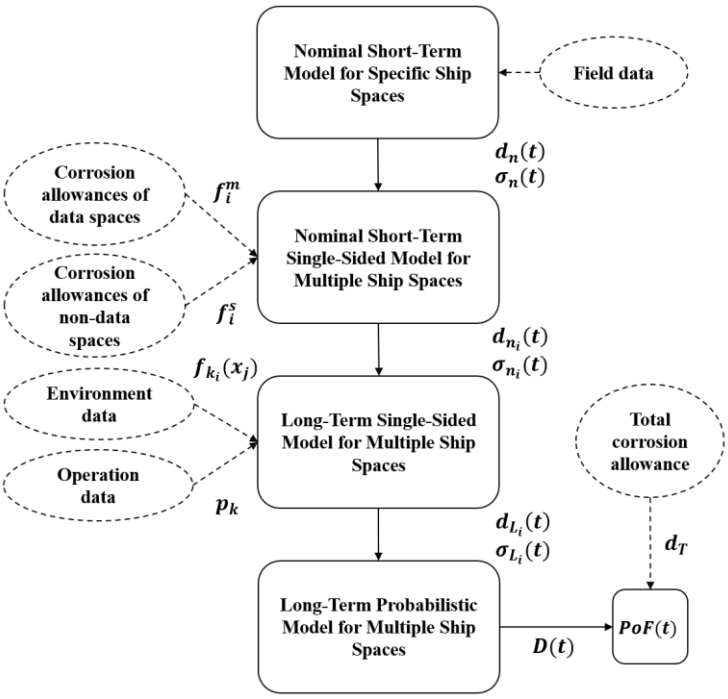


Since environmental and operational effects are just described by a constant factor, the product of factors f_{CS_i} and $f_{e\&o}$ is the Total Factor f_{T_i} (Appendix Equation A.16) that modify $\sigma_n(t)$ to define $\sigma_{L_i}(t)$ (Equation 4).

$$f_{T_i} = f_{CS_i} f_{e\&o} \tag{A.16}$$

The time-based probabilistic corrosion model framework is presented in (Appendix Figure A.4).

Appendix Figure A.4. Probabilistic corrosion model framework.



According to the developments of this Appendix and the considerations from Section 2.3, 17 spaces were modeled in a list for general corrosion, as presented in Appendix Table A.5.

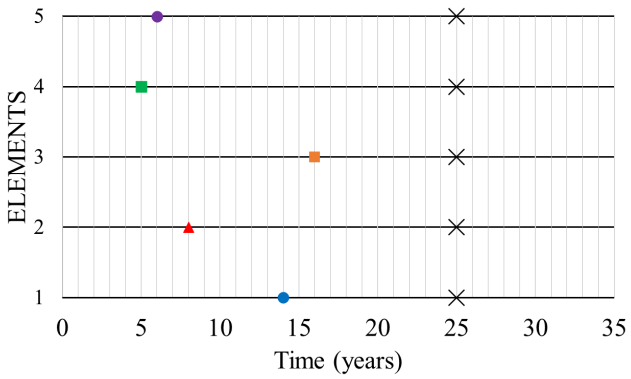
Appendix Table A.5. List of Corrosion Models.

CORROSION MODEL	CLASSIFICATION	REFERENCE SPACE	LONG TERM THICKNESS FOR CALIBRATED DOUBLE-SIDE MODELS	f_m	LONG TERM THICKNESS	CORROSION ADDITION REFERENCE	CORROSION ADDITION IACS (OIL TANKERS)	fs	MODIFIED LONG TERM THICKNESS	TRANSITION TIME	COATING TIME	f_T
SEA WATER	I	I	1.42	0.45	0.64	1	1	1.0	0.64	11.89	3.17	0.45
SEA WATER QUAY	H	I	1.42	0.45	0.64	1	1.5	1.5	0.96	14.97	3.17	0.68
UP BALLAST TOP	F	F	1.85	0.50	0.93	1.7	1.7	1.0	0.93	14.70	10.54	0.50
BALLAST TOP	G	G	1.42	0.55	0.78	1.2	1.2	1.0	0.78	13.41	3.17	0.55
BALLAST SIDE	G	G	1.42	0.55	0.78	1.2	1.2	1.0	0.78	13.41	3.17	0.55
BALLAST BOTTOM	G	G	1.42	0.55	0.78	1.2	1.2	1.0	0.78	13.41	3.17	0.55
UP OIL TOP	D	D	1.91	0.50	0.96	1.7	1.7	1.0	0.96	14.94	11.49	0.50
OIL TOP	E	D	1.91	0.50	0.96	1.7	1	0.6	0.56	10.91	11.49	0.29
OIL SIDE	E	D	1.91	0.50	0.96	1.7	1	0.6	0.56	10.91	11.49	0.29
OIL BOTTOM	C	D	1.91	0.50	0.96	1.7	2.1	1.2	1.18	16.54	11.49	0.62
ATMOSPHERE	B	A	1.91	0.50	0.96	1.7	1	0.6	0.56	10.91	11.49	0.29
ATMOSPHERE WET DECK	A	A	1.91	0.50	0.96	1.7	1.7	1.0	0.96	14.94	11.49	0.50
DRY ACCOMMODATION	-	-	-	-	-	0	0	0	-	-	-	-
MACHINE ROOM BOTTOM	C	D	1.91	0.50	0.96	1.7	1	0.6	0.56	10.91	11.49	0.29
COMPENSATED TOP	E	D	1.91	0.50	0.96	1.7	1	0.6	0.56	10.91	11.49	0.29
COMPENSATED SIDE	G	G	1.42	0.55	0.78	1.2	1.2	1.0	0.78	13.41	3.17	0.55
COMPENSATED BOTTOM	G	G	1.42	0.55	0.78	1.2	1.2	1.0	0.78	13.41	3.17	0.55

Appendix B: Time-Grouping Demonstration

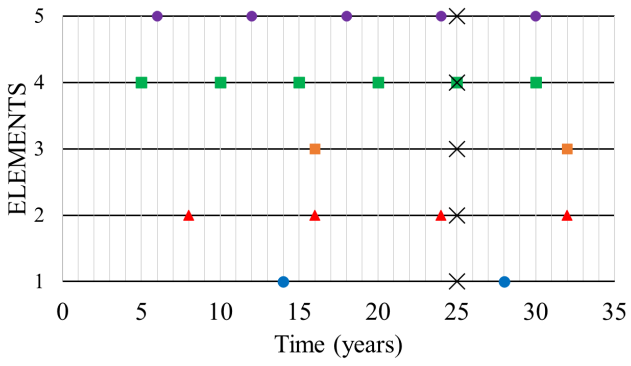
B.1 Step 1: Single element time threshold

Appendix Figure B.1. Grouping Strategy (Step 1).



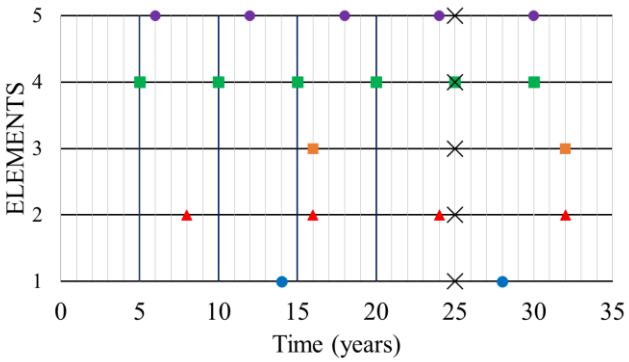
B.2 Step 2: Single element repair (time threshold repetitions)

Appendix Figure B.2. Grouping Strategy (Step 2).

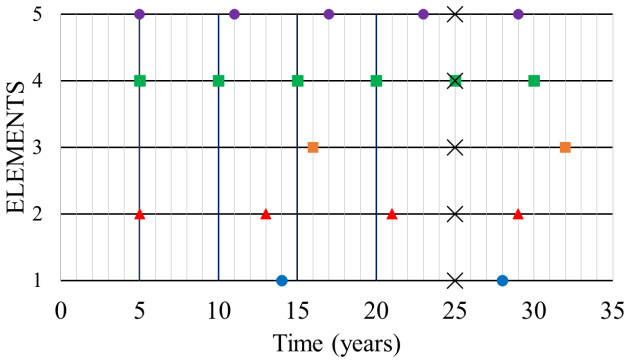


B.3 Step 3: Grouping and Anticipation

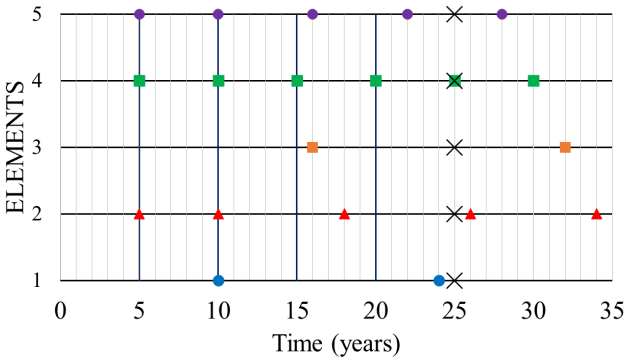
Appendix Figure B.3. Grouping Strategy (Step 3): Input Solution.



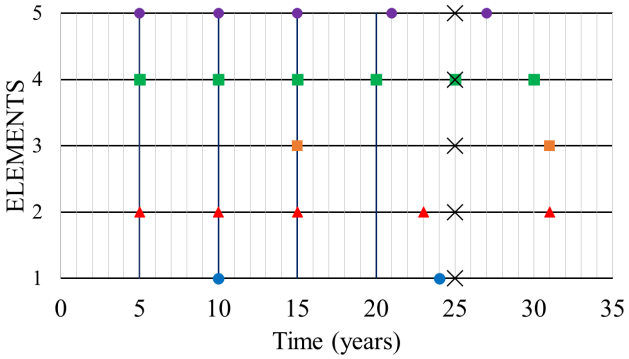
Appendix Figure B.4. Grouping Strategy (Step 3): Iteration 1.



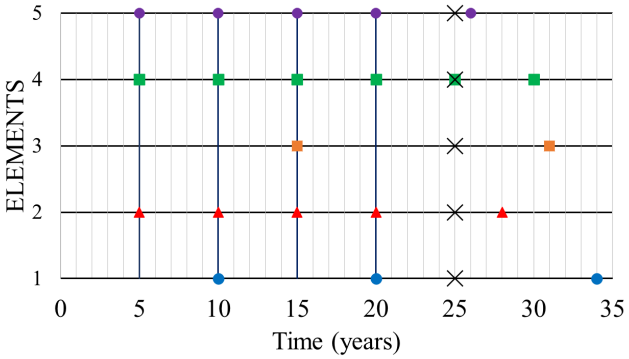
Appendix Figure B.5. Grouping Strategy (Step 3): Iteration 2.



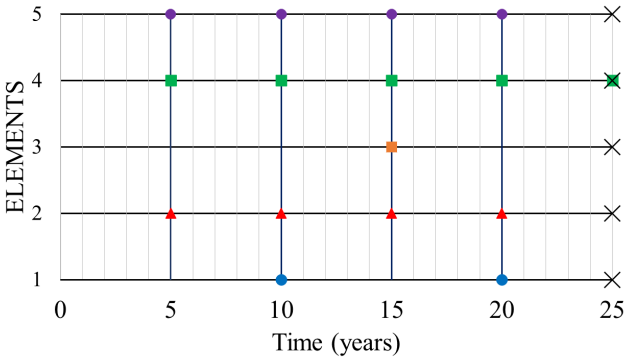
Appendix Figure B.6. Grouping Strategy (Step 3): Iteration 3.



Appendix Figure B.7. Grouping Strategy (Step 3): Iteration 4.



Appendix Figure B.8. Grouping Strategy (Step 3): Grouping Solution.



Appendix C: Elements' Parameters

The parameters' values presented in this Appendix are based on the generic naval vessel cross-section illustrated by Figure 13 with its five associated elements described in Chapter 2. The values are the author's choice solely for framework simulation and testing. Therefore, there is no intention to represent a specific ship, although the values are referred to a real order of magnitude.

Appendix Table C.1. Elements' Parameters.

ELEMENT LOCALIZATION PARAMETERS	ELEMENT CODE	1	2	3	4	5
	COMPARTMENT 1 NAME	BALLAST TANK	BALLAST TANK	BALLAST TANK	SEAWATER QUAY	SEAWATER
	COMPARTMENT 2 NAME	OIL TANK	BALLAST TANK	BALLAST TANK	FOOD STORAGE	OIL TANK
COMPARTMENT PARAMETERS	COMPARTMENT 1 TYPE	BALLAST TANK	BALLAST TANK	BALLAST TANK	NO TANK	NO TANK
	COMPARTMENT 2 TYPE	OIL TANK	BALLAST TANK	BALLAST TANK	NO TANK	OIL TANK
	COATING TYPE COMPARTMENT 1	TANK	TANK	TANK	OUTER HULL	OUTER HULL
	COATING TYPE COMPARTMENT 2	TANK	TANK	TANK	INTERNAL	TANK
	TANK 1 VOLUME [m^3]	40.00	40.00	40.00	-	-
	TANK 2 VOLUME [m^3]	25.00	-	-	-	25.00
ELEMENT PARAMETERS	STRUCTURAL ELEMENT TYPE	PLATE	LONG STIFF	LONG STIFF	PLATE	PLATE
	STRUCTURAL ELEMENT SHAPE	FLAT	FLAT	FLAT	CURVED	CURVED
	ORIGINAL THICKNESS [mm]	6.50	5.00	10.00	7.50	8.00
	AREA [mm^2]	9,000,000.00	463,500.00	270,000.00	6,750,000.00	9,000,000.00
	VOLUME [mm^3]	58,500,000.00	2,317,500.00	2,700,000.00	50,625,000.00	72,000,000.00
	MASS [kg]	459.23	18.19	21.20	397.41	565.20
	WELD LENGTH [mm]	13,000.00	9,000.00	9,000.00	12,000.00	13,000.00
DAMAGE PARAMETERS	CORROSION MODEL SIDE 1	BALLAST TOP	BALLAST BOTTOM	BALLAST BOTTOM	SEAWATER QUAY	SEAWATER
	CORROSION MODEL SIDE 2	OIL TOP	BALLAST BOTTOM	BALLAST BOTTOM	DRY ACCOMMODATION	OIL BOTTOM
	THICKNESS [mm]	6.50	5.00	10.00	7.50	8.00
	% FOR FAILURE	25%	25%	25%	25%	25%
	WASTAGE FOR FAILURE [mm]	1.63	1.25	2.50	1.88	2.00
	DAMAGE SETTING	IMPAIRED OP	OPERATIONAL	OPERATIONAL	IMPAIRED OP	IMPAIRED OP
OTHER PARAMETERS	SCAFFOLD 1	NO	NO	NO	NO	NO
	SCAFFOLD 2	NO	NO	NO	NO	NO
	INTERFERENCE REMOVAL TIME (h)	0	0	0	0.5	0
	INTERFERENCE REINSTALL TIME (h)	0	0	0	1	0
	DRYDOCK	YES	YES	YES	NO	YES

Appendix D: Costs' Parameters

The parameters' values presented in this Appendix are the author's choice solely for framework simulation and test, although they were based on a comprehensive cross-search for a reasonable order of magnitude. This search is based on the U.S. reference, by considering the LCS Freedom Class benchmark, the Congressional Budget Office (CBO) and the U.S. Government Accountability Office (GAO) reports; the World Bank and Federal Reserve websites; and the author's experience.

D.1 Cost of Failure Parameters (Except Structural)

Appendix Table D.1. Cost of Failure Parameters (Except for Structural).

1	SUPPLY SHIP [YES: 1 | NO: 0]	0.00	
2	GROSS DOMESTIC PRODUCT PER CAPITA (GDP)	82,769.41	USD
3	LIFE EXPECTANCY	78.00	years
4	LABOR UTILIZATION (hours worked per capta)	1,765.34	hours
5	PROPORTION OF LIFE SPENT IN ECONOMIC ACTIVITY	0.20	
6	OPTIMUM ACCEPTABLE IMPLIED COST OF AVERTING A FATALITY (ICAF) [USD/fatality]	6,395,031.94	USD/fatality
7	NEW SHIP PRICE	500,000,000.00	USD
8	SHIP DEPRECIATION RATE	0.03	USD/year
9	NEW PAYLOAD PRICE	15,000,000.00	USD
10	PAYLOAD DEPRECIATION RATE	0.05	USD/year
11	OIL PRICE	1,000.00	USD/mt
12	OIL DENSITY	0.85	mt/m^3
13	CARGO TANK OIL VOLUME	0.00	m^3
14	TOTAL SHIP OIL	600.00	m^3

D.2 Cost of Opportunity Parameters

Appendix Table D.2. Cost of Opportunity Parameters.

1	FEDERAL FUNDS RATE	0.045	%/year
2	TARGET INFLATION	0.02	%/year
3	ALPHA - PERCENTAGE OF NON-IDLE O&S EXPENDITURES	0.3	%/year
4	O&S EXPENDITURES	145,000,000.00	USD

D.3 Structural Cost Parameters

Appendix Table D.3. Structural Cost Parameters (1-30).

1	MEAN TIME TO ENTER DRYDOCK	12.00	h
2	FIXED COST TO ENTER DRYDOCK	10,000.00	USD
3	NUMBER OF HULL CLEANNING WORKERS	2.00	workers
4	MEAN TIME TO CLEAN HULL	0.02	h.worker/m^2
5	HULL CLEANING LABOR COST	15.00	USD/(h.worker)
6	HULL CLEANING FIXED COST	2.00	USD/m^2
7	NUMBER OF TANK DRAINERS	2.00	drainers
8	MEAN TIME TO DRAIN TANK	0.10	h.drainer/m^3
9	DRAINING TANK LABOR COST	5.00	USD/(h.drainer)
10	DRAINING TANK FIXED COST	20.00	USD/m^3
11	NUMBER OF OIL TANK CLEANING WORKERS	2.00	workers
12	MEAN TIME TO CLEAN OIL TANK	0.50	h.worker/m^3
13	OIL TANK CLEANNING LABOR COST	20.00	USD/(h.worker)
14	OIL TANK CLEANNING FIXED COST	5.00	USD/m^3
15	NUMBER OF NON OIL TANK CLEANING WORKERS	2.00	workers
16	MEAN TIME TO CLEAN NON OIL TANK	0.17	h.worker/m^3
17	NON OIL TANK CLEANNING LABOR COST	10.00	USD/(h.worker)
18	NON OIL TANK CLEANNING FIXED COST	2.00	USD/m^3
19	NUMBER OF DEGASSING PUMPS	2.00	pumps
20	MEAN TIME TO DEGAS TANK	0.50	h.pump/m^3
21	TANK DEGASSING LABOR COST	5.00	USD/(h.pump)
22	TANK DEGASSING FIXED COST	200.00	USD/pump
23	NUMBER OF WORKERS TO BUILD SCAFFOLD	4.00	workers
24	MEAN TIME TO BUILD SCAFFOLDS	8.00	h.worker/scaffold
25	BUILD SCAFFOLD LABOR COST	10.00	USD/(h.worker)
26	BUILD SCAFFOLD FIXED COST	150.00	USD/scaffold
27	NUMBER OF HULL SURVEYORS	2.00	surveyors
28	MEAN TIME TO SURVEY HULL	0.01	h.surveyor/area
29	HULL SURVEY LABOR COST	15.00	USD/(h.surveyor)
30	HULL SURVEY FIXED COST	2.00	USD/m^2

Appendix Table D.4. Structural Cost Parameters (31-70).

31	**NUMBER OF NON OIL TANK SURVEYORS**	2.00	surveyors
32	**MEAN TIME TO SURVEY NON OIL TANK**	0.02	h.surveyor/m^3
33	**NON OIL TANK SURVEY LABOR COST**	20.00	USD/(h.surveyor)
34	**NON OIL TANK SURVEY FIXED COST**	4.00	USD/m^3
35	**NUMBER OF OIL TANK SURVEYORS**	2.00	surveyors
36	**MEAN TIME TO SURVEY OIL TANK**	0.02	h.surveyor/m^3
37	**OIL TANK SURVEY LABOR COST**	25.00	USD/(h.surveyor)
38	**OIL TANK SURVEY FIXED COST**	8.00	USD/m^3
39	**NUMBER OF ULTRASOUND SURVEYORS**	4.00	surveyors
40	**MEAN TIME TO ULTRASOUND SURVEY**	0.05	h.surveyor/m^2
41	**ULTRASOUND SURVEY COST**	25.00	USD/(h.surveyor)
42	**ULTRASOUND FIXED COST**	500.00	USD
43	**MEAN TIME TO REPORT SURVEY**	1.00	h/compartment
44	**REPORT SURVEY LABOR COST**	20.00	USD/h
45	**REPORT SURVEY FIXED COST**	500.00	USD
46	**NUMBER OF WORKERS TO REMOVE INTERFERENCES**	2.00	workers
47	**REMOVE INTERFERENCES LABOR COST**	15.00	USD/(h.worker)
48	**REMOVE INTERFERENCES FIXED COST**	300.00	USD/interference
49	**STEEL YELD LOSS**	20.00	%
50	**STEEL COST**	10.00	USD/kg
51	**NUMBER OF FLAT PLATE PROCESS WORKSTATIONS FOR FLAT PLATE**	2.00	workstations
52	**NUMBER OF FLAT PLATE PROCESS WORKSTATIONS FOR CURVED PLATE**	2.00	workstations
53	**MEAN TIME FOR FLAT PLATE FABRICATION**	0.33	h.workstation/element
54	**STD TIME FOR FLAT PLATE FABRICATION**	0.50	h.workstation/element
55	**PLATE CUTTING COST**	40.00	USD/(h.workstation)
56	**FLAT PLATE FABRICATION FIXED COST**	500.00	USD/workstation
57	**HOLDING COST PER FLAT PLATE**	500.00	USD/element
58	**NUMBER OF FLAT PROFILE PROCESS WORKSTATIONS FOR FLAT PROFILE**	2.00	workstations
59	**NUMBER OF FLAT PROFILE PROCESS WORKSTATIONS FOR CURVED PROFILE**	2.00	workstations
60	**MEAN TIME FOR FLAT PROFILE FABRICATION**	0.50	h.workstation/element
61	**STD TIME FOR FLAT PROFILE FABRICATION**	0.75	h.workstation/element
62	**PROFILE CUTTING COST**	40.00	USD/(h.workstation)
63	**FLAT PROFILE FABRICATION FIXED COST**	500.00	USD/workstation
64	**HOLDING COST PER FLAT PROFILE**	250.00	USD/element
65	**NUMBER OF CURVED PLATE PROCESS WORKSTATIONS**	2.00	workstations
66	**MEAN TIME TO BEND PLATE**	0.67	h.workstation/element
67	**STD TIME TO BEND PLATE**	1.00	h.workstation/element
68	**PLATE BENDING COST**	80.00	USD/(h.workstation)
69	**CURVED PLATE FABRICATION FIXED COST**	500.00	USD/workstation
70	**HOLDING COST PER CURVED PLATE**	1,000.00	USD/element

Appendix Table D.5. Structural Cost Parameters (71-110).

71	**NUMBER OF CURVED PROFILE PROCESS WORKSTATIONS**	2.00	workstation
72	**MEAN TIME TO BEND PROFILE**	0.67	h.workstation/element
73	**STD TIME TO BEND PROFILE**	1.00	h.workstation/element
74	**PROFILE BENDING COST**	80.00	USD/(h.workstation)
75	**CURVED PROFILE FABRICATION FIXED COST**	500.00	USD/workstation
76	**HOLDING COST PER CURVED PROFILE**	1,000.00	USD/element
77	**NUMBER OF WELDERS FOR CONNECTION**	4.00	welder
78	**MEAN TIME TO CONNECT ELEMENTS**	1.75	h.welder/element
79	**STD TIME TO CONNECT ELEMENTS**	2.63	h.welder/element
80	**ELEMENT CONNECTION LABOR COST**	20.00	USD/(h.welder)
81	**ELEMENT CONNECTION FIXED COST**	500.00	USD/welder
82	**HOLDING COST PER ELEMENT FOR CONNECTTION**	1,000.00	USD/element
83	**NUMBER OF WELDERS**	4.00	welder
84	**MEAN TIME TO WELD ELEMENT**	2.40	h.welder/m
85	**STD TIME TO WELD ELEMENT**	3.60	h.welder/m
86	**WELD LABOR COST**	20.00	USD/(h.welder)
87	**WELD FIXED COST**	500.00	USD/welder
88	**HOLDING COST PER ELEMENT FOR WELD**	1,500.00	USD/element
89	**NUMBER OF WELD SURVEYORS**	2.00	surveyors
90	**MEAN TIME TO SURVEY WELD**	0.17	h.surveyors/m
91	**STD TIME TO SURVEY WELD**	0.25	h.surveyors/m
92	**WELD SURVEY LABOR COST**	15.00	USD/(h.surveyor)
93	**WELD SURVEY FIXED COST**	500.00	USD/surveyor
94	**HOLDING COST PER ELEMENT FOR WELD SURVEY**	1,500.00	USD/element
95	**FLAT PLATE WIP LEVEL**	5.00	elements
96	**CURVED PLATE WIP LEVEL**	5.00	elements
97	**FLAT PROFILE WIP LEVEL**	5.00	elements
98	**CURVED PROFILE WIP LEVEL**	5.00	elements
99	**NUMBER OF INTERNAL COATERS**	3.00	coaters
100	**MEAN TIME TO COAT INTERNAL**	2.00	h.coater/m^2
101	**INTERNAL COATING LABOR COST**	15.00	USD/(h.coater)
102	**INTERNAL COATING FIXED COST**	5.00	USD/m^2
103	**NUMBER OF EXTERNAL COATERS**	3.00	coaters
104	**MEAN TIME TO COAT EXTERNAL**	3.00	h.coater/m^2
105	**EXTERNAL COATING LABOR COST**	15.00	USD/(h.coater)
106	**EXTERNAL COATING FIXED COST**	5.00	USD/m^2
107	**NUMBER OF OUTER HULL COATERS**	4.00	coaters
108	**MEAN TIME TO COAT OUTER HULL**	16.00	h.coater/m^2
109	**HULL COATING LABOR COST**	15.00	USD/(h.coater)
110	**HULL COATING FIXED COST**	30.00	USD/m^2

Appendix Table D.6. Structural Cost Parameters (111-133).

111	**NUMBER OF TANK COATERS**	3.00	tank coaters
112	**MEAN TIME TO COAT TANK**	8.00	h.coater/m^2
113	**TANK COATING LABOR COST**	15.00	USD/(h.coater)
114	**TANK COATING FIXED COST**	10.00	USD/m^2
115	**NUMBER OF WORKERS TO REINSTALL INTERFERENCES**	2.00	workers
116	**REINSTALL INTERFERENCES LABOR COST**	15.00	USD/(h.worker)
117	**REINSTALL INTERFERENCES FIXED COST**	300.00	USD/interference
118	**NUMBER OF WORKERS TO REMOVE SCAFFOLD**	3.00	workers
119	**MEAN TIME TO REMOVE SCAFFOLDS**	3.00	h.worker/scaffold
120	**REMOVE SCAFFOLD LABOR COST**	10.00	USD/(h.worker)
121	**REMOVE SCAFFOLD FIXED COST**	150.00	USD/scaffold
122	**MEAN TIME TO EXIT DRYDOCK**	12.00	h
123	**FIXED COST TO EXIT DRYDOCK**	10,000.00	USD
124	**DRYDOCK COST PER DAY**	15,000.00	USD/day
125	**MEAN TIME TO ENTER QUAY**	2.00	h
126	**FIXED COST TO ENTER QUAY**	2,000.00	USD
127	**MEAN TIME TO EXIT QUAY**	2.00	h
128	**FIXED COST TO EXIT QUAY**	2,000.00	USD
129	**QUAY COST PER DAY**	3,000.00	USD/day
130	**WORKHOURS PER DAY**	12.00	h/day
131	**SHIPYARD PERCENTUAL PRICE OVER TIME-BASED COST**	20.00	%
132	**SHIPYARD PERCENTUAL PRICE OVER FIXED COST**	20.00	%
133	**HULL AREA**	3,000.00	m^2

Appendix E: Time-Grouping Hand Calculation Results

This Appendix presents the results of the time-grouping intervention's cost and time for all tasks in each downtime; the Structural Cost C_S, the Expected Cost of Failure C_{EF}, and the Expected Cost of Opportunity C_{EO}.

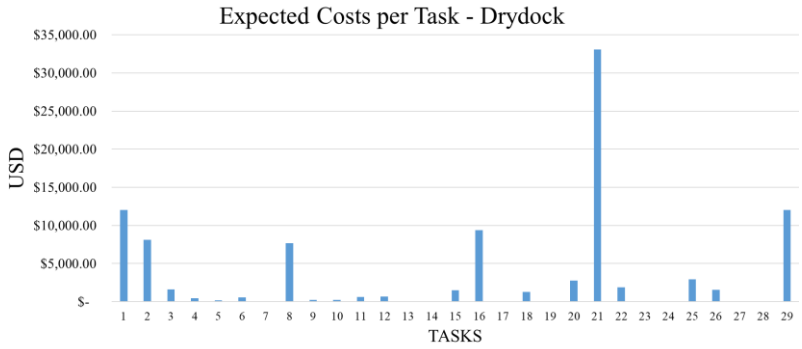
E.1 Structural Cost

1. Year 5: Elements [2, 4, 5]

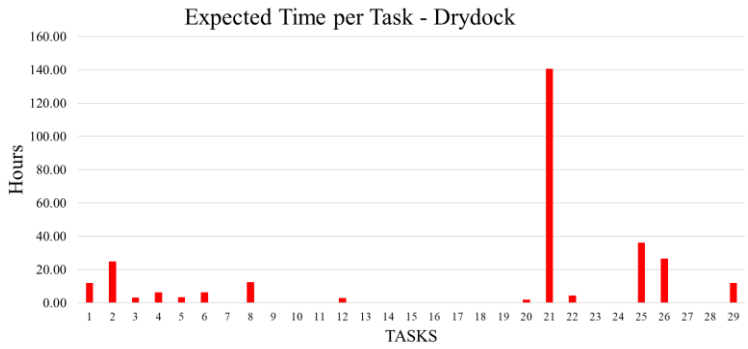
Appendix Table E.1. Drydock Costs in PV for Downtime at Year 5.

TASKS		DURATION TIME	END TIME	SHIPYARD PRICES		
TASK NUMBER	TASK DISCRIPTION	MEAN TIME [h] or [day] for downtime	MEAN TIME [h]	FIXED PRICES [USD]	TIME-BASED PRICES [USD]	TOTAL PRICE [USD]
1	ENTER DRY DOCK	12.00	12.00	$ 12,000.00	$ -	$ 12,000.00
2	CLEAN HULL	25.00	37.00	$ 7,200.00	$ 900.00	$ 8,100.00
3	DRAIN TANK	3.25	15.25	$ 1,560.00	$ 39.00	$ 1,599.00
4	CLEAN OIL TANK	6.25	21.50	$ 150.00	$ 300.00	$ 450.00
5	CLEAN NON OIL TANK	3.33	18.58	$ 96.00	$ 80.00	$ 176.00
6	DEGAS TANKS	6.25	27.75	$ 480.00	$ 75.00	$ 555.00
7	BUILD SCAFFOLD	0.00	37.00	$ -	$ -	$ -
8	HULL VISUAL SURVEY	12.50	49.50	$ 7,200.00	$ 450.00	$ 7,650.00
9	NON OIL TANK VISUAL SURVEY	0.33	18.92	$ 192.00	$ 16.00	$ 208.00
10	OIL TANK VISUAL SURVEY	0.21	27.96	$ 240.00	$ 12.50	$ 252.50
11	ULTRASOUND SURVEY	0.12	49.62	$ 600.00	$ 14.20	$ 614.20
12	SURVEY REPORT	3.0	52.62	$ 600.00	$ 72.00	$ 672.00
13	REMOVE INTERFERENCES AND OUTLINE REPAIR	0.0	52.62	$ -	$ -	$ -
14	PROCESS FLAT PLATE	0.0	52.62	$ -	$ -	$ -
15	PROCESS FLAT PROFILE	0.3	52.87	$ 1,464.55	$ 24.33	$ 1,488.88
16	PROCESS FLAT PLATE FOR BENDING	0.2	52.79	$ 9,342.30	$ 16.14	$ 9,358.45
17	PROCESS FLAT PROFILE FOR BENDING	0.0	52.62	$ -	$ -	$ -
18	PROCESS CURVED PLATE	0.3	53.13	$ 1,213.82	$ 65.16	$ 1,278.98
19	PROCESS CURVED PROFILE	0.0	52.62	$ -	$ -	$ -
20	CONNECT ELEMENTS	1.9	54.83	$ 2,556.78	$ 184.77	$ 2,741.55
21	WELD	140.6	195.47	$ 19,570.23	$ 13,501.77	$ 33,071.99
22	WELD SURVEY	4.5	199.96	$ 1,748.13	$ 161.51	$ 1,909.63
23	INTERNAL COAT	0.0	199.96	$ -	$ -	$ -
24	EXTERNAL COAT	0.0	199.96	$ -	$ -	$ -
25	OUTER HULL COAT	36.0	235.96	$ 324.00	$ 2,592.00	$ 2,916.00
26	TANK COAT	26.5	226.43	$ 119.12	$ 1,429.49	$ 1,548.61
27	REINSTALL INTERFERENCES	0.0	235.96	$ -	$ -	$ -
28	REMOVE SCAFFOLDS	0.0	235.96	$ -	$ -	$ -
29	EXIT DRYDOCK	12.0	247.96	$ 12,000.00	$ -	$ 12,000.00
30	DRYDOCK TIME AND COST	21	-	$ -	$ 378,000.00	$ 378,000.00
			TOTAL PRICE	$ 78,656.93	$ 397,933.86	$ 476,590.79

Appendix Figure E.1. Drydock Costs in PV for Downtime at Year 5.



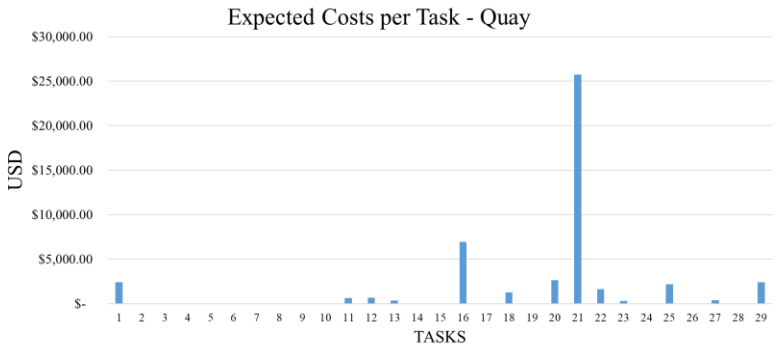
Appendix Figure E.2. Drydock Times for Downtime at Year 5.



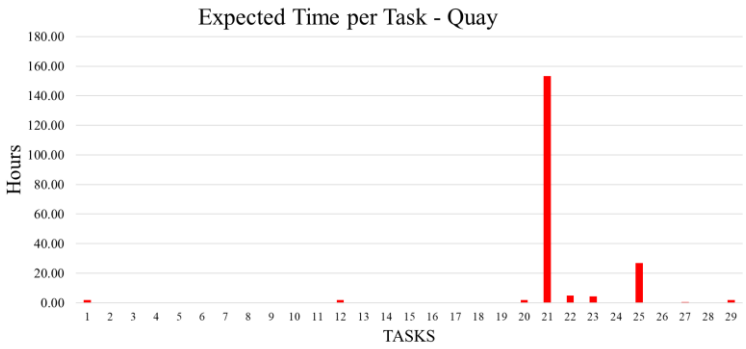
Appendix Table E.2. Quay Costs in PV for Downtime at Year 5.

TASKS		DURATION TIME	END TIME	SHIPYARD PRICES		
TASK NUMBER	TASK DISCRIPTION	MEAN TIME [h] or [day] for downtime	MEAN TIME [h]	FIXED PRICES [USD]	TIME-BASED PRICES [USD]	TOTAL PRICE [USD]
1	ENTER QUAY	2.00	2.00	$ 2,400.00	$ -	$ 2,400.00
2	CLEAN HULL	0.00	2.00	$ -	$ -	$ -
3	DRAIN TANK	0.00	2.00	$ -	$ -	$ -
4	CLEAN OIL TANK	0.00	2.00	$ -	$ -	$ -
5	CLEAN NON OIL TANK	0.00	2.00	$ -	$ -	$ -
6	DEGAS TANKS	0.00	2.00	$ -	$ -	$ -
7	BUILD SCAFFOLD	0.00	2.00	$ -	$ -	$ -
8	HULL VISUAL SURVEY	0.00	2.00	$ -	$ -	$ -
9	NON OIL TANK VISUAL SURVEY	0.00	2.00	$ -	$ -	$ -
10	OIL TANK VISUAL SURVEY	0.00	2.00	$ -	$ -	$ -
11	ULTRASOUND SURVEY	0.08	2.08	$ 600.00	$ 10.13	$ 610.13
12	SURVEY REPORT	2.0	4.08	$ 600.00	$ 48.00	$ 648.00
13	REMOVE INTERFERENCES AND OUTLINE REPAIR	0.3	4.33	$ 360.00	$ 9.00	$ 369.00
14	PROCESS FLAT PLATE	0.0	4.33	$ -	$ -	$ -
15	PROCESS FLAT PROFILE	0.0	4.33	$ -	$ -	$ -
16	PROCESS FLAT PLATE	0.2	4.50	$ 6,925.84	$ 16.13	$ 6,941.97
17	PROCESS FLAT PROFILE	0.0	4.33	$ -	$ -	$ -
18	PROCESS CURVED PLATE	0.3	4.84	$ 1,212.65	$ 65.06	$ 1,277.72
19	PROCESS CURVED PROFILE	0.0	4.33	$ -	$ -	$ -
20	CONNECT ELEMENTS	1.9	6.75	$ 2,471.29	$ 183.30	$ 2,654.59
21	WELD	153.4	160.14	$ 10,990.59	$ 14,725.73	$ 25,716.31
22	WELD SURVEY	4.9	165.04	$ 1,474.09	$ 176.19	$ 1,650.28
23	INTERNAL COAT	4.5	169.54	$ 40.50	$ 243.00	$ 283.50
24	EXTERNAL COAT	0.0	165.04	$ -	$ -	$ -
25	OUTER HULL COAT	27.0	192.04	$ 243.00	$ 1,944.00	$ 2,187.00
26	TANK COAT	0.0	165.04	$ -	$ -	$ -
27	REINSTALL INTERFERENCES	0.5	192.54	$ 360.00	$ 18.00	$ 378.00
28	REMOVE SCAFFOLDS	0.0	192.04	$ -	$ -	$ -
29	EXIT QUAY	2.0	194.54	$ 2,400.00	$ -	$ 2,400.00
30	QUAY TIME AND COST	17	-	$ -	$ 61,200.00	$ 61,200.00
			TOTAL PRICE	$ 30,077.96	$ 78,638.54	$ 108,716.50

Appendix Figure E.3. Quay Costs in PV for Downtime at Year 5.



Appendix Figure E.4. Quay Times for Downtime at Year 5.

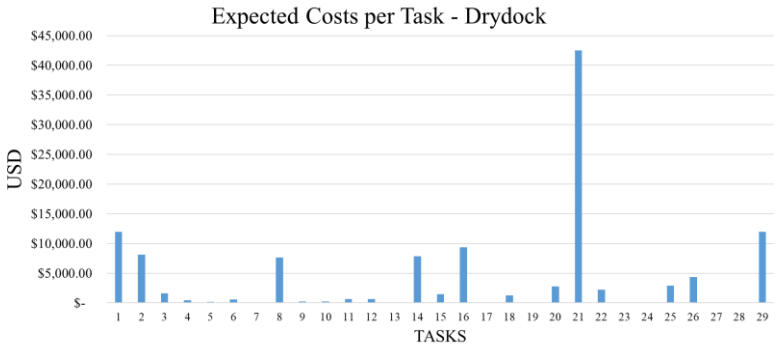


2. Year 10 and 20: Elements [1, 2, 4, 5]

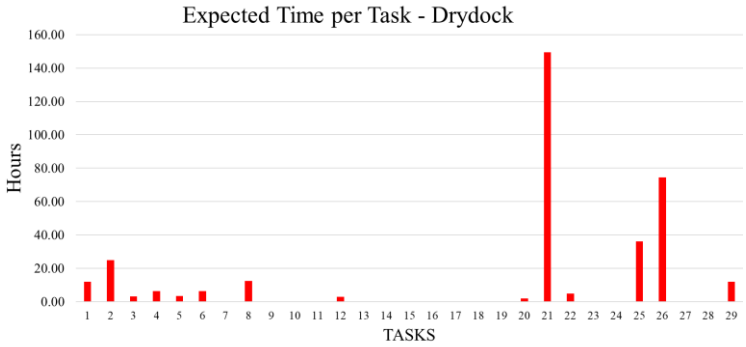
Appendix Table E.3. Drydock Costs in PV for Downtime at Year 10 and 20.

TASKS		DURATION TIME	END TIME	SHIPYARD PRICES		
TASK NUMBER	TASK DISCRIPTION	MEAN TIME [h] or [day] for downtime	MEAN TIME [h]	FIXED PRICES [USD]	TIME-BASED PRICES [USD]	TOTAL PRICE [USD]
1	ENTER DRY DOCK	12.00	12.00	$ 12,000.00	$ -	$ 12,000.00
2	CLEAN HULL	25.00	37.00	$ 7,200.00	$ 900.00	$ 8,100.00
3	DRAIN TANK	3.25	15.25	$ 1,560.00	$ 39.00	$ 1,599.00
4	CLEAN OIL TANK	6.25	21.50	$ 150.00	$ 300.00	$ 450.00
5	CLEAN NON OIL TANK	3.33	18.58	$ 96.00	$ 80.00	$ 176.00
6	DEGAS TANKS	6.25	27.75	$ 480.00	$ 75.00	$ 555.00
7	BUILD SCAFFOLD	0.00	37.00	$ -	$ -	$ -
8	HULL VISUAL SURVEY	12.50	49.50	$ 7,200.00	$ 450.00	$ 7,650.00
9	NON OIL TANK VISUAL SURVEY	0.33	18.92	$ 192.00	$ 16.00	$ 208.00
10	OIL TANK VISUAL SURVEY	0.21	27.96	$ 240.00	$ 12.50	$ 252.50
11	ULTRASOUND SURVEY	0.23	49.73	$ 600.00	$ 27.70	$ 627.70
12	SURVEY REPORT	3.0	52.73	$ 600.00	$ 72.00	$ 672.00
13	REMOVE INTERFERENCES AND OUTLINE REPAIR	0.0	52.73	$ -	$ -	$ -
14	PROCESS FLAT PLATE	0.2	52.90	$ 7,816.07	$ 16.14	$ 7,832.20
15	PROCESS FLAT PROFILE	0.3	52.98	$ 1,464.40	$ 24.31	$ 1,488.71
16	PROCESS FLAT PLATE FOR BENDING	0.2	52.90	$ 9,342.11	$ 16.14	$ 9,358.24
17	PROCESS FLAT PROFILE FOR BENDING	0.0	52.73	$ -	$ -	$ -
18	PROCESS CURVED PLATE	0.3	53.24	$ 1,213.02	$ 65.09	$ 1,278.11
19	PROCESS CURVED PROFILE	0.0	52.73	$ -	$ -	$ -
20	CONNECT ELEMENTS	1.9	54.85	$ 2,620.55	$ 183.77	$ 2,804.32
21	WELD	149.4	204.22	$ 28,193.32	$ 14,339.29	$ 42,532.61
22	WELD SURVEY	4.8	208.98	$ 2,022.37	$ 171.31	$ 2,193.68
23	INTERNAL COAT	0.0	208.98	$ -	$ -	$ -
24	EXTERNAL COAT	0.0	208.98	$ -	$ -	$ -
25	OUTER HULL COAT	36.0	244.98	$ 324.00	$ 2,592.00	$ 2,916.00
26	TANK COAT	74.5	283.45	$ 335.12	$ 4,021.49	$ 4,356.61
27	REINSTALL INTERFERENCES	0.0	283.45	$ -	$ -	$ -
28	REMOVE SCAFFOLDS	0.0	283.45	$ -	$ -	$ -
29	EXIT DRYDOCK	12.0	295.45	$ 12,000.00	$ -	$ 12,000.00
30	DRYDOCK TIME AND COST	25	-	$ -	$ 450,000.00	$ 450,000.00
			TOTAL PRICE	$ 95,648.96	$ 473,401.72	$ 569,050.68

Appendix Figure E.5. Drydock Costs in PV for Downtime at Year 10 and 20.



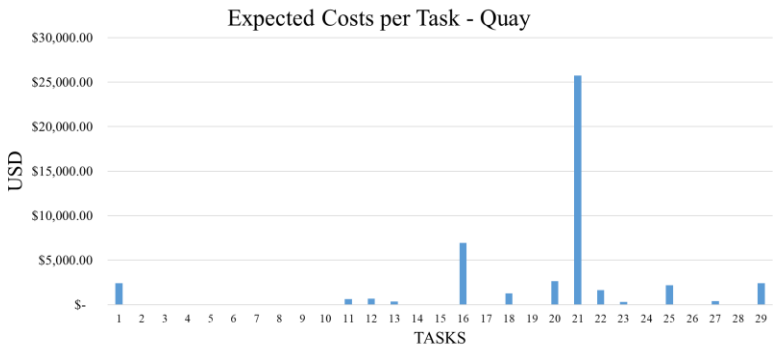
Appendix Figure E.6. Drydock Times for Downtime at Year 10 and 20.



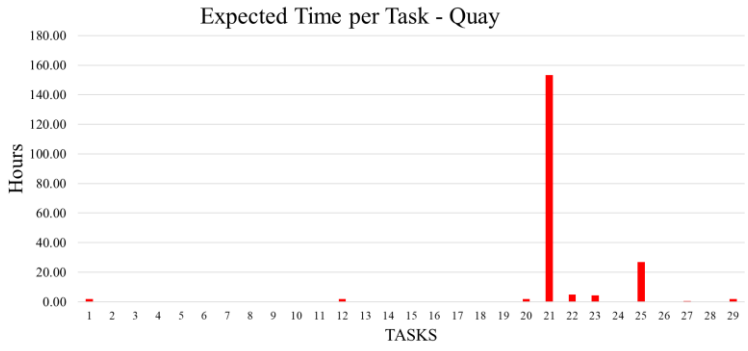
Appendix Table E.4. Quay Costs in PV for Downtime at Year 10 and 20.

TASKS		DURATION TIME	END TIME	SHIPYARD PRICES		
TASK NUMBER	TASK DISCRIPTION	MEAN TIME [h] or [day] for downtime	MEAN TIME [h]	FIXED PRICES [USD]	TIME-BASED PRICES [USD]	TOTAL PRICE [USD]
1	ENTER QUAY	2.00	2.00	$ 2,400.00	$ -	$ 2,400.00
2	CLEAN HULL	0.00	2.00	$ -	$ -	$ -
3	DRAIN TANK	0.00	2.00	$ -	$ -	$ -
4	CLEAN OIL TANK	0.00	2.00	$ -	$ -	$ -
5	CLEAN NON OIL TANK	0.00	2.00	$ -	$ -	$ -
6	DEGAS TANKS	0.00	2.00	$ -	$ -	$ -
7	BUILD SCAFFOLD	0.00	2.00	$ -	$ -	$ -
8	HULL VISUAL SURVEY	0.00	2.00	$ -	$ -	$ -
9	NON OIL TANK VISUAL SURVEY	0.00	2.00	$ -	$ -	$ -
10	OIL TANK VISUAL SURVEY	0.00	2.00	$ -	$ -	$ -
11	ULTRASOUND SURVEY	0.08	2.08	$ 600.00	$ 10.13	$ 610.13
12	SURVEY REPORT	2.0	4.08	$ 600.00	$ 48.00	$ 648.00
13	REMOVE INTERFERENCES AND OUTLINE REPAIR	0.3	4.33	$ 360.00	$ 9.00	$ 369.00
14	PROCESS FLAT PLATE	0.0	4.33	$ -	$ -	$ -
15	PROCESS FLAT PROFILE	0.0	4.33	$ -	$ -	$ -
16	PROCESS FLAT PLATE	0.2	4.50	$ 6,925.84	$ 16.13	$ 6,941.97
17	PROCESS FLAT PROFILE	0.0	4.33	$ -	$ -	$ -
18	PROCESS CURVED PLATE	0.3	4.84	$ 1,212.65	$ 65.06	$ 1,277.72
19	PROCESS CURVED PROFILE	0.0	4.33	$ -	$ -	$ -
20	CONNECT ELEMENTS	1.9	6.75	$ 2,471.29	$ 183.30	$ 2,654.59
21	WELD	153.4	160.14	$ 10,990.59	$ 14,725.73	$ 25,716.31
22	WELD SURVEY	4.9	165.04	$ 1,474.09	$ 176.19	$ 1,650.28
23	INTERNAL COAT	4.5	169.54	$ 40.50	$ 243.00	$ 283.50
24	EXTERNAL COAT	0.0	165.04	$ -	$ -	$ -
25	OUTER HULL COAT	27.0	192.04	$ 243.00	$ 1,944.00	$ 2,187.00
26	TANK COAT	0.0	165.04	$ -	$ -	$ -
27	REINSTALL INTERFERENCES	0.5	192.54	$ 360.00	$ 18.00	$ 378.00
28	REMOVE SCAFFOLDS	0.0	192.04	$ -	$ -	$ -
29	EXIT QUAY	2.0	194.54	$ 2,400.00	$ -	$ 2,400.00
30	QUAY TIME AND COST	17	-	$ -	$ 61,200.00	$ 61,200.00
			TOTAL PRICE	$ 30,077.96	$ 78,638.54	$ 108,716.50

Appendix Figure E.7. Quay Costs in PV for Downtime at Year 10 and 20.



Appendix Figure E.8. Quay Times for Downtime at Year 10 and 20.

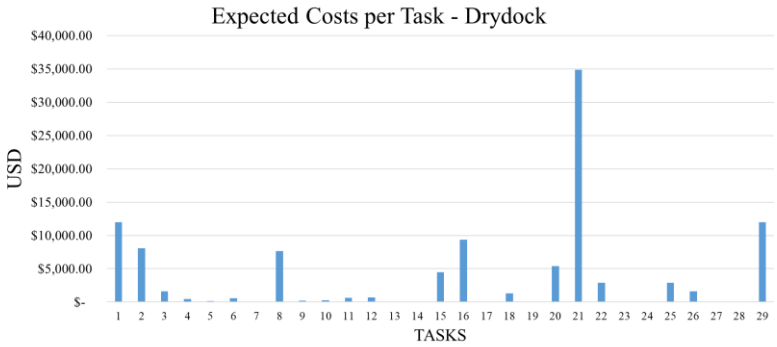


3. Year 15: Elements [2, 3, 4, 5]

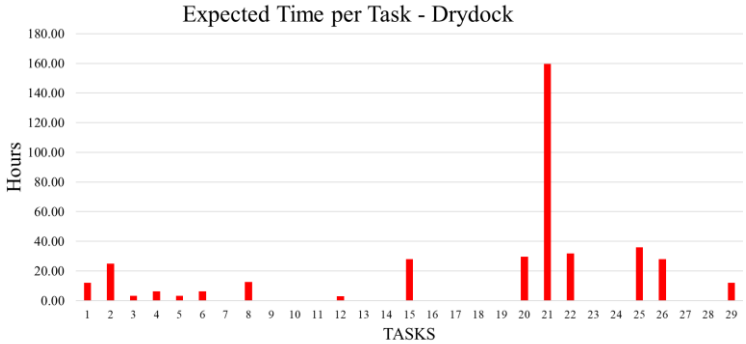
Appendix Table E.5. Drydock Costs in PV for Downtime at Year 15.

TASKS		DURATION TIME	END TIME	SHIPYARD PRICES		
TASK NUMBER	TASK DISCRIPTION	MEAN TIME [h] or [day] for downtime	MEAN TIME [h]	FIXED PRICES [USD]	TIME-BASED PRICES [USD]	TOTAL PRICE [USD]
1	ENTER DRY DOCK	12.00	12.00	$ 12,000.00	$ -	$ 12,000.00
2	CLEAN HULL	25.00	37.00	$ 7,200.00	$ 900.00	$ 8,100.00
3	DRAIN TANK	3.25	15.25	$ 1,560.00	$ 39.00	$ 1,599.00
4	CLEAN OIL TANK	6.25	21.50	$ 150.00	$ 300.00	$ 450.00
5	CLEAN NON OIL TANK	3.33	18.58	$ 96.00	$ 80.00	$ 176.00
6	DEGAS TANKS	6.25	27.75	$ 480.00	$ 75.00	$ 555.00
7	BUILD SCAFFOLD	0.00	37.00	$ -	$ -	$ -
8	HULL VISUAL SURVEY	12.50	49.50	$ 7,200.00	$ 450.00	$ 7,650.00
9	NON OIL TANK VISUAL SURVEY	0.33	18.92	$ 192.00	$ 16.00	$ 208.00
10	OIL TANK VISUAL SURVEY	0.21	27.96	$ 240.00	$ 12.50	$ 252.50
11	ULTRASOUND SURVEY	0.12	49.62	$ 600.00	$ 14.60	$ 614.60
12	SURVEY REPORT	3.0	52.62	$ 600.00	$ 72.00	$ 672.00
13	REMOVE INTERFERENCES AND OUTLINE REPAIR	0.0	52.62	$ -	$ -	$ -
14	PROCESS FLAT PLATE	0.0	52.62	$ -	$ -	$ -
15	PROCESS FLAT PROFILE	27.9	80.55	$ 1,769.93	$ 2,681.58	$ 4,451.51
16	PROCESS FLAT PLATE FOR BENDING	0.2	52.79	$ 9,342.53	$ 16.15	$ 9,358.68
17	PROCESS FLAT PROFILE FOR BENDING	0.0	52.62	$ -	$ -	$ -
18	PROCESS CURVED PLATE	0.3	53.13	$ 1,214.73	$ 65.24	$ 1,279.96
19	PROCESS CURVED PROFILE	0.0	52.62	$ -	$ -	$ -
20	CONNECT ELEMENTS	29.6	82.49	$ 2,567.90	$ 2,843.16	$ 5,411.06
21	WELD	159.7	214.48	$ 19,550.60	$ 15,328.57	$ 34,879.16
22	WELD SURVEY	31.9	218.70	$ 1,748.03	$ 1,148.18	$ 2,896.20
23	INTERNAL COAT	0.0	218.70	$ -	$ -	$ -
24	EXTERNAL COAT	0.0	218.70	$ -	$ -	$ -
25	OUTER HULL COAT	36.0	254.70	$ 324.00	$ 2,592.00	$ 2,916.00
26	TANK COAT	27.9	246.61	$ 125.60	$ 1,507.25	$ 1,632.85
27	REINSTALL INTERFERENCES	0.0	254.70	$ -	$ -	$ -
28	REMOVE SCAFFOLDS	0.0	254.70	$ -	$ -	$ -
29	EXIT DRYDOCK	12.0	266.70	$ 12,000.00	$ -	$ 12,000.00
30	DRYDOCK TIME AND COST	23	-	$ -	$ 414,000.00	$ 414,000.00
			TOTAL PRICE	$ 78,961.31	$ 442,141.22	$ 521,102.53

Appendix Figure E.9. Drydock Costs in PV for Downtime at Year 15.



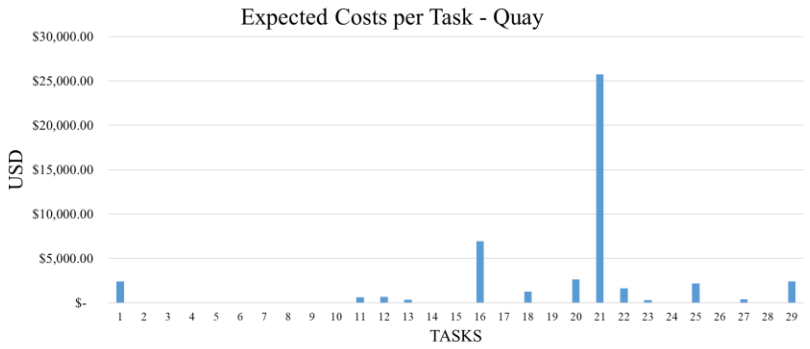
Appendix Figure E.10. Drydock Times for Downtime at Year 15.



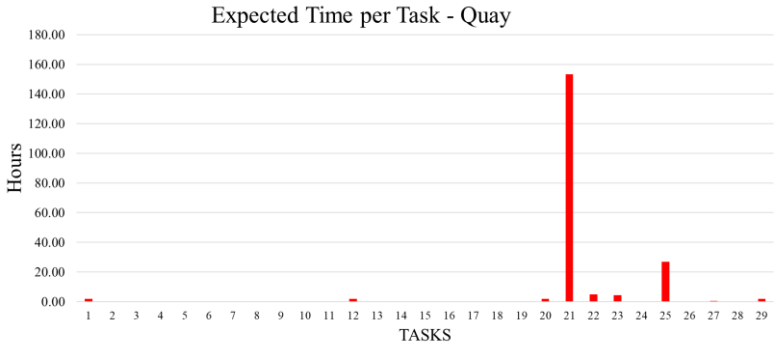
Appendix Table E.6. Quay Costs in PV for Downtime at Year 15.

TASKS		DURATION TIME	END TIME	SHIPYARD PRICES		
TASK NUMBER	TASK DISCRIPTION	MEAN TIME [h] or [day] for downtime	MEAN TIME [h]	FIXED PRICES [USD]	TIME-BASED PRICES [USD]	TOTAL PRICE [USD]
1	ENTER QUAY	2.00	2.00	$ 2,400.00	$ -	$ 2,400.00
2	CLEAN HULL	0.00	2.00	$ -	$ -	$ -
3	DRAIN TANK	0.00	2.00	$ -	$ -	$ -
4	CLEAN OIL TANK	0.00	2.00	$ -	$ -	$ -
5	CLEAN NON OIL TANK	0.00	2.00	$ -	$ -	$ -
6	DEGAS TANKS	0.00	2.00	$ -	$ -	$ -
7	BUILD SCAFFOLD	0.00	2.00	$ -	$ -	$ -
8	HULL VISUAL SURVEY	0.00	2.00	$ -	$ -	$ -
9	NON OIL TANK VISUAL SURVEY	0.00	2.00	$ -	$ -	$ -
10	OIL TANK VISUAL SURVEY	0.00	2.00	$ -	$ -	$ -
11	ULTRASOUND SURVEY	0.08	2.08	$ 600.00	$ 10.13	$ 610.13
12	SURVEY REPORT	2.0	4.08	$ 600.00	$ 48.00	$ 648.00
13	REMOVE INTERFERENCES AND OUTLINE REPAIR	0.3	4.33	$ 360.00	$ 9.00	$ 369.00
14	PROCESS FLAT PLATE	0.0	4.33	$ -	$ -	$ -
15	PROCESS FLAT PROFILE	0.0	4.33	$ -	$ -	$ -
16	PROCESS FLAT PLATE	0.2	4.50	$ 6,925.84	$ 16.13	$ 6,941.97
17	PROCESS FLAT PROFILE	0.0	4.33	$ -	$ -	$ -
18	PROCESS CURVED PLATE	0.3	4.84	$ 1,212.65	$ 65.06	$ 1,277.72
19	PROCESS CURVED PROFILE	0.0	4.33	$ -	$ -	$ -
20	CONNECT ELEMENTS	1.9	6.75	$ 2,471.29	$ 183.30	$ 2,654.59
21	WELD	153.4	160.14	$ 10,990.59	$ 14,725.73	$ 25,716.31
22	WELD SURVEY	4.9	165.04	$ 1,474.09	$ 176.19	$ 1,650.28
23	INTERNAL COAT	4.5	169.54	$ 40.50	$ 243.00	$ 283.50
24	EXTERNAL COAT	0.0	165.04	$ -	$ -	$ -
25	OUTER HULL COAT	27.0	192.04	$ 243.00	$ 1,944.00	$ 2,187.00
26	TANK COAT	0.0	165.04	$ -	$ -	$ -
27	REINSTALL INTERFERENCES	0.5	192.54	$ 360.00	$ 18.00	$ 378.00
28	REMOVE SCAFFOLDS	0.0	192.04	$ -	$ -	$ -
29	EXIT QUAY	2.0	194.54	$ 2,400.00	$ -	$ 2,400.00
30	QUAY TIME AND COST	17	-	$ -	$ 61,200.00	$ 61,200.00
			TOTAL PRICE	$ 30,077.96	$ 78,638.54	$ 108,716.50

Appendix Figure E.11. Quay Costs in PV for Downtime at Year 15.



Appendix Figure E.12. Quay Times in PV for Downtime at Year 15.



E.2 Expected Cost of Failure

Appendix Table E.7. Cost of Failure for Single Elements and Associated Unavailability Time.

	STRUCTURAL MAINTENANCE COST [USD]	SOCIAL COSTS [USD]	COST OF FAILURE [USD]	UNAVAILABILITY TIME [DAYS]
ELEMENT 1	$ 518,223.09	$ 639,503.19	$ 1,157,726.29	24
ELEMENT 2	$ 358,239.84	$ 63,950.32	$ 422,190.16	16
ELEMENT 3	$ 358,222.42	$ 63,950.32	$ 422,172.74	16
ELEMENT 4	$ 108,716.50	$ 639,503.19	$ 748,219.69	17
ELEMENT 5	$ 503,123.61	$ 639,503.19	$ 1,142,626.81	23

Appendix Table E.8. Probability of Failure Up to First Threshold.

YEARS	ELEMENT 1 P_f	ELEMENT 2 P_f	ELEMENT 3 P_f	ELEMENT 4 P_f	ELEMENT 5 P_f
1	0.00E+00	0.00E+00	0.00E+00	0.00E+00	0.00E+00
2	0.00E+00	0.00E+00	0.00E+00	0.00E+00	0.00E+00
3	0.00E+00	0.00E+00	0.00E+00	0.00E+00	0.00E+00
4	0.00E+00	7.60E-03	2.51E-03	1.29E-03	8.17E-04
5	0.00E+00	2.05E-02	6.96E-03	3.61E-03	2.25E-03
6	0.00E+00	3.51E-02	1.24E-02		4.12E-03
7	0.00E+00	4.99E-02	1.84E-02		
8	1.11E-16	6.43E-02	2.46E-02		
9	2.09E-09		3.07E-02		
10	8.46E-07		3.66E-02		
11	1.78E-05		4.23E-02		
12	2.84E-04		4.76E-02		
13	1.10E-03		5.27E-02		
14	3.10E-03		5.74E-02		
15			6.18E-02		
16			6.59E-02		
17					
18					
19					
20					
21					
22					
23					
24					
25					

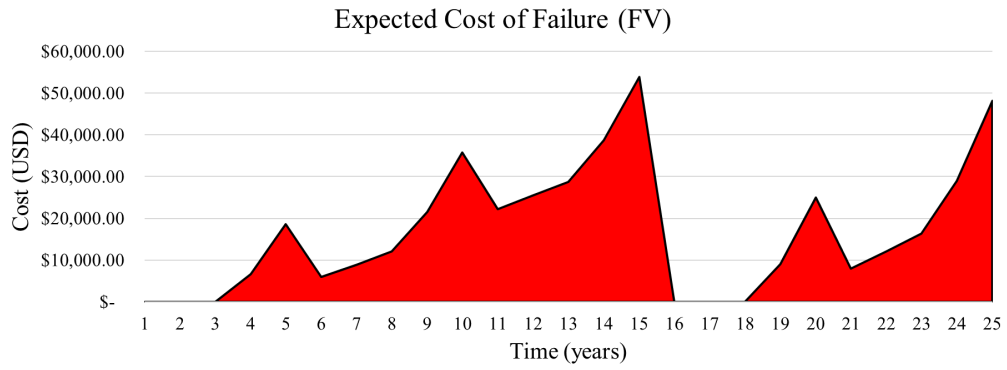
Appendix Table E.9. Expected Cost of Failure Up to First Threshold.

YEARS	ELEMENT 1 RISK	ELEMENT 2 RISK	ELEMENT 3 RISK	ELEMENT 4 RISK	ELEMENT 5 RISK
1	$ -	$ -	$ -	$ -	$ -
2	$ -	$ -	$ -	$ -	$ -
3	$ -	$ -	$ -	$ -	$ -
4	$ -	$ 3,207.43	$ 1,060.64	$ 963.82	$ 933.94
5	$ -	$ 8,653.34	$ 2,937.74	$ 2,700.62	$ 2,572.16
6	$ -	$ 14,820.08	$ 5,254.67		$ 4,710.75
7	$ -	$ 21,088.16	$ 7,783.49		
8	$ 0.00	$ 27,157.28	$ 10,379.24		
9	$ 0.00		$ 12,952.98		
10	$ 0.98		$ 15,450.79		
11	$ 20.57		$ 17,840.78		
12	$ 329.29		$ 20,105.10		
13	$ 1,271.72		$ 22,235.01		
14	$ 3,587.39		$ 24,227.69		
15			$ 26,084.19		
16			$ 27,808.07		
17					
18					
19					
20					
21					
22					
23					
24					
25					

Appendix Table E.10. Expected Cost of Failure Over Time with Interventions.

YEARS	ELEMENT 1 RISK	ELEMENT 2 RISK	ELEMENT 3 RISK	ELEMENT 4 RISK	ELEMENT 5 RISK	SUM PV	SUM FV
1	$ -	$ -	$ -	$ -	$ -	$ -	$ -
2	$ -	$ -	$ -	$ -	$ -	$ -	$ -
3	$ -	$ -	$ -	$ -	$ -	$ -	$ -
4	$ -	$ 3,207.43	$ 1,060.64	$ 963.82	$ 933.94	$ 6,165.82	$ 6,674.08
5	$ -	$ 8,653.34	$ 2,937.74	$ 2,700.62	$ 2,572.16	$ 16,863.85	$ 18,619.06
6	$ -	$ -	$ 5,254.67	$ -	$ -	$ 5,254.67	$ 5,917.61
7	$ -	$ -	$ 7,783.49	$ -	$ -	$ 7,783.49	$ 8,940.78
8	$ 0.00	$ -	$ 10,379.24	$ -	$ -	$ 10,379.24	$ 12,160.94
9	$ 0.00	$ 3,207.43	$ 12,952.98	$ 963.82	$ 933.94	$ 18,058.16	$ 21,581.18
10	$ 0.98	$ 8,653.34	$ 15,450.79	$ 2,700.62	$ 2,572.16	$ 29,377.89	$ 35,811.48
11	$ -	$ -	$ 17,840.78	$ -	$ -	$ 17,840.78	$ 22,182.77
12	$ -	$ -	$ 20,105.10	$ -	$ -	$ 20,105.10	$ 25,498.13
13	$ -	$ -	$ 22,235.01	$ -	$ -	$ 22,235.01	$ 28,763.36
14	$ -	$ 3,207.43	$ 24,227.69	$ 963.82	$ 933.94	$ 29,332.87	$ 38,704.10
15	$ -	$ 8,653.34	$ 26,084.19	$ 2,700.62	$ 2,572.16	$ 40,010.31	$ 53,848.60
16	$ -	$ -	$ -	$ -	$ -	$ -	$ -
17	$ -	$ -	$ -	$ -	$ -	$ -	$ -
18	$ 0.00	$ -	$ -	$ -	$ -	$ 0.00	$ 0.00
19	$ 0.00	$ 3,207.43	$ 1,060.64	$ 963.82	$ 933.94	$ 6,165.82	$ 8,982.44
20	$ 0.98	$ 8,653.34	$ 2,937.74	$ 2,700.62	$ 2,572.16	$ 16,864.83	$ 25,060.26
21	$ -	$ -	$ 5,254.67	$ -	$ -	$ 5,254.67	$ 7,964.32
22	$ -	$ -	$ 7,783.49	$ -	$ -	$ 7,783.49	$ 12,033.12
23	$ -	$ -	$ 10,379.24	$ -	$ -	$ 10,379.24	$ 16,367.02
24	$ -	$ 3,207.43	$ 12,952.98	$ 963.82	$ 933.94	$ 18,058.16	$ 29,045.42
25	$ -	$ 8,653.34	$ 15,450.79	$ 2,700.62	$ 2,572.16	$ 29,376.91	$ 48,195.93
					TOTAL	$ 317,290.31	

Appendix Figure E.13. Expected Cost of Failure C_{EF} in FV – Time-Grouping.



E.3 Expected Cost of Opportunity

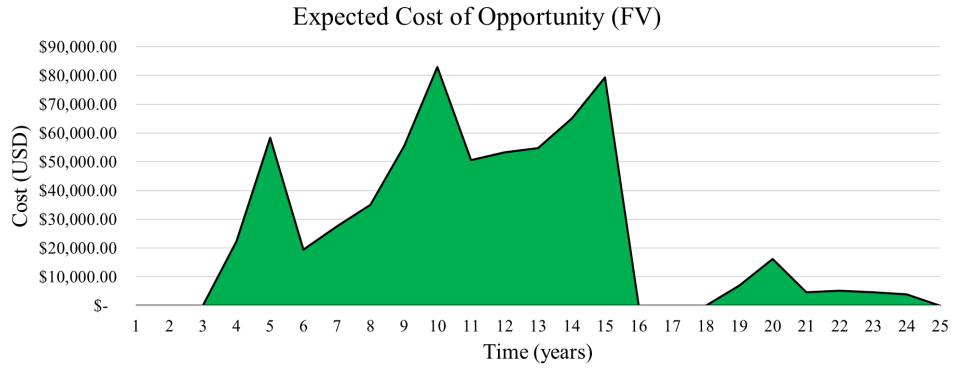
Appendix Table E.11. Expected Cost of Opportunity Up to First Threshold (without return of capital).

YEARS	ELEMENT 1 RISK	ELEMENT 2 RISK	ELEMENT 3 RISK	ELEMENT 4 RISK	ELEMENT 5 RISK
1	$ -	$ -	$ -	$ -	$ -
2	$ -	$ -	$ -	$ -	$ -
3	$ -	$ -	$ -	$ -	$ -
4	$ -	$ 17,693.98	$ 5,851.26	$ 3,573.63	$ 3,174.41
5	$ -	$ 47,736.70	$ 16,206.79	$ 10,013.34	$ 8,742.63
6	$ -	$ 81,755.96	$ 28,988.70		$ 16,011.57
7	$ -	$ 116,334.23	$ 42,939.58		
8	$ 0.00	$ 149,814.92	$ 57,259.69		
9	$ 0.01		$ 71,458.37		
10	$ 3.40		$ 85,238.18		
11	$ 71.38		$ 98,423.15		
12	$ 1,142.84		$ 110,914.85		
13	$ 4,413.63		$ 122,665.02		
14	$ 12,450.38		$ 133,658.14		
15			$ 143,900.00		
16			$ 153,410.23		
17					
18					
19					
20					
21					
22					
23					
24					
25					

Appendix Table E.12. Expected Cost of Opportunity Over Time with Interventions.

YEARS	ELEMENT 1 RISK	ELEMENT 2 RISK	ELEMENT 3 RISK	ELEMENT 4 RISK	ELEMENT 5 RISK	SUM PV	SUM FV
1	$ -	$ -	$ -	$ -	$ -	$ -	$ -
2	$ -	$ -	$ -	$ -	$ -	$ -	$ -
3	$ -	$ -	$ -	$ -	$ -	$ -	$ -
4	$ -	$ 12,024.51	$ 3,976.41	$ 2,428.58	$ 2,157.27	$ 20,586.77	$ 22,283.78
5	$ -	$ 30,485.44	$ 10,349.92	$ 6,394.68	$ 5,583.19	$ 52,813.23	$ 58,310.07
6	$ -	$ -	$ 17,354.09	$ -	$ -	$ 17,354.09	$ 19,543.52
7	$ -	$ -	$ 24,031.51	$ -	$ -	$ 24,031.51	$ 27,604.65
8	$ 0.00	$ -	$ 29,867.70	$ -	$ -	$ 29,867.70	$ 34,994.77
9	$ 0.00	$ 8,572.83	$ 34,621.98	$ 1,731.45	$ 1,538.02	$ 46,464.28	$ 55,529.12
10	$ 1.52	$ 21,400.27	$ 38,212.12	$ 4,488.96	$ 3,919.30	$ 68,022.18	$ 82,918.66
11	$ -	$ -	$ 40,646.19	$ -	$ -	$ 40,646.19	$ 50,538.42
12	$ -	$ -	$ 41,982.50	$ -	$ -	$ 41,982.50	$ 53,243.96
13	$ -	$ -	$ 42,305.80	$ -	$ -	$ 42,305.80	$ 54,727.06
14	$ -	$ 5,522.06	$ 41,712.92	$ 1,115.28	$ 990.69	$ 49,340.95	$ 65,104.34
15	$ -	$ 13,370.31	$ 40,304.17	$ 2,804.58	$ 2,448.67	$ 58,927.73	$ 79,308.97
16	$ -	$ -	$ -	$ -	$ -	$ -	$ -
17	$ -	$ -	$ -	$ -	$ -	$ -	$ -
18	$ 0.00	$ -	$ -	$ -	$ -	$ 0.00	$ 0.00
19	$ 0.00	$ 2,825.61	$ 934.41	$ 570.69	$ 506.93	$ 4,837.64	$ 7,047.53
20	$ 0.45	$ 6,272.99	$ 2,129.70	$ 1,315.83	$ 1,148.85	$ 10,867.83	$ 16,149.03
21	$ -	$ -	$ 3,009.40	$ -	$ -	$ 3,009.40	$ 4,561.25
22	$ -	$ -	$ 3,301.65	$ -	$ -	$ 3,301.65	$ 5,104.29
23	$ -	$ -	$ 2,898.77	$ -	$ -	$ 2,898.77	$ 4,571.07
24	$ -	$ 442.35	$ 1,786.46	$ 89.34	$ 79.36	$ 2,397.51	$ 3,856.24
25	$ -	$ -	$ -	$ -	$ -	$ -	$ -
					TOTAL	$ 519,655.72	

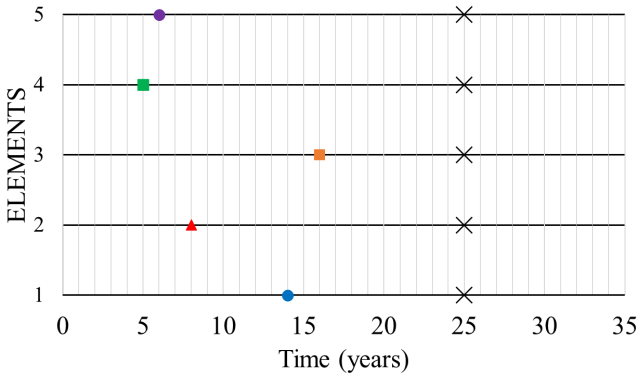
Appendix Figure E.14. Expected Cost of Opportunity C_{EO} in FV – Time-Grouping.



Appendix F: Policy-Grouping Demonstration

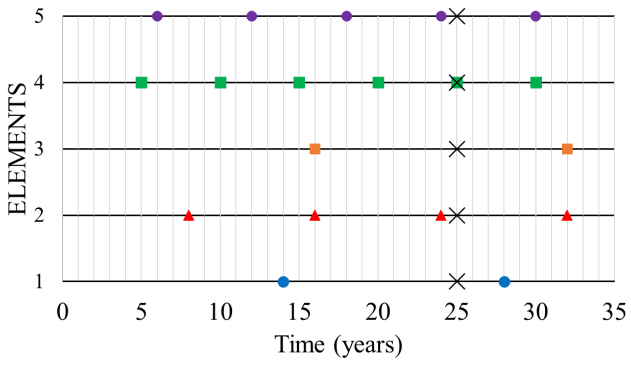
F.1 Step 1: Single element time threshold

Appendix Figure F.1. Grouping Strategy (Step 1).



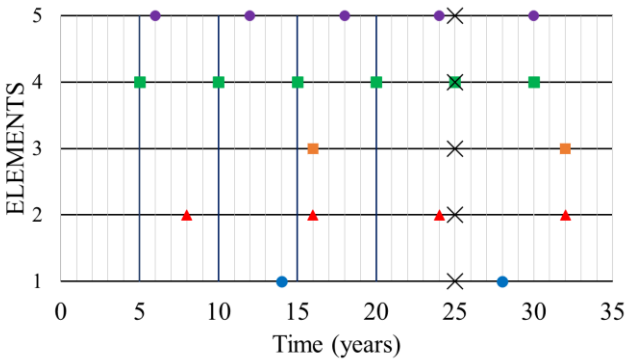
F.2 Step 2: Single element repair (time threshold repetitions)

Appendix Figure F.2. Grouping Strategy (Step 2).

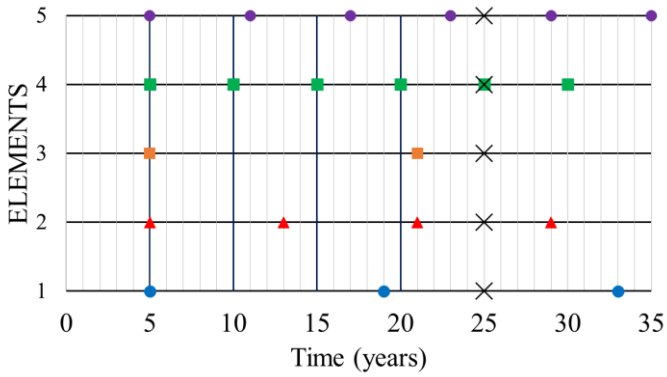


F.3 Step 3: Grouping, Policy Application, and Anticipation

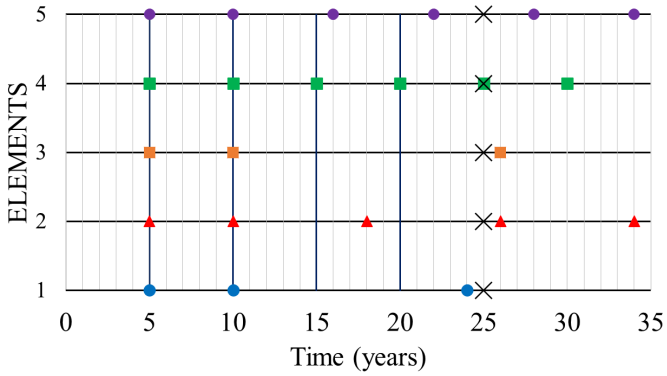
Appendix Figure F.3. Grouping Strategy (Step 3): Input Solution.



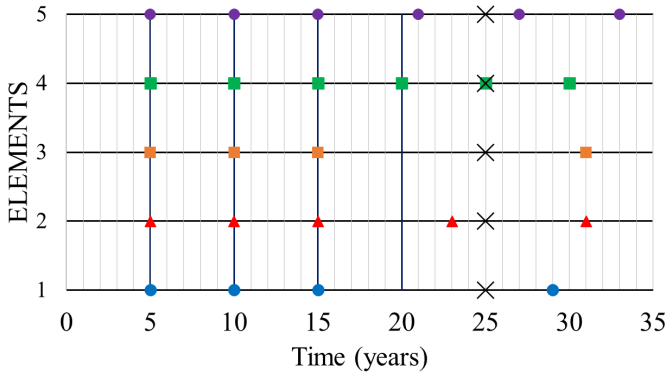
Appendix Figure F.4. Grouping Strategy (Step 3): Iteration 1.



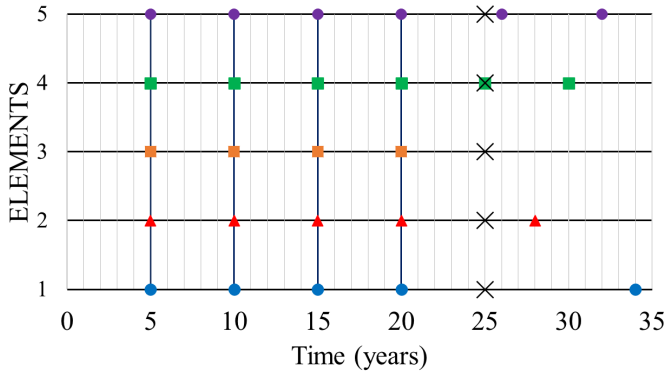
Appendix Figure F.5. Grouping Strategy (Step 3): Iteration 2.



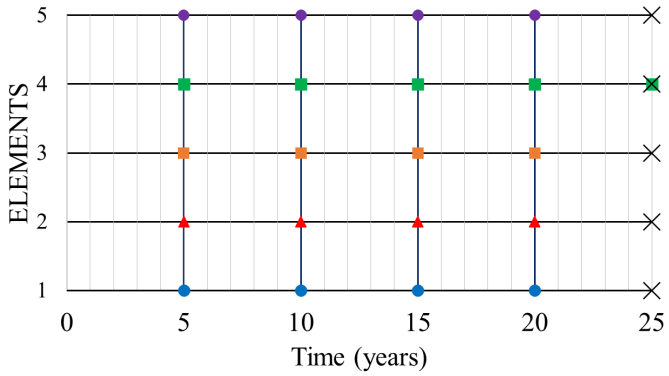
Appendix Figure F.6. Grouping Strategy (Step 3): Iteration 3.



Appendix Figure F.7. Grouping Strategy (Step 3): Iteration 4.



Appendix Figure F.8. Grouping Strategy (Step 3): Grouping Solution.



Appendix G: Policy-Grouping Hand Calculation Results

This Appendix presents the results for the policy-grouping intervention's cost and time for all tasks in each downtime; the Structural Cost C_S, the Expected Cost of Failure C_{EF}, and the Expected Cost of Opportunity C_{EO}.

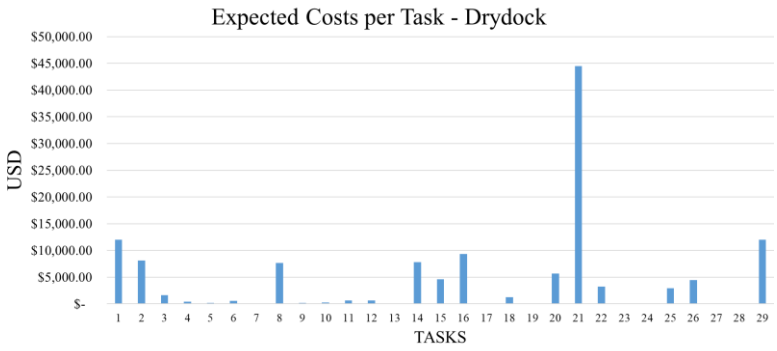
G.1 Structural Cost

Year 5, 10, 15, and 20: Elements [1, 2, 3, 4, 5]

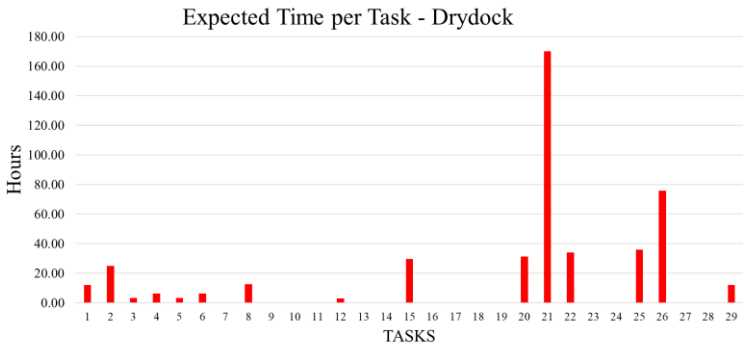
Appendix Table G.1. Drydock Costs in PV for Downtime at Year 5, 10, 15, and 20.

TASKS		DURATION TIME	END TIME	SHIPYARD PRICES		
TASK NUMBER	TASK DISCRIPTION	MEAN TIME [h] or [day] for downtime	MEAN TIME [h]	FIXED PRICES [USD]	TIME-BASED PRICES [USD]	TOTAL PRICE [USD]
1	ENTER DRY DOCK	12.00	12.00	$ 12,000.00	$ -	$ 12,000.00
2	CLEAN HULL	25.00	37.00	$ 7,200.00	$ 900.00	$ 8,100.00
3	DRAIN TANK	3.25	15.25	$ 1,560.00	$ 39.00	$ 1,599.00
4	CLEAN OIL TANK	6.25	21.50	$ 150.00	$ 300.00	$ 450.00
5	CLEAN NON OIL TANK	3.33	18.58	$ 96.00	$ 80.00	$ 176.00
6	DEGAS TANKS	6.25	27.75	$ 480.00	$ 75.00	$ 555.00
7	BUILD SCAFFOLD	0.00	37.00	$ -	$ -	$ -
8	HULL VISUAL SURVEY	12.50	49.50	$ 7,200.00	$ 450.00	$ 7,650.00
9	NON OIL TANK VISUAL SURVEY	0.33	18.92	$ 192.00	$ 16.00	$ 208.00
10	OIL TANK VISUAL SURVEY	0.21	27.96	$ 240.00	$ 12.50	$ 252.50
11	ULTRASOUND SURVEY	0.23	49.73	$ 600.00	$ 28.10	$ 628.10
12	SURVEY REPORT	3.0	52.73	$ 600.00	$ 72.00	$ 672.00
13	REMOVE INTERFERENCES AND OUTLINE REPAIR	0.0	52.73	$ -	$ -	$ -
14	PROCESS FLAT PLATE	0.2	52.90	$ 7,816.27	$ 16.14	$ 7,832.41
15	PROCESS FLAT PROFILE	29.7	82.45	$ 1,769.76	$ 2,852.64	$ 4,622.40
16	PROCESS FLAT PLATE FOR BENDING	0.2	52.90	$ 9,342.30	$ 16.14	$ 9,358.45
17	PROCESS FLAT PROFILE FOR BENDING	0.0	52.73	$ -	$ -	$ -
18	PROCESS CURVED PLATE	0.3	53.24	$ 1,213.82	$ 65.16	$ 1,278.98
19	PROCESS CURVED PROFILE	0.0	52.73	$ -	$ -	$ -
20	CONNECT ELEMENTS	31.4	84.30	$ 2,635.18	$ 3,013.09	$ 5,648.26
21	WELD	170.1	225.02	$ 28,168.22	$ 16,330.08	$ 44,498.30
22	WELD SURVEY	33.9	229.50	$ 2,022.25	$ 1,222.12	$ 3,244.37
23	INTERNAL COAT	0.0	229.50	$ -	$ -	$ -
24	EXTERNAL COAT	0.0	229.50	$ -	$ -	$ -
25	OUTER HULL COAT	36.0	265.50	$ 324.00	$ 2,592.00	$ 2,916.00
26	TANK COAT	75.9	305.42	$ 341.60	$ 4,099.25	$ 4,440.85
27	REINSTALL INTERFERENCES	0.0	305.42	$ -	$ -	$ -
28	REMOVE SCAFFOLDS	0.0	305.42	$ -	$ -	$ -
29	EXIT DRYDOCK	12.0	317.42	$ 12,000.00	$ -	$ 12,000.00
30	DRYDOCK TIME AND COST	27	-	$ -	$ 486,000.00	$ 486,000.00
			TOTAL PRICE	$ 95,951.40	$ 518,179.22	$ 614,130.63

Appendix Figure G.1. Drydock Costs in PV for Downtime at Year 5, 10, 15, and 20.



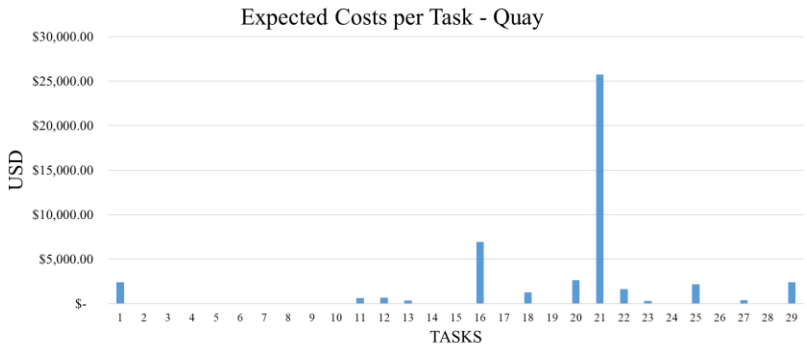
Appendix Figure G.2. Drydock Times for Downtime at Year 5, 10, 15 and 20.



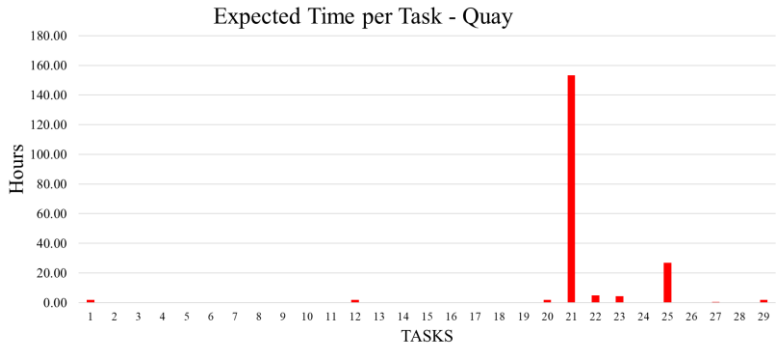
Appendix Table G.2. Quay Costs in PV for Downtime at Year 5, 10, 15, and 20.

TASKS		DURATION TIME	END TIME	SHIPYARD PRICES		
TASK NUMBER	TASK DISCRIPTION	MEAN TIME [h] or [day] for downtime	MEAN TIME [h]	FIXED PRICES [USD]	TIME-BASED PRICES [USD]	TOTAL PRICE [USD]
1	ENTER QUAY	2.00	2.00	$ 2,400.00	$ -	$ 2,400.00
2	CLEAN HULL	0.00	2.00	$ -	$ -	$ -
3	DRAIN TANK	0.00	2.00	$ -	$ -	$ -
4	CLEAN OIL TANK	0.00	2.00	$ -	$ -	$ -
5	CLEAN NON OIL TANK	0.00	2.00	$ -	$ -	$ -
6	DEGAS TANKS	0.00	2.00	$ -	$ -	$ -
7	BUILD SCAFFOLD	0.00	2.00	$ -	$ -	$ -
8	HULL VISUAL SURVEY	0.00	2.00	$ -	$ -	$ -
9	NON OIL TANK VISUAL SURVEY	0.00	2.00	$ -	$ -	$ -
10	OIL TANK VISUAL SURVEY	0.00	2.00	$ -	$ -	$ -
11	ULTRASOUND SURVEY	0.08	2.08	$ 600.00	$ 10.13	$ 610.13
12	SURVEY REPORT	2.0	4.08	$ 600.00	$ 48.00	$ 648.00
13	REMOVE INTERFERENCES AND OUTLINE REPAIR	0.3	4.33	$ 360.00	$ 9.00	$ 369.00
14	PROCESS FLAT PLATE	0.0	4.33	$ -	$ -	$ -
15	PROCESS FLAT PROFILE	0.0	4.33	$ -	$ -	$ -
16	PROCESS FLAT PLATE	0.2	4.50	$ 6,925.84	$ 16.13	$ 6,941.97
17	PROCESS FLAT PROFILE	0.0	4.33	$ -	$ -	$ -
18	PROCESS CURVED PLATE	0.3	4.84	$ 1,212.65	$ 65.06	$ 1,277.72
19	PROCESS CURVED PROFILE	0.0	4.33	$ -	$ -	$ -
20	CONNECT ELEMENTS	1.9	6.75	$ 2,471.29	$ 183.30	$ 2,654.59
21	WELD	153.4	160.14	$ 10,990.59	$ 14,725.73	$ 25,716.31
22	WELD SURVEY	4.9	165.04	$ 1,474.09	$ 176.19	$ 1,650.28
23	INTERNAL COAT	4.5	169.54	$ 40.50	$ 243.00	$ 283.50
24	EXTERNAL COAT	0.0	165.04	$ -	$ -	$ -
25	OUTER HULL COAT	27.0	192.04	$ 243.00	$ 1,944.00	$ 2,187.00
26	TANK COAT	0.0	165.04	$ -	$ -	$ -
27	REINSTALL INTERFERENCES	0.5	192.54	$ 360.00	$ 18.00	$ 378.00
28	REMOVE SCAFFOLDS	0.0	192.04	$ -	$ -	$ -
29	EXIT QUAY	2.0	194.54	$ 2,400.00	$ -	$ 2,400.00
30	QUAY TIME AND COST	17	-	$ -	$ 61,200.00	$ 61,200.00
			TOTAL PRICE	$ 30,077.96	$ 78,638.54	$ 108,716.50

Appendix Figure G.3. Quay Costs in PV for Downtime at Year 5, 10, 15, and 20.



Appendix Figure G.4. Quay Times for Downtime at Year 5, 10, 15, and 20.



G.2 Expected Cost of Failure

Appendix Table G.3. Cost of Failure for Policy Elements and Associated Unavailability Time.

	STRUCTURAL MAINTENANCE COST [USD]	SOCIAL COSTS [USD]	COST OF FAILURE [USD]	UNAVAILABILITY TIME [DAYS]
ELEMENT 1, 2, 3	$ 534,782.60	$ 639,503.19	$ 1,174,285.79	24
ELEMENT 1, 2, 3	$ 534,782.60	$ 63,950.32	$ 598,732.92	24
ELEMENT 1, 3	$ 490,260.28	$ 63,950.32	$ 554,210.60	22
ELEMENT 4	$ 108,716.50	$ 639,503.19	$ 748,219.69	17
ELEMENT 5	$ 503,123.61	$ 639,503.19	$ 1,142,626.81	23

Appendix Table G.4. Probability of Failure Up to First Threshold.

YEARS	ELEMENT 1 P_f	ELEMENT 2 P_f	ELEMENT 3 P_f	ELEMENT 4 P_f	ELEMENT 5 P_f
1	0.00E+00	0.00E+00	0.00E+00	0.00E+00	0.00E+00
2	0.00E+00	0.00E+00	0.00E+00	0.00E+00	0.00E+00
3	0.00E+00	0.00E+00	0.00E+00	0.00E+00	0.00E+00
4	0.00E+00	7.60E-03	2.51E-03	1.29E-03	8.17E-04
5	0.00E+00	2.05E-02	6.96E-03	3.61E-03	2.25E-03
6	0.00E+00	3.51E-02	1.24E-02		4.12E-03
7	0.00E+00	4.99E-02	1.84E-02		
8	1.11E-16	6.43E-02	2.46E-02		
9	2.09E-09		3.07E-02		
10	8.46E-07		3.66E-02		
11	1.78E-05		4.23E-02		
12	2.84E-04		4.76E-02		
13	1.10E-03		5.27E-02		
14	3.10E-03		5.74E-02		
15			6.18E-02		
16			6.59E-02		
17					
18					
19					
20					
21					
22					
23					
24					
25					

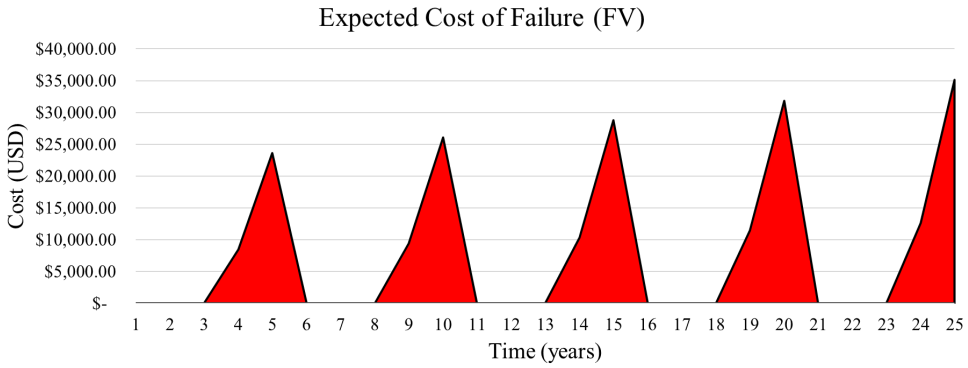
Appendix Table G.5. Expected Cost of Failure Up to First Threshold.

YEARS	ELEMENT 1, 2, 3 RISK	ELEMENT 1, 2, 3 RISK	ELEMENT 1,3 RISK	ELEMENT 4 RISK	ELEMENT 5 RISK
1	$ -	$ -	$ -	$ -	$ -
2	$ -	$ -	$ -	$ -	$ -
3	$ -	$ -	$ -	$ -	$ -
4	$ -	$ 4,548.64	$ 1,392.36	$ 963.82	$ 933.94
5	$ -	$ 12,271.81	$ 3,856.54	$ 2,700.62	$ 2,572.16
6	$ -	$ 21,017.24	$ 6,898.11		$ 4,710.75
7	$ -	$ 29,906.38	$ 10,217.84		
8	$ 0.00	$ 38,513.35	$ 13,625.43		
9	$ 0.00		$ 17,004.13		
10	$ 0.99		$ 20,283.15		
11	$ 20.86		$ 23,420.63		
12	$ 334.00		$ 26,393.13		
13	$ 1,289.91		$ 29,189.19		
14	$ 3,638.70		$ 31,805.09		
15			$ 34,242.23		
16			$ 36,505.27		
17					
18					
19					
20					
21					
22					
23					
24					
25					

Appendix Table G.6. Expected Cost of Failure Over Time with Interventions.

YEARS	ELEMENT 1, 2, 3 RISK	ELEMENT 1, 2, 3 RISK	ELEMENT 1,3 RISK	ELEMENT 4 RISK	ELEMENT 5 RISK	SUM PV	SUM FV
1	$ -	$ -	$ -	$ -	$ -	$ -	$ -
2	$ -	$ -	$ -	$ -	$ -	$ -	$ -
3	$ -	$ -	$ -	$ -	$ -	$ -	$ -
4	$ -	$ 4,548.64	$ 1,392.36	$ 963.82	$ 933.94	$ 7,838.76	$ 8,484.92
5	$ -	$ 12,271.81	$ 3,856.54	$ 2,700.62	$ 2,572.16	$ 21,401.13	$ 23,628.58
6	$ -	$ -	$ -	$ -	$ -	$ -	$ -
7	$ -	$ -	$ -	$ -	$ -	$ -	$ -
8	$ -	$ -	$ -	$ -	$ -	$ -	$ -
9	$ -	$ 4,548.64	$ 1,392.36	$ 963.82	$ 933.94	$ 7,838.76	$ 9,368.04
10	$ -	$ 12,271.81	$ 3,856.54	$ 2,700.62	$ 2,572.16	$ 21,401.13	$ 26,087.86
11	$ -	$ -	$ -	$ -	$ -	$ -	$ -
12	$ -	$ -	$ -	$ -	$ -	$ -	$ -
13	$ -	$ -	$ -	$ -	$ -	$ -	$ -
14	$ -	$ 4,548.64	$ 1,392.36	$ 963.82	$ 933.94	$ 7,838.76	$ 10,343.07
15	$ -	$ 12,271.81	$ 3,856.54	$ 2,700.62	$ 2,572.16	$ 21,401.13	$ 28,803.10
16	$ -	$ -	$ -	$ -	$ -	$ -	$ -
17	$ -	$ -	$ -	$ -	$ -	$ -	$ -
18	$ -	$ -	$ -	$ -	$ -	$ -	$ -
19	$ -	$ 4,548.64	$ 1,392.36	$ 963.82	$ 933.94	$ 7,838.76	$ 11,419.59
20	$ -	$ 12,271.81	$ 3,856.54	$ 2,700.62	$ 2,572.16	$ 21,401.13	$ 31,800.95
21	$ -	$ -	$ -	$ -	$ -	$ -	$ -
22	$ -	$ -	$ -	$ -	$ -	$ -	$ -
23	$ -	$ -	$ -	$ -	$ -	$ -	$ -
24	$ -	$ 4,548.64	$ 1,392.36	$ 963.82	$ 933.94	$ 7,838.76	$ 12,608.15
25	$ -	$ 12,271.81	$ 3,856.54	$ 2,700.62	$ 2,572.16	$ 21,401.13	$ 35,110.82
					TOTAL	$ 146,199.43	

Appendix Figure G.5. Expected Cost of Failure C_{EF} in FV – Policy-Grouping.



G.3 Expected Cost of Opportunity

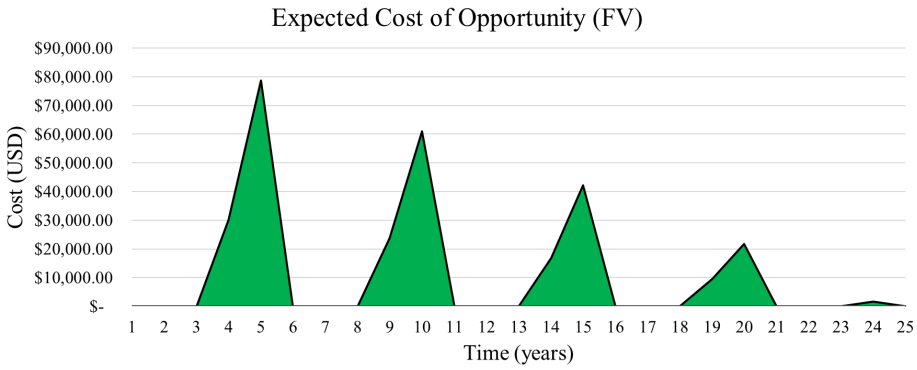
Appendix Table G.7. Expected Cost of Opportunity Up to First Threshold (without return of capital).

YEARS	ELEMENT 1, 2, 3 RISK	ELEMENT 1, 2, 3 RISK	ELEMENT 1, 3 RISK	ELEMENT 4 RISK	ELEMENT 5 RISK
1	$ -	$ -	$ -	$ -	$ -
2	$ -	$ -	$ -	$ -	$ -
3	$ -	$ -	$ -	$ -	$ -
4	$ -	$ 26,278.47	$ 7,979.47	$ 3,573.63	$ 3,174.41
5	$ -	$ 70,896.85	$ 22,101.48	$ 10,013.34	$ 8,742.63
6	$ -	$ 121,421.06	$ 39,532.39		$ 16,011.57
7	$ -	$ 172,775.48	$ 58,557.46		
8	$ 0.00	$ 222,499.81	$ 78,086.05		
9	$ 0.01		$ 97,449.04		
10	$ 3.41		$ 116,240.81		
11	$ 71.68		$ 134,221.39		
12	$ 1,147.55		$ 151,256.54		
13	$ 4,431.82		$ 167,280.45		
14	$ 12,501.69		$ 182,271.96		
15			$ 196,238.97		
16			$ 209,208.23		
17					
18					
19					
20					
21					
22					
23					
24					
25					

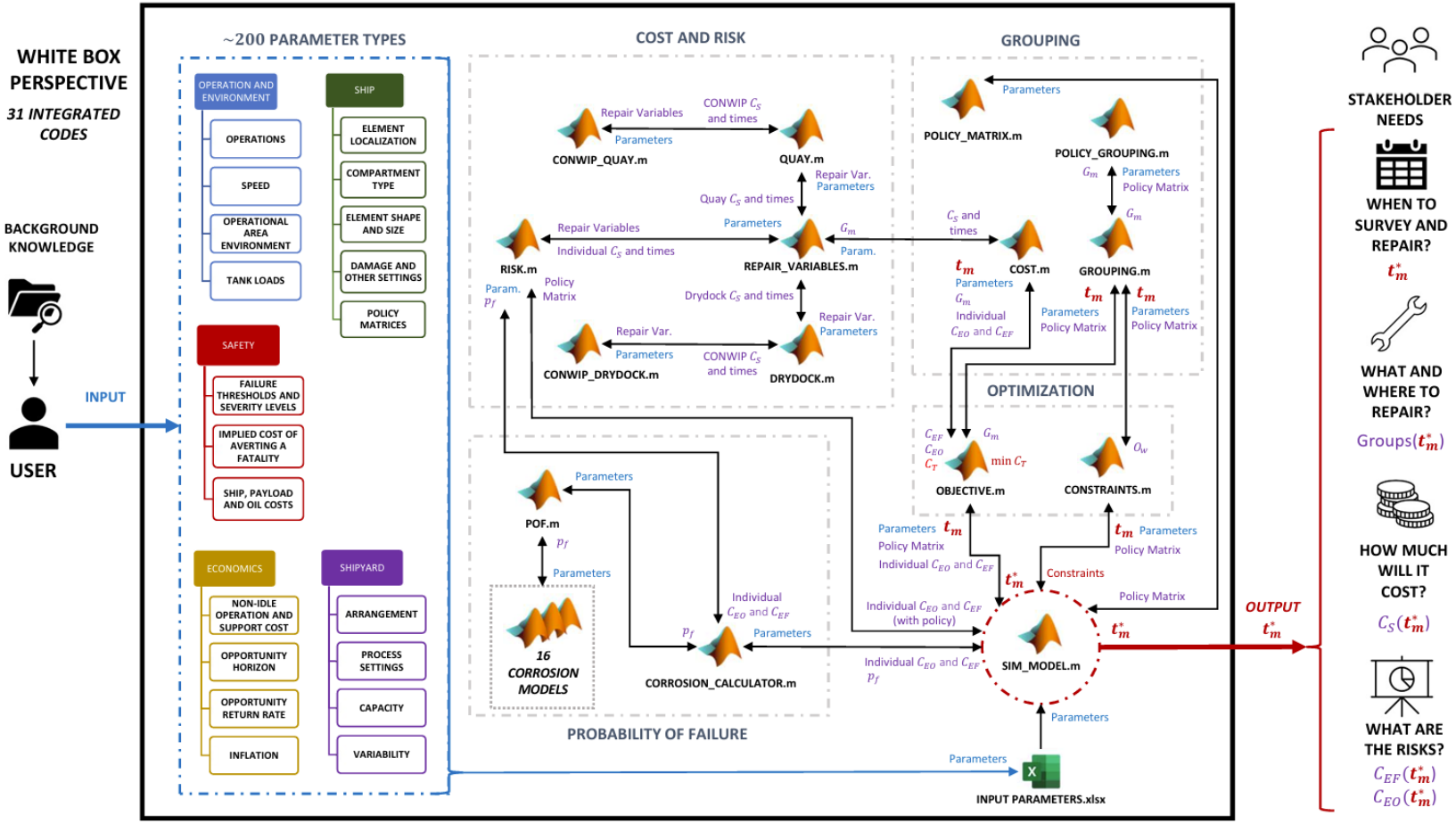
Appendix Table G.8. Expected Cost of Opportunity Over Time with Interventions.

YEARS	ELEMENT 1, 2, 3 RISK	ELEMENT 1, 2, 3 RISK	ELEMENT 1, 3 RISK	ELEMENT 4 RISK	ELEMENT 5 RISK	SUM PV	SUM FV
1	$ -	$ -	$ -	$ -	$ -	$ -	$ -
2	$ -	$ -	$ -	$ -	$ -	$ -	$ -
3	$ -	$ -	$ -	$ -	$ -	$ -	$ -
4	$ -	$ 17,858.37	$ 5,422.70	$ 2,428.58	$ 2,157.27	$ 27,866.92	$ 30,164.05
5	$ -	$ 45,275.89	$ 14,114.37	$ 6,394.68	$ 5,583.19	$ 71,368.13	$ 78,796.18
6	$ -	$ -	$ -	$ -	$ -	$ -	$ -
7	$ -	$ -	$ -	$ -	$ -	$ -	$ -
8	$ -	$ -	$ -	$ -	$ -	$ -	$ -
9	$ -	$ 12,732.07	$ 3,866.10	$ 1,731.45	$ 1,538.02	$ 19,867.63	$ 23,743.66
10	$ -	$ 31,782.93	$ 9,908.05	$ 4,488.96	$ 3,919.30	$ 50,099.24	$ 61,070.70
11	$ -	$ -	$ -	$ -	$ -	$ -	$ -
12	$ -	$ -	$ -	$ -	$ -	$ -	$ -
13	$ -	$ -	$ -	$ -	$ -	$ -	$ -
14	$ -	$ 8,201.16	$ 2,490.29	$ 1,115.28	$ 990.69	$ 12,797.42	$ 16,885.92
15	$ -	$ 19,857.11	$ 6,190.28	$ 2,804.58	$ 2,448.67	$ 31,300.65	$ 42,126.55
16	$ -	$ -	$ -	$ -	$ -	$ -	$ -
17	$ -	$ -	$ -	$ -	$ -	$ -	$ -
18	$ -	$ -	$ -	$ -	$ -	$ -	$ -
19	$ -	$ 4,196.50	$ 1,274.27	$ 570.69	$ 506.93	$ 6,548.39	$ 9,539.76
20	$ -	$ 9,316.43	$ 2,904.32	$ 1,315.83	$ 1,148.85	$ 14,685.43	$ 21,821.78
21	$ -	$ -	$ -	$ -	$ -	$ -	$ -
22	$ -	$ -	$ -	$ -	$ -	$ -	$ -
23	$ -	$ -	$ -	$ -	$ -	$ -	$ -
24	$ -	$ 656.96	$ 199.49	$ 89.34	$ 79.36	$ 1,025.15	$ 1,648.89
25	$ -	$ -	$ -	$ -	$ -	$ -	$ -
					TOTAL	$ 235,558.96	

Appendix Figure G.6. Expected Cost of Opportunity C_{EO} in FV – Policy-Grouping.



Appendix H: The OMCRO Framework



Bibliography

Aven, Terje. 2010. "On How to Define, Understand and Describe Risk." *Reliability Engineering and System Safety* 95 (6): 623–31. https://doi.org/10.1016/j.ress.2010.01.011.

Ayyub, Bilal, U.O. Akpan, P.A. Rushton, T.S. Koko, Jonathan Ross, and James Lua. 2002. "SSC-421 Risk-Informed Inspection of Marine Vessels."

Baker, Kenneth R., and Dan Trietsch. 2009. *Principles of Sequencing and Scheduling*. Edited by Inc. John Wiley & Sons. https://onlinelibrary.wiley.com/doi/.

Benoit, Emile. 1973. *Defence and Economic Growth in Developing Countries*. Lexington, MA: Lexington Books.

Benoit, Emile. 1978. "Growth and Defense in Developing Countries." *The University of Chicago Press Journals* 26 (2): 271–80. https://about.jstor.org/terms.

Blanchard, Benjamin S. 1998. *Logistics Engineering and Management*. Edited by Prentice Hall. 5th ed. Upper Saddle River, NJ.

Casares, João F C, and Nickolas Vlahopoulos. 2024. "Optimizing Ship Structural Integrity Management: Opportunistic Maintenance with Corrosion Prediction." www.sname.org.

Devore, Jay. 2009. *Probability and Statistics for Engineering and The Sciences*. Seventh. Brooks/Cole CENGAGE Learning.

DNV. 2002. "Marine Risk Assessment. Offshore Technology Report 2001/063." London, UK: HSE Books.

DoDI 4151.22. 2020. "DoD Instruction 4151.22 - Condition-Based Maintenance Plus for Materiel Maintenance." https://www.esd.whs.mil/DD/.

Dong, Fang. 2013. "Dynamic Control of Flexible Queueing Networks with Application to Shipbuilding." Ann Arbor, MI: The University of Michigan.

Dufresne, Daniel. 2008. "Sums of Lognormals." *Actuarial Research Clearing House*.

Dunne, J. Paul, Ron P. Smith, and Dirk Willenbockel. 2005. "Models of Military Expenditure and Growth: A Critical Review." *Defence and Peace Economics* 16 (6): 449–61. https://doi.org/10.1080/10242690500167791.

Dylan, by W. 2015. “A Multi-Objective Collaborative Optimization Framework to Understand Trade-Offs Between Naval Lifetime Costs Considering Production, Operation, and Maintenance.” PhD Thesis, University of Michigan.

Eck, Nees Jan Van, and Ludo Waltman. 2010. “Software Survey: VOSviewer, a Computer Program for Bibliometric Mapping.” *Scientometrics* 84 (2): 523–38. https://doi.org/10.1007/s11192-009-0146-3.

Einstein, Albert. 1929. “What Life Means to Einstein.” *The Saturday Evening Post*, October 26, 1929.

Eisenhower, Dwight D. 1953. “The Chance for Peace : Address by Dwight D. Eisenhower, President of the United States, April 16, 1953.” *Department of State Publication ; 5042. General Foreign Policy Series ; 78*. Washington, DC: Govt. Print. Off.

Elveren, Adem Y. 2022. “Military Spending and Profit Rate: A Circuit of Capital Model with a Military Sector.” *Defence and Peace Economics* 33 (1): 59–76. https://doi.org/10.1080/10242694.2020.1832394.

Emi, Hirohiko, Atsushi Kumano, Norio Yamamoto, Yasushi Nakamura, Nobuhiro Baba, and Hiromi Shihara. 1991. “A Basic Study on Life Assessment of Ships and Offshore Structures.”

EMSA. 2005. “Double Hull Tankers: High Level Panel of Experts.”

Fenton, Lawrence F. 1960. “The Sum of Log-Normal Probability Distributions in Scatter Transmission Systems.” *IRE Transactions on Communications Systems*.

Fisher, Irving. 1907. *THE RATE OF INTEREST: Its Nature, Determination and Relation to Economic Phenomena*. Norwood, MA: The Macmillan Company.

Flanders, Ralph E. 1924. “Design, Manufacture, and Production Control of a Standard Machine.” *Transactions of ASME* 46:691–713.

Franklin, Benjamin. 1762. *Advice to a Young Tradesman*. Boston: Sold [by Benjamin Mecom] at the new printing-office, in Boston.

GAO. 2020. “GAO-20-588 Report to Congressional Committees.”

GAO. 2025. “GAO-25-106990 Q&A Report to the Committee on Armed Services, House of Representatives.”

Garbatov, Y. 2020. “Risk-Based Corrosion Allowance of Oil Tankers.” *Ocean Engineering* 213 (October). https://doi.org/10.1016/j.oceaneng.2020.107753.

Garbatov, Y., C. Guedes Soares, and G. Wang. 2007. “Nonlinear Time Dependent Corrosion Wastage of Deck Plates of Ballast and Cargo Tanks of Tankers.” *Journal of Offshore Mechanics and Arctic Engineering* 129 (1): 48–55. https://doi.org/10.1115/1.2426987.

Garbatov, Y., and C. Guedes Soares. 2008. “Corrosion Wastage Modeling of Deteriorated Bulk Carrier Decks.” *International Shipbuilding Progress* 55 (1–2): 109–25. https://doi.org/10.3233/ISP-2008-0041.

Gardiner, C. P., and R. E. Melchers. 2001. “Enclosed Atmospheric Corrosion in Ship Spaces.” *British Corrosion Journal* 36 (4): 272–76. https://doi.org/10.1179/000705901101501730.

Gold, David. 1997. “Evaluating the Trade-off between Military Spending and Investment in the United States.” *Defence and Peace Economics* 8 (3): 251–66. https://doi.org/10.1080/10430719708404880.

Grobar, Lisa M, and Richard C Porter. 1987. *BENOIT REVISITED: DEFENSE SPENDING AND ECONOMIC GROWIH IN LDCs*. Ann Arbor, MI: Research Seminar in International Economics, Department of Economics, University of Michigan.

Gudze, M. T., and R. E. Melchers. 2008. “Operational Based Corrosion Analysis in Naval Ships.” *Corrosion Science* 50 (12): 3296–3307. https://doi.org/10.1016/j.corsci.2008.08.048.

Guedes Soares, C., and Y. Garbatov. 1999. “Reliability of Maintained, Corrosion Protected Plates Subjected to Non-Linear Corrosion and Compressive Loads.” *Marine Structures* 12:425–45.

Guedes Soares, C., Y. Garbatov, and A. Zayed. 2011. “Effect of Environmental Factors on Steel Plate Corrosion under Marine Immersion Conditions.” *Corrosion Engineering Science and Technology* 46 (4): 524–41. https://doi.org/10.1179/147842209X12559428167841.

Guedes Soares, C., Y. Garbatov, A. Zayed, and G. Wang. 2005. “Non-Linear Corrosion Model for Immersed Steel Plates Accounting for Environmental Factors.” In *SNAME Maritime Convention 2005*, 306–29. http://onepetro.org/SNAMESMC/proceedings-pdf/SMC05/2-SMC05/D021S003R003/2453248/sname-smc-2005-d21.pdf.

Guedes Soares, C., Y. Garbatov, A. Zayed, and G. Wang. 2008. “Corrosion Wastage Model for Ship Crude Oil Tanks.” *Corrosion Science* 50 (11): 3095–3106. https://doi.org/10.1016/j.corsci.2008.08.035.

Guedes Soares, C., Y. Garbatov, A. Zayed, and G. Wang. 2009. “Influence of Environmental Factors on Corrosion of Ship Structures in Marine Atmosphere.” *Corrosion Science* 51 (9): 2014–26. https://doi.org/10.1016/j.corsci.2009.05.028.

Hopp, Wallace J, and Mark L Spearman. 2011. *Factory Physics*. *Factory Physics*. 3rd ed. Long Grove, Ill.: Waveland Press.

IACS. 2010. "Common Structure Rules for Double Hull Oil Tankers."

IACS. 2022. "UR Z7 Hull Classification Surveys."

INCOSE. 2023. *Systems Engineering Handbook*. Edited by International Council on Systems Engineering. 5th ed. San Diego, CA, USA: Wiley.

ISO 31073. 2022. "ISO 31073:2022 Risk Management—Vocabulary." Edited by International Organization for Standardization (ISO). Geneva: ISO.

ISO/IEC/IEEE 15288. 2023. "Systems and Software Engineering - System Life Cycle Processes." The International Organization for Standardization, The International Electrotechnical Commission, and The Institute of Electrical and Electronics Engineers.

Kennedy, John F. 1962. "Address to Congress on the State of the Union January 11." *State of the Union - 2006*.

Kim, Do Kyun, Eileen Wee Chin Wong, and Nak Kyun Cho. 2020. "An Advanced Technique to Predict Time-Dependent Corrosion Damage of Onshore, Offshore, Nearshore and Ship Structures: Part I = Generalisation." *International Journal of Naval Architecture and Ocean Engineering* 12 (January):657–66. https://doi.org/10.1016/j.ijnaoe.2020.06.007.

Koch, Gerhardus. 2017. "Cost of Corrosion." In *Trends in Oil and Gas Corrosion Research and Technologies: Production and Transmission*, edited by A. M El-Sherik, 26–54. Chantilly: Elsevier Science & Technology. http://ebookcentral.proquest.com/lib/umichigan/detail.action?docID=4875092.

Kuznecovs, Artjoms, Jonas W. Ringsberg, Anirudh Mallaya Ullal, Pavan Janardhana Bangera, and Erland Johnson. 2022. "Consequence Analyses of Collision-Damaged Ships — Damage Stability, Structural Adequacy and Oil Spills." *Ships and Offshore Structures*. https://doi.org/10.1080/17445302.2022.2071014.

Liker, Jeffrey K., and Thomas Lamb. 2002. "What Is Lean Ship Construction and Repair?" *Journal of Ship Production* 18 (3): 121–42. https://doi.org/10.5957/jsp.2002.18.3.121.

Lödding, Hermann. 2013. *Handbook of Manufacturing Control*. Springer.

Mankiw, N. Gregory. 2015. *Principles of Economics*. 7th ed. Stamford, CT: CENGAGE Learning.

Mansour, A., P. Wirsching, P. Lucket, and A. Plumpton. 1997. "SSC-398 Assessment of Reliability of Ship Structures."

McIntyre, Dale R. 2017. *Forms of Corrosion: Recognition and Prevention*. 2nd ed.

Melchers, R. E. 2003a. "Modeling of Marine Immersion Corrosion for Mild and Low-Alloy Steels: Part 1: Phenomenological Model." http://meridian.allenpress.com/corrosion/article-pdf/59/4/319/1535906/1_3277564.pdf.

Melchers, R. E. 2003b. "Modeling of Marine Immersion Corrosion for Mild and Low-Alloy Steels: Part 2: Uncertainty Estimation." *Corrosion* 59 (April). http://meridian.allenpress.com/corrosion/article-pdf/59/4/335/1535898/1_3277565.pdf.

Melchers, R. E. 2019. "Predicting Long-Term Corrosion of Metal Alloys in Physical Infrastructure." *Npj Materials Degradation* 3 (1). https://doi.org/10.1038/s41529-018-0066-x.

Melchers, R. E. 2014. "Corrosion Wastage in Aged Structures." In *Condition Assessment of Aged Structures*, 77–106.

Melchers, R. E. and André Beck. 2018. *Structural Reliability Analysis and Prediction*. Third. John Wiley & Sons Ltd.

Melchers, R. E. 1997. "Modeling of Marine Corrosion of Steel Specimens." In *Corrosion Testing in Natural Waters*, Second Volume:20–33.

Paik, J. K., J. M. Lee, Y. Park, J. S. Hwang, and C. W. Kim. 2003. "Time-Variant Ultimate Longitudinal Strength of Corroded Bulk Carriers." *Marine Structures* 16 (8): 567–600. https://doi.org/10.1016/j.marstruc.2004.01.003.

Paik, J. K., A. K. Thayamballi, Y. I. Park, and J. S. Hwang. 2004. "A Time-Dependent Corrosion Wastage Model for Seawater Ballast Tank Structures of Ships." *Corrosion Science* 46 (2): 471–86. https://doi.org/10.1016/S0010-938X(03)00145-8.

Paik, J.K., S.K. Kim, and S.K. Lee. 1998. "Probabilistic Corrosion Rate Estimation Model for Longitudinal Strength Members of Bulk Carriers." *Ocean Engng* 25 (10): 837–60.

Pinciroli, Luca, Piero Baraldi, and Enrico Zio. 2023. "Maintenance Optimization in Industry 4.0." *Reliability Engineering and System Safety* 234 (June). https://doi.org/10.1016/j.ress.2023.109204.

Plutarch. 1905. *Plutarch's Lives*. Edited by Arthur Hugh Clough and John Dryden. New York: Colonial Co.

Qin, Shengping, and Weicheng Cui. 2003. "Effect of Corrosion Models on the Time-Dependent Reliability of Steel Plated Elements." *Marine Structures*. Vol. 16.

Rodzewicz, Thomas C, Jonathan H Potterton, Katherine M Lappe, Brent C Yezefski, and David J Singer. 2010. “A New Approach to Ship Repair Using CONWIP and Parts Kits.” *Journal of Ship Production and Design*. Vol. 26.

Sadeghian, M. 2022. “The Reliability Assessment of a Ship Structure under Corrosion and Fatigue, Using Structural Health Monitoring.” *International Journal of Engineering, Transactions B: Applications* 35 (9): 1765–78. https://doi.org/10.5829/ije.2022.35.09c.13.

Samuelson, Paul A., and William D. Nordhaus. 1998. *Economics*. 16th ed. New Delhi: Tata McGraw-Hill Publising Company Limited.

Sandler, Todd, and Keith Hartley. 1995. *The Economics of Defense*. Cambridge, England: Cambridge University Press.

Saydam, Duygu, and Dan M. Frangopol. 2015. “Risk-Based Maintenance Optimization of Deteriorating Bridges.” *Journal of Structural Engineering* 141 (4). https://doi.org/10.1061/(asce)st.1943-541x.0001038.

Scopus®. 2023. “Www.Scopus.Com.” September 3, 2023.

Smith, Ronald P. 1977. “Military Expenditure and Capitalism.” *Cambridge Journal of Economics* 1 (March):61–76. https://academic.oup.com/cje/article/1/1/61/1734958.

Smith, Ronald P. 1980. “Military Expenditure and Investment in OECD Countries, 1954-1973.” *JOURNAL OF COMPARATIVE ECONOMICS* 4:19–32.

Spearman, Mark L., David L. Woodruff, and Wallace J. Hopp. 1990. “CONWIP: A Pull Alternative to Kanban.” *International Journal of Production Research* 28 (5): 879–94. https://doi.org/10.1080/00207549008942761.

Storch, Richard Lee, and Sanggyu Lim. 1999. “Improving Flow to Achieve Lean Manufacturing in Shipbuilding.” *Production Planning and Control* 10 (2): 127–37. https://doi.org/10.1080/095372899233280.

Vu, Hai Canh, Phuc Do, Anne Barros, and Christophe Bérenguer. 2014. “Maintenance Grouping Strategy for Multi-Component Systems with Dynamic Contexts.” *Reliability Engineering and System Safety* 132:233–49. https://doi.org/10.1016/j.ress.2014.08.002.

Wang, G., B. Boon, F. P. Brennan, Y. Garbatov, C. Ji, J. Parunov, T. A. Rahman, et al. 2009. “Condition Assessment of Aged Ships and Offshore Structures.” In *17th International Ship and Offshore Structures Congress*. Seoul, Korea.

Woloszyk, K., and Y. Garbatov. 2024. “A Probabilistic-Driven Framework for Enhanced Corrosion Estimation of Ship Structural Components.” *Reliability Engineering and System Safety* 242 (February). https://doi.org/10.1016/j.ress.2023.109721.

Yamamoto, N, and K Ikegami. 1996. “A Study on the Degradation of Coating and Corrosion of Ship’s Hull Based on the Probabilistic Approach.” http://asmedigitalcollection.asme.org/offshoremechanics/article-pdf/120/3/121/5748397/121_1.pdf.

Young, Neil. 1987. *Rust Never Sleeps*. Burbank, CA: Reprise Records.

Zayed, A., Y. Garbatov, and C. Guedes Soares. 2007. “Corrosion Modeling of Single Hull Crude Oil Tanker Subjected to Multiple Deterioration Environments.” In *Proceedings of the 26th International Conference on Offshore Mechanics and Artic Engineering - OMAE*. San Diego, California.

Zayed, A., Y. Garbatov, and C. Guedes Soares. 2018. “Corrosion Degradation of Ship Hull Steel Plates Accounting for Local Environmental Conditions.” *Ocean Engineering* 163 (September):299–306. https://doi.org/10.1016/j.oceaneng.2018.05.047.